



# Etude fondamentale du comportement au feu de composites silicones : stabilité thermique, résidus sous pyrolyse et tests calorimétriques

Siska Devarennnes-Hamdani

## ► To cite this version:

Siska Devarennnes-Hamdani. Etude fondamentale du comportement au feu de composites silicones : stabilité thermique, résidus sous pyrolyse et tests calorimétriques. Matériaux. Université Montpellier II - Sciences et Techniques du Languedoc, 2011. Français. NNT : . tel-00726168

**HAL Id: tel-00726168**

**<https://theses.hal.science/tel-00726168>**

Submitted on 29 Aug 2012

**HAL** is a multi-disciplinary open access archive for the deposit and dissemination of scientific research documents, whether they are published or not. The documents may come from teaching and research institutions in France or abroad, or from public or private research centers.

L'archive ouverte pluridisciplinaire **HAL**, est destinée au dépôt et à la diffusion de documents scientifiques de niveau recherche, publiés ou non, émanant des établissements d'enseignement et de recherche français ou étrangers, des laboratoires publics ou privés.

ACADEMIE DE MONTPELLIER  
*UNIVERSITE MONTPELLIER 2*  
*SCIENCES ET TECHNIQUES DU LANGUEDOC*

**T H E S E**

pour obtenir le grade de  
**DOCTEUR DE L'UNIVERSITE MONTPELLIER 2**

***Discipline : Chimie des Matériaux***

***Ecole Doctorale : Sciences Chimiques***

présentée et soutenue publiquement

par

Siska HAMDANI-DEVARENNES

le 25 Février 2011

---

**Etude fondamentale du comportement au feu  
de composites silicones: stabilité thermique,  
résidus sous pyrolyse et tests calorimétriques**

---

**JURY**

M. Jean-Jacques ROBIN, Professeur, Université Montpellier II	, Président
M. José-Marie LOPEZ-CUESTA, Professeur EMA, Montpellier II	, Directeur de Thèse
M. François GANACHAUD, Chargé de Recherche ENSCM, Montpellier II	, Directeur de Thèse
M. Frédéric LEISING, Directeur de Recherche et Développement, Chryso	, Rapporteur
M. Eric LEROY, Chargé de Recherche, Université de Nantes	, Rapporteur
M. Philippe CASSAGNAU, Professeur, Université Claude Bernard	, Examineur
M. Giovanni CAMINO, Professeur, Politecnico di Torino	, Examineur
M. Damien DJIAN, Manager du HCR-LSR, Blustar Silicones	, Invité
Mlle. Claire LONGUET, Ingénieur de Recherche EMA	, Invité





# *Remerciements*

*Une bonne chose de faite ! C'est donc avec la plus profonde gratitude que je tiens à remercier toutes les personnes qui ont contribué à la réussite de ces trois ans et demie de thèse. Je ne saurais oublier toutes les personnes dont la disponibilité et la rigueur m'ont permis de garder ma persévérance, mon ardeur au travail et un sentiment de forte implication dans la recherche scientifique. Que ces personnes trouvent ici, en témoignage de ma profonde affection et de ma reconnaissance, mes plus chaleureux remerciements pour leur soutien sans faille depuis ma première année de thèse et pendant toute la durée de mon séjour en France. Je désire exprimer ma plus profonde gratitude pour chacun d'eux avec un remerciement plus particulier à Monsieur Yannick Vimont pour m'avoir accueilli au sein du CMGD lorsqu'il en était le Directeur. Je ne saurais oublier son soutien sans faille qui m'a permis de dépasser les difficultés rencontrées lors de mon séjour au laboratoire. Je remercie également M. le Professeur Bernard Boutevin pour m'avoir accueilli au sein de son laboratoire de Macromoléculaire IAM-ENSCM.*

*Je voudrais également exprimer ma profonde reconnaissance à mes directeurs de thèse, Monsieur François Ganachaud et Monsieur José-Marie Lopez-Cuesta. Il m'est impossible d'exprimer toute la gratitude que j'éprouve pour eux pour m'avoir proposé ce sujet de recherche, et pour tout le dynamisme qu'ils ont su montrer au cours des ces trois ans et demi passés à leur côté ; mais également pour leurs compétences scientifiques qui m'ont permis de mener à bien cette étude. Leurs conseils et leurs commentaires précieux m'ont permis de surmonter mes difficultés et de progresser dans mes études. Je les remercie également pour m'avoir apporté une aide précieuse tant sur le plan scientifique que sur le plan humain. J'ai beaucoup*

*apprécié leur générosité exceptionnelle, leurs qualités humaines, et surtout la complicité que nous avons développée. José, tu as su me laisser la liberté nécessaire à l'accomplissement de mes travaux, tout en gardant un œil critique et avisé. François l'occasion m'est ici offerte de te dire combien je te suis redevable pour l'humilité, l'amour du travail bien fait, la volonté de bien faire, ton sacré caractère, et surtout pour le temps que tu as consacré à la correction de nos articles composant ce manuscrit. Vous êtes scientifiquement et humainement indispensables pour moi dans cette expérience doctorale. Sans vous cette thèse ne serait pas ce qu'elle est.*

*Je remercie et exprime ici toute mon amitié doublée de ma reconnaissance à Claire Longuet, mon encadrante de proximité pour tous ses conseils sur le plan scientifique ainsi que sur le plan humain, sa disponibilité, et son dynamisme, pour sa compagnie au cours des longues journées ainsi que pour m'avoir donné son amitié. J'espère qu'il y aura toujours de la place pour moi dans ton bureau, pas seulement juste pour papoter entre filles, mais aussi pour le 'brainstorming' scientifique.*

*Mes plus vifs remerciements s'adressent aux membres du jury qui ont accepté de juger ce travail :*

*Je remercie sincèrement Monsieur le Professeur Jean-Jacques Robin, qui m'a fait l'honneur de présider le jury de cette thèse.*

*Je remercie tout particulièrement Monsieur Frédéric Leising, Directeur de Recherche et Développement à Chryso, ainsi que Monsieur Eric Leroy, Chargé de Recherche à l'Université de Nantes, pour avoir accepté de juger ce travail et d'en être les rapporteurs. Je tiens surtout à les remercier pour la rapidité avec laquelle ils ont lu mon manuscrit et l'intérêt qu'ils ont porté à mon travail.*

*Je présente toute ma reconnaissance à Monsieur le Professeur Giovanni Camino, de la Politecnico di Torino pour le grand honneur qu'il m'a fait en*

*acceptant d'examiner mon travail et de participer à la soutenance de cette thèse. J'éprouve un profond respect pour son travail. Certaines de ses publications scientifiques m'ont beaucoup aidée pour le développement de certains points traités au cours de mon doctorat.*

*Je voudrais également exprimer mes remerciements les plus sincères à Monsieur Damien Djian, le Manager formulation du HCR-LSR de Blustar Silicones, pour la collaboration enrichissante entretenue au cours de ces années, aussi que pour l'aide apportée au cours de nos discussions, pour ses précieux conseils et pour sa rapidité lors de l'envoi des différents échantillons.*

*Je veux adresser tous mes remerciements à Monsieur le Professeur Philippe Cassagnau, de l'Université Claude Bernard de Lyon, pour le temps qu'il a su prendre pour examiner mon manuscrit et pour sa participation à ce jury de thèse.*

*La qualité des données présentées ici sont le fruit d'un travail d'équipe qui a permis d'aboutir à ce manuscrit de thèse. Cette étude a également été enrichie grâce à de nombreuses discussions que j'ai pu avoir avec les différents ingénieurs de recherche et doctorants de mes deux laboratoires d'accueil.*

*Mes remerciements vont tout particulièrement à Etienne Delebecq pour son amitié, sa sympathie et surtout pour notre collaboration, et sa contribution indispensable. Etienne, le « cœur d'or », tu travailles toujours énormément, et je t'apprécie beaucoup pour ces qualités, et ce fut un grand plaisir de travailler à tes côtés.*

*J'exprime toute ma gratitude à Rodolphe Sonnier pour ses conseils, et plus particulièrement sur le travail du dernier chapitre. Je te remercie pour toutes tes remarques, tes suggestions, et tes conseils amicaux. Malgré l'encadrement de plusieurs thésards, tu as quand même trouvé le temps de*

*lire intensivement ce chapitre. C'est fini, tu n'auras plus 44 pages à lire et corriger en une nuit.*

*Merci également à Didier Perrin, pour ses remarques notamment sur le premier chapitre. J'espère qu'un jour, pour toi comme pour moi, que nos yeux se rétabliront. En attendant, rien ne peut nous empêcher de faire les choses bien et surtout de bien faire les choses.*

*Je voudrais également exprimer mes remerciements les plus sincères à Belkacem Otazaghine, qui par son expérience et son enthousiasme, a su me doner de nombreux conseils, surtout lors de la caractérisation et de l'interprétation des analyses du Py-GC/MS.*

*Ce travail n'aurait pu être mené à bien sans l'aide de différents fournisseurs qui, au travers de leur soutien matériel, ont reconnu mon travail et m'ont fait confiance :*

*Merci aux Bluestar Silicones pour m'avoir fourni les matrices ainsi que d'autres composés nécessaires au cours de ce travail de cette thèse. Je remercie également NYCO Mineral, Nabaltec AG, Evonik Degussa International AG, Gelest Inc.*

*Et comme mon travail s'est déroulé à la fois au laboratoire CMGD, en grande partie, et à l'ENSCM, en petite partie, je tiens à remercier tous les membres de l'équipe du CMGD et de l'IAM-ENSCM pour leur accueil, leur sympathie ainsi que leurs idées constructives.*

*Je remercie vivement Jean-Marie Taulemesse et Pierre Gaudon avec qui j'ai eu tant de discussions fructueuses, pour leurs conseils avisés et pour leur aide indispensable lors de la caractérisation et l'interprétation effectué avec le MEB/EDX et la DRX. Je tiens également à remercier Laurent Clerc, Marc Longerey, Robert Lorquet, et Benjamin Gallard pour leur aide précieuse et la patience dont ils ont fait preuve, lors des caractérisations de la variation de volumes, résistance à la compression, et les DRX des composants et pour les*

*coups de mains lors des pannes de certains appareillages. Je les remercie vivement pour leurs précieux conseils techniques.*

*J'ai eu également le plaisir de collaborer avec des étudiants motivés lors de stages sur mon sujet de thèse. Je remercie « ma poupette » Audrey Pommier et « ma grande-petite » Julia Raeke pour leur aide indispensable lors de ma première et deuxième année de thèse. Je vous adore, parce que vous êtes adorables. J'aimerais bien un jour vous réunir, pour voir qui est la plus grande d'entre vous ?*

*Je souhaite évidemment remercier les différentes personnes du CMGD pour leur soutien scientifique mais aussi et surtout pour avoir réussi à créer une super ambiance au sein et en dehors du labo.*

*Pour leur généreuse assistance, je voudrais aussi remercier les personnels administratifs, notre adorable secrétaire Sylvie Cruvellier, et aussi Michèle Brun, ainsi que pour leur amitié. Je leur adresse mes remerciements pour toute la sympathie qu'elles m'ont témoignée dès le début jusqu'à ce-jour. Grâce à elle, j'ai pu faire mon travail plus tranquillement sans soucis administratif.*

*Au delà des cadres scientifiques du CMGD, je suis redevable envers mes amis et les collègues et envers les permanents avec qui j'ai pu partager un café, un repas, un barbecue (bientôt la saison !!) pendant ces trois ans et demie. Je me souviendrai toujours de leur gentillesse et surtout des moments formidables de joie et de convivialité passés ensemble. Une spéciale dédicace aux membres des 'Daltons': notre « organisatrice » Lucie, « ma créatrice Dinette » Amandine, « ma poupette » Audrey, « notre « autre copine » Hossein : j'aime beaucoup tes pompons, notre « galette » Gaëlle, et « ma caroni » Caroline, le « philosophe » Nicolas, la « sage » Aurélie, la « calme et douce » Joana, Yen, Hang, Tao, et tous les autres que je n'ai pu citer ici. Merci pour votre amitié et pour tous les moments de détente et rires inoubliables passés ensemble, et aussi pour vos encouragements et votre*

soutien. Tous ce que vous avez fait pour moi est inoubliable même si je ne vous connais que depuis peu (par rapport à mon séjour sur terre :D) et malgré mon titre « despote du CMGD », je vous adore. Merci à Hossein pour sa sagesse et les discussions constructive, sa gentillesse et sa disponibilité mais aussi pour « les coups des mains ». Merci à Dinette pour le BD ce que tu as fait et le reste, même si c'est un grand cadeau des Daltons, c'est un de le plus précieux cadeau de ma soutenance. Je l'ai montré à tous mes proches, je suis fière de ton travail. Lulu, avec qui j'ai partagé mon bureau depuis ce trois ans, maintenant c'est à moi de t'encourager...aller tu vas y arriver, on est tous avec toi ! Ma Poupette, qui est toujours à l'écoute, qui a le cœur sur la main, et qui toujours est disponible pour les autres. J'adore nos fous rires pendant la détente et à la gym avec Joana. Gaëlle « galette », j'adore ton café, il faut que tu me donnes ta recette même si je ne crois pas arriver à faire aussi bien que toi, je te remercie également pour ta participation dans l'avancée des manipulations lors ton projet long quand tu étais petite. Et Ma Caroni j'adore ton rire. Merci aux thésards Vietnamiens, avec qui j'arrivé à me sentir à la maison, même si je ne comprends pas le vietnamien, mais leurs sourires suffisent !

Cette gratitude va également à mes collègues et tout le personnel d'IAM-ENSCM pour la bonne ambiance qu'il y régnait tout au long de ces années. Je pense particulièrement à Claire, David, Nelly, les anciens thésards mes compatriotes « option matériaux » Julien et Guillaume. Merci pour votre accueil chaleureux, les coups des mains, les encouragements, et parfois les précieux conseils techniques que vous m'avez donné.

Je réserve un remerciement chaleureux à Christine Joly-Duhamel qui m'a beaucoup encouragée dans les bons moments ainsi que dans les moments plus difficiles. Plus qu'une encadrante, j'ai trouvé en elle, une 'maman scientifique', sur qui je peux compter, et qui m'a toujours amicalement assistée surtout au début quand je faisais mes premiers pas en France en 2005.

*Et bien sur, je n'oublierai pas remercier Mme. Jacqueline Raymond lorsqu'il en était la Directrice de la relation internationale à ENSCM et aussi pour Claudia et Frédéric pour ses chaleureuse accueil, ses guides et ses aides même avant que j'ai mis mes pieds en France.*

*J'ai la chance aussi de connaître et croise ma route avec les grand hommes dans ses domaines avec qui j'ai appris beaucoup des choses, mon grand-père « faire pas les choses moitié-moitié », Bapak Rusdi Djamal, le Professeur à l'université Andalas : « va jusqu'à bout de ton étude », Bapak Budi Liputra, le manager du Buckman Laboratories Asia pacifique : « n'attend pas les choses vient sur toi, et toujours 'work smart' », et Denis Poncelet, le professeur à ONIRIS Nantes et le président de BRG (Bioencapsulation Research Group) : « celui qui joue qui gagne ». Merci pour votre précieuses conseils, j'aurai toujours les besoin.*

*Je ne pourrais jamais oublier l'aide des personnes de ma merveilleuse famille pour leur soutien constant tout au long de mes études et de mon doctorat, malgré tout ce que j'ai pu affronter sur ce chemin. Ma famille et mes amis, avec leurs encouragements constants, « tu vas y arriver » bien qu'angoissée et fréquemment en période de doute, m'ont permis de ne jamais dévier de mon objectif final. Donc, dans ce travail, je ne saurais oublier de citer les deux hommes extraordinaires qui ont illuminé ma vie, mon père Yulizar, et mon mari Jérôme, et, une femme, la plus extraordinaire que je n'ai jamais rencontrée, ma mère Yasmaermi. Je n'oublierai jamais l'amour et la douceur de ma mère. Mes parents, qui m'ont fait telle que je suis maintenant. Mon « deux-tiers » Jérôme, plus qu'un mari, j'ai trouvé en lui, un ami avec son amour affectueux et l'amitié dont il a toujours fait preuve, son soutien et sa complicité m'ont été indispensables. Je t'aime, mon « deux- tiers ». Avec mes parents, ils m'ont soutenu du début jusqu'à la fin. Ils ont toujours insisté pour que je continue mon rêve jusqu'au bout et pour ne jamais baisser les bras même si ce n'était pas toujours facile pour eux. Des pensées affectueuses vont à ma sœur, à mon frère, à Retta, à Pak Gangan's family, à mbak Jenny, et à*



*ma famille française : Papy, « papa » Etienne, Taty Marlène, tonton André, taty Conchita et tonton Felix. Merci d'être toujours là pour nous, ainsi de nous accueillir toujours à bras ouverts. Je n'y serais jamais arrivé sans votre soutien unanime. Et enfin une pensée toute particulière pour Jerry, mon gros chat noir (je dois le mettre au régime), qui m'a accompagné pendant les nuits blanches de rédaction, même si la plupart du temps il m'a juste embêtée en me demandant à boire sous le robinet, et pour me fait rire quand il fait son beau pour que je le trouve mignon.*

*Pour vous tous, le seul mot merci ne sera jamais assez. J'espère que cette thèse sera un remerciement suffisant au soutien et à la confiance sans cesse renouvelée dont vous avez fait preuve à mon égard.*

*À mon mari, à mes parents*

# Sommaire

Introduction Générale .....	1
Retardateurs de flamme à base de silicone .....	7
Flame retardancy of Polydimethylsiloxane .....	11
Synergie entre la silice et le platine pour obtenir un haut taux de résidu et une résistance au feu améliorée lors de la pyrolyse de formulations à base de silicone.....	43
High Residue Contents Indebted by Platinum and Silica Synergistic Action during the Pyrolysis of Silicone Formulations.....	47
Etude des propriétés thermiques d’une matrice silicone contenant des charges à base de calcium ou d’aluminium : Préparation des mélanges et analyse de leur comportement thermique. ....	63
Calcium and aluminum-based fillers as flame-retardant additives in silicone matrices. I. Blend preparation and thermal properties .....	65
Etude de la cohésion du résidu des composites à matrice silicone contenant des charges minérales à base de calcium ou d’aluminium après pyrolyse en conditions extrêmes .....	77
Calcium and Aluminum-based fillers as flame retardant additives in Silicone matrices II. Analysis on composite residues from an industrial-based pyrolysis test .....	81
Etude du comportement au feu de composites silicone comportant des charges minérales à base de calcium ou d’aluminium .....	97
Calcium and aluminum-based fillers as flame-retardant additives in silicone matrices. III. Investigations on fire reaction .....	99
Conclusion générale et perspectives .....	137



# *Introduction Générale*





## Introduction Générale

Selon les statistiques des principaux pays industrialisés, 10 à 20 décès et 100 à 200 blessés par million d'habitants et par an sont imputables à des incendies. De plus, la perte économique totale attribuée au feu en Europe est plus importante qu'aux Etats Unis (Figure 1). En France par exemple, la perte économique et le taux de mortalité assignés aux incendies sont supérieurs à ceux des autres pays européens considérés, probablement du fait que les dispositifs anti-incendie y sont moins drastiques.

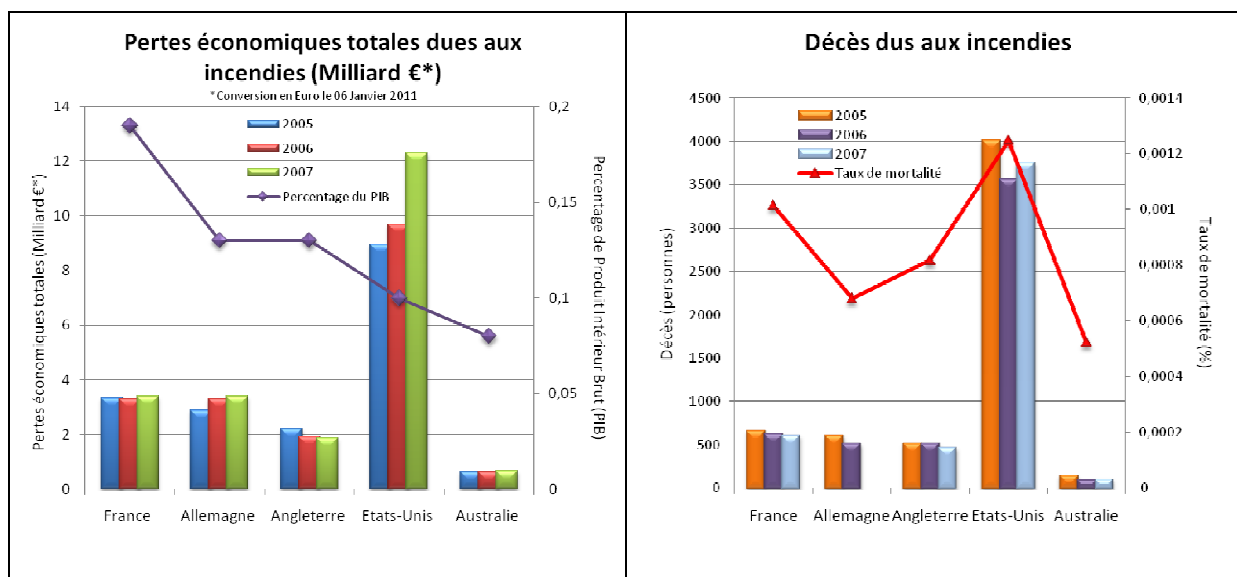


Figure 1. Pertes économiques et décès provoqués par des incendies [1]

Les feux accidentels dans les lieux d'habitation ont des conséquences plus graves que dans des locaux professionnels, de par l'absence de réglementation imposant l'installation de détecteurs de fumée chez les particuliers ou de l'absence de sorties de secours. Environ 80% des décès pour cause d'incendie sont répertoriés dans des bâtiments privés, et 10% de ces accidents sont provoqués par un défaut électrique. Lorsque les câbles ne sont pas protégés vis-à-vis du risque incendie, la surchauffe des fils, la formation d'arcs électriques ou de courts-circuits peuvent entraîner l'inflammation de la matière isolante puis sa combustion, propageant ainsi le feu à travers le bâtiment. Les câbles contribuent également et de façon significative, au dégagement de chaleur et à la production de fumées (suffisamment pour limiter la visibilité et inhiber l'action des secours), ainsi qu'à l'intensification de la production de monoxyde de carbone (CO), considéré comme le gaz le plus mortel libéré au cours des incendies, et de gaz corrosifs tels qu'HCl [2]. Pour preuve, une étude réalisée en 2005 en

Grande Bretagne montre que l'intoxication par les gaz ou la fumée est la première cause de décès lors d'un incendie (Figure 2).

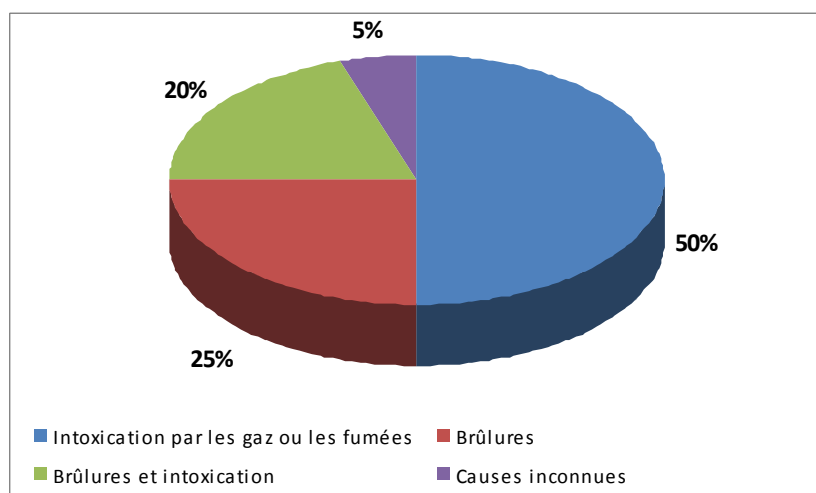
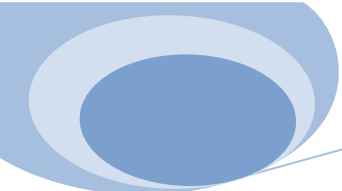


Figure 2. Causes de décès lors d'incendies rapportés en Grande Bretagne [3]

L'amélioration des performances feu de la câblerie est nécessaire pour permettre une réduction notable du nombre de décès et des pertes financières provoquées par les incendies. Il s'agit notamment de maximiser la durée de fonctionnement de systèmes d'alarmes, ascenseurs, et téléphones, afin de permettre aux secours d'intervenir dans de meilleures conditions. Pour cette raison, la tenue au feu d'un câble est testée et certifiée selon des normes nationales et internationales. En France, selon la norme NFC 32-070, le câble est dit « non-propagateur de flamme » s'il satisfait la catégorie C2, « non-propagateur d'incendie » s'il satisfait la catégorie C1 et « résistant au feu » s'il satisfait la catégorie CR1. Cette norme française NFC 32-070 CR1 s'appuie sur les normes internationales IEC 60331 ou EN 50265-2-1, appliquées dans le monde et l'Union Européenne, respectivement. Dans les deux cas, les câbles sont pyrolysés jusqu'à 750°C ou 850°C, respectivement, tout en exerçant un choc mécanique toutes les 5 minutes. En Angleterre, la norme BS8434 catégorie 1 dite « standard » et catégorie 2 dite « améliorée » impose à la fois des chocs mécaniques et l'application d'un jet d'eau à des températures atteignant 830°C et 930°C, respectivement. Depuis le 1<sup>er</sup> Mars 2009, la norme BS8434-1 a été remplacée par la norme BS EN 50200:2006, afin de s'aligner sur la norme européenne [4]. Afin d'homogénéiser les normes présentes dans les différents pays européens, l'Union Européenne a mis en place une classification des matériaux utilisés dans le secteur du bâtiment, dénommée « Euroclasses » et en fonction depuis les années 2000 [5].

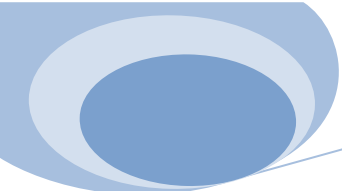


A l'heure actuelle, la plupart des formulations appliquées en câblerie utilisent des polymères organiques thermoplastiques, tels que le polychlorure de vinyle (PVC), le poly(éthylène vinyl acétate) (EVA), le polyéthylène basse densité (PE bd), le polyamide (PA) ou le polypropylène (PP). Pour améliorer leur propriétés feu, des stratégies basées sur l'emploi de retardateurs de flamme halogénés ou d'hydroxydes métalliques ont été développées [6]. Les inconvénients de ces additifs sont pour les premiers, une corrosivité des effluents et un risque environnemental et pour les seconds, le risque d'une détérioration des propriétés mécaniques. Jusqu'aux années 90, les câbles de haut voltage étaient préférentiellement réalisés en PVC, or il s'avère que ces derniers peuvent produire de l'acide chlorhydrique lors de leur combustion [7]. Par mesure de sécurité publique et par respect pour l'environnement, les gouvernements ont donc limité l'utilisation de ces polymères en câblerie dans la plupart des pays.

Face à ces limites, la formulation de câbles à base de silicone apparaît comme une alternative prometteuse pour obtenir de meilleures propriétés à hautes températures. En effet, le silicone, comparé aux polymères organiques, possède une excellente stabilité thermique, produit un faible taux de COV (composés organiques volatiles) et les fumées produites lors de sa combustion sont non-toxiques, non-corrosives, et très peu opaques [8,9,10]. Malgré tous ces avantages, les propriétés du silicone seul ou chargé en silice, ne sont pas suffisantes pour satisfaire certains domaines d'application feu [11]. Dans le domaine de la câblerie, par exemple, le maintien du fonctionnement du câble en cas d'incendie nécessite l'incorporation, dans la gaine de silicone, d'une forte quantité de particules minérales de structures adéquates, afin que le résidu après dégradation du polymère conserve une intégrité suffisante pour continuer à assurer le bon fonctionnement électrique. Ce type d'applications impose aux matériaux de présenter après combustion, des résidus cohésifs possédant de bonnes propriétés mécaniques permettant de passer la norme NFC 32-070 CR1, c'est-à-dire capable de supporter sans se fendiller les chocs mécaniques exercés sur la gaine du câble. A l'heure actuelle, aucune formulation élaborée par les industriels ne donne de résultats totalement satisfaisants à ce test applicatif [12].

De nombreux brevets et articles ont été publiés, mais la connaissance des mécanismes d'action des différents additifs et charges minérales incorporés dans les gaines en silicone est encore très limitée. L'amélioration de la compréhension des processus de dégradation thermique et de céramisation des résidus des composites à matrice silicone reste donc d'actualité. De même, une formulation unique permettant de répondre à la norme quelle que



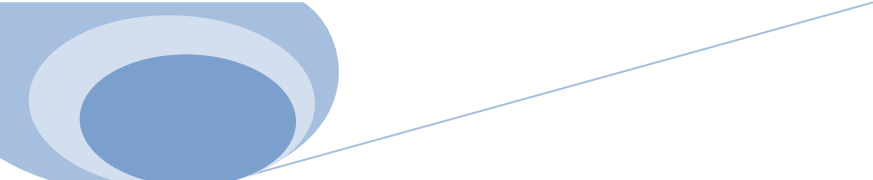


soit l'application visée, notamment dans le domaine de la câblerie, n'a toujours pas été développée. Au vu de ce manque de connaissances, nous avons décidé, dans le cadre de ce travail de thèse, de réaliser une étude fondamentale afin de comprendre les différents mécanismes mis en jeu lors de la dégradation d'une matrice silicone comportant différents types d'additifs et de charges minérales. Ce manuscrit comporte trois grandes parties, développées au travers de cinq chapitres. Ces chapitres comprennent chacun un article en anglais publié, soumis ou en fin de rédaction. Préalablement, un résumé en français donne les résultats principaux et les conclusions marquantes de l'étude présentée.

La première partie du travail consistera à faire le point sur l'état des connaissances concernant le comportement au feu des silicones, développé ici au travers d'une étude bibliographique. Dans ce premier chapitre, nous compilerons les brevets et les articles scientifiques traitant de la stabilité thermique du silicone seul ou additivé. Nous décrirons ainsi le mécanisme de dégradation du silicone, le rôle des charges ou des additifs employés pour améliorer les propriétés thermiques et le comportement au feu du silicone, ainsi que l'introduction des silicones comme retardateurs de flamme dans d'autres matrices polymères.

Dans une deuxième partie, nous considérerons le comportement au feu de la matrice silicone, afin d'expliquer l'effet bien connu du platine sur sa résistance thermique et de développer le mécanisme de céramisation observé au cours d'une pyrolyse. Le platine est un additif couramment utilisé dans les formulations silicone comme agent de catalyse pour les réactions d'hydrosilylation [13]. Par ailleurs, il a été montré, par analyse thermique, que ce dernier, en présence de silice, catalysait les réactions de réticulation responsables d'une augmentation du taux de résidu [14,15,16]. Nous fournirons ici des explications à ces phénomènes, et suggérerons de nouvelles formulations moins onéreuses aboutissant à de fort taux de résidus.

Dans une dernière partie, nous étudierons l'influence de deux familles de charges, l'une à base de calcium, et l'autre à base d'aluminium, sur les composites à matrice silicone chargé de silice. Les différentes propriétés étudiées sont le comportement thermique, la cohésion des résidus et enfin le comportement au feu. Ainsi, la stabilité thermique des composites avec les différents types de charges par thermogravimétrie (ATG) sera présentée dans le chapitre trois, où la microscopie électronique à balayage (MEB) couplée à l'analyse élémentaire X (EDX) et la diffraction des rayons X (DRX), permettent de déterminer les composés présents dans les résidus. La cohésion des résidus des composites sera présentée dans le chapitre quatre, où différents tests sont réalisés : résistance à la compression et mesure de la variation de volume



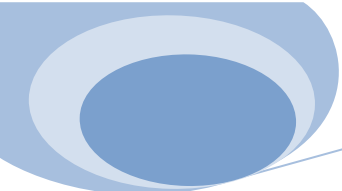
couplés à l'imagerie électronique et aux analyses par diffraction et microanalyse X. Le comportement au feu des composites sera finalement abordé dans le chapitre cinq, où l'influence de chaque charge sur l'action retardatrice du silicone en phase condensée est décrite.

Enfin, nous concluerons sur l'influence de chaque charge étudiée dans la matrice silicone réticulée vis-à-vis de la stabilité thermique, de la cohésion du résidu, et du comportement au feu, avant de donner quelques perspectives de développement destinées à fournir la meilleure formulation de composite à matrice silicone en fonction du comportement souhaité et/ou de l'application visée.

## Références

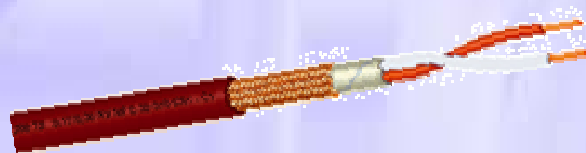
---

- 1 Annual report of United Nations Fire Statistics Study at the meeting in Geneve in Septembre 2010. World Fire Statistics No. 26/ Octobre 2010. The Geneva Association.
- 2 Fire safety of cables. European Flame Retardants Association consulté en janvier 2011 <http://www.cefic-efra.com/Objects/2/Files/Fire%20safety%20of%20cables.pdf>
- 3 Fire statistics. European Flame Retardants Association consulté en janvier 2011 <http://www.flameretardants.eu/Content/Default.asp?PageName=openfile&DocRef=2006-02-13-00005>
- 4 BS EN 50200 :2006. Method of test for resistance to fire of unprotected small cables for use in emergency circuits. British Standards Institution. June 2006
- 5 Mitzlaff M., Troitzsch J., National and international fire protection regulations and test procedures : Building. In Plastics flammability Handbook 3rd Ed: Principles, Regulations, Testing, and Approval. Troitzsch J., , Munich: Hanser Publishers, 2004.p.227-432
- 6 Troitzsch HJ. In: Gachter R, Muller H, editors. Flame Retardants: Plastics Additives. Cincinnati: Hanser Publisher, 1993.p.709-748
- 7 Bensheim A. H. PVC stabilizers, In: Gachter R, Muller H, editors. Flame Retardants: Plastics Additives. Cincinnati: Hanser Publisher, 1993.p.p. 271-326,
- 8 Dvornic PR. In: Jones RG, Ando W, Chojnowski J, editors. Thermal Stability of Polysiloxanes: Silicone-Containing Polymers. Dordrecht, the Netherlands: Kluwer Academic Publisher, 2000.p.185-212
- 9 Jovanovic JD, Govedarica MN, Dvornic PR, Popovic IG. The thermogravimetric analysis of some polysiloxanes. Polym Degrad Stab 1998;61:87-93.
- 10 Buch RR. Rates of heat release and related fire parameters for silicones. Fire Safety 1991;17:1-12

- 
- 
- 11 Hshieh F-Y. Shielding effects of silica-ash layer on the combustion of silicones and their possible applications on the fire retardancy of organic polymers. *Fire Mater* 1998;22:69-76.
  - 12 George C, Pouchelon A, Thiria R. Composition Polyorganosiloxanes vulcanisables à chaud utilisable notamment pour la fabrication de fils ou câbles électriques. France Patent 2,899,905; 2006.
  - 13 Karstedt B.D., Platinum Vinylsiloxanes, US Patent 3715334, 1970.
  - 14 MacLaury M. R., The Influence of Platinum, Fillers and Cure on the Flammability of Peroxide Cured Silicone Rubber, *J. Fire Flam.* 1979, 10, 175-98
  - 15 Lagarde R, Lahaye J, Bargain M. Mécanisme d'ignifugation d'élastomères organosiliciques par le platine, *European Polymer Journal* 1977;13:769-774.
  - 16 Hayashida K, Tsuge S, Ohtani H. Flame retardant mechanism of polydimethylsiloxane material containing platinum compound studied by analytical pyrolysis techniques and alkaline hydrolysis gas chromatography. *Polymer* 2003;44:5611–5616.

# *Chapitre 1.*

## *Etude Bibliographique*





## Retardateurs de flamme à base de silicone

Les polymères synthétiques font partie intégrante de notre quotidien, à tel point qu'ils ont rapidement remplacé les matériaux plus traditionnels, tels que les métaux ou les céramiques, et même les polymères naturels comme le bois, le coton, le caoutchouc naturel, etc. Un des points faibles des polymères en général, par rapport à d'autres types de matériaux, réside cependant dans leur forte combustibilité. Il s'avère nécessaire que les produits finis contenant des polymères synthétiques (par exemple, les câbles, les tapis, ou les meubles) présentent un degré de réaction au feu satisfaisant pour assurer la sécurité publique face aux incendies.

Les matériaux à base de silicones sont commercialisés depuis le début des années 1940, et utilisés dans de nombreuses applications en génie civil, en construction, électricité, transport, aéronautique, défense, textile et dans l'industrie cosmétique [1]. Le produit majoritaire de la gamme des silicones est le polydiméthylsiloxane (PDMS). Les éléments structuraux principaux des polysiloxanes ont une influence directe ou indirecte sur leur stabilité thermique, par exemple la force inhérente à la liaison siloxane (Si-O) ou la flexibilité importante du segment de chaîne  $-\text{[Si-O]}_x-$ . Ainsi, les siloxanes cycliques (faible poids moléculaire) montrent une plus haute stabilité entropique par rapport aux siloxanes linéaires (haut poids moléculaire), et donc une dégradation thermique retardée [2]. Les silicones présentent également un faible taux de dégagement de chaleur (HRR), une sensibilité minimale à un flux thermique externe et une faible production de monoxyde de carbone. Le HRR pour la plupart des silicones se situe dans une fourchette de  $60\text{-}150\text{ kW}\cdot\text{m}^{-2}$  pour une irradiance de  $50\text{ kW}\cdot\text{m}^{-2}$  [3]. Les silicones possèdent également une vitesse de combustion lente, sans gouttes enflammées et à l'état pur, aucune émission de fumées toxiques. Il n'est donc pas surprenant qu'en raison de ses propriétés de réaction au feu, le PDMS ait été mis en tête de liste des polymères pour les applications en câblerie.

Contrairement aux polymères organiques, les silicones exposés à des températures élevées sous oxygène conduisent à la formation de silice. C'est sur cette base que les silicones ont été sélectionnés comme retardateurs de flamme : en effet, le résidu de silice sert de « couverture isolante », il agit comme une barrière de transport de masse retardant la volatilisation des produits de décomposition, réduisant la quantité de substances volatiles disponibles pour la combustion en phase gazeuse et donc, diminuant la quantité de chaleur disponible à la surface du polymère. Le résidu de silice permet également d'isoler la surface du polymère du flux de

chaleur incident. Cependant, même si l'épaisseur de la couche de silice, obtenue suite à la combustion de la matrice silicone seule dans l'air, varie en fonction de la rampe de température et de la température finale, en aucun cas, elle ne présente une cohésivité suffisante pour toutes les applications visées. Diverses méthodes ont donc été proposées pour former une couche protectrice sur les surface brûlées des polymères, comme l'ajout de charges inorganiques agissant de telle sorte à diluer les gaz et réduire ainsi la chaleur en surface due à la grande quantité de cendres produites [4]. Le réseau physique formé par ces additifs de grande surface spécifique dans le polymère fondu réduit également le phénomène de chute de gouttes, mais, d'autre part, limite considérablement la mise en œuvre de certains systèmes. Des phénomènes similaires se produisent lorsque des charges poreuses comme les zéolithes sont utilisées à des concentrations élevées, surtout si la taille moyenne des pores ( $> 10$  nm) permet aux chaînes de polymère d'y pénétrer [5].

Différents travaux de recherche en cours visent à améliorer les propriétés ignifuges du silicone, en ajoutant des charges, en modifiant le squelette siloxane ou en incorporant des hétéroatomes retardateurs de flamme. La revue suivante vise à décrire la plupart des travaux portant sur les applications des silicones en tant qu'agents ignifugeants et/ou sur le développement des propriétés retardatrices de flamme des silicones eux-mêmes. Nous avons essayé d'être le plus exhaustif possible mais toutes les publications traitant de la résistance au feu des silicones ainsi que les brevets n'ont pu être cités ici. Cette revue est divisée en trois parties principales. Dans la première partie nous discutons de la dégradation thermique des silicones, en insistant sur les mécanismes de dépolymérisation, l'effet de la structure du polymère, des conditions de chauffage, et de l'ajout d'additifs (i.e. à moins de 5% en poids de charges). Ensuite, l'influence de plusieurs types de charges minérales (contenant jusqu'à 60% en poids) en tant qu'agents retardateur de flamme du PDMS est présentée. Enfin, nous décrivons l'ajout dans d'autres matrices polymères, de PDMS ou de PDMS fonctionnalisés comme retardateurs de flamme.

## Références

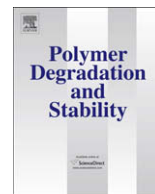
---

- 1 Biron M. Silicones ou siloxanes Applications. *Techniques de l'Ingénieur* Oct 2007, N2882.
- 2 Dvornic PR. In: Jones RG, Ando W, Chojnowski J, editors. Thermal Stability of Polysiloxanes: Silicone-Containing Polymers. Dordrecht, the Netherlands: Kluwer Academic Publisher, 2000.p.185-212

- 3 Buch RR. Rates of heat release and related fire parameters for silicones. Fire Safety 1991;17:1-12
- 4 Marosi G, Mårton A, Anna P, Bertalan G, Marosfoi B, Szép A. Ceramic precursor in flame retardant systems. Polym Degrad Stab 2002;77:259-265.
- 5 Wen J, Mark J. Mechanical properties and structural characterization of poly(dimethylsiloxane) elastomers reinforced with zeolite fillers. J Mater Sci, 1994;29(2):499-503







## Review article

## Flame retardancy of silicone-based materials

Siska Hamdani<sup>a</sup>, Claire Longuet<sup>a</sup>, Didier Perrin<sup>a</sup>, José-Marie Lopez-cuesta<sup>a</sup>, François Ganachaud<sup>b,\*</sup><sup>a</sup> Centre des Matériaux de Grande Diffusion, Ecole des Mines d'Alès, 6 avenue de Clavières 30319 ALES Cedex, France<sup>b</sup> Institut Charles Gerhardt UMR5253 CNRS/UM2/ENSCM/UM1, Equipe Ingénierie et Architectures Macromoléculaires, Ecole Nationale Supérieure de Chimie de Montpellier, 8 Rue de l'Ecole Normale 34296 Montpellier Cedex, France

## ARTICLE INFO

## Article history:

Received 25 June 2008

Received in revised form

4 November 2008

Accepted 18 November 2008

Available online 3 December 2008

## Keywords:

Flame retardancy

Silicone

Mineral fillers

Ceramization

## ABSTRACT

This review describes some recent works related to the development of the flame retardation of silicone elastomers and/or applications of silicones as flame retardant agents in other polymers. First, the thermal degradation of silicones themselves is discussed, focussing on depolymerization mechanisms, effect of structure, heating conditions, and effect of additives (i.e. less than 5 wt% fillers) on thermal degradation of silicones. Then, the influence of several types of mineral fillers (of up to 80 wt% content) as ceramization agents of silicones is presented. Finally, the introduction of (functionalized) silicones as flame retardants into other polymers is described.

© 2008 Elsevier Ltd. All rights reserved.

## 1. Introduction

Synthetic polymers are a crucial part of today's life, they can be found nearly everywhere. Today, synthetic polymer materials are rapidly replacing more traditional materials such as metals, ceramics, and natural polymers such as wood, cotton, natural rubber etc. However, one weak aspect of synthetic polymer materials compared with other materials is that polymers are combustible. Thus, the majority of polymer-containing end-products (e.g., cables, carpets, furniture cabinets, etc.) must have a satisfactory degree of fire resistance to ensure public safety from fire. Silicone materials have been produced commercially since the beginning of the 1940s. Over the past 60 years, silicone materials have grown into a billion-dollar industry, and are used in many applications in civil engineering, construction building, electrical, transportation, aerospace, defence, textiles, and cosmetics industries [1]. The dominant polymer in the silicone industry is polydimethylsiloxane (PDMS). The main structural elements of polysiloxanes have direct or indirect influence on their stability at elevated temperatures, including: inherent strength of the siloxane (Si–O) bond, pronounced flexibility of the  $-\text{[Si-O]}_x-$  chain segments, and entropically higher stability of low molecular weight cyclic siloxanes compared to their high molecular weight linear counterparts

against thermal degradation [2]. Silicones have comparatively low heat release rates (HRR)<sup>1</sup>, minimal sensitivity to external heat flux and low yields of carbon monoxide release. The HRR for most silicones falls within the range of 60–150 kW m<sup>−2</sup> [3]. Silicones also show a slow burning rate without a flaming drip and when pure, no emissions of toxic smokes. Based on these fire properties, silicones offer significant advantages for flame retardant applications. It is not surprising that due to their properties against flames, PDMS has been put in the top list of polymers for applications at high temperature such as in electrical wires and cables. Unlike organic polymers, silicones exposed to elevated temperatures under oxygen leave behind an inorganic silica residue. The shielding effects provide some of the fundamentals for the development of silicone-based fire retardants. Silica residue serves as an “insulating blanket”, which acts as a mass transport barrier delaying the volatilization of decomposition products. Therefore, it reduces the amount of volatiles available for burning in the gas phase and thus, the amount of heat that feeds back to the polymer surface. The silica residue also serves to insulate the underlying polymer surface from incoming external heat flux. It was reported by Hsieh [4] that the silica ash layer integrity governs the efficiency of the diffusion barrier that restricts the diffusion of fuels into the combustion zone and the access of oxygen to the unburned fuels. Even if the strength

\* Corresponding author. Tel.: +33 4 67 14 72 96; fax: +33 4 67 14 72 20.  
E-mail address: [francois.ganachaud@enscm.fr](mailto:francois.ganachaud@enscm.fr) (F. Ganachaud).

<sup>1</sup> Readers not familiar with techniques applied to polymer to determine their flame retardancy are directed to Appendix, where their basics are briefly described.

of the silica powder obtained by firing silicone polymer alone in air varies with the temperature ramp and final temperature, by no means however does it exhibit enough cohesion for any useful structural applications. Various methods have then been proposed for forming inorganic protective layers on the surface of burning polymers, since inorganic filler particles act through a dilution effect and reduce heat feedback due to large amount of ash [5]. The physical network formed by such additives of high surface area (e.g. aerosil) in the polymer melt also reduces dripping but, on the other hand, significantly restricts the processability of such systems. Similar problems occur when porous fillers like zeolites are used in high concentrations, especially if the average pore size ( $>10$  nm) allows the polymer chains to penetrate [6]. For instance, Mansouri et al. [7] improved the strength of PDMS residue by adding certain inorganic fillers into silicone-based polymers to generate ceramics with good integrity and shape retention after firing at temperatures up to  $1050^{\circ}\text{C}$ . More research described in this review addresses current efforts to improve flame retardant properties of silicone, including addition of fillers, modification of the structure of silicone by incorporation of flame retardant heteroatoms into siloxane backbone, or formulation issues. This review aims at describing most of the recent work related to the applications of silicones as flame retardant agents and/or development in the flame retardation of silicones themselves. Though trying to be as exhaustive as possible, all publications dealing with the flame retardancy of silicone, particularly patents, may not have been quoted here. This review is divided into three main parts. First, the thermal degradation of silicones is discussed, focusing on depolymerization mechanisms, effect of structure, heating conditions, and effect of additives (i.e. less than 5 wt% fillers) on the thermal degradation of silicone. Then, the influence of several types of mineral fillers (in contents up to 80 wt%) as ceramization agents of PDMS is presented. Finally, the introduction of PDMS or functionalized PDMS as flame retardants into other polymers is described.

## 2. Thermal degradation of silicones

### 2.1. Depolymerization

Numerous studies have already established that the differences in degradation behaviour of polysiloxanes result from two main factors: (i) the type and concentration of polymer end-groups and (ii) the presence of catalytic amounts of impurities in the polymer. The depolymerization process is thus a conjunction of three different reaction mechanisms, named “unzipping”, “random scission”, and “externally catalyzed” mechanisms [2].

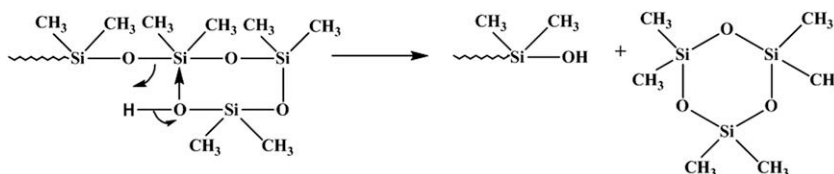
#### 2.1.1. Unzipping reaction

Polysiloxanes containing silanol ( $\text{Si}-\text{OH}$ ) (and to a lower extent hydroxyalkyl  $\text{Si}-\text{R}-\text{OH}$ ) end-groups are principally depolymerized by the “unzipping” mechanism. As the polymer is heated, its viscosimetric molecular weight first sharply increases, which is typical of an intermolecular reaction between the polymer chain-ends through silanol condensation reactions. Further increasing the temperature leads to a decrease of the polymer molecular weight.

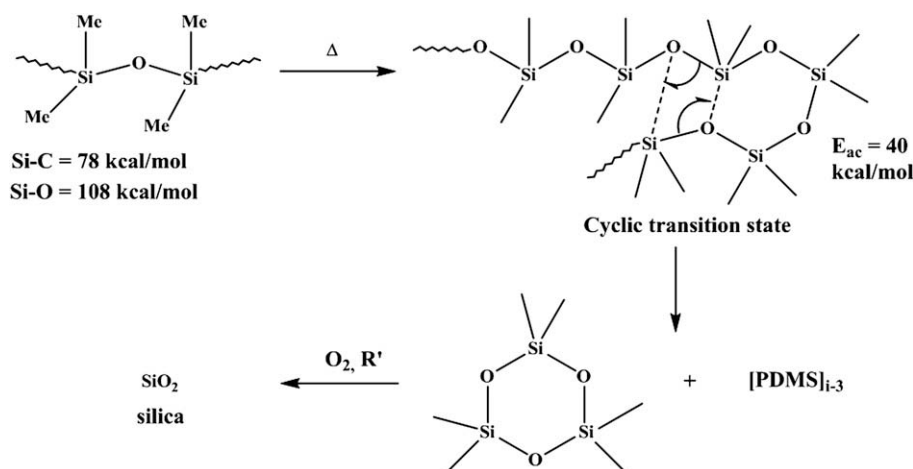
Indeed, silanol functions can ‘back-bite’ to promote intramolecular redistribution reactions which generate low molecular weight cyclic siloxanes, as shown in Scheme 1. Cyclic trimer and tetramer are the most prominent products of this fragmentation because of their thermodynamic stability at the temperatures of degradation. Their evaporation adds an additional driving force for the completion of the degradation process. The decrease in molar mass was found to be linear with the extent of volatilization, confirming the stepwise nature of the formation of volatiles characteristic of the unzipping reaction. The thermally weakest bond in PDMS is the  $\text{C}-\text{Si}$  ( $326\text{ kJ mol}^{-1}$ ) bond, however the cyclic oligomers formed by its decomposition suggest that the  $\text{Si}-\text{O}$  bond ( $451\text{ kJ mol}^{-1}$ ) should break instead. This fact suggests that the depolymerization of PDMS could be governed mainly by the molecular structure and kinetic considerations, and not by bond energies. According to Camino et al. [8] the formation of an intramolecular, cyclic transition state is the rate-determining step. Silicon d-orbital participation was postulated with siloxane bond rearrangement leading to the elimination of cyclic oligomers and shortening of the chain.

#### 2.1.2. Random scission reaction

Polysiloxanes end-capped with inert groups (most likely trimethylsilyl moieties) [2] are degraded either by inter- or intramolecular redistribution reactions that occur randomly between the siloxane bonds of the polymer backbone. The thermal degradation mechanism of PDMS results in the formation of the smallest cyclic product, hexamethylcyclotrisiloxane, as illustrated in Scheme 2. Random scission requires a sufficient flexibility of the polymer chain segments, high polarity of the siloxane bonds, and higher thermodynamic stability of the degradation products than that of the reagents (i.e. open chain macromolecules). This reaction is always possible when polymers are exposed to high enough temperatures. In a clear contrast to unzipping, the random scission mechanism results in a dramatic decrease of polymer molecular weight from the very onset of the degradation and in simultaneous broadening of the molecular weight distribution. Both effects are ascribed to the most probable location for the occurrence of random scission being towards the middle of the polymer chain. The transition state can be formed at any point of the polymer chain, and splitting of PDMS chains proceeds until the residual linear structure is too short to form new cycles and/or the evaporation of the shortened chain fragments favourably competes with cyclization. Thermal oxidation to  $\text{SiO}_2$ ,  $\text{H}_2\text{O}$ ,  $\text{CO}_2$  mostly takes place by reaction in the gas phase between oxygen and volatile cyclic oligomers formed by thermal degradation, the latter increasing smoke opacity. In addition, holes form in the material, which leads to the loss of the integrity of the residue after combustion. Radhakrishnan [9] has evaluated the degradation of hydroxyl- and vinyl-terminated PDMS. Vinyl-terminated PDMS depolymerizes by random decomposition along the chain, whereas hydroxyl-terminated PDMS depolymerizes through its chain-ends as well as by random decomposition, making this latter less stable against thermal degradation. The relative contribution of each process to depolymerization depends on the temperature of degradation (random scission predominates at high temperatures), but also on



Scheme 1. Intramolecular mechanism of degradation of the hydroxyl-terminated PDMS by unzipping reaction.



**Scheme 2.** Depolymerization mechanism of PDMS by random scission.

sample history and pyrolysis conditions. Decomposition products of silanol and vinyl-terminated PDMS at elevated temperatures and under inert atmosphere are principally some cyclic oligomers, with small amounts of methane and traces of linear oligomers (see also part 2.3.1 [9]).

### 2.1.3. Externally catalyzed reaction

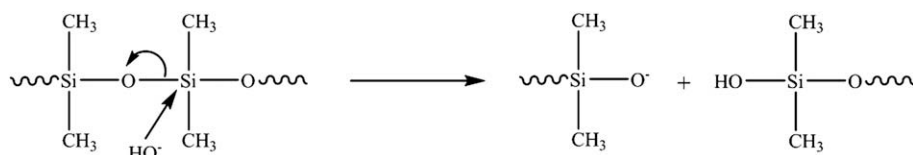
Polysiloxanes which contain ionic, polar impurities or additives, even in very small amounts, are degraded by externally catalyzed mechanism [2]. In contrast to unzipping and random scission, this mechanism involves hydrolytic cleavage of the Si–O backbone bonds by foreign species, which initiate the degradation process as shown in Scheme 3. Like random scission, the extent of the externally catalyzed reaction depends on the nature of polymer end-groups. Such degradation frequently yields unusual by-products (such as methane), which results from reactions between two methyl groups (*vide infra*). In fact, the presence of ionic impurities in polysiloxanes may completely ruin the exceptional thermal properties of PDMS even at moderate temperatures [2]. For instance, Grassie and Macfarlane [10] showed that the presence of traces of KOH (a conventional catalyst of ring opening polymerization or polycondensation) caused an accelerated decomposition of the polymer by forming many short oligomers such as those presented in Scheme 3, accompanied by the formation of siloxy ion.

### 2.2. Oxidative vs. inert degradation

According to Camino et al. [11], the products of the thermal degradation of polydimethylsiloxane (PDMS) are determined by the heating conditions and the nature of the gaseous environment, where two thermal mechanisms of degradation, i.e. molecular and radical mechanisms, are competing.

#### 2.2.1. Molecular mechanism

The molecular mechanism implies Si–O bond scission that takes place at low temperature range and during slow heating, leading to the formation of cyclic oligomers. Camino et al. [8] studied the thermal degradation of PDMS end-blocked with trimethylsiloxy groups at different heating rates. At a slow heating rate of  $1^\circ\text{C min}^{-1}$ , thermal oxidative degradation of PDMS is significantly different from degradation under a nitrogen flow (Fig. 1(a)). In the presence of nitrogen, one step of thermal degradation beginning at  $514^\circ\text{C}$  produces a mixture of oligomers, whereas in presence of air, at least two stages of degradation are observed, the first starting at  $339^\circ\text{C}$  and the second at  $400^\circ\text{C}$ . In both steps the major degradation products are similar to those produced in inert atmosphere, i.e. composed of various oligomers, but with additional  $\text{CO}_2$  and water. In this case as well, finely divided silica powder appears at  $500^\circ\text{C}$  for a final residue around 60%. The two-step process can be explained by assuming that oxygen catalyzes the depolymerization of PDMS to volatile cyclic oligomers, leading to a temperature of initial weight loss lower ( $290^\circ\text{C}$ ) than that observed in nitrogen ( $400^\circ\text{C}$ ). This process competes with oxidative crosslinking which stabilizes the material. Further decomposition to cyclic oligomers occurs above  $400^\circ\text{C}$ , as in nitrogen, although accelerated by competing oxidation. Interaction of oxygen with the degrading condensed phase depends on a complex competition between oxygen diffusion and solubility, on one hand, and degradation reaction and product evaporation on the other hand. At a higher heating rate of  $50^\circ\text{C min}^{-1}$ , weight loss shifts to a higher temperature both in nitrogen and in air (Fig. 1(b)) and the final silica residue decreases to 10%. At this rate, chemical reactions start to occur at higher temperatures than before, where the solubility of oxygen in the condensed phase decreases and the rate of thermal degradation reactions increases, making the heterogeneous phase reaction of active species with oxygen less probable. The first step of weight loss in air overlaps with the second, while stabilization



**Scheme 3.** Degradation of PDMS by externally catalyzed mechanism (here provoked by a hydroxyl anion).

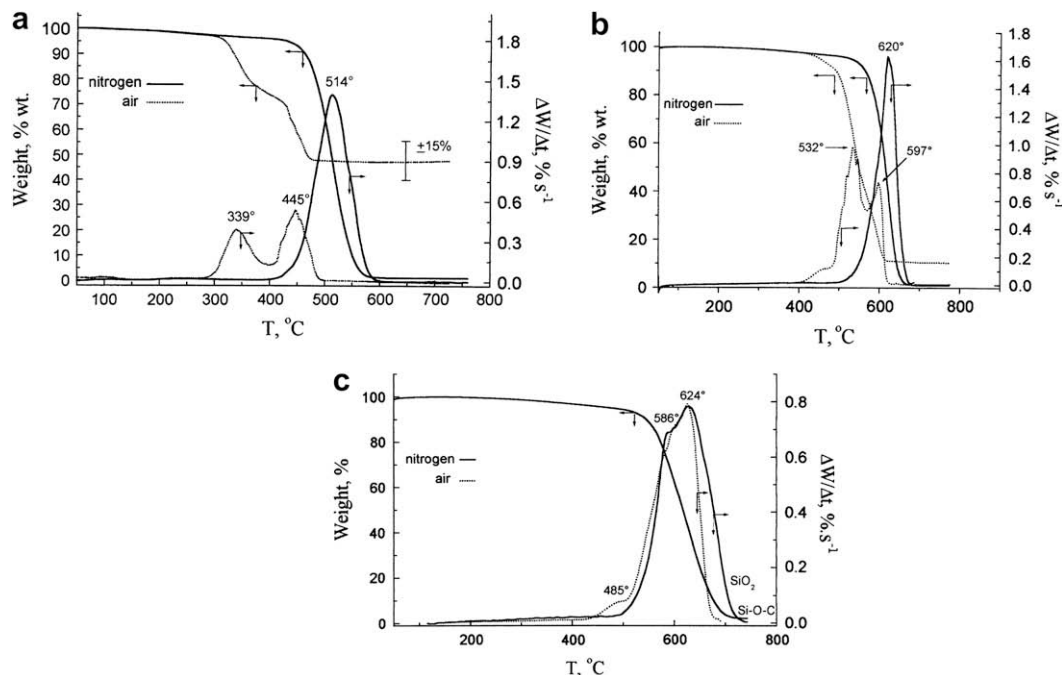


Fig. 1. TG and DTG curves of PDMS in nitrogen (solid line) and in air (dotted line) at a heating rate of (a) 1 °C min<sup>-1</sup>, (b) 50 °C min<sup>-1</sup>, and (c) 100 °C min<sup>-1</sup> [8].

induced by oxidative crosslinking takes place. Finally, at a heating rate of 100 °C min<sup>-1</sup>, thermal degradation behaviour of PDMS in nitrogen and in air tends to overlap. In nitrogen fluxed degradation, a small amount (4%) of a black residue (e.g. silicon carbide or oxycarbide) was observed at 700–800 °C (Fig. 1(c)). In thermo-oxidative degradation, such black stable residue was difficult to detect in an overwhelming amount of white silica. Here, the thermal decomposition is strongly reduced due to the low rate of reaction between the material and oxygen, low oxygen solubility and high thermal degradation rate. The direct reaction of oxygen with the condensed phase either does not take place or at a limited extent. Another study by Camino et al. [11] showed that the heating rate influences the nature of volatile products formed during the thermal degradation of PDMS in helium or in air. At a slow heating rate of 10 °C min<sup>-1</sup>, cyclic oligomers, with trimer as primary product, were exclusively formed. Whereas at fast heating rate (80 °C min<sup>-1</sup> up to 800 °C, also called “flash pyrolysis”), formation of cyclic oligomers, tetramer being the most abundant one, was accompanied by the generation of linear pentasiloxane or rearranged oligomeric siloxane compounds (e.g. tetrasiloxane, 3,5-diethoxy-1,1,1,7,7,7-hexamethyl-3,5-bis(trimethylsiloxy)).

#### 2.2.2. Radical mechanism

The radical mechanism occurs through homolytic Si–CH<sub>3</sub> bonds scission, which prevails at high temperatures and results in oligomers and methane release (Scheme 4). Cross-linking of the macroradicals by coupling of radicals I and II decreases the flexibility of the PDMS chain and hinders further splitting of cyclic oligomers. The thermal stability of this heavily crosslinked PDMS increases

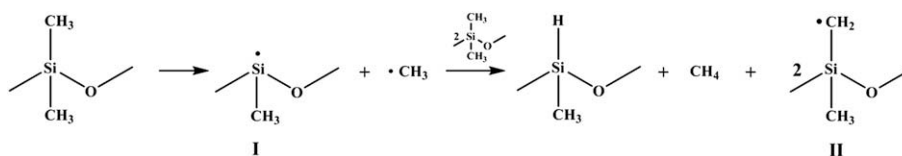
and reorganization of atomic bonds can take place with formation of black ceramic silicon-oxycarbide.

#### 2.3. Structure/degradation relationship

From the different thermal degradation pathways presented above, it is anticipated that certain types of polysiloxanes will display higher thermal resistance than others. The chemical nature of polymer functional groups (either at the end or inside the chain) as well as their molecular weight has been shown to influence the degradation of PDMS significantly.

##### 2.3.1. Influence of end-groups

As briefly depicted above, Grassie and Macfarlane [10] showed that hydroxyl end-groups lower the thermal stability of PDMS considerably compared to vinyl or methyl end-groups because of “back-biting” reactions. The product of degradation of pure hydroxyl-terminated PDMS is a mixture of cyclic oligomers with the trimer predominating and steadily decreasing amounts of tetramer, pentamer, etc. Grassie and Macfarlane [10] also reported that the replacement of hydroxyl end-groups by methyl enhances the thermal stability of PDMS considerably whereas no change in the distribution of by-products was observed. Jovanovic et al. [13] suggested that vinyl end-groups, as compared to methyl, change the degradation mechanism of the polysiloxanes. Introduction of vinyl end-groups decreases the thermal stability and thermo-oxidative stability of PDMS by reducing the amount of degradation residue in comparison with methyl end-groups. Later on, Radhakrishnan [9] reported that the decomposition products of



Scheme 4. Proposed radical mechanism in silicone thermal degradation.

vinyl-terminated PDMS at elevated temperatures are principally cyclic oligomers, with small amounts of methane and traces of linear oligomers. This conclusion was also supported by Deshpande and Rezac [12] who reported that the decomposition products of vinyl-terminated PDMS at 364 °C are principally the cyclic oligomers, hexamethyltrisiloxane (trimer) and octamethyltetrasiloxane (tetramer).

### 2.3.2. Influence of side-groups

Jovanovic et al. [13] found that the introduction of methylhydrosiloxy units in the polysiloxane backbone decreases their thermal stability in comparison to the dimethylsiloxy units. PDMS is thermo-oxidatively more stable than Si–H based homo- or copolymers, i.e. degradation starts at lower temperatures for these latter. On the other hand, the final content of residue is always larger for the SiH-based copolymers, presumably because cross-linking reactions occur both in air and under nitrogen. In contrast, substituting methyl by vinyl groups in the PDMS backbone decreases the weight loss after thermal degradation. Grassie and Macfarlane [10] studied the effect of incorporating phenyl groups into siloxane backbone. PDMS is naturally stable in vacuum until approximately 340 °C; the introduction of a small amount of methylphenylsiloxane or diphenylsiloxane into a PDMS skeleton can increase the onset temperature up to 400 °C [14]. Grassie et al. [15] measured both the onset temperature of thermal degradation and residue content of PDMS containing phenyl groups, and showed a neat, direct correlation between increasing phenyl content and final weight of residue. The products of degradation of poly(dimethyl/diphenyl siloxane) are benzene and complex mixtures of cyclic oligomers. Deshpande and Rezac [12] confirmed that the degradation of poly(diphenyl-dimethyl)siloxane resulted in the release of benzene in the initial stages of the reaction whereas no cyclic oligomers were traced.

### 2.3.3. Influence of molecular weight

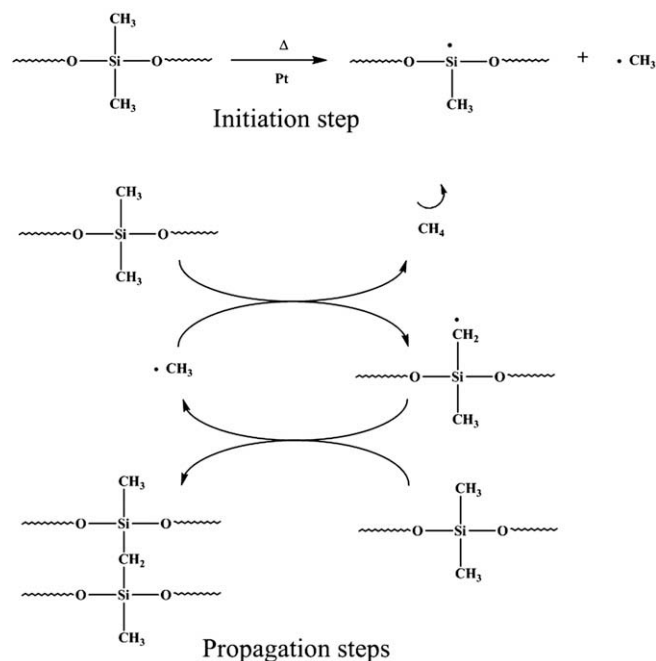
Connell et al. [16] found that as the length of the siloxane chain is increased, the time to ignition in a cone calorimetry test decreases because the amount of combustible hydrocarbon in the samples increases with increasing chain length. Grassie et al. [15] showed that the amount of residue is strictly proportional to the polymer molecular weight.

## 2.4. Effects of additives

We consider in this part all types of compounds that have been introduced in a silicone formulation at less than 5 wt%.

### 2.4.1. Platinum compounds

Addition of a conventional hydrosilylation catalyst, i.e. platinum (0)-1,3-divinyl-1,1,3,3-tetramethyldisiloxane, into silicone rubber improves its fire retardancy uniquely [17]. Indeed, only a few ppm are a priori sufficient to dramatically modify the burning behaviour of silicone, in contrast to ordinary flame retardants whose contents are generally of about 10% or more. It has been found that cross-linking reactions of various polymer materials during their thermal degradation are closely related to their efficient flame retardancy. During the thermal treatment at around 400–500 °C, the platinum compound induces the cleavage of methyl–silicon bonds in silicone rubber and radical coupling that leads to the formation of cross-linking points (Scheme 5). This radical mechanism is initiated by Pt-catalyzed homolytic breaking of Si–CH<sub>3</sub> bond to produce a methyl and a silyl radicals, the former which abstracts hydrogen from another methyl group to yield methane and a radical methylene grafted on the chain siloxane. Finally, this macroradical attacks an adjacent polymer chain inducing a meso-cross-linking of the



**Scheme 5.** Pathway for the methylene-bridge structure formation induced by platinum-catalysed radical chain-reaction.

matrix. According to Lagarde et al. [18], the action of Pt as flame retardant in PDMS occurs by preventing the formation of the complex of transition which supports the backbiting degradation of the polysiloxanes. Pt thus limits the quantity of condensates formed. Smith [19] used platinum or a platinum compound to improve flame retardancy of polyorganosiloxane foams used in coating applications or protective filling, wherein fire retarding is important. The flame retardancy can be further improved by addition of 0.2 wt% of carbon black: the foams are self-extinguishing in short times without releasing toxic fumes during combustion.

### 2.4.2. Transition metal oxides

Transition metal oxides such as FeO, Fe<sub>2</sub>O<sub>3</sub>, CeO, TiO<sub>2</sub>, etc or a mixture of two or more were used by Fujiki and Tanaka [20] to impart high-temperature resistance to silicone as coating and air-bag-based material. A thickness of 5–20 μm of this silicone was used for coating materials, such as polyamide fibres, polyester fibres, polyurethane sheets and so on. Silicone rubbers filled with titanium dioxide as heat resistant additive showed deteriorated mechanical and electrical properties when immersed in water. Even mixtures of platinum and fumed titanium compounds incorporated in silicone rubber did not improve their flame retardant properties when heated or exposed to moisture [21]. Therefore, Hatanaka et al. [21] proposed to use platinum and titanium dioxides treated with an organosilane or an organosiloxane in silicone rubber. The treated titanium dioxide imparted more efficient flame retardancy at smaller amount than the original untreated titanium dioxide. Even after a prolonged exposure to the atmosphere, the electrical and mechanical properties (including high elasticity) as well as the flame retardancy of the resulting silicone rubbers were not adversely affected. They suggested use of surface modified TiO<sub>2</sub> having an average particle size of less than 0.1 μm at composition of 1–20 phr (parts per hundred) loading levels. Noteworthy, they reported that an excessive use of TiO<sub>2</sub> decreased the mechanical properties, especially the tensile strength, of the resulting silicone rubber and increased its tendency





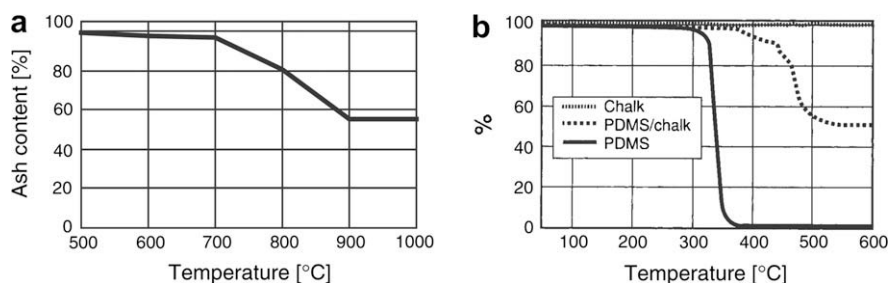


**Fig. 3.** TGA in technical air of (a) chalk between 500 and 1000 °C (10 °C min<sup>-1</sup>); (b) PDMS, chalk and a model mixture (30/70 wt%) of chalk and PDMS between 50 and 600 °C (10 °C min<sup>-1</sup>) [44].

[33]. More details about flame retardancy of several inorganic fillers in PDMS are discussed in this part.

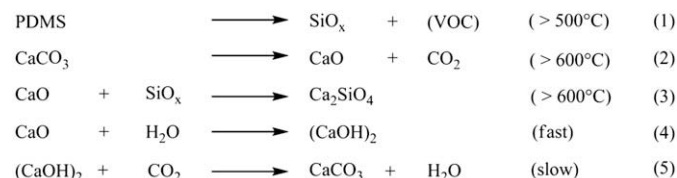
### 3.1. Silica particles

Silica is the most common filler introduced in PDMS because of its reinforcing effect [34,35] induced by hydrogen bonding between oxygen of Si–O–Si in PDMS chain and hydrogen of silanol groups on the surface of silica [36]. As a component of flame retardant systems material, silica has been applied to several polymers such as polypropylene, poly(methyl methacrylate) (PMMA), epoxy resin, poly(ethylene-co-vinyl acetate) (EVA), butadiene–acrylonitrile rubbers, and of course, PDMS. The thermal decomposition of PDMS [37] is greatly enhanced by the physically absorbed and chemically combined water on the silica surface, whose release at high temperature catalyses the decomposition of PDMS by hydrolyzing the siloxane chain. This defect can be strongly reduced, even suppressed by surface treatment of silica before incorporating it into PDMS. The deposition of amorphous silica ash (a major combustion product of silicones) on the fuel surface is believed to play a significant role in mediating the fuel formation rate in silicone in fires. Some studies have reported some improved flame retardancy due to silica in PDMS with emphasis on techniques used to incorporate the silica, the effect of different sizes or different types of silica, etc. The flame retardant effectiveness and mechanism of silica is based on specific physical processes in the condensed phase rather than chemical reactions, as proven by Kashiwagi et al. [38]. The balance between the density and the surface area of the additive and polymer melt viscosity determines whether the additive accumulates near the sample surface or sinks through the polymer melt layer. From the synthesis point of view, elastomeric networks of poly(dimethyl siloxane) (PDMS) reinforced with silica particles can be prepared by different manners. Yuan and Mark [36] have reported that silica can be generated in situ through the hydrolysis and condensation of the precursor tetraethoxysilane (TEOS), as described in Scheme 6. They found that the in situ precipitation technique could control the size and size distribution and provides better dispersion of filler particles throughout polymer matrices and stronger polymer–filler interactions. Tanahashi et al. [39] made use of this new and simple method for the dispersion of ultrafine silica particles into thermoplastic resin by mechanical methods without any surface modification of dispersed fillers or any organic reactions. A clear advantage of this method is a good nanodispersion of silica particles in various polymer compositions regardless of the degree of chemical affinity between the dispersed silica and matrix resin and without complicated chemical reactions at the organic–inorganic interface. Later on, Liu and Li [40] prepared a hybrid material which silica core is surrounded by PDMS arms. Nanosilica-cored star polymers were prepared by grafting monoglycidylether-terminated

polydimethylsiloxane (PDMS-G) onto nanosilica particles. The moderate grafting yield of 50–60% was ascribed to steric hindrance from the growing shell of PDMS. The organic layer thus generated is able to separate the silica particles from each others and to prevent particle aggregation. They showed that this star PDMS/silica hybrid could effectively increase the thermal stability and char formation of the grafted PDMS arms in comparison to the starting PDMS arm (Fig. 2). The authors finally noted that the synthesis employed here could be applied to prepare other star polymers from nanosilica cores.

### 3.2. Calcium carbonate

Calcium carbonate has been extensively employed as a filler in polymer composites, because of its several remarkable benefits such as abundant raw material resource, low price, and stable properties. Several types of calcium carbonates, such as natural calcium carbonates or precipitated calcium carbonate, have been introduced in different proportions as fillers in PVC (65%), polyester (20%), polyolefins (5%), etc [41]. Recently, Deodhar et al. [42] used calcium carbonate nanoparticles (70 nm) as flame retardant agent in PP. Calcium carbonate in the silicone industry was mainly used in sealant formulations [43]. Chalk is a natural calcium carbonate whose thermal stability and degradation were studied by Hermansson et al. [44]. Chalk action as flame retardant starts at high temperature by releasing CO<sub>2</sub> gas and by providing an endothermic effect inside the matrix. The weight loss starts slowly from 500 °C and remains constant above 900 °C, finally providing a residue of 56 wt%. The content of residue correlates well with the theoretical value when all CaCO<sub>3</sub> has been transformed into CaO (Fig. 3(a)). According to Hermansson et al. [44], chalk has a positive effect on silicone elastomers, because it neutralizes acidic residues remaining from polymerization processes, which are otherwise destructive for the elastomer. TG curves typically show enhancement of thermal stability of silicone by addition of chalk (Fig. 3(b)). PDMS degrades around 300 °C, whereas when mixed with chalk, some residue remains in samples treated at 500 °C. The silicone elastomer stabilized by chalk thus survives at higher temperatures in addition to taking an active part in the formation of the intumescent structure. After treatment at 500 °C, the intumescent structure consists of calcium carbonate and silicon oxides. At higher



**Scheme 7.** Successive reactions in the degradation of chalk-filled silicone elastomers.



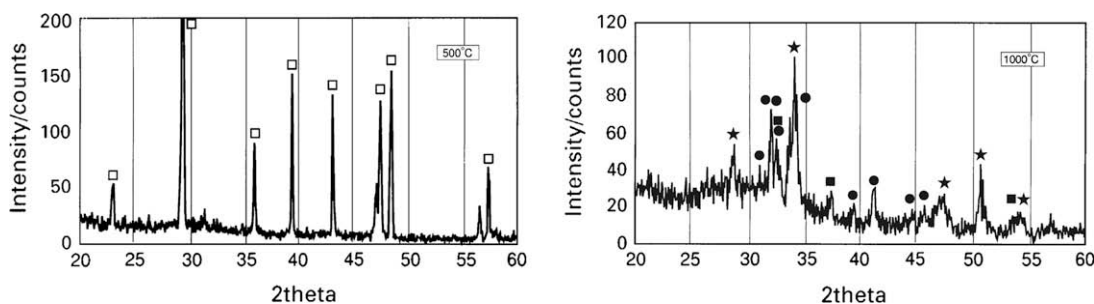


Fig. 4. XRD diffractograms of chalk:silicone flame retardant system embedded in a matrix polymer treated at 500 °C and 1000 °C respectively (1 h, air) and expected peaks for (□)  $\text{CaCO}_3$ ; (●)  $\text{Ca}_2\text{SiO}_4$ ; (★)  $\text{Ca(OH)}_2$ ; (■)  $\text{CaO}$  [44].

temperatures, calcium silicate ( $\text{Ca}_2\text{SiO}_4$ ) forms through a sintering reaction between calcium oxide ( $\text{CaO}$ ), formed from the degradation of chalk, and silicon oxides as shown in Scheme 7. The formation of  $\text{CaO}$ ,  $\text{Ca(OH)}_2$  and  $\text{Ca}_2\text{SiO}_4$  explains the presence of calcium, oxygen and silicon in the fired sample treated at 1000 °C as shown by XRD analysis (Fig. 4). Therefore, flame retarding action of calcium carbonate seems identical to those of metal hydroxides with a decomposition temperature range shifted toward higher temperatures. In a silicone matrix, calcium carbonate releases  $\text{CO}_2$  and  $\text{H}_2\text{O}$  gases during combustion that cool the polymer substrate and in the same time dilute flammable gases available for burning in the vapour phase. Therefore the heat feedback to the polymer substrate is reduced and in turn the emission of flammable gases decreases. Moreover, calcium carbonate contributes to the constitution of a mineral or ceramic-like calcium silicate residue after degradation which acts as flame retardant by barrier effect [44].

### 3.3. Wollastonite

Wollastonite, also known as calcium metasilicate, is a naturally occurring mineral. It consists of pure white, non-hydrated needle-shaped crystals. The particle lengths are typically larger than the widths by a factor of between one and two, but the aspect ratio (diameter divided by thickness) can be much higher, up to 15. Consequently, wollastonite reinforcing property can compete with or partially replace other reinforcing fillers and fibres as its cost is competitive [45]. Wollastonite is used in composites to increase mechanical properties such as tensile, flexural, and impact strengths, as well as to increase dimensional stability and minimize distortion at elevated temperatures. Park [46] reported the use of non-treated wollastonite and surface-treated wollastonite with 3-aminopropyl triethoxysilane (APTS) or allyltrimethoxysilane (ATMS) to improve mechanical properties of silicone rubber. Incorporation of 10 wt% of wollastonite into compression-moulded silicone rubber decreased tensile strength, increased tear strength, and decreased elongation at break. Lower values of tensile strength and elongation at break are a consequence of weaker adhesion. An increase in weight percentage of filler reduced the deformability of the matrix, and, in turn, reduced also the ductility in the skin area so that the composite tended to form a weak structure. In contrast, the silane treated wollastonite composites developed higher tensile strength than untreated composites and a significant improvement in tear strength. Silane coupling agents are predominately used as mediators, binding organic materials to inorganic materials. These react with the silanols on the filler surface through a covalent bond, whereas the allyl functional group bonds to the rubber during vulcanization; the case of aminosilanes may however be more complex and its action is not fully understood yet. Filler–polymer bonding helps to increase tensile strength and to improve other compound properties such as higher strength and abrasion

resistance. Application of wollastonite as flame retardants in PDMS has also been patented by several authors. Nicholson et al. [47] from Dow Corning Corporation incorporated 21.1 wt% of wollastonite into 66.4 wt% of dimethylvinylsiloxane terminated dimethyl siloxane to obtain a cured silicone foam exhibiting high flame resistance and forming hard ceramized char with few cracks on burning. The form of wollastonite used was a needle-like shape with particle size from about 5–15  $\mu\text{m}$  and aspect ratio 15:1. Compositions with <1 wt% wollastonite did not exhibit char formation or low heat release rate, but if wollastonite content >60 wt%, uncured compositions were too stiff, and therefore difficult to process, and did not blow into uniform foams. Moreover, for wire and cable coating applications, Shephard [48] from Dow Corning proposed a curable silicone composition, made by mixing ingredients comprising: 30–90 wt% of a heat-curable non-halogenated organosiloxane polymer, containing at least 2 alkenyl groups per molecule, 1–65 wt% of a reinforcing silica filler, 5–70 wt% of wollastonite having an average particle size of 2–30  $\mu\text{m}$  and aspect ratio of at least 3:1, and curing component sufficient to cure the composition (a peroxide catalyst). Addition of 38.7 wt% wollastonite into silicone resulted in a tough resinous char with few surface cracks and high surface integrity while sample containing 8 wt% amorphous silica and 60 wt% wollastonite resulted in hard and resinous char structure with no vertical expansion; in the latter case, the weight loss was only 6 wt% and the fire did not penetrate through the 1/4" thick sample. Substitution of a part of wollastonite with diatomaceous earth (5  $\mu\text{m}$ ) resulted in a self-extinguishing material with a hard and resinous char structure and a weight loss of only 8 wt%. High consistency rubbers were systematically formulated for plenum

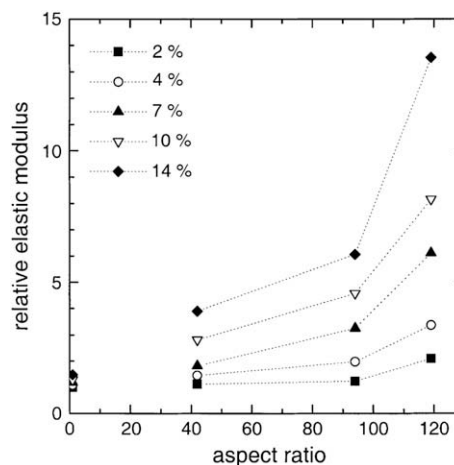
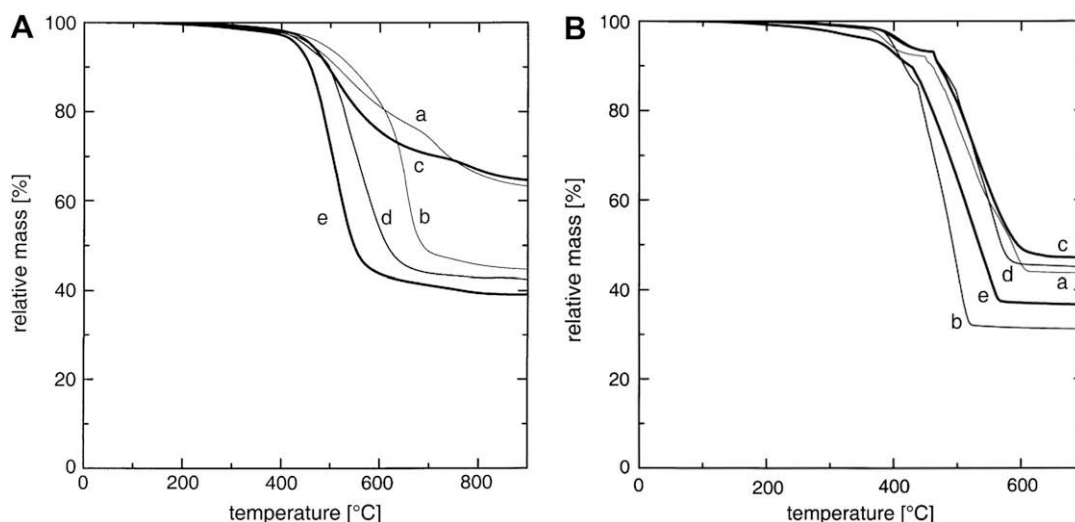


Fig. 5. Dependence of the relative elastic modulus on the aspect ratio (diameter divided by thickness) of the filler particles at different loading levels (vol%) [51].



**Fig. 6.** TG traces of PDMS composites at 10 vol% filler under nitrogen (A) and air (B) at heating rate of  $20\text{ }^{\circ}\text{C min}^{-1}$ : (a) unfilled PDMS, (b) spherigglass with aspect ratio 1, (c) mica with aspect ratio 42, (d) mica with aspect ratio 94, and (e) mica fines with aspect ratio 119 [51].

cable coatings with different sizes of wollastonite. A sample containing wollastonite with an average particle size of  $12\text{ }\mu\text{m}$  and a particle size range of  $1\text{--}393\text{ }\mu\text{m}$  was compared with a sample containing wollastonite with an average particle size of  $10\text{ }\mu\text{m}$ , and a particle size range of  $1\text{--}119\text{ }\mu\text{m}$ . Both samples showed very similar HRR peaks without significant difference in the char structures of the two materials [48]. Compositions with less than about 5 wt% of wollastonite did not exhibit the char formation and low heat release rate of the present invention. The upper limit of wollastonite that is useful would depend on the properties desired in the uncured and cured compositions. Generally, wollastonite present at greater quantity than about 70 wt% resulted in uncured compositions that are too stiff and therefore difficult to process, and in cured compositions that have reduced tensile strength and elongation. George et al. [49] used modified wollastonite (with functional alkoxysilanes) to improve flame retardant of PDMS by adding 3.5 wt% of wollastonite into 65 wt% of dimethylvinylsiloxyl terminated dimethyl siloxane. The matrix also contained other fillers such as silica, mica,  $\text{TiO}_2$  and other additives. This formulation resulted in a ceramized char with good cohesivity that is required for cable application.

### 3.4. Mica

#### 3.4.1. Structure and reinforcing effect of mica

Mica [50] corresponds to a group of aluminosilicate minerals characterized by a layered structure which can be cleaved to give thin, flexible sheets. The two most common classes of commercially available mica are muscovite and phlogopite. Muscovite mica is a 2:1 layered aluminosilicate (ideal formula  $\text{KAl}_2(\text{Si}_3\text{Al})\text{O}_{10}(\text{OH})_2$ ). Each 2:1 layer consists of two tetrahedral silica sheets sandwiching an alumina octahedral sheet of about 1 nm thick. Since on average, one Si atom out of four in the tetrahedral sheets is replaced by Al, the layers are negatively charged. These charges are compensated by interlayer cations, mostly potassium, and the layers are held together in stacks by electrostatic and Van der Waals forces. Phlogopite mica is a trioctahedral alkali aluminium silicate ( $\text{KMg}_3(\text{Si}_3\text{Al})\text{O}_{10}(\text{OH})_2$ ). Phlogopite has a layered structure of magnesium aluminium silicate sheets weakly bonded together by layers of potassium ions. Both mica types are typically present in the form of thin plates or flakes with sharply defined edges. Mica is chemically inert and is stable to about  $600\text{ }^{\circ}\text{C}$  where

dehydroxylation takes place. The key characteristic of mica as a filler for plastics is its ability to be processed to give thin and plate-shaped particles, with aspect ratios higher than for any other minerals. The aspect ratio of the final flakes depends upon the origin of the mica and the processing method, designed to achieve a high aspect ratio while keeping undamaged flat flakes. This ideal becomes increasingly difficult with decreasing particle size. For certain applications, mica needs surface treatment, among which silane coating is the most popular technique. Indeed, hydroxyl groups on the mica surface are well suited to react with the silanol groups of hydrolyzed silanes. It should be noted here that uncoated mica gives adequate interaction with polar resins such as thermoplastic polyesters and polyamides, so that the additional benefits of silane coating are rarely worth the extra cost, and even in non-polar resins, most applications do not justify the additional expense of silane surface treatment. Taking into account compounding costs, mica filled compounds are generally more expensive than the unfilled resin. Consequently, mica is not viewed as a cost-saving filler, but rather as a means to modify mechanical properties. Mica affects some properties such as stiffness, dimensional stability, flexural, tensile, and impact strengths. Only glass fibre rivals on the high aspect ratio of mica as a tool in stiffening polymer compounds. Osman et al. [51] reported the reinforcing effect of mica to silicone network. The elastic modulus of PDMS networks was dramatically increased by the incorporation of plate-like particles such as mica. The modulus enhancement depends on the aspect ratio and volume fraction of the particles (agglomerates or primary particles), as well as on their distribution in the matrix. They showed that at the same loading level, mica with higher aspect ratio increased dramatically the reinforcing effect on PDMS composite (Fig. 5). At all loading levels, mica is uniformly distributed in the PDMS matrix, except in the 14 vol% of high aspect ratio (119) mica composite. This is probably due to the attractions between the platelets which seem to increase with increasing interfacial area and decreasing inter-particle distance, so that the fine mica particles tend to agglomerate above 10 vol%.

#### 3.4.2. Thermal degradation of mica/silicone elastomers

Mica is one of the most popular flame retardant fillers in silicone polymer especially for electric cable applications, both from the electrical and the mechanical points of view. Osman et al. [51] reported that the thermal degradation of PDMS composites was

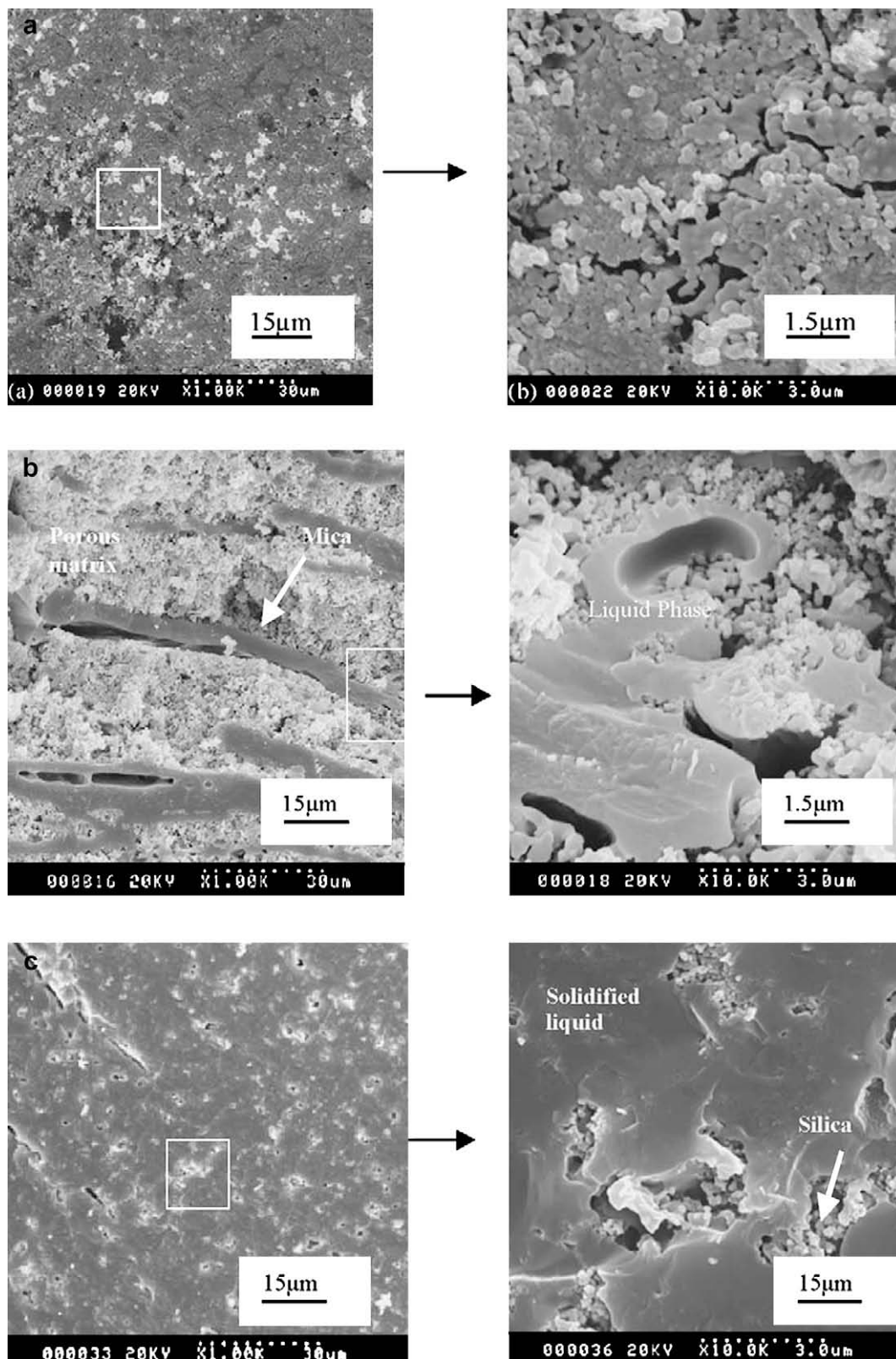


Fig. 7. SEM micrographs of (a) silicone, (b) silicone filled with coarse grade mica, and (c) silicone filled with fine grade mica after firing at 1100 °C at heating rate 10 °C min<sup>-1</sup> [53].

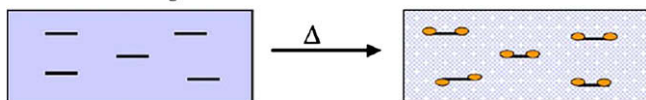
increased by increasing the aspect ratio of mica (Fig. 6). The weight loss of the 10 vol% composites under nitrogen atmosphere showed that mica with high aspect ratio strongly enhanced the amount of residue, while mica with small aspect ratio did not. The oxidative

degradation of the same composites showed that only the mica with high aspect ratio enhanced the oxidation of PDMS. Note that the unfilled PDMS was extraordinary stable under these thermal conditions, a result which let us think that other fire retardant



additives are present in the sample. Also, mica is able to form a ceramized residue in silicone composite after pyrolysis at high temperature. Hanu et al. [52] reported that addition of 20 wt% of mica with average particle size 110  $\mu\text{m}$  into silicone increased residue yield from 54% to 63% in comparison to pristine PDMS, while smaller mica (20  $\mu\text{m}$ ) increased residue yield to 60%. This residue showed a ceramized structure as sought in electrical cable application. They suggested that the formation of this ceramized residue was due to the reaction between inorganic fillers and the silica issued from the decomposed polymer matrix, which formed a eutectic liquid phase at the edges of the fillers able to penetrate into matrix region. The extent of eutectic formation was shown to be influenced by factors such as particle size and chemical composition of the fillers. The size of muscovite particles in silicone-based composites was shown to have significant effects on the orientation of the particles, on the tensile properties of polymer composites and on the strength of resultant ceramics. Therefore, Hanu et al. [53] used coarse and fine grade muscovite mica as fillers in PDMS, with average particle sizes 95  $\mu\text{m}$  and 7  $\mu\text{m}$  respectively. They found that, at 20 wt% loading levels of mica in silicone, the strength of ceramic formed through high temperature pyrolysis of polymer composites was improved with increased amount of eutectic liquid and particle size, as observed in SEM studies with an improvement in the ultimate strength of the ceramic residue (Fig. 7). The residue of fired silicone polymer is highly porous and contains micro-cracks (Fig. 7(a)). There is some evidence of solidification of silica particles, but the amount of liquid is too low to produce a strong char after firing at 1100  $^{\circ}\text{C}$ . Addition of coarse muscovite to silicone polymer resulted in a stronger residue after firing and a higher resistance to heat distortion with shrinkage reduction (around 50%, Fig. 7(b)). On firing at 1100  $^{\circ}\text{C}$ , a eutectic reaction took place between the coarse muscovite and the silica matrix, but the temperature was not high enough to melt the entire muscovite particle. Instead, it produced a liquid phase around the surface of the muscovite particles. Overall, in sample containing coarse mica, the preferential orientation and the low surface area of the muscovite particles left many silica regions poorly infiltrated by the liquid phase and thus weakly bonded. Hanu et al. schematized the effect of filler particle size on the strength of the samples after firing (Fig. 8). With a reduction in filler particle size and the same volume percentage of filler, reduced inter-particle distance and higher surface area of filler resulted in an increased amount of reactivity of the filler particles and a greater amount of eutectic liquid being formed. The increased amount of liquid led to a higher strength ceramic material and greater observed shrinkage after firing (Fig. 7(c)). Mansouri et al. [7] have studied the mechanism of ceramization structure of mica-PDMS composite after firing at 1050  $^{\circ}\text{C}$ . 20 wt% mica flake (muscovite) with particle size 114  $\mu\text{m}$  was added into a silicone gum containing 40 wt% silica with particle sizes between 20 and 40 nm and 1.44 g dicumyl peroxide

**Silicone + Coarse grade mica**



**Silicone + Fine grade mica**

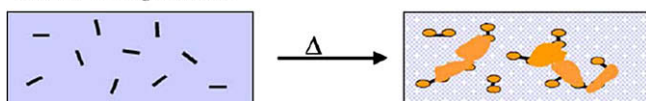


**Fig. 8.** Influence of muscovite particle size and preferential orientation within the polymer matrix on the sintering and solidification of ceramic composites [53].

(DCP) for cable formulation. This cable was fired in air to 1050  $^{\circ}\text{C}$  for 30 min, then sprayed with a water jet (fire test conditions for cables according to Australian Standard, AS/NZS3013:1995). Upon firing, the cable formed a coherent and strong ceramic with no visible cracks, thus able to withstand small mechanical shocks from the water spray applied at the end of firing. The inner and outer surfaces of cable were observed by SEM: on the outside, the shape of mica plates at the edges was clearly altered after heating to 1050  $^{\circ}\text{C}$  (Fig. 9(a,b)) whereas the inner surface in contact with the copper conductor, has formed a more liquid phase and micro-bridges

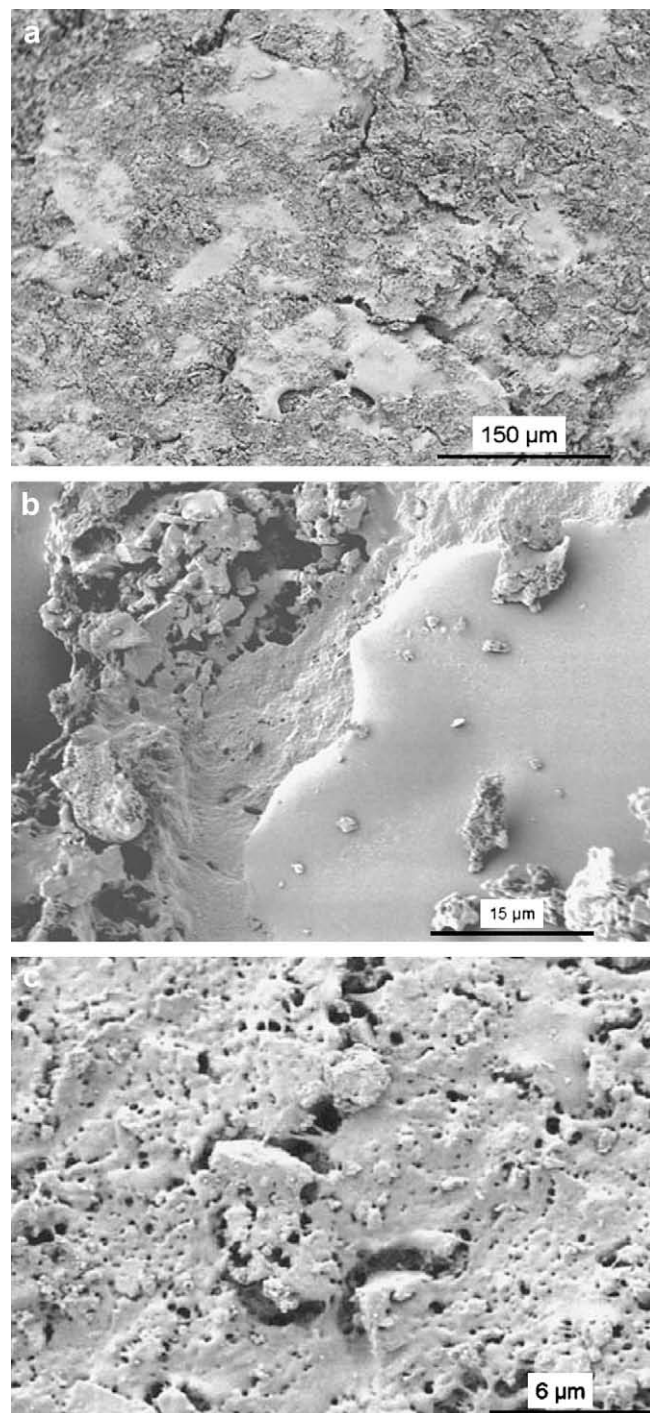


**Fig. 9.** Scanning electron micrographs of (a, b) the outer surface of the cable at different magnifications, (c) the inner side of the cable after fire test [7].

responsible for the strength of the residue (Fig. 9(c)). They showed that edge melting and joining of mica plates after firing at 1050 °C result from eutectic reactions at the interfaces between the mica particles and silica formed from decomposition of the silicone polymer matrix. Ordinarily, silicon dioxide and mica each have melting points well above 1050 °C. However, when mica decomposes and reacts with silica on heating, an eutectic can form at the interface around 900 °C. This eutectic liquid is believed to infiltrate the silica matrix and so acts as a bridge between the silicone dioxide particles and the mica particles, giving a coherent structure at the firing temperature. The presence of micro-bridge filling pores with regions up to 5–10 µm thick is believed to improve ash strength. The weight loss of mica occurred when temperature rose from 600 to 900 °C due to dehydration and decomposition of mica. As a result, muscovite-filled silicone offers some improvement in fire performance in terms of both time to ignition and rate of heat release when compared to muscovite-unfilled silicone. Upon addition of muscovite, the TTI is increased from 75 to 92 s and the peak rate of heat release is decreased from 144 to 98 kW m<sup>-2</sup>. Latter on, Mansouri et al. [54] studied the pyrolysis behaviour of silicone–mica composites. They observed the presence of skin formation and preferential positioning of silica on the surface. These effects were more pronounced at higher temperatures. Either silica has diffused into the surface upon firing and has formed a skin layer upon cooling, as suggested by the authors, and/or silica formed preferentially at the surface where oxygen is present. Silica from silicone decomposition (mainly fumed silica) has a large surface area (high pore volume) and low density, tending to accumulate near the surface without sinking through the polymer melt layer during the burning process. Samples fired at 1000 °C showed continuous skin formation richer in silicon (30–40 wt%) than that for the sample fired at 600 °C (20–25 wt%). At lower firing temperature (600 °C), eutectic reaction occurred between the product of pyrolysis (silica) and filler to form a compact powder with no or limited binding whereas at higher firing temperature (1000 °C), mica flakes melted at the edges and diffused into the matrix, and pyrolysis products acted as a binder to join the mica plates together.

### 3.4.3. Effect of additives + mica on ceramization

Mansouri et al. [54] suggested that the addition of certain inorganic materials to the mica–silicone composite could produce a liquid phase at lower temperature to facilitate the formation of a strong ceramic. Among inorganic materials that are commonly used to improve the ceramization of the residue resulting from silicone–mica composite fire burning, one finds glass frits, zinc oxide, ferric oxide, and zinc borate. Ariagno et al. [55] have proposed the formulation of a heat-vulcanisable silicone elastomer which is well adapted for conversion into mechanically strong flame-retardant protective sheathings/coatings for, e.g., electrical wires and cables. This formulation comprises at least one polydiorganosiloxane polymer containing a fireproofing and mechanical strength-enhancing amount of mica and ZnO. They found that mica has synergistic effect with zinc oxide in obtaining silicone elastomers with good mechanical properties, mainly elongation at break (at least 180%) and better ceramized residue. They observed that the composite containing only ZnO has fragile residue and cracks. Therefore, they proposed to use the composition containing about 1.5–15 wt% mica and 0.5–5 wt% of ZnO in order to obtain a good ceramized residue. They noted that incorporation of both fillers may not exceed 40 wt%. Branlard et al. [56] from Rhodia disclosed mica in the silicone elastomer composition for making electric wires or cables displaying an enhanced reaction to fire. These silicone elastomers contained 8–30 wt% of mica and about 6–20 wt% of ZnO. For cable application, they suggested to use 6.26 wt% of mica and 3.48 wt% of ZnO among other fillers in their

silicone composition to obtain ceramized residue after firing at high temperature according to NFC 32070 CR1 standard. On the contrary, another patent by Rhodia suggested using lower mica content but higher ZnO content in the silicone formulation for wire and cable application. George et al. [49] disclosed that silicone containing 0.74 wt% of mica and 2.05 wt% of ZnO produced ceramized residue after firing at 940 °C thus satisfying the cable standard test NFC 32070 CR. The mica used does not need a special particle size if smaller than 100 µm, as long as it gives a good dispersion in polymer matrix. The variation in mica's content in silicone formulation is probably due to the existence of other fillers that promote ceramization residue. Alexander et al. [57] proposed to use a composition consisting essentially of the silicone polymer, mica, glass additive and crosslinking agent for cable application. A composition containing 5–30 wt% of mica and 0.3–8 wt% of glass frits in silicone polymer formed a strong ceramized residue at elevated temperature (1050 °C) of substantially the same shape and volume as the pristine material. For cable application, where the electrical resistivity of the composition is important, the levels of mica and/or glass additive must be selected carefully. For a given composition, if the level of mica is too high, electrical integrity problems arise due to an unacceptable reduction in electrical resistivity of the composition and/or from dielectric breakdown. The preferred level of mica is from 15% to 30% by weight and more preferably from 20 wt% to 30 wt%, the mean particle size being of 50–200 µm. Muscovite mica is the type generally preferred for those applications because compositions containing phlogopite mica display greater mechanical strength when heated to about 1000 °C to form ceramics, but on the opposite greater shrinkage than that containing muscovite mica. Typically, mica with a mean particle size from 15 µm to 250 µm was selected. Micas at the lower end of this range (e.g. less than 50 µm mean particle size) result in ceramics that are mechanically stronger but display greater shrinkage that can result in cracking. Micas at the middle and upper end of the range are preferable for use in cable applications or other applications where shape retention is particularly important. If the mean particle size of the mica is too large or the amount of mica present is too high, the resultant composition tends to be difficult to process, for instance by extrusion. In addition, the mechanical properties of crosslinked silicone polymers containing coarser particle size grades of mica or high mica levels are poorer. In another study, Alexander et al. [57] reported that replacement of the low-melting glass with zinc borate was undertaken to improve the fire resistance of the ceramizable system, while maintaining high stiffness and good shape retention. Decreasing weight loss from 32% to 25% and cohesive residue were observed by addition of zinc borate. Hanu et al. [58] used two types of mica (muscovite and phlogopite) in addition with glass frit or ferric oxide as flame retardant fillers in silicone rubber. Incorporation of 20 wt% of mica or mica mixture containing 15 wt% of mica and 5% glass frit or ferric oxide has found to have a stabilizing effect on the thermal stability of silicone polymer. It was found that this composition improved silicone thermal stability through several ways: (i) adsorption of

**Table 1**  
Flammability of silicone–mica composites using different additives [58].

Sample	Filler	TTI (s)	Average HRR (kW m <sup>-2</sup> )	Peak HRR (kW m <sup>-2</sup> )
HTVSi	None	67	117	144
SiEAPI	Glass frit	62	117	130
SiMO	Ferric oxide	55	102	117
SiGAI	Muscovite	87	93	98
SiGAEAPI	Muscovite + glass frit	66	121	134
SiGAMO	Muscovite + ferric oxide	69	87	95



polymer chains onto the mica surface resulting in restriction of segmental mobility and thus suppressing redistribution and chain transfer reactions; (ii) shielding effects which reduce mass transport rates (i.e. a reduction in diffusion of fuel products into the gas phase due to an increase in the polymer melt viscosity); (iii) cross-linking promotion and hence lower segmental mobility to suppress redistribution reactions resulting in an overall improvement in residue yield. Cone calorimeter test at incident heat flux of  $50 \text{ kW m}^{-2}$  showed that both ferric oxide and glass frit effectively reduce the time to ignition, an undesirable effect in the field of passive fire protection. However, ferric oxide was considered better than glass frit because, unlike glass frit, it actually lowered the heat release rate of silicone polymer (Table 1). The adsorption of polymer chains onto the surface of mica and ferric oxide particles reduced segmental mobility and suppressed redistribution and chain transfer reactions (typical of silicone depolymerization), which explain the observed delay in the onset of degradation. Ferric oxide was also found to delay the onset of degradation, but resulted in residual yield lower than that of neat silicone. The differences in the residual yields of silicone–mica composites compared to the silicone–ferric oxide composites is explained by the fact that mica addition has a diluting effect on yield, whereas Fe ion in ferric oxide catalyses hydroperoxide decomposition during oxidation, which ultimately catalyzes depolymerization and degradation. Glass frits were found to reduce the thermal stability of silicone polymer due to the increased concentration of metal ions present in these fillers. As mentioned above, glass frits react with fillers and the silica matrix to form a liquid phase which bonds the fillers and silica matrix together, conferring strength to the char. Thus, low temperature ceramization has important role in ceramization residue. The requirement for low temperature ceramization would be insufficient if it relied purely on the mica–silica eutectic reaction, which takes place above  $800^\circ\text{C}$ . The addition of glass frits is a useful technique for lowering the temperatures. These glass frits melt at temperatures below the mica–silica eutectic temperature and combine with the inorganic fillers and pyrolysis products of silicone rubber to assist the formation of a ceramic. Typically, Mansouri et al. [59] studied the influence of various glass frits on the ceramization residue and thus dimensional changes at different temperature. They used two different sizes of muscovite mica, coarse muscovite mica A with particle sizes between 63 and  $150 \mu\text{m}$ , and dry-ground fine muscovite mica B with particle sizes between 38 and  $75 \mu\text{m}$ . Muscovite mica was chosen as it is expected that its alkali component would promote the formation of

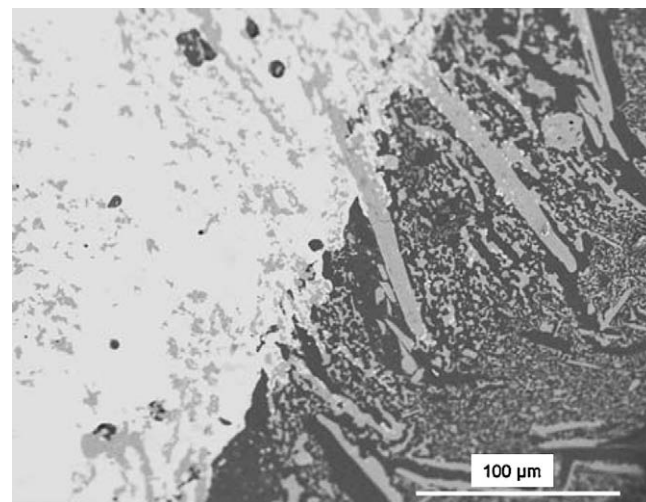


Fig. 10. Scanning electron micrograph of a cross-section of cable showing the interaction between mica particles and copper. Bright area is conductor and grey area is ceramized insulation [59].

a liquid phase during heating at elevated temperatures. Three types of glass frits with softening point of  $525^\circ\text{C}$  (glass frits C and D) and  $800^\circ\text{C}$  (glass frit E) with different compositions were selected [59]. The dimensional changes of ceramized samples were measured and showed that shrinkage at  $1000^\circ\text{C}$  (Table 2) increased when low temperature glass frits (C and D) were added, compared with the high temperature glass frit E. This is expected if liquid phase sintering occurs via the densification mechanism, as a greater volume of liquid phase would allow for more rapid particle rearrangement. Compositions made with glass frits C and D showed limited shrinkage at 600 and  $800^\circ\text{C}$ , which contrasts with other compositions, expanding at these temperatures. When high softening point glass frit E was added to the base composition, no significant dimensional changes occurred up to  $800^\circ\text{C}$ . In contrast to the results for the lower temperature, heating at  $1000^\circ\text{C}$  caused significant shrinkage, due to the formation of a liquid phase that allows densification via liquid phase sintering. This mechanism was not observed at lower temperatures, because insignificant amounts of low viscosity liquid phase were produced. However, at high temperatures, alkali metal ions, from either the mica or the glass additives, tend to provide conductive pathways in the liquid phase. It is thus appropriate either to limit the level of mica and/or the level of glass additive or to select a glass additive having a low alkali metal oxide content (e.g. preferably less than 30% alkali metal oxide content) and/or a fine particle size to reduce the overall level of the additive required to achieve the desired mechanical properties [57]. Finally, Mansouri et al. [59] have unexpectedly observed the interaction between copper of the electric cable and ceramic at the interface (Fig. 10). The XRD spectrum for the residue remaining after the fire test showed the presence of cuprite ( $\text{Cu}_2\text{O}$ ). The diffusion of copper oxides towards the insulation layer has previously been observed by Henrist et al. [60] for a cable sheathed with a zinc–borate filled composition.

### 3.5. Kaolin

Kaolin is also called china clay or porcelain earth. Kaolin is a dioctahedral 1:1 layered clay mineral and its structural formula is  $\text{Al}_2\text{Si}_2\text{O}_5(\text{OH})_4$ . Each layer consists of two sheets: a tetrahedral sheet in which silicon atoms are tetrahedrally coordinated by oxygen atoms; and an octahedral sheet where aluminium atoms are octahedrally coordinated to hydroxyl groups and share apical

Table 2  
Dimensional changes of different silicone compositions at different temperatures<sup>a</sup> [59].

Compositions	Shrinkage (–)/expansion (+) (%)		
	$600^\circ\text{C}$	$800^\circ\text{C}$	$1000^\circ\text{C}$
Silicone/mica A/peroxide (78:20:2)	1.5	0.57	–0.73
Silicone/mica A/peroxide/glass frit E (75.5:20:2:2.5) (composition H)	0.64	0.59	–3.5
Silicone/mica A/peroxide/glass frit D (76.75:20:2:1.25)	–0.37	–1.2	–5.7
Silicone/mica A/peroxide/glass frit D (75.5:20:2:2.5)	–0.8	–1.96	–5.4
Silicone/mica A/peroxide/glass frit D/glass frit E (75.5:20:2:1.25:1.25)	0.26	–0.17	–5.9
Silicone/mica A/mica B/peroxide (68:20:10:2) (composition F)	1.10	0.3	–1.3
Silicone/mica A/mica B/peroxide/glass frit C(65.5:20:10:2:2.5) (composition G)	0.92	0.2	–6.3

<sup>a</sup> Numbers in brackets are weight percent of each component in the composition. Peroxide: dicumyl peroxide.

**Table 3**  
Composition, thermal and modulus properties of kaolin/PDMS composites [61].

Composition (wt%)	Thermogravimetric mass loss step: $T$ ( $^{\circ}\text{C}$ ), (rate (% $\text{min}^{-1}$ ))		Mass loss at 900 $^{\circ}\text{C}$ (%)	TTI (s)	Peak HRR ( $\text{kW m}^{-2}$ ) <sup>a</sup>	Density ( $\text{g cm}^{-3}$ )	Modulus (MPa)
	Step 2	Step 3					
PDMS	510 (1.6)	730 (1.2)	28.1	123	74/72	$0.48 \pm 0.02$	$6.2 \pm 0.7$
PDMS:kaolin (72:28)	529 (3.6)	726 (0.7)	31.5	148	80/71	$0.62 \pm 0.02$	$12.3 \pm 0.6$

<sup>a</sup> Composites display two peaks, the higher HRR peak is indicated in italics.

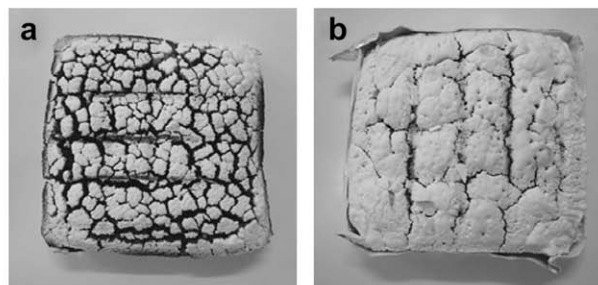
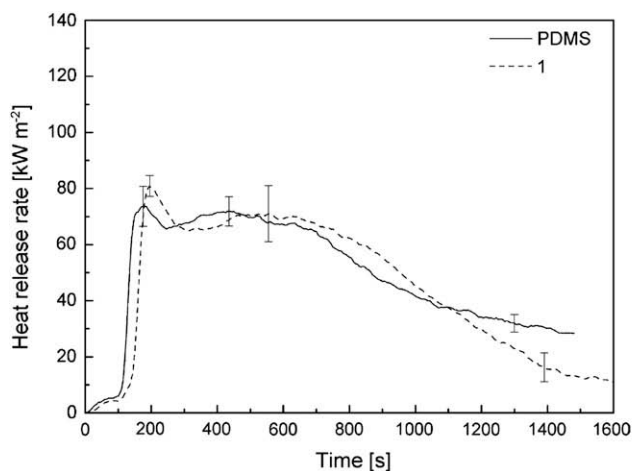


**Fig. 11.** Cone calorimetry experiments (incident heat flux  $35 \text{ kW m}^{-2}$ ) on PDMS/kaolin composite (left): heat release rate curves for PDMS and PDMS/kaolin composite (1); (right): residues of (a) PDMS foam, (b) composite PDMS containing calcinated kaolin [61].

oxygen from the silica tetrahedral sheet. Such typical structure of clay in kaolin crystal foreshadows that kaolin could have the potential flame retardancy that montmorillonite has (*vide infra*). Kaolin is a hydrous aluminosilicate of two varieties, i.e. naturally occurring (hydrous form) and calcined kaolin (anhydrous form). Calcined kaolin is obtained when the clay is heated at more than  $600^{\circ}\text{C}$ , therefore this variety is harder than the hydrous one, i.e. 6–8 on the Mohs scale<sup>2</sup>, against 2 for the former [45]. Addition of calcined kaolin ( $\sim 28 \text{ wt\%}$ ) into PDMS has improved its fire retardancy properties and strength residual [61]. Composite PDMS containing kaolin exhibits a greater mass loss at lower temperature compared to PDMS alone. The incorporation of kaolin was expected to provide an increased torturous pathway for the pyrolysis gases to diffuse through and to reinforce the polymer matrix; however this was not the case. Such increase in mass loss cannot be ascribed to calcined kaolin, which exhibits a very small amount of mass loss ( $<1\%$  by TGA). Rather, the aluminosilicate mineral ( $\text{Al}_2\text{SiO}_5(\text{OH})_4$ ) entails dehydroxylation during calcination process which increased the catalytic activity of the particle surfaces. The mass loss of this composite at  $900^{\circ}\text{C}$  was greater (32%) than theoretically calculated based on the mass loss of PDMS (21%). The structural change may be described by the observation of greater mass loss rate at  $529^{\circ}\text{C}$ . Detail information about composition, thermal and modulus properties of PDMS composites are shown in Table 3. Test by cone calorimeter at a constant incident heat flux of  $35 \text{ kW m}^{-2}$  has shown an increasing TTI from 123 to 148 s because of the retarding effect of the mineral in degrading the polymer. The formation of an insulating char on the surface resulted in decreasing the HRR to a minimum of about  $66 \text{ kW m}^{-2}$  before reaching a similar HRR to the PDMS at later time (Fig. 11). All composites exhibited two peak

HRRs, the first similar to PDMS but the second peak being shifted to higher HRR. This behaviour is ascribed to the disruption and breakdown of the PDMS foam structure during the combustion test due to filler addition which increases stiffness of PDMS foam. Fig. 11 also shows that the composites reveal crack formation that occurred during the test resulting in opening foamed structure. The increased surface area exposed to the heat implies that an increase in fuel for fire is available for combustion. Addition of kaolin into PDMS increased the mass loss at  $900^{\circ}\text{C}$ , which suggests that kaolin promotes the decomposition of PDMS. Adding to the formulation a combination with magnesium hydroxide and zinc borate decreased the mass loss of PDMS at  $900^{\circ}\text{C}$  while maintaining char density. The residual char surface exhibited a thicker silica ash deposit and less cracks compared to another composites containing magnesium hydroxide and zinc borate. In conclusion, addition of kaolin into PDMS matrix does not change significantly the fire property of PDMS according to cone calorimeter test but nonetheless, induces a better ceramization residue after firing.

### 3.6. Metal hydrates

Among the metallic hydroxide flame retardants, aluminium trihydrate ( $\text{Al}(\text{OH})_3$  abbreviated ATH) or magnesium dihydroxides ( $\text{Mg}(\text{OH})_2$  or MDH) are popular flame retardants and smoke suppressants. ATH offers numerous benefits since it is cheap, safe and easily incorporated into many plastics/polymers. It is also halogen-free and produces nontoxic fume, which makes it a valuable competitive fire retardant [62]. The flame retarding property of ATH in polymers is based on its thermal decomposition, in the temperature range from  $180$  to  $200^{\circ}\text{C}$ , where it is converted into aluminium oxide in an endothermic reaction with release of water vapour (Scheme 8) [63]. ATH typically loses 34.6% of its mass as water vapour after heating to temperatures above  $350^{\circ}\text{C}$  [64]. Flame retardants containing MDH act similarly to those containing

<sup>2</sup> The Mohs scale is a qualitative and somewhat arbitrary hardness indexing scheme, based on scratch tests of natural minerals on a softer material. The Mohs scale ranges from 1 for talc to 10 for diamond.



Scheme 8. Thermal decomposition of ATH.

ATH, but start to decompose at a higher temperature range of 250–300 °C. The exothermic breakdown of the ATH, the formation of aluminium oxide, the liberation of water vapour, effect the combustion by physical ways including [65]: (i) diluting the polymer in the condensed phase, (ii) decreasing the amount of available fuel, (iii) increasing the amount of thermal energy needed to raise the temperature of the composition to the pyrolysis level, due to the high heat capacity of the fillers, (iv) increasing the enthalpy of decomposition – emission of water vapour, (v) diluting gaseous phase by water vapour which decreases the amount of fuel and oxygen in the flame, (vi) possibly generating endothermic interactions between the water and decomposition products in the flame, (vii) decreasing feedback energy to the pyrolysing polymer, and finally (viii) creating an insulating effect by the oxides remaining in the char. Besides, due to the high specific surface area of the oxide layer, absorption of smoke and other toxic or decomposed carbonaceous gaseous products takes place, making ATH a very effective smoke suppressant as well [66]. To date, most application of ATH is as flame retardant fillers in electrical/electronic cables used in critical environments such as subways, airports, ships and nuclear power stations, whereas cables containing MDH are generally reserved for automotive and special applications. ATH or MDH also can be used in combination with co-additives such as organomodified clays, zinc borate, red phosphorus or nitrogen/phosphorous compounds. Some studies related to improving residue properties after/during combustion have also been reported. Specific effects of transition metals, when co-precipitated with magnesium hydroxide as solid solutions, included [67]: (i) facilitating and lowering the temperature of the dehydration of the additive; (ii) catalyzing the dehydrogenation of the polymer; (iii) promoting carbonization; and (iv) improving acid resistance. However, the use of ATH in polymers does present some disadvantages, for example loadings as high as 60 wt% are required to impart significant flame retardancy, which affects the physical properties of the composites. In addition, ATH is less ideal for use as flame retardant agent in polymer such as PDMS for security cable application because of its relatively low decomposition temperature and cracks generation which is of inconvenience in terms of residual cohesivity. Nicholson et al. [47] reported that incorporation of 13.8 wt% of ATH into silicone formulation for electric wires or cables gave a significantly poorer fire performance. The char structure of residue after combustion was cracked and friable. Genevose and Shanks [61] reported that the combination of zinc borate (ZB) and MDH improves fire performance and increases the strength of the residual char of PDMS. The hydrated fire retardants reject water that cools on the substrate. MDH and ZB were incorporated into PDMS matrix in the presence of kaolin (Table 4). The fire performance behaviour measured by cone calorimetry showed

Table 4

Composition, thermal and modulus properties of composites PDMS containing MDH [61].

Sample	Composition (wt%)	Mass loss at 900 °C (%)	TTI (s)	Peak HRR (kW m <sup>-2</sup> ) <sup>a</sup>	Density (g cm <sup>-3</sup> )	Modulus (MPa)
1	PDMS	28.1	123	74/72	0.48 ± 0.02	6.2 ± 0.7
2	PDMS:kaolin: MDH (73:16:11)	23.5	144	78/118	0.66 ± 0.01	11.6 ± 0.8
3	PDMS:kaolin: MDH:ZB (73: 16:10:1)	22.3	155	82/116	0.71 ± 0.03	8.2 ± 0.9
4	PDMS:kaolin: MDH:ZB (73:16:6:5)	24.1	109	84/108	0.65 ± 0.02	13.6 ± 0.9

<sup>a</sup> Composites display two peaks, the higher HRR peak is indicated in italics.

decreasing of both TTI and peak HRR compared to unfilled PDMS. Magnesium oxide is retained in the composite thus insulating and limiting the diffusion of combustible volatiles. However, addition of fillers increased the density and stiffness of the PDMS foam (Tables 3 and 4). The loss of water and volatiles caused the PDMS to lose its flexibility and to become rigid and brittle (ceramic precursor). The pressure of gases through the structure, accompanied by changes in internal stresses (shrinkage) caused formation of cracks in the composites during the test at 900 °C and therefore resulting in open foam structure (Fig. 12). The increased surface area exposed to the heat implies that an increase in fuel for fire is available for combustion. Reduction of MDH content in PDMS matrix (substituted by ZB) resulted in less cracks in the residue due to less water release from hydrothermal degradation of MDH.

### 3.7. Talc

Talc [45] is a naturally occurring hydrated magnesium sheet silicate, 3MgO·4SiO<sub>2</sub>·H<sub>2</sub>O. The elementary sheet is composed of a layer of magnesium–oxygen/hydroxyl octahedral, sandwiched between two layers of silicon–oxygen tetrahedral. The main or basal surfaces of this elementary sheet do not contain hydroxyl groups or active ions, which explains its hydrophobic nature and inertness. Most of talcs are lamellar in nature, they are chemically inert, organophilic and water-repellent to a great extent. Above 900 °C, talc progressively loses its hydroxyl groups and above 1050 °C, it re-crystallizes into different forms of enstatite (anhydrous magnesium silicate). Similarly to clays, talc belongs to the phyllosilicate group, but in contrast to montmorillonite, hectorite or saponite, talc cannot be exfoliated by using cationic surfactant due to the absence of metallic cations between the layers. Therefore, lamellar talc particles may have effects similar to those of clay platelets in the material. Optionally, talc has been used as non-reinforcing filler in silicone elastomer useful as insulation for electrical equipment, as encapsulants and as sealants where flame retardancy is necessary [68]. Tkaczyk et al. [69] from General Electric used 20 wt% of talc, chosen among ground silicate minerals,

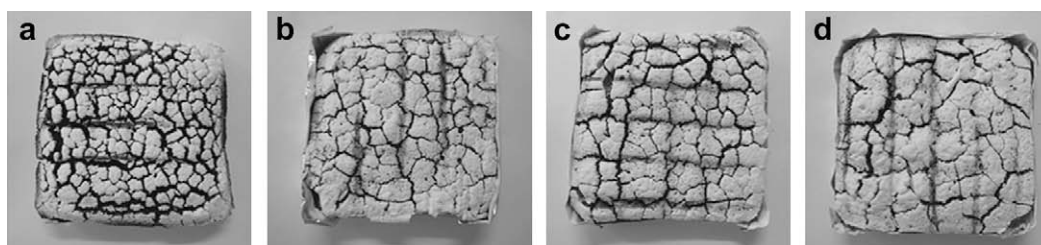
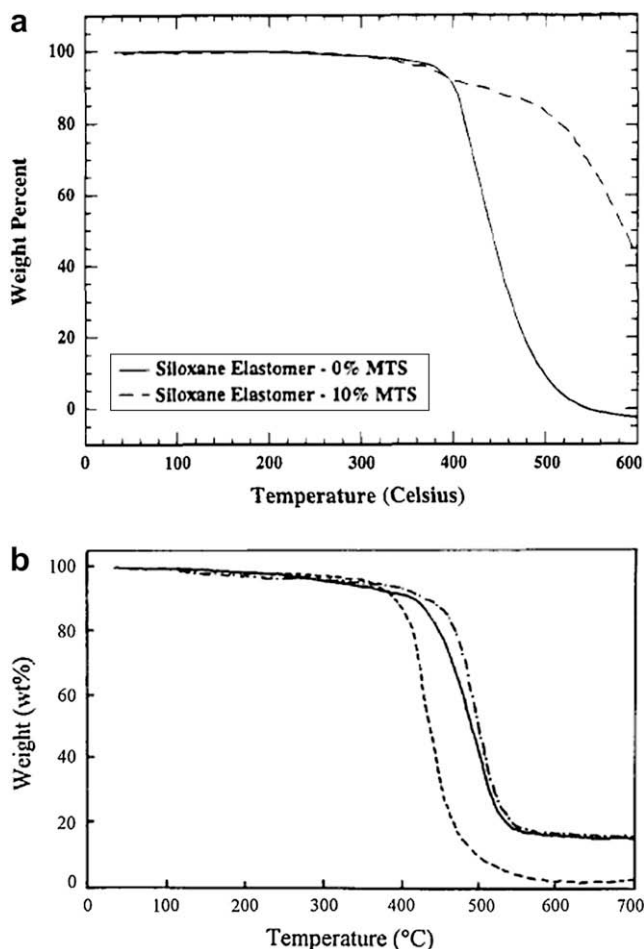


Fig. 12. Photos of MDH-filled PDMS composites residues after cone calorimetry experiments (incident heat flux 35 kW m<sup>-2</sup>): (a) PDMS foam, (c) composite 2, (d) composite 3, (e) composite 4 (see Table 4) [61].





**Fig. 13.** Two different TGA studies on MMT/silicone composites: (a) PDMS (solid line) and PDMS nanocomposite (dashed line) containing 10 wt% of S04682 silicate [73]; (b) silicone rubber without filler (—); silicone rubber/oMMT hybrid (—●—); silicone rubber/aerosilica (—●—) [76].

to make silicone composite useful in insulating electrical wires. They found that talc which surface was treated with a silane provided a lower conductivity than untreated talc, a better compatibility with silicone and improved mechanical properties of silicone composite. Talc-filled silicone composite also exhibited a lower conductivity at higher temperatures compared to mica or wollastonite, making these very resistant to electrical breakdown during fire. Sweet and Gallmeyer from Dow Corning Corp. [70] and George et al. from Rhodia [49] used talc as filler in preparation of silicone rubber. The invention of Dow Corning Corp. deals with flame retardant silicone rubbers useful as marine deck coatings, firewall construction and fire-blanket applications. Rhodia's one

deals with organopolysiloxane-based compositions vulcanizable by hot process into silicone elastomers, useful in particular for making electric wires or cables. Rhodia used talc alone or in combination with calcinated kaolin or calcium carbonate as semi-reinforcing filler.

### 3.8. Montmorillonite (MMT)

According to Gilman et al. [71], the general flame retardant mechanism of clay based nanocomposites is a build-up of a high-performance carbonaceous silicate char on the surface during burning. This layer insulates the underlying material and slows the mass loss rate of decomposition products. Recently Leszczyńska et al. [72] studied in detail the factors and mechanism that controls thermal stability of polymer/MMT nanocomposites. According to these authors, there are several factors that influence thermal stability of polymer/MMT nanocomposites, among which : (i) a labyrinth effect induced by intercalated or exfoliated structure of MMT, which limits oxygen diffusion inside the nanocomposite sample; (ii) a steric effect, in that MMT layers strongly interact with polymer matrix thus limiting the polymer chain motion; (iii) a mass barrier effect, which protects the bulk of sample from heat, decreases the rate of mass loss during thermal degradation of polymer nanocomposite and generates more intensive char formation on the surface; (iv) a heat barrier effect, that could also provide superheated conditions inside the polymer melt thus leading to extensive random scission of polymer chain and to the release of numerous chemicals. These degradation products trapped between clay layers have more opportunity to undergo secondary reactions; (v) a catalytic effect of the nanodispersed clay effectively promoting char-forming reactions. It was also suggested that the more effective char production during thermal decomposition of polymer/clay nanocomposites may be favoured by chemical interactions between the polymer matrix and the clay layer surface during thermal degradation. Nanodispersed MMT layers were also found to interact with polymer chains in a way that forces the arrangement of macro-chains and restricts the thermal motions of polymer domains. Generally, the thermal stability of polymeric nanocomposites containing MMT is related to the organoclay content and the dispersion. Burnside and Giannelis [73] reported the synthesis of PDMS/organo-montmorillonite nanocomposites using melt intercalation. The organosilicate was prepared by ion-exchanging  $\text{Na}^+$ -MMT with dimethyl ditallow ammonium bromide and the hybrids were prepared by a sonication method. Fig. 13(a) shows the TG curves for both the unfilled PDMS and the PDMS nanocomposite containing 10 wt% of S04682 (a commercial organosilicate). The nanocomposite shows delayed decomposition compared to the unfilled polymer. Whereas PDMS decomposes into volatile cyclic materials, the permeability of the MMT/PDMS nanocomposite is dramatically decreased thus hindering volatile decomposition products. Besides, Burnside and Giannelis [74] observed an increase and a broadening of the glass-transition

**Table 5**

TGA analysis and corresponding flammability performances of fire-retardant MMT-filled silicone rubbers<sup>a</sup> [77].

Sample	oMMT	SiO <sub>2</sub>	MDH	RP	LOI (%)	UL-94 test	T <sub>5%</sub> (°C)	T <sub>50%</sub> (°C)	Residue at 750 °C (%)
MVMQ0	0	0	0	0	27.1	V-1			
MVMQ1	0	20	20	5	29.0	V-0	229.4	545.5	29.9
FSNC0	1	0	0	0	29.4	V-0	336.8	556.8	32.53
FSNC1	1	20	20	5	31.1	V-0	358.7	594.7	33.50
FSNC2	3	20	20	5	29.5	V-0	327.8	548.3	31.37
FSNC3	5	20	20	5	29.8	V-0	311.2	553.2	34.21
FSNC4	7	20	20	5	30.2	V-0	299.6	549.8	35.28

<sup>a</sup> Each sample contain 100 parts of MVMQ and 2.8 parts of bis(2,4-dichlorobenzoyl) peroxide. Heating rate for TGA is 10 °C min<sup>-1</sup>. For abbreviations, see text.

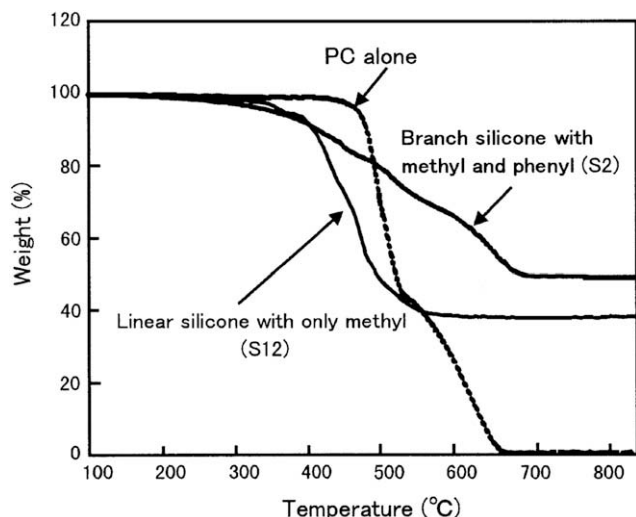


Fig. 14. Thermogravimetric analysis of PC/silicone derivative blends [79].

temperature and loss of the crystallization transition of the bound polymer chains of PDMS nanocomposites. Ma et al. [75] prepared exfoliated/intercalated polydimethylsiloxane (PDMS) nanocomposites by two steps, i.e. preparation of treated MMT solution and solution blending with PDMS. Incorporation of 10 wt% Na<sup>+</sup>-

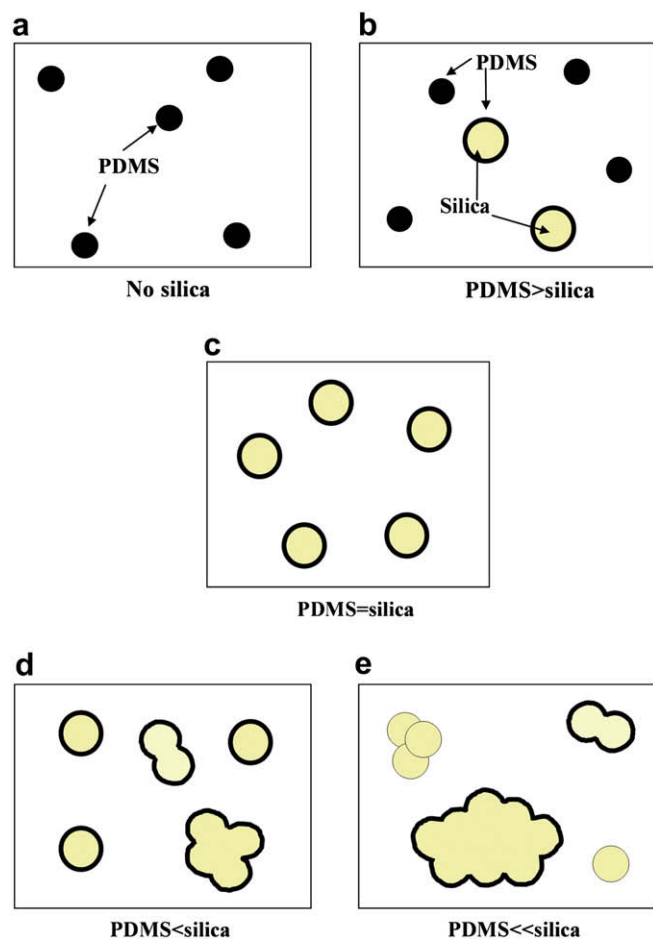


Fig. 15. Schematic distribution of PDMS in the PC-PDMS block copolymers containing nanosized silica [81].

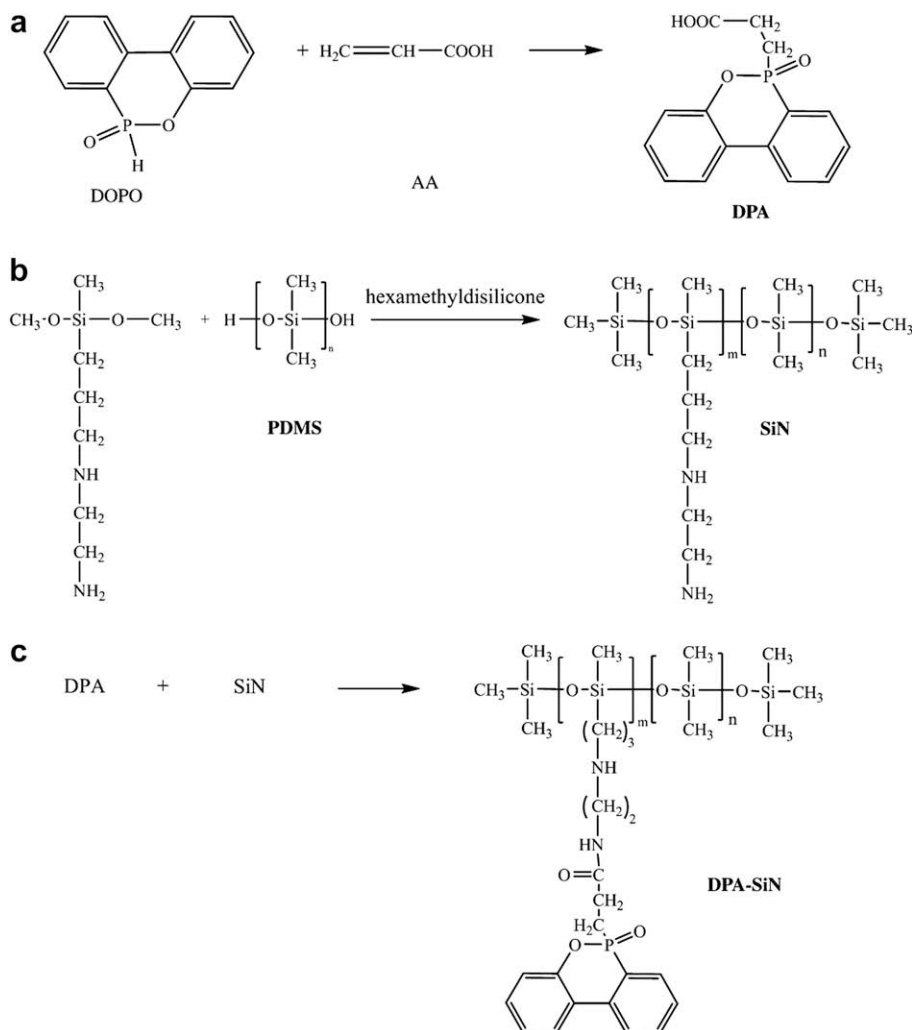
MMT into the PDMS matrix shifted decomposition temperature of PDMS nanocomposite from 395 to 463 °C. The nanocomposites displayed delayed decomposition temperature compared to the pristine polymers again because of hindered diffusion of the volatile decomposition products. They found that PDMS was grafted onto MMT layer surface via condensation of hydroxyl groups of PDMS and those on MMT layer surface, then preventing nanolayers of MMT to re-aggregate. Wang et al. [76] synthesized silicone rubber/oMMT hybrid nanocomposites via melt-intercalation process. oMMT (organo-modified montmorillonite) was synthesized by dissolving 5 wt% of Na<sup>+</sup>-MMT in an excess of hexadecyltrimethylammonium bromide. This process advantageously does not need any solvent, so it is easy to apply in industry. oMMT particles were exfoliated into nano-scale layers of about 50 nm thickness from their original 40 μm particle size and uniformly dispersed in silicone rubber matrix (hydroxyl-terminated polydimethylsiloxane). The mechanical properties and thermal stability of the hybrids were very close to those of aerosilica-filled silicone rubber. In terms of thermal properties, silicone rubber/oMMT hybrid nanocomposites showed the enhancement of thermal stability of PDMS. Fig. 13(b) shows the TG traces of unfilled silicone rubber and filled silicone rubber with 8.1 vol% of filler (oMMT or aerosilica). Decomposition temperatures of the filled silicone rubber were 433 °C for the hybrid and 440 °C for the aerosilica-filled silicone rubber, both higher than that of the unfilled silicone rubber (381 °C). Yang et al. [77] prepared flame-retardant methyl vinyl silicone rubber (MVMQ)/montmorillonite nanocomposites by solution intercalation method, using magnesium hydroxide (MDH) and red phosphorus (RP) as synergistic flame retardant additives, and aerosilica (SiO<sub>2</sub>) as synergistic reinforcement filler (Table 5). The oMMT used was montmorillonite modified by hexadecyl trimethyl ammonium bromide with average particle size 5 μm. In this report, they showed that the nano-dispersed lamellae of oMMT (exfoliation or intercalation) in MVMQ rubber matrix have the main flame-retardant effect and this nanocomposite have a good flame retardant synergistic effect with MDH and RP. The nanocomposites show higher thermal stabilities, flame-retardant properties, and excellent mechanical properties. The nanocomposite containing 1 wt% of oMMT enhanced LOI of MVMQ/oMMT from 27.1 to 29%, while the MVMQ/oMMT/MH/RP/SiO<sub>2</sub> hybrids had LOI of 31.1% and achieved V-0 rating on the UL-94 test. The synergistic flame retardant mechanism by using MVMQ/oMMT nanocomposites is mainly ascribed to the physical process occurring in condensed phase. A silicate layers may protrude on the surface of a burning nanocomposite, creating a physical protective barrier on the surface of the material. These layers act as a protective barrier and can limit the oxygen diffusion to the substrate.

#### 4. Silicone and modified silicone as flame retardants in other polymer matrices

In a number of studies, silicones have been used as flame retardant synergists to modify the manner in which more conventional plastics burn. Silicones can be used as flame retardant agents through direct blending within the polymer matrix, incorporation into porous fillers, or by synthesizing block/graft

Table 6  
LOI of different particles size silica in PC-PDMS block copolymers (1 wt% PDMS) [81].

Silica types	Average particle sizes	Silica content (wt%)	LOI (%)
Colloidal silica	50 nm	0.5	38
	20 nm	0.5	40
Microsilica	16 μm	0.5	27
Nanosized-silica	50 nm	0.5	40
	50 nm	2	34



**Scheme 9.** The synthesis route of DPA-SiN flame retardant.

copolymers including silicone segments. Cone calorimeter evaluations reported by Pape and Romenesco [78] showed that the silicone powder additives give improved fire retardant properties such as reduced peak and heat release rate, reduced levels of carbon monoxide generation and reduced levels of smoke evolution in a variety of polymer systems including polyolefins, polycarbonate, polystyrene, PPO, polyamide, even at addition levels of 1–5 wt%. Silicone powder additive is a combination of polydimethylsiloxane and fumed silica. This combination is necessary to give a free flowing powder, as well as to affect burning characteristics. This powder has been modified with organofunctional reactivity (amino, epoxy, or methacrylate) to enhance the compatibility in various polymer systems. Combination with conventional fire retardant systems, such as halogen/antimony, ammonium polyphosphate, and water evolving fire retardant products such as magnesium hydroxide also gave improvements in flame retardancy.

#### 4.1. Polycarbonate (PC)–PDMS block copolymer

Iji and Serizawa [79] used several types of silicone polymers as flame retardant in polycarbonate (PC). Silicones tested varied in their chain structure (linear or branched type), the nature of functional groups in the chain (methyl, phenyl, mixture of them) and the type of end-groups (methyl, phenyl, hydroxyl, methoxy,

vinyl). Branched silicone polymers containing a mixture of methyl and phenyl groups along the chain and end-capped by methyl groups proved the most effective in enhancing LOI values and final residue (Fig. 14). According to the authors, the superior flame-retardant effect of the silicone derivatives (branched silicone with methyl and phenyl) is due to their excellent dispersion and migration on the surface of PC during combustion, where they form a uniform and highly flame resistant barrier. The formation of a highly flame-resistant char resulted from combination of polysiloxane and condensed aromatic compounds onto the PC surface. Furthermore, the efficiency of the branched silicones was observed to increase with decreasing molecular weight due to accelerated migration to PC surface as a result of its lower viscosity. Nodera and Kanai [80] reported the different flame retardancy effects between nano-sized and micro-sized silica in PC–PDMS block copolymer. They found that the thermal stability and the amount of residue for PC–PDMS block copolymer were slightly enhanced by adding the nano-sized silica. It is thought that the maximum loss rate decreases with increasing nano-sized silica content because the residue has a good sealing efficiency. Meanwhile, micro-sized silica or silica aggregated at more than 1.0 wt% of silica in PC–PDMS block copolymer has little effect on the sealing efficiency of residue because micro-sized silica cannot cover on enough of the surface of the residue. Furthermore, when the nano-sized PDMS domains (~50 nm, which has high flame retardancy) move to surface of the

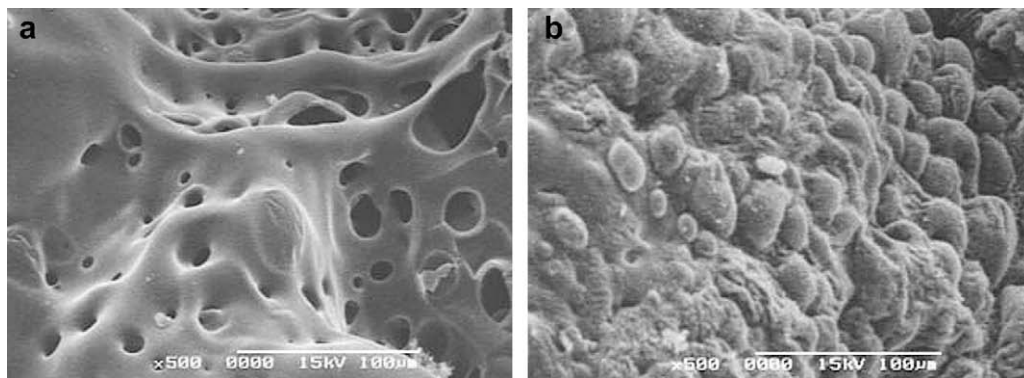
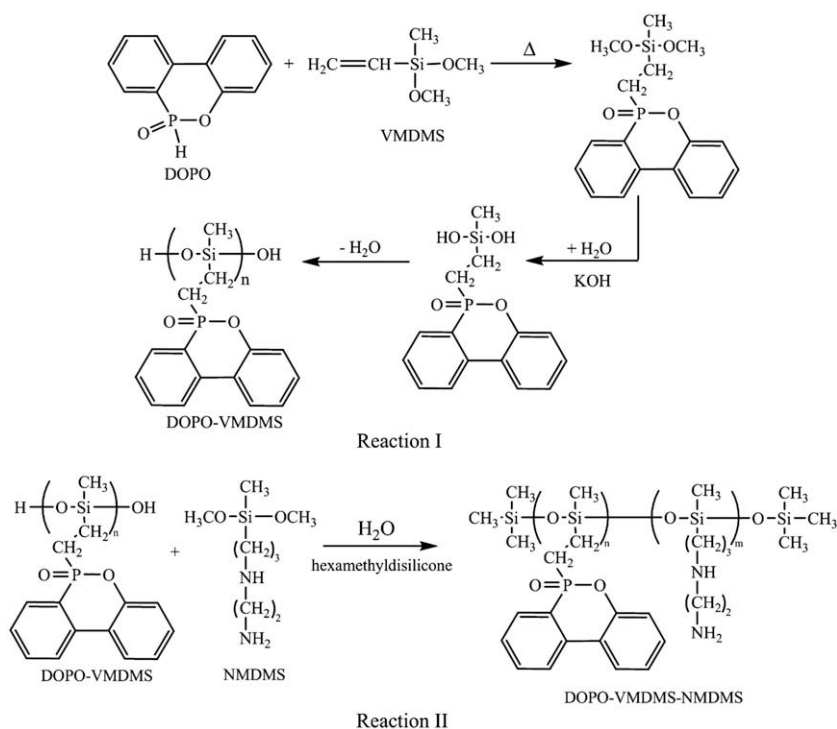


Fig. 16. SEM micrographs of (a) the inner surface and (b) the outer surface of the char layer [85].

micro-sized silica particles, the interaction between PC and PDMS decreases and so the flame retardancy of PC–PDMS block copolymer decreases. Further works by Nodera and Kanai [81] showed that monodisperse nano-sized silica (50 nm, in powder form) had a positive effect on the flame retardant mechanism of PCD–PDMS, whereas colloidal silica (nano-sized silica dispersed in liquid polyethyleneglycol) with a median particle size of 20 nm has higher flame retardancy as compared with this of 50 nm. The enhancement of the flame retardancy was ascribed to the fact that the PC–PDMS block copolymer is mainly distributed on the surface of the nano-sized silica through physical interactions. Indeed, the size of silica is almost the same as the size of PDMS domains effective in flame retardancy (domain size  $\sim 50$  nm). Furthermore, micro-sized silica has a little effect on the sealing efficiency of residue because micro-sized silica cannot cover enough on the surface of the residue. It is supposed that the PDMS on the surface of micro-sized silica has a behaviour similar to large PDMS domain ineffective in flame retardancy. Therefore, polymers with micro-sized silica or a lot of aggregated nano-sized silica have lower LOI values (Table 6). Based on such results, Nodera and Kanai [81] proposed

a conceptual model of silica distributions in PDMS which influence the flame retardancy efficiency of PDMS (Fig. 15). When the nano-sized silica content is less than the PDMS content (Fig. 15(b)), silica is perfectly dispersed in the matrix and fully covered with PDMS. The monodisperse silica is effective in the flame retardant enhancement of matrix polymer. In that case, it is thought that PDMS located on the surface of nano-sized silica particle exhibits higher thermal stability than PDMS alone and generates high sealing residue covered with more nano-sized silica particles in combustion. As the nano-sized silica content increases, a part of the silica particles aggregates but still the aggregated silica surface is covered with PDMS (Fig. 15(d)). At large silica content, the content of uncovered aggregated silica particles and single silica particle increased (Fig. 15(e)). Since the flame retardancy of PDMS is low, the thermal degradation behaviour of the polymer composite is decreased. Yasuhiro and Kazuhiko [82] used both PDMS and  $\text{TiO}_2$  which surfaces were treated with siloxane to provide remarkable flame retardancy to PC resin composition. In this composition, PC resin achieved V-0 rate in flammability test according to UL-94 standard. In other work to improve flame retardancy of PC, Barren



Scheme 10. The synthesis route for DOPO–VMDMS–NMDMS (DVN).



et al. [83] used TiO<sub>2</sub> surface treated with PDMS as pigment and flame retardant agent in PC. Lupinski and Howkins [84] also used up to 9 wt% of PDMS-treated fillers such as TiO<sub>2</sub>, clay or carbon black in PC resin order to improve flame retardancy of resin by achieving V-0 rate for UL-94 test.

#### 4.2. PC/poly(acrylonitrile–butadiene–styrene) (ABS)

Silicone additives can be modified by introduction of heteroatom-containing molecules that may have synergistic effect in flame retardant action. Zhong et al. [85] used flame retardant containing phosphorous, nitrogen and silicon elements simultaneously in a PC/ABS alloy. This type of flame retardant was synthesized through a simple method depicted Scheme 9. 9-(9,10-Dihydro-9-oxa-10-phosphaphenanthrene-10-oxide)-propionic acid (DPA) was synthesized through direct addition reaction of 9,10-dihydro-9-oxa-10-phosphaphenanthrene-10-oxide (DOPO) and acrylic acid (AA). DOPO has high thermal stability, oxidation resistance, and good water resistance. DPA was introduced into *N*-*b*-(aminoethyl)-*c*-aminopropyl methyl dimethoxy silane/dimethyl siloxane copolymer (SiN) to form the flame retardant called DPA–SiN. Incorporation of 30 wt% of DPA–SiN into PC/ABS improved the LOI value from 21 to 27 with 2.2 wt% of P, 2.4 wt% of Si and 1.2 wt% of N. At this loading level, the HRR, THR and EHC are reduced to about half of unmodified PC/ABS. It was reported that the addition of DPA–SiN changed the thermal behaviour of PC/ABS by forming more stable char layer during thermal decomposition. Unfortunately, this type of flame retardant could not increase TTI as expected, because it decomposed earlier than the polymer. The morphological structure of char formed by DPA–SiN modified PC/ABS blends indicates that a smooth and compact char layer was obtained at 800 °C whereas char layer could swell well to form a barrier to resist the transfer of heat and mass during a fire (Fig. 16). Another type of flame retardant containing Si, P and N for PC/ABS alloys has also been developed by Zhong et al. [86]. This type of flame retardant called DVN was synthesized from the reaction of DOPO, vinylmethyldimethoxy silane (VMDMS) and *N*- $\beta$ -(aminoethyl)- $\gamma$ -aminopropyl methyl dimethoxy silane (NMDMS) (Scheme 10). In PC/ABS, DVN has activity in both condensed phase and gas phase. Incorporation of up to 30 wt% DVN into PC/ABS alloys has improved thermal stability and flame retardancy by enhancing LOI of PC/ABS alloys from 21.2 to 27.2. The highest LOI was obtained if DVN contain 2.8 wt% P, 3 wt% Si and 0.5 wt% N. At the same loading level of flame retardant DVN (typically 30 wt%), Zhong et al. [87] observed a decrease in LOI by decreasing P and increasing Si and N contents. The morphological structures of the chars obtained after the LOI test were observed by SEM (Fig. 17) [86]. The outer surface is smooth and plain while the internal surface exhibits cell structure. The swollen internal structure, dense and smooth outer surface provide a good barrier to the transfer of heat and mass during the fire. The char retards the overflow of the flammable volatiles at high temperature. The thermal decomposition performance of PC/ABS/DVN occurs through decomposition of phosphorus-containing groups to hydrate the char source-containing groups in a fire or during heating. Then, they form a continuous and protective carbon–silica layer. The gases generated by the nitrogen-containing groups form the carbon–silica layer. SiO<sub>2</sub> reacts easily with phosphate to yield silicophosphate which is known to stabilize phosphorus species.

#### 4.3. Ethylene butyl acrylate (EBA)

In the early 1990s, Davidson and Wilkinson [88] reported the improvement of flame retardancy of acrylate-based copolymers in wire and cable applications by addition of chalk and silicone. 5 wt%

of trimethylsilyl chain-ended PDMS gum containing nominally 0.2 mol% vinyl groups and 30 wt% of stearate coated calcium carbonate having an average particle size of 1.5 microns were added into 65 wt% of EBA copolymer (noted CaSiEBA in the following). This formulation successfully increased the LOI value of EBA copolymer from 18 to 34. Later on, the flame retardancy of EBA copolymer containing silicone and chalk has been investigated in detail by two groups in Sweden, namely the group of researchers from Borelys Technology Oy (Hermansson, Sultan, or Huhtala), and Krämer et al. [89]. Beside the development of flame retardancy of CaSiEBA type, they also studied CaSiEBA application as flame retardant in polyolefin polymers. Both of these groups used EBA, chalk and silicone from the same supplier i.e. Borealis AB (Sweden). Table 7 compares the results gained on the cone calorimeter and LOI tests using two slightly different CaSiEBA formulations. Increasing silicone content in CaSiEBA slightly increased flame retardancy in term of cone calorimeter test results. This is probably due to the role of silicone in the formation of heat barrier layer (i.e. CaSiO<sub>4</sub>) through its reaction with chalk at high temperature. Hermansson's team observed that at 1000 °C the char of CaEBA collapsed during burning while CaSiEBA formed an intumescent structure with a compact and flat char, even though LOI test did not show much differences between CaEBA and SiEBA (Table 8). According to Hermansson et al. [44], ester pyrolysis of ethyl butyl acrylate (EBA) which occurs at 300 °C, results in a reaction between the chalk and the carboxylic acid, leading to formation of gases and ionomers. The volatile species dilute and reduce the combustible gases transported to the flame front and cause the melt to effervesce hence generating an intumescent structure. The intumescent structure acts as a heat insulating layer protecting the material underneath from burning and preventing new combustible gases to reach the flame front. The intumescent structure is reinforced by the ionomers creating crosslinks in the melt. In addition, cross-linked points through the reaction between carboxylic acid (after ester pyrolysis of EBA) and calcium ions in chalk increases the melt viscosity and thus the stability of the (initial) melt. Hermansson et al. [90] also showed that the reinforcement of intumescent structure through an insulation effect is triggered by temperature. At high temperature (above 700 °C) intumescent structure was stabilized by the presence of some calcium silicate. The fact that some calcium silicate is present in the surface layer shows that chalk to a small extent has been converted to calcium oxide, although the conversion rate is slow below 700 °C. The final ash residue consists of cavities of different sizes due to insulation effect of outer layer. Two layers can be seen, where the bulk layer consists mainly of chalk and the protective surface layer consists of chalk and traces of amorphous silica. The flame retardancy of composites is known to be strongly affected by the dispersibility of flame retardant agents in the matrix, enhanced by a good adhesion at the filler–matrix interface [91]. Hermansson et al. [92] thus studied the effect of chalk and silicone distributions to flame retardant efficiency. A homogeneous distribution of chalk particles in the polymer matrix leads to a larger contact area between the chalk particles and polymer matrix, which is positive for the interactions and the chemical mechanisms occurring between the solid phase and the melt phase. Homogeneous dispersion of silicone elastomer is also important, as it facilitates the formation a uniform thickness of SiO<sub>2</sub> at the surface that withstands the pressure of volatile gases formed in the bulk, and the initial crack propagation that occurs at the weakest spots (lowest thickness) can most likely be reduced or perhaps entirely avoided. Indeed, more extensive mixing provided a better dispersion of chalk particles and silicone elastomer, as well as improved flame retardant properties as shown by cone calorimeter test at incident heat flux of 35 kW m<sup>−2</sup> (Table 9). CaSiEBA manufactured in a full scale extruder (i.e. a 300 mm/7D

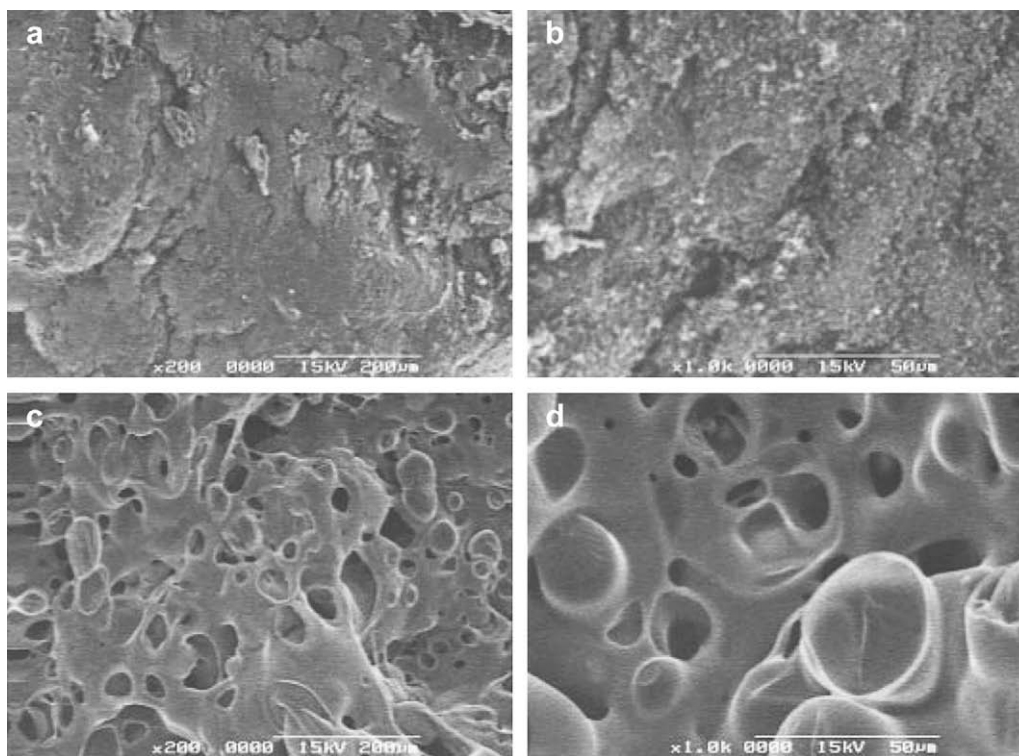


Fig. 17. The outer (a, b) and internal (c, d) surfaces of PC/ABS/DVN-30 after LOI test [86].

Buss-co-kneader, FSE in Table 9) has higher oxygen index (LOI) value than that of produced on a laboratory two-roll mill (TRM-4 min, TRM-10 min, etc. in Table 9). The two-roll mill was run at a rotation speed of 5 rpm during addition of fillers and, thereafter, of 22 rpm, on both rolls. According to author, the oxygen index of materials produced on the two-roll mill is optimal at a mixing time of 20 min. The flame retardancy of CaSiEBA can be further improved by introduction of some additives such as metal oxides. For cable and wire applications, Sultan et al. [93] from Borealis Technology Oy added 2 wt% of metal oxide such as  $\text{Al}_2\text{O}_3$  (110  $\mu\text{m}$ ),  $\text{Fe}_2\text{O}_3$  (7  $\mu\text{m}$ ), or  $\text{TiO}_2$  (3  $\mu\text{m}$ ) into CaSiEBA flame retardant in order to enhanced the LOI value of initial CaSiEBA (35) to 36, 39 and 39.5, respectively [93]. Moreover, Huhtala and Mohta [94], still from Borealis Technology Oy, disclosed that the partial substitution of calcium carbonates with oMMT nanofillers reduced dripping properties of burned materials. The particles of the nanofiller are dispersed in the polymer matrix so that the maximum thickness in polymer matrix in at least one dimension is below 10 nm. 12 wt% of silicone in combination with 34 wt% of calcium carbonate was also used as a flame retardant agent of other acrylate-based polymers enhanced by PDMS addition in ethylene butyl acrylate (EBA) for wire and cable TG measurements (Fig. 18), which show that

Table 7

Result of the cone calorimeter tests of CaSiEBA compositions studied by Hermansson et al. [44] and Krämer et al. [89] groups<sup>a</sup>.

Material	Hermansson	Kramer
Chalk (wt%)	30	30–40
Silicone (wt%)	12.5	5–7
EBA (wt%)	57.3	NC <sup>b</sup>
Additives (wt%)	0.2 (antioxidant Irganox 1010)	–
Peak HRR ( $\text{kW m}^{-2}$ )	326	$284 \pm 32$
Ignition time (s)	148	$197 \pm 4$
Mass loss (%)	65.9	$62 \pm 2$

<sup>a</sup> Cone calorimeter with 35  $\text{kW m}^{-2}$  external heat flux.

<sup>b</sup> Not communicated.

applications. Substitution with 4 wt% of alkyl quarternary ammonium montmorillonite decreased HRR average of EBA composite from 257 to 215  $\text{kW m}^{-2}$ . Silicone and chalk not only improve flame retardancy of EBA, but combination of these compounds has also been used as flame retardant in other polymers. A commercial flame retardant with silicone, calcium carbonate in the form of chalk and EBA is currently available under the trend name Casico<sup>TM</sup> [44]. The flame retardant mechanism of Casico is complex and is related to a number of reactions, e.g. ester pyrolysis, formation of carbon dioxide, ionomer formation and formation of an intumescent structure stabilized by a protecting char. Later studies by Krämer et al. [89] have confirmed the role of chalk and silicone in an ethylene–acrylate based copolymer by using these materials as flame retardant agent in PP. Formulations were based on an ethylene–butyl acrylate copolymer blended with polypropylene with a ratio 4:3 (CaSiEBA-PP), and an ethylene–methacrylic acid copolymer (CaSiEMAA, see also next part). In all formulations, the acrylate content is 8 wt% in the EBA copolymer, the chalk filling level 30–40 wt% and the silicone amount 5–7 wt%. Fig. 18 shows the TGA of these blends. The mass loss in a nitrogen atmosphere was very similar for all three formulations, proceeding principally in a single step which led to significant mass losses above 400 °C with a maximum rate at 460–470 °C. The more pronounced mass loss for CaSiEBA compared to CaSiEBA-PP is consistent with the higher butyl acrylate content in the former material (Fig. 18(a)) [89]. Under thermo-oxidative degradation, CaSiEBA-PP and CaSiEBA polymers displayed degradation in the three temperature regions, with

Table 8

Effect of chalk and silicone additions to flame retardancy of EBA copolymers [44].

Material	LOI (%)	Peak HRR ( $\text{kW m}^{-2}$ )	Ignition time (s)	Mass loss (%)
EBA	18	1304	77	98.1
SiEBA	19	1044	84	98.7
CaEBA	20	656	102	71.7
CaSiEBA	30.5	326	148	65.9

**Table 9**

Cone calorimetry results and LOI data for different mixing times of CaSiEBA composite<sup>a</sup> [92].

Material <sup>b</sup>	Mixing time (min)	Max HRR (kW m <sup>-2</sup> )	Average HRR (kW m <sup>-2</sup> )	Average ignition time (s)	LOI (%)
TRM-4 min	4	–	–	–	31.5
TRM-10 min	10	384	264	109	32.0
TRM-20 min	20	326	194	148	34.0
TRM-30 min	30	–	–	–	32.5
FSE	–	364	226	139	38.0

<sup>a</sup> Formulation: 30 wt% of chalk, 12.5 wt% of silicone and 57.3 wt% of EBA; cone calorimetry with incident heat flux of 35 kW m<sup>-2</sup>.

<sup>b</sup> TRM: two roll mill, FSE: full scale extruder.

a minor mass loss at 250 °C, followed by two major steps at 355 °C and 430 °C. The subsequent mass loss above 600 °C was due to degradation of the chalk filler. Acrylic acid and butyl acrylate polymers are known to show a significant decomposition at 360 °C (Fig. 18(b)). The higher initial mass loss of CaSiEBA-PP at 250 °C as compared to CaSiEBA, indicates the earlier decomposition of PP. Ignition of CaSiEBA-PP occurred as the surface layer reached temperatures between 350 and 400 °C, as was seen in Fig. 18(b). At these temperatures, CaSiEBA-PP has a significant mass loss, yielding the volatiles necessary for the ignitable gas. IR spectroscopy analysis confirmed that the decomposition of PP preceded the decomposition of EBA and provided a significant contribution to the ignitable gases. Therefore, the combustion of CaSiEBA-PP self-accelerates and leads to a rapid pyrolysis on the polymer surface.

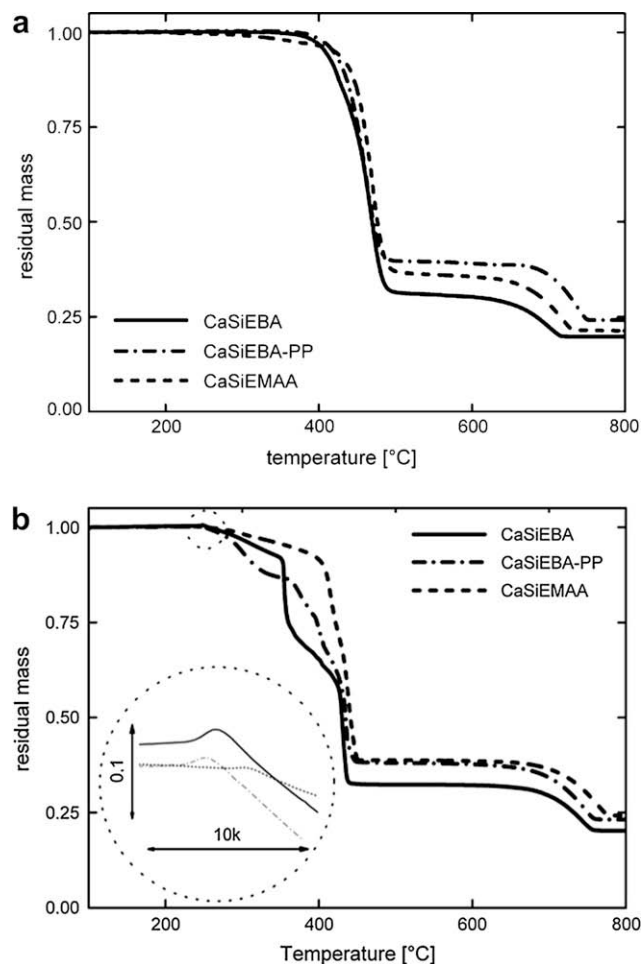


**Fig. 18.** TG data of several ethylene acrylate-based polymers containing flame retardant chalk and silicone at a heating rate of 10 °C min<sup>-1</sup>: (a) in nitrogen, (b) in air [89].

Moreover, the inner part of the composite did not have much time to undergo the beneficial calcium salt formation, which might lead to char expansion. This explained why the melt viscosity of CaSiEBA-PP was much lower than that for CaSiEBA [89].

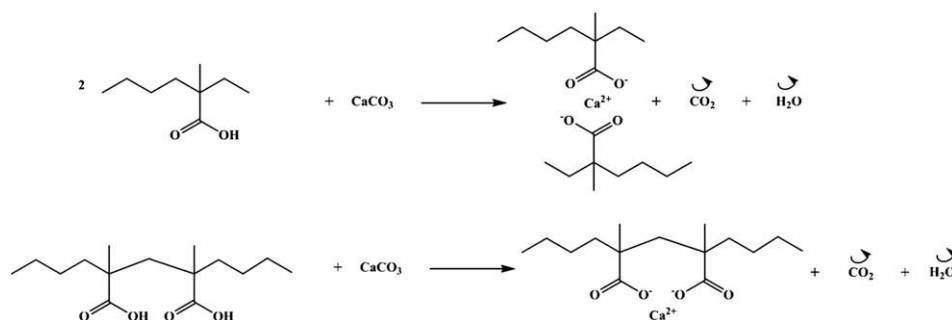
#### 4.4. Ethylene-methacrylic acid (EMAA), ethylene-methyl acrylate (EMA), and ethylene-ethyl acrylate (EEA) copolymers

Silicone as flame retardant in EMAA was studied by Krämer et al. [89]. EMAA copolymers were blended with chalk and silicone to form an ethylene-methacrylic acid copolymer (CaSiEMAA). The acrylate content of EMAA is 9 wt%, the chalk filling level amounted to 30–40 wt% and the silicone amounted to 5–7 wt% of the blends. The TGA showed the enhancement of thermal stability of EMAA by addition of chalk and silicone (Fig. 18). Thermo-oxidative degradation of CaSiEMAA displayed degradation in three temperature regions, with a minor mass loss at 250 °C, followed by major step at above 415 °C, and increasing further at 430 °C, while the mass loss at 600 °C was due to degradation of chalk (Fig. 18(b)). In their previous work, Krämer et al. [95] demonstrated the significant effect of coated and uncoated precipitated calcium carbonate nanoparticles with an average size of 70 nm on the thermal and thermo-oxidative stabilities of EMAA with a low filler content (5 wt%). Here, the high thermal stability of the EMAA formulation does not rely strongly on the silicone glass layer, but may rather be due to an interaction between calcium ions and carboxylate ions (Scheme 11). The char of the highly crosslinked samples was more stable but dissected by a myriad of small cracks. These observations agree with the assumption that the formation of calcium salt stabilises the polymer chains of EMAA and prevents a reduction in molar mass, rather than inducing a strong inter-chain cross-linking in the polymer. The increased melt viscosity shortens the time to ignition but significantly reduces heat release rate as measured by cone calorimetry. Two factors contributed to the melt viscosity of the polymer [89]: (i) Surface cross-linking on the particle surface between polymer and chalk. Calcium salt formation in polymer surface stabilizes the polymer chains and prevents a reduction in molar mass. Low viscosity suggests that inter-chain crosslinking by the calcium ion bonds is weak. (ii) Oxygen contributes to the increase in “complex viscosity”. Char formation is stronger in an oxidative environment, whereas the materials melt and form a pool in nitrogen. Oxygen may lead to cross-linking of the polymer chains to form a silicon oxide network on the sample surface through reactions with the silicone in the formulation. Note that studying the char stability and melt viscosity in detail is important, since it can be related to melt dripping which presents a major hazard in a fire: indeed, it increases the burning surface area which can lead to more intense fire and faster fire spread. Thermal improvement of other acrylate polymers thanks to PDMS was extensively studied by several authors. Santra et al. [96] reported that blends of ethylene methyl acrylate (EMA)–PDMS have different thermal stabilities depending on the composition of PDMS. Lower content of PDMS i.e. 30 wt% showed lower thermal stability compared to higher contents, i.e. above 50 wt%. The authors explained this result by formation of new C–C bond between EMA and PDMS as the result of crosslinking between radicals from EMA degradation and vinyl groups in PDMS. Later on, PDMS blended with ethylene ethyl acrylate (EEA) was reported to give the same beneficial effect as in EMA–PDMS blend [97].

#### 4.5. Low density polyethylene (LDPE)

Silicone elastomer containing chalk was used by Hermansson et al. [44] to improve flame retardancy of LDPE. LOI and cone calorimeter tests were performed on a composition containing





**Scheme 11.** Reaction scheme of calcium salt formation in EMAA/chalk composite.

about 12.5 wt% of silicone elastomer, 30 wt% of chalk and 57.3 wt% of LDPE, a halogen-free flame-retardant material with intumescent behaviour. The LOI value increased from 18 to 24.5, while cone calorimeter test at heat flux of  $35 \text{ kW m}^{-2}$  also showed a remarkable improvement in term of HRR, TTI, and mass loss (Table 10). According to Hermansson et al. [44], the flame retardancy in LDPE was exerted through synergetic formation from silicone and chalk of stable intumescent structure covered by chars as heat barrier, thus preventing combustible gases to maintain the flame. Addition of silicone only to LDPE could not lead to the formation of this heat barrier. TGA showed that there was no more residue of SiLDPE at a temperature of  $500^\circ\text{C}$ , whereas in CaSiLDPE they found 29.8 wt% of residue at  $500^\circ\text{C}$  and 17.2 wt% of residue at  $1000^\circ\text{C}$  respectively. Silicone alone has also been studied to enhance thermal stability of LDPE. Increasing thermal stability of LDPE by PDMS was explained by crosslinking formation between radicals from degradation product of LDPE and vinyl groups in PDMS backbone [97]. Degradation of LDPE, which is the source of radicals in the melt of the components, begins before the degradation of PDMS ceases, to favour crosslinking together with formation of new alkyl groups on the silicon atoms. Since blends of LDPE–PDMS are immiscible, ethylene–methyl acrylate copolymer was introduced as a chemical compatibiliser in the 50:50 blend of LDPE and PDMS rubber previously studied by Santra et al. [98]. EMA reacted with PDMS rubber during melt-mixing at  $180^\circ\text{C}$  to form EMA-grafted PDMS rubber (EMA-g-PDMS) in situ. An optimum proportion of the compatibiliser (EMA) was found to be 6 wt%. Later on, Jana and Nando [99] confirmed this result after investigating the thermal stability of blends of LDPE and PDMS (50:50) compatibilised with various proportions of EMA as polymeric compatibiliser. In addition to C–C crosslinks in the blend system, EMA-g-PDMS acts as virtual bridges between the two components holding the continuous (LDPE) and dispersed (PDMS) phases together. Therefore, formation of intra- as well as inter-molecular crosslinking between LDPE and PDMS matrix enhances the mechanical strength and stability of the blend. At higher proportions of EMA (beyond 6 wt%), most likely EMA-g-PDMS tends to form a separate phase with respect to LDPE and PDMS. In another study of EMA incorporation as compatibiliser in 75:25 LDPE–PDMS rubber blends, Jana et al. [100] found that the addition of 2 wt% EMA showed the optimum thermal stability compared to other compositions with 0 and 6 wt% EMA. Thus the quantity of compatibiliser (EMA) required for the different compositions of LDPE–PDMS needs to be systematically optimized.

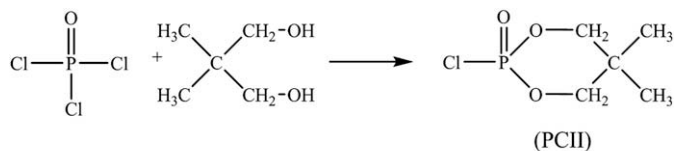
**Table 10**  
TGA, LOI and cone calorimeter results of CaSiLDPE [44].

Material	Peak HRR ( $\text{kW m}^{-2}$ )	Ignition time (s)	Mass loss (%)	LOI (%)
LDPE	1420	76	99.4	18
SiLDPE				0
CaLDPE				17.2
CaSiLDPE	320	95	69.4	24.5

#### 4.6. Polypropylene (PP)

Modified silicone-based flame retardant containing phosphorus, nitrogen and silicon called PSiN has been synthesized and used in polypropylene (PP) [101]. PSiN was prepared with various ratios of  $\alpha,\omega$ -dihydroxy-polydimethylsiloxane (PDMS), *N*- $\beta$ -(aminoethyl)- $\gamma$ -aminopropyl methyl dimethoxy silane (HD-103) in SiN synthesis by the route showed in Scheme 9(b) and neopentyl glycol phosphonyl chloride (PCII) (Scheme 12). Li et al. [102] reported that PSiN application in PP provided flame retardant performance as well as thermal stability for PP. At 30 wt% loading of PSiN, LOI value of PP/PSiN was enhanced from 17 to 26, and the char yield at  $800^\circ\text{C}$  was improved from 0 to 27 wt% with 4.4 wt% of P, 2 wt% of Si, and 1 wt% of N. The phosphorus in PSiN provides possibility for the PP blends to form char, and the silicon improves the thermal stability of char because when temperatures of PP/PSiN increased, silicon-containing compounds melt and migrate to the surface of the materials due to their low surface energy. Phosphorus-containing compounds degrade at relatively low temperature to form protective phosphorus–carbon layer with weak phosphate bonds. The nitrogen-containing compounds in the sample decompose to generate ammonia or other molecules. The high heat-insulating, heat-resistant generation and incombustible ammonia gas plays a role in reducing the flammability of materials. It is not flammable and can dilute the concentration of the oxygen near the surface of materials as well as swell the carbon layer during a fire. The silicon containing compounds degrade to generate silicon dioxide that could not be oxidized further and be left in the carbon layer, therefore it improves the thermal stability of the char layer. The foamed and thermally stable carbon layer shows good insulation properties in heat and mass transfer, which results in the improvement of fire performance of the polymer. A filler such as wollastonite was also added into PDMS to enhance flame retardancy of polypropylene. In a patent of Dow Corning, Romenesco and Shephard [103] proposed to disperse wollastonite in conjunction with a silicone gum or silicone base in a thermoplastic polyolefin (mainly polypropylene and polyethylene) resin. These materials were prepared with a view to improve insulation and jacketing materials for transmission media cable applications. They mentioned that the wollastonite used should have a particle size of  $2\text{--}30 \mu\text{m}$ , a needle-like shape, an aspect ratio (length:diameter) of 3:1 or greater. When burned, these thermoplastic silicone vulcanisates develop char structures with good integrity, and exhibit extremely low flame spread and smoke and heat generation properties. They showed that a better char structure is formed on burning when the calcium silicate is added at a ratio above 25 wt%, based on the total formulation. The upper limit of calcium silicate that is useful will depend on the properties desired in the uncured and cured compositions. Generally, calcium silicate present at greater than about 60 wt% of the total formulation results in uncured compositions too stiff and therefore difficult to process.





**Scheme 12.** The synthesis route of PSiN flame retardant.

#### 4.7. Poly(vinyl acetate) (PVAc)

Zulfiqar and Ahmad [104] studied the thermal stability of PVAc blended with several types of siloxane such as PDMS, polydiphenylsiloxane (PDPS) and poly(dimethyl/diphenylsiloxane) (PDMDPS). The thermal stability of PVAc–PDMS blends of different compositions is shown in Fig. 19. Polysiloxanes are substantially more stable than PVAc, so that increasing the quantity of polysiloxane in the blends, gradually increases the stability. Blends of PVAc and PDMS also led to slightly larger residue contents than the pure siloxane. This behaviour was explained by authors on the basis of crosslinking induced by the presence of catalysing agents such as  $\text{CH}_3\text{COOH}$  or acetate radicals which are released by PVAc. The free radicals diffusing from the PVAc phase are responsible for abstraction of hydrogen atoms from methyl groups in PDMS.

#### 4.8. Ethylene vinyl acetate (EVA)

In EVA copolymer for wire and cable applications, Davidson and Wilkinson [88] reported that the addition of 5 wt% of trimethylsilyl chain-ended PDMS gum and a stearate coated calcium carbonate (average particle size of 1.5  $\mu\text{m}$ ) remarkably improved flame retardancy of EVA copolymer (Table 11). Andreasson et al. [105] reported that, silicone together with calcium carbonate and MDH improved flame retardancy of EVA composites for cable and wire applications in terms of LOI. LOI of 40.8 was obtained when EVA composites contain 6.25 wt% of silicone, 29 wt% of calcium carbonate and 29 wt% of precipitated MDH. Addition of 2 wt% of  $\text{TiO}_2$  having average particle size of 2.5  $\mu\text{m}$  into EVA composites filled with MDH remarkably improved flame retardancy compared to EVA alone by LOI enhancement of about 36 to 37.

#### 4.9. Polystyrene (PS)

A composition containing 80:20 of PS–PDMS blend was synthesized and the thermal degradation and pyrolysis mechanisms were studied in detail by Lomakin et al. [106]. According to these authors, the flame retardation mechanism of PS by PDMS occurs both from thermal stabilization of PS in one hand and thermal destabilization of PDMS on the other hand, via cross-linking reactions of styrene and dimethylsiloxane fragments (Scheme 13). This mechanism has been proven by analyses of pyrolysis products formed from the PS–PDMS blend. At 600 °C they observed two new compounds. The first compound, apparently formed by the cross-reaction (termination) of two macro-radical fragments of the PS and PDMS chains, was identified as 3-phenyl-1-(3',3',5',5',7',7',9',9'-octamethylcyclopentasiloxo)butane (I in Scheme 13) and the second compound is a radical fragment of PS. Then at 800 °C, they found a new product identified as phenyl(3',3',5',5',7',7'-hexamethylcyclotetrasiloxo)propane, and formed by the cross-reaction of radical fragments of PS and PDMS degraded chains.

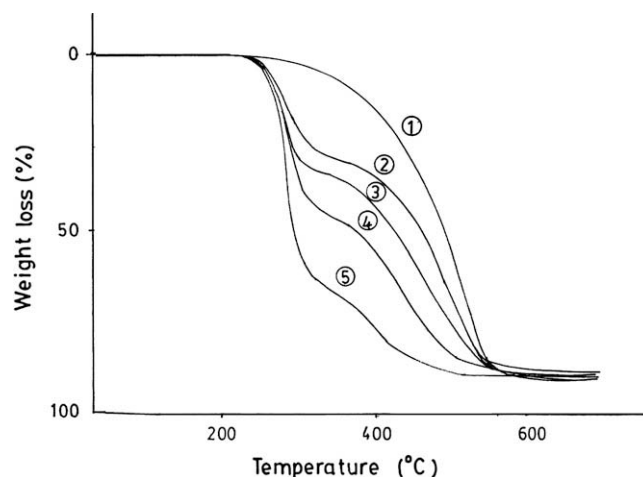


**Fig. 19.** TG curves (dynamic nitrogen, heating rate 10 °C/min) for PDMS:PVAc blends: 100% PDMS (1), 75% PDMS (2), 50% PDMS (3), 25% PDMS (4) and 0% PDMS (5).

#### 4.10. Poly(vinyl chloride) (PVC)

McNeill and Basan [107] reported the thermal degradation of blends of PVC with PDMS by thermogravimetry over the whole composition range. The results show destabilization at low loadings of PDMS, but for compositions with 50% or more PDMS, both polymers are stabilized. Similar effects were reported in the case of PVC blending with other polysiloxane polymers such as PDPS and PDMDPS [108] blends. Blends of higher siloxane contents show stability throughout the decomposition range, which increases with the siloxane concentrations due to delay in the release of chloride radicals.

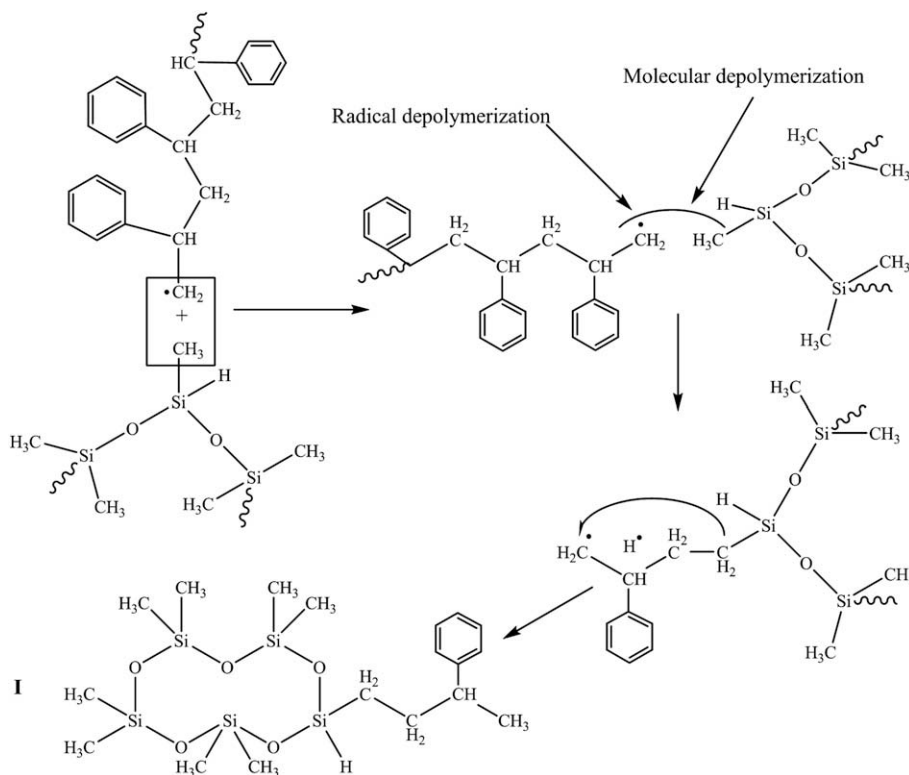
#### 4.11. Polyurethane (PU)

Belva et al. [109] reported that PDMS could not enhance the heat stability of polyurethane (PU) in thermo-oxidative conditions, but the amount of high temperature residue increased and depended on the amount of PDMS incorporated in PU chains due to formation and accumulation of silica (Fig. 20). PU/PDMS hybrid formed a protective layer limiting heat transfer between the flame and the substrate. In order to improve miscibility of PDMS in PU–PDMS blend, Santra et al. [110] proposed the addition of ethylene–methyl acrylate (EMA). The effect of EMA copolymer as a reactive polymeric compatibiliser in the blend was proven by mechanical property measurements and phase morphology studies. Similar to its compatibilising properties in LDPE–PDMS blend [98], EMA reacted with PDMS rubber during melt mixing to produce EMA-g-PDMS rubber in situ, which acted as the compatibiliser for the binary system of TPU and PDMS rubbers. EMA-g-PDMS rubber is believed to undergo specific interaction via hydrogen bonding with the TPU matrix through the ketone ( $\text{C}=\text{O}$ ) group of EMA and the unassociated amine ( $-\text{NH}-$ ) group of TPU, whereas the PDMS

**Table 11**

LOI value enhancement of different types of EVA copolymers by addition of silicone and stearate coated  $\text{CaCO}_3$  [88].

Vinyl acetate content in EVA copolymer (%)	EVA content (wt%)	Silicone (wt%)	$\text{CaCO}_3$ (wt%)	LOI (%)
28	65	5	30	27
28	60	5	35	28
28	55	5	40	29
28	50	5	45	34
18	50	5	45	29
40	50	5	45	30



**Scheme 13.** Pyrolysis mechanism of polystyrene–polydimethylsiloxane blend.

rubber in the EMA-g-PDMS disperses well with the bulk PDMS matrix.

#### 4.12. Polyamide-6 (PA-6)

Dong et al. [111] have developed two elastomeric flame retardants to improve flame retardancy of polyamide 6. S-ENP is made of resin silicone nanoparticles with  $T_g$  of  $-120^\circ\text{C}$  and particle size of  $\sim 100$  nm, and S-ENPC is S-ENP where unmodified clay with a dry weight ratio of 4/1 has been added. It has been found that S-ENP not only increases the toughness and improves the flame retardancy of polyamide-6, but also helps, in S-ENPC, unmodified clay exfoliate in polyamide-6 matrix (Fig. 21). The flammability properties of polyamide-6 composites characterized by cone calorimetry showed that nanocomposite containing 10 phr of S-ENP decreased the lower peak heat release rate (PHRR) down to 60% compared to pure polyamide-6, compared to 68% lower for composites containing 10 phr of S-ENPC. In S-ENPC, S-ENP and clay were found to have a synergistic flame retardant effect on polyamide-6 resulting from the formation of two barriers, coat-like layer and island-like flocculates, on the surface of the nanocomposite residue at the end of combustion.

#### 4.13. Epoxy resin

Liu and Chou [112] compared nano-scale silica, diglycidylether terminated-polydimethylsiloxane (PDMS-DG) and TEOS as silicon-source additive in phosphorus epoxy resin. Nano-scale silica could not migrate to surface of degraded residues during thermal degradation of epoxy resin, so it failed to show synergism with phosphorus on flame retardation. PDMS-DG and TEOS showed significant performance in silicon migration and could form a protective layer for preventing/retarding further degradation of char, but self-degradation of PDMS-DG during the heating period

resulted in some silicon loss in the condensed phase. Thus, formation of epoxy–silica hybrid structure through sol–gel reactions by using TEOS was a good approach for achieving phosphorus–silicon synergism of flame retardation in epoxy resins. Hsiue et al. [113] found that synergistic effect of phosphorus–silicon on epoxy resin fire resistance can be further levelled up by using modified siloxane reagents to replace silanes. They mixed 44.3 wt% of bis(3-glycidyloxy)phenylphosphine oxide (BGPPPO) with 34.6 wt% of diamine aminopropyl-terminated polydimethylsiloxane (PDMS-NH<sub>2</sub>) in place of the triglycidyloxy phenyl (TGPS). They obtained a high LOI value of 45 for the resin with

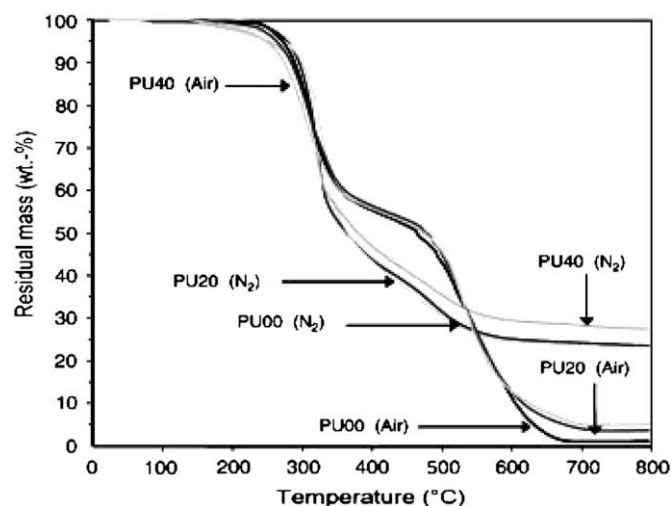


**Fig. 20.** TG curves of neat PU (PU00) and PU/PDMS hybrid (PU20: PU containing 20 wt% of PDMS and PU40: PU containing 40 wt% of PDMS) in nitrogen and air fluxes [109].

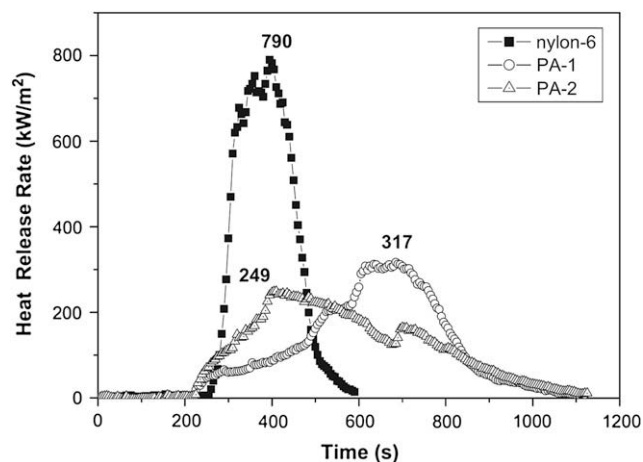


Fig. 21. Heat release rate (HRR) plots for pure polyamide-6, composite polyamide-6-S-ENP (PA-1) and composite polyamide-6-S-ENPC (PA-2) at a heat flux of  $35 \text{ kW m}^{-2}$  [111].

a phosphorus content of 4.8 wt% and a silicon content of 12.7 wt%. Furthermore, the LOI values increased with the increase in silicon content. This highly synergistic flame retardation efficiency of siloxane with phosphorus mainly comes from the formation of a continuous silica layer, which reduces thermal oxidation of the phosphorus char.

#### 4.14. Poly(bisphenol fluorenone carbonate) (BPFPC)

Only 5–10 wt% of silicone in multi-sequenced copolymers of bisphenol fluorenone carbonate and PDMS could enhance the LOI values of BPFPC from 38 to 51 [114]. Above 15 wt% of silicone blocks, LOI started to decrease. The residue changed from a fine, black, friable char formed with the homopolymer, to a more voluminous, very strong and large black char at moderate amounts of silicone, and to a gray, coarse, weak residue at high silicone contents. It was noticed that the mechanical properties of the formed char depended on the silicone content and represented an important requirement for obtaining higher LOI values.

## 5. Conclusions

Silicones are greatly acknowledged for their better thermal and thermo-oxidative stabilities compared to most carbon-based polymers. This acute resistance against flame has put PDMS in the top list of polymers for applications at high temperature where flame retarding behaviour is required. As a flame retardant, PDMS offers outstanding advantages such as halogen-free flame retardant with very low or almost zero emission of toxic smokes, thus considered to be among the “environmentally friendly” category of additives. Silicones can be used as flame retardant agents through direct blending within the polymer matrix, incorporation into porous filler, or by synthesizing block/graft copolymers including silicone segments. Silicone acts as a flame retardant through condensed phase by favouring the formation of a silica layer as a heat and mass transfer barrier. Therefore, the basic strategy of the flame retardation of silicone is to avoid ring formation and to increase the formation of silica as the pyrolysis product. Flame retardancy of silicone can be improved by filler addition. Several types of fillers have been used to improve flame retardancy of silicone, such as silica, calcium carbonate, wollastonite, mica, talc, kaolin, montmorillonite, carbon black, aluminium trihydrate, and magnesium dihydrate. Generally, calcium carbonate, wollastonite and mica improve flame retardancy of silicone by ceramization phenomena. Talc, kaolin, and

montmorillonite improve flame retardancy of silicone by catalytic effect which accelerates silica layer formation. Fillers such as calcium carbonate, wollastonite, mica, kaolin, and montmorillonite also improve the mechanical properties of the silica layer, an important issue when one knows that the fragile ash of silica residue formed by firing silicone may not be strong enough to function as a barrier in flame retardation for certain applications. Metal hydrate (ATH or MDH) favours heat absorption but ATH is less ideal for use as flame retardant agent in PDMS formulations applied in wire and cable applications because of its relatively low decomposition temperature and crack generation which is of inconvenience in terms of residue cohesion. For this reason, probably boehmite would be a better choice to avoid crack generation in the residue of firing silicone. The technology of fire-resistant silicones passes through the addition of low contents of additives such as stabilizers, synergistic agents, etc. depending on final product application. For instance, platinum, ZnO,  $\text{TiO}_2$ ,  $\text{ZrO}_2$ , CeO, FeO, and  $\text{Fe}_2\text{O}_3$  are additives that were commonly used to improve flame retardancy of silicone. Carbon nanotubes have hardly been tested as flame retardant fillers in PDMS, despite their known ability to dissipate heat. Finally, some works have shown that PDMS alone can enhance thermal stability of polycarbonate (PC), bisphenol fluorenone carbonate (BPFPC), nylon, and polyurethane. PDMS filled with flame retardants are used in some polymers such as PC-PDMS block copolymer, ethylene butyl acrylate (EBA), ethylene-methacrylic acid copolymer, polypropylene, low density polyethylene (LDPE), and ethylene vinyl acetate (EVA). Structure modification of silicone by incorporating some flame-retardant elements such as phosphorus and/or nitrogen has showed improved flame retardancy and intumescent char formation by synergistic effects. This type of silicone-based flame retardant has been widely used as additives in other polymer matrixes than silicone, such as polyurethane, PC/ABS alloy, polypropylene and epoxy resin.

## Appendix

Main techniques of fire retardancy evaluation quoted in this review are summarized below.

#### Cone calorimeter test

The cone calorimeter test is at present the most advanced method for assessing materials' reaction to fire. Indeed, this test gives a possibility to evaluate: (i) the ignitability; (ii) the combustibility; (iii) the smoke production and (iv) the production of toxic gases. Fig. 22 shows the principle of the cone calorimeter, based on the principle of oxygen consumption calorimetry. Generally, the heat of combustion of any organic material is directly related to the amount of oxygen required for combustion in which 13.1 MJ of heat is released per kg of oxygen consumed. The cone calorimeter brings quantitative analysis to materials flammability research by investigating parameters such as heat release rate (HRR), time to ignition (TTI), total heat release (THR) and mass loss rate (MLR). The HRR measurements can be further interpreted by looking at average HRR, peak HRR and time to peak HRR. Heat release rate is the key measurement required to assess the fire hazard of materials and products as it quantifies fire size, rate of fire growth and consequently the release of associated smoke and toxic gases. The cone calorimeter, if so configured, can also measure and quantify smoke output as well as  $\text{CO}/\text{CO}_2$  release rates [115]. Cone calorimeter tests can be conducted in accordance with national and international standards including BS 476 (Part 15), ASTM E1354 and ASTM E1474, and ISO 5660-1. An example of cone calorimeter test according to ISO 5660-1:1993 is given hereafter [116]. The surface of the test specimen is exposed to a constant level of heat irradiance, within

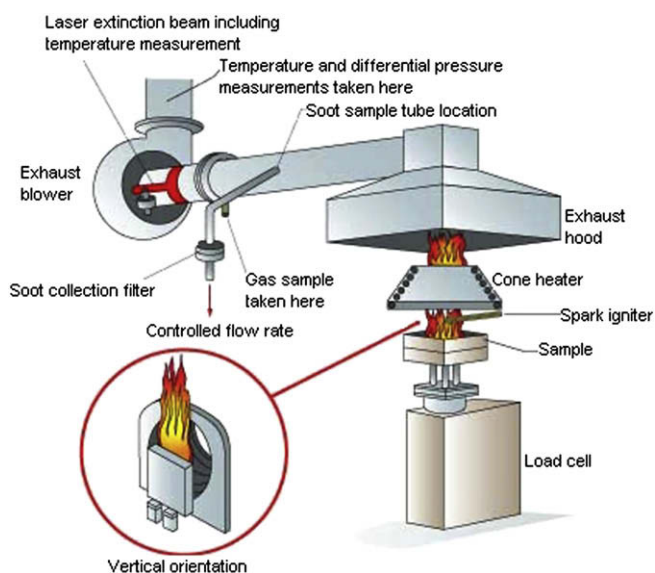


Fig. 22. Schematic principle of cone calorimeter [124].

the range  $0\text{--}100\text{ kW m}^{-2}$ , from a conical heater. Volatile gases from the heated specimen are ignited by an electrical spark igniter. Combustion gases are collected by an exhaust hood for further analysis. This gas analysis makes it possible to calculate heat release rate and to assess production of toxic gases from the specimen. Smoke production is assessed by measuring attenuation of a laser beam by smoke in the exhaust duct. The attenuation is related to volume flow, resulting in a measure of smoke density called smoke extinction area [ $\text{m}^2\text{ s}^{-1}$ ]. The specimen is mounted on a load cell which records the mass loss rate of the specimen during combustion. A thorough analysis requires testing at several irradiance levels. Typical levels of irradiance are 25, 35, 50 and  $75\text{ kW m}^{-2}$ . According to ISO 5660-1:1993(E), three specimens shall be tested at each heat flux level. The test result contains information about dimensions, pre-treatment and conditioning of the test specimens, and information about the test conditions. The following test results are tabulated: (i) time to ignition [TTI, s]; (ii) total heat released [THR,  $\text{MJ m}^{-2}$ ], (iii) maximum heat release rate [MHR,  $\text{kW m}^{-2}$ ], (iv) average heat release rate after 180 s and after 300 s [average  $\text{HRR}_{180}$ , or average  $\text{HRR}_{300}$ ,  $\text{kW m}^{-2}$ ], (v) effective heat of

combustion [EHC,  $\text{MJ kg}^{-1}$ ]; (vi) average smoke production [ $\text{m}^2\text{ s}^{-1}$ ], (vii) production of carbon monoxide (CO) [g]. It is also possible to measure production of other gas components, like cyanhydric acid (HCN). The following results are given graphically for each of the applied irradiation levels: (i) heat release rate [HRR,  $\text{kW m}^{-2}$ ]; (ii) rate of smoke production [ $\text{m}^2\text{ s}^{-1}$ ]; (iii) rate of production of CO and HCN [ $\text{g s}^{-1}$ ]; (iv) specimen mass as a function of time [ $\text{g s}^{-1}$ ]. The unit  $\text{m}^2$  is related to specimen area. The surface of the specimens shall be essentially flat. The specimens shall be representative of the product, and as far as possible be similar to the final product. A complete test requires that at least 12 specimens with dimensions of  $100\text{ mm} \times 100\text{ mm}$  and of maximum thickness of 50 mm be tested. Different types of typical burning behaviour give rise to characteristic curves of HRR vs. time. Some are illustrated in Fig. 23 [117].

#### Limiting oxygen index (LOI) test

The limiting oxygen index (LOI) or oxygen index (OI) is a method for evaluation of the flammability of materials. LOI is defined as the minimum concentration of oxygen in an oxygen–nitrogen mixture, required to sustain combustion of a vertically mounted test specimen. Hence, higher LOI values represent better flame retardancy [118]. Preliminary tests are first carried out in order to ascertain the approximate  $\text{O}_2/\text{N}_2$  ratio required for the material under investigation. This is reached when the materials burns at a uniform slow rate after ignition. The oxygen content of the  $\text{O}_2/\text{N}_2$  mixture is then lowered until the test specimen just continues to burn. After the next lower  $\text{O}_2$  concentration (a reduction of 0.2% in the oxygen content) the test specimen must be extinguished. Table 12 reports the oxygen index test specifications [118]. The oxygen index is determined by the US standard ASTM D 2863-77 [119] procedure which has been introduced as Nordtest method NT Fire 013. Fig. 24 shows the principle of the measurement and a figure of LOI test equipment.

#### UL-94 test

UL-94 is the standard applied by the American Underwriters Laboratories for testing the flammability and fire safety of plastic materials used in devices and appliances [120]. The standard classifies plastics according to the way they burn in various orientations and thicknesses. UL-94 applies not only to the electrical industry but also to all areas of applications except the use of plastics in building. UL-94 is particularly significant for plastics used in electrical products since a UL listing of the product frequently requires

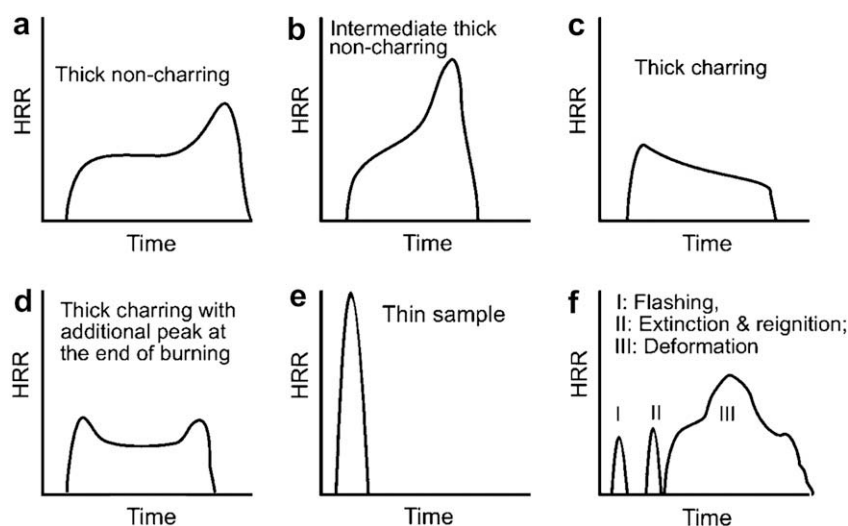


Fig. 23. Typical HRR curves for different characteristic burning behaviors [117].



**Table 12**  
Oxygen index test specifications.

Specimens	10 specimens 150 mm × 6 mm × 3 mm
Specimen position	Clamped vertically
Ignition source	Gas pilot flame
Test duration	Until the minimum oxygen concentration of an O <sub>2</sub> /N <sub>2</sub> mixture required to sustain combustion is reached
Results	Expressed as = $100 \times \text{O}_2 / \text{O}_2 + \text{N}_2$ (%)

a favourable flammability classification of the materials used [121]. UL-94 contains test procedures for both horizontally and vertically positioned test specimens in the form of rods. In the UL-94 HB (Horizontal Burning) test, the burning of a horizontal plastic specimen is tested, and in the most demanding HB, specifications are: slow burning on a horizontal specimen; burning rate < 76 mm/min for thickness < 3 mm. In UL-94 V (Vertical Burning) tests, the test specimen is vertical and ignited by a Bunsen burner to be classified according to their burning times as V-0, V-1, V-2. These tests are more rigorous than the HB test since the vertical specimens are burned by their lower ends, thus preheating material above it, and the samples must extinguish themselves. The test layout is illustrated in Fig. 25. A flame is applied twice to the lower end of the vertically suspended test specimen for 10 s. The top class, i.e. V-0 is achieved if the mean inter-flame time of five samples after 10 applications of the flame does not exceed 5 s. The material is placed in class V-1 if the mean after-flame time is less than 25 s. If flaming drippings occur, the material is classified in V-2; the ignition of surgical cotton placed below the specimen serves as a criterion for this phenomenon.

#### Relation between LOI, cone calorimeter and UL-94 tests

Since cone calorimeter measures flammability in different manner than LOI and UL-94 fire tests, one should not be surprised by the poor correlation between them. Morgan and Bundy [116]

tried to explain differences among LOI, cone calorimeter and UL-94 test. LOI is a small-scale test that uses a variable percentage oxygen atmosphere to maintain a candle-like burn, and UL-94 V applies a small calibrated flame twice under the sample (configured vertically) for 10 s followed by measuring time to extinguishment after each flame application. Cone calorimetry, on the other hand, uses a forced combustion in which radiant heat is projected onto a sample before ignition and during burning of the sample. The sample is usually in a horizontal configuration, thus eliminating any physical effects of polymer burning (dripping away from the flame, for example) that are sometimes used to pass the UL-94 V test, especially under the V-2 rating. Further, the sample in the cone calorimeter exposed to continuous heat during the test is well ventilated, whereas UL-94 is not. In effect, cone calorimeter measures the material response to constant fire threat with time, whereas UL-94 measures the material response to remove a fire threat and its time to self-extinction. Therefore, some studies have been conducted to show correlations between UL-94, LOI and cone calorimeter tests.

**LOI and UL-94 relationship:** there have been many efforts to correlate LOI and UL-94 tests systematically. Generally, the LOI values of UL-94 V-1, V-0 rated materials were higher than those of HB materials. However, it does not mean that higher LOI gives better UL-94 V ratings [122]. Weil et al. [123] reported that the LOI value might be levelled with UL-94 or cone calorimeter data to some degree in certain conditions but it was hard to show close relations between LOI and UL-94 or cone calorimeter data because of the downward burning test condition of LOI.

**Cone calorimeter and UL-94 relationship:** studies about the quantitative relationship between UL-94 V and cone calorimeter remain elusive, even if the cone calorimeter can be used to understand why a material passes or fails a particular UL-94 V rating [116]. In particular, a  $\text{HRR}_0 > 100 \text{ kW m}^{-2}$  for materials showed sustained ignition (HB) in the UL-94 test, while a  $\text{HRR}_0 < 100 \text{ kW m}^{-2}$  correlated well with self-extinguishing behaviour [124].

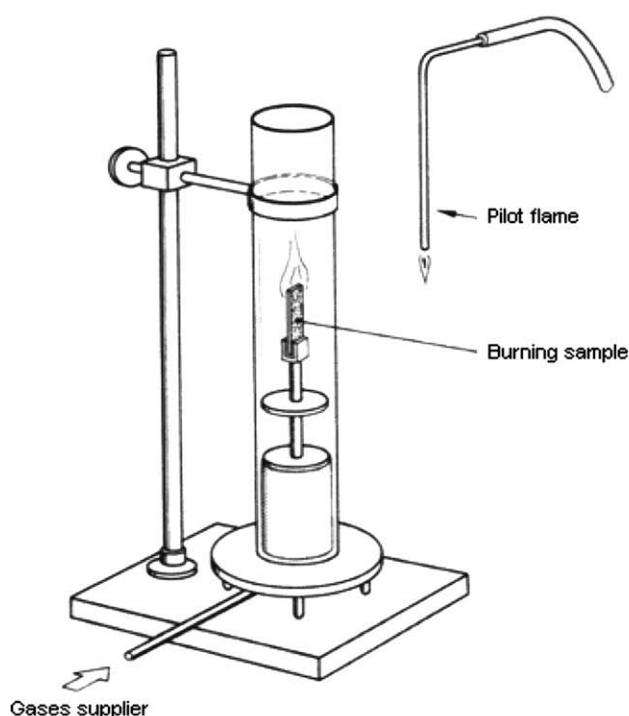


**Fig. 24.** Installation scheme and a photo of LOI test equipment [118].

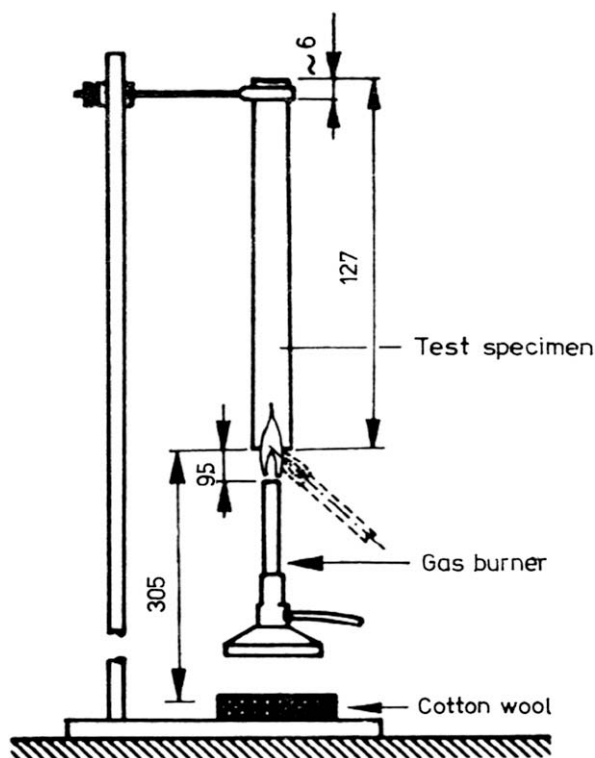


Fig. 25. Installation scheme of UL-94 equipment [121].

*LOI, UL-94 and HRR (cone calorimeter) relationship:* Hong et al. [122] showed that HRR obtained from the cone calorimeter was more related to UL-94 ratings than LOI. The lower the HRR, the better the UL-94 rating obtained. Still, it seems that more studies are required to clarify the correlation between HRR and UL-94.

## References

- [1] Biron M. Silicones or siloxanes applications. *Techniques de l'Ingénieur* Oct 2007;N2882 (in French).
- [2] Dvornic PR. In: Jones RG, Ando W, Chojnowski J, editors. *Thermal stability of polysiloxanes: silicone-containing polymers*. Dordrecht, the Netherlands: Kluwer Academic Publisher; 2000. p. 185–212.
- [3] Buch RR. Rates of heat release and related fire parameters for silicones. *Fire Safety* 1991;17:1–12.
- [4] Hsieh F-Y. Shielding effects of silica-ash layer on the combustion of silicones and their possible applications on the fire retardancy of organic polymers. *Fire Mater* 1998;22:69–76.
- [5] Marosi G, Márton A, Anna P, Bertalan G, Marosfoi B, Szép A. Ceramic precursor in flame retardant systems. *Polym Degrad Stab* 2002;77:259–65.
- [6] Wen J, Mark J. Mechanical properties and structural characterization of poly(dimethylsiloxane) elastomers reinforced with zeolite fillers. *J Mater Sci* 1994;29(2):499–503.
- [7] Mansouri J, Burford RP, Cheng YB, Hanu L. Formation of strong ceramified ash from silicone-based compositions. *J Mater Sci* 2005;40:5741–9.
- [8] Camino G, Lomakin S, Lazzari M. Polydimethylsiloxane thermal degradation. Part 1. Kinetic aspects. *Polymer* 2001;42(6):2395–402.
- [9] Radhakrishnan TS. New method for evaluation of kinetic parameters and mechanism of degradation from pyrolysis–GC studies: thermal degradation of polydimethylsiloxanes. *J Appl Polym Sci* 1999;73:441–50.
- [10] Grassie N, Macfarlane IG. The thermal degradation of polysiloxane-I poly (dimethylsiloxane). *Eur Polym J* 1978;14:875–84.
- [11] Camino G, Lomakin S, Lagard M. Thermal polydimethylsiloxane degradation. Part 2. The degradation mechanisms. *Polymer* 2002;43(7):2011–5.
- [12] Deshpande G, Rezac ME. The effect of phenyl content on the degradation of poly(dimethyl/diphenylsiloxane) copolymers. *Polym Degrad Stab* 2001;74:363–70.
- [13] Jovanovic JD, Govedarcia MN, Dvornic PR, Popovic IG. The thermogravimetric analysis of some polysiloxanes. *Polym Degrad Stab* 1998;61:87–93.
- [14] Grassie N, Francey K. The thermal degradation of polysiloxanes. Part 3. Poly(dimethyl/methyl phenyl siloxane). *Polym Degrad Stab* 1980;2(1):53–66.
- [15] Grassie N, Francey KF, Macfarlane IG. The thermal degradation of PDMS. Part 4: poly(dimethyl/diphenyl siloxane). *Polym Degrad Stab* 1980;2(1):67–83.
- [16] Connell JE, Metcalfe E, Thomas MJK. Silicate–siloxane fire retardant composites. *Polym Int* 2000;49:1092–4.
- [17] Hayashida K, Tsuge S, Ohtani H. Flame retardant mechanism of polydimethylsiloxane material containing platinum compound studied by analytical pyrolysis techniques and alkaline hydrolysis gas chromatography. *Polymer* 2003;44:5611–6.
- [18] Lagarde R, Lahaye J, Bargain M. Mécanisme d'ignifugation d'élastomères organosilicés par le platine. *Eur Polym J* 1977;13:769.
- [19] Smith SB. Method of preparing fire retardant siloxane foams and foams prepared therefrom, US Patent 3,923,705; 1975.
- [20] Fujiki H, Tanaka M. Silicone coated base material and air bag base material, European Patent 0,669,419; 1995.
- [21] Hatanaka M, Mahekawa R, Maruyama H. Flame retardant silicone rubber compositions, US Patent 3,862,082; 1975.
- [22] Schroeder RM, Tselepis AJ, Wolf ATF. Sprayable silicone emulsions which form elastomers having smoke and fire resistant properties, European Patent 0,839,853; 1998.
- [23] Ota K, Hirai K. Flame retardant silicone rubber composition for coating electrical wire and cable, US Patent 6,011,105; 1998.
- [24] Gun'ko VM, Borysenko MV, Pissis P, Spanoudaki A, Shinyashiki N, Sulim IY, et al. Polydimethylsiloxane at the interfaces of fumed silica and zirconia/fumed silica. *Appl Surf Sci* 2007;253:7143–56.
- [25] Anon, Composition organopolysiloxaniques, French Patent 2,166,313; 1972.
- [26] Dubois R, Pouchelon A, Pusineri C. Utilisation de mélanges à base de Pt et de composé de métaux de transition autres que le Pt pour améliorer les propriétés de résistance à l'arc des élastomères silicones, World Patent 98,029,488; 1998.
- [27] Alexandre M, Dubois P, Devalckenaere M, Claes M. Fireproof composition. World Patent 2007,048,208; 2007.
- [28] Hancock M. In: Rothon R, editor. *Filled thermoplastic: particulate-filled polymer composites*. New York, USA: Longman Scientific and Technical; 2003. p. 279–316.
- [29] Harper CA. *Modern plastics handbook*. Maryland, USA: McGraw Hill; 1999. pp. 4.26–4.36.
- [30] Hornsby PR, Rothon RN. In: Le Bras M, Wilkie CA, Bourbigot S, Duquesne S, Jama C, editors. *Fire retardant fillers for polymers: fire retardancy of polymers: new applications of mineral fillers*. Cambridge, United Kingdom: RSC; 2005. p. 19–41.
- [31] Osman MA, Atallah A, Kahr G, Suter UW. Reinforcement of poly(-dimethylsiloxane) networks by montmorillonite platelets. *J Appl Polym Sci* 2002;83:2175–83.
- [32] Clerc L, Ferry L, Leroy E, Lopez-Cuesta J-M. Influence of talc physical properties on the fire retarding behaviour of (ethylene-vinyl acetate copolymer/magnesium hydroxide/talc) composites. *Polym Degrad Stab* 2005;88:504–11.
- [33] Szép A, Szabo A, Tóth N N, Anna P, Marosi G. Role of montmorillonite in flame retardancy of ethylene-vinyl acetate copolymer. *Polym Degrad Stab* 2006;91:593–9.
- [34] Demir MM, Menciloglu YZ, Erman B. Effect of filler amount on thermoelastic properties of poly(dimethylsiloxane) networks. *Polymer* 2005;46:4127–34.
- [35] Arrighi V, Higgins JS, Burgess AN, Floudas G. Local dynamics of poly(dimethyl siloxane) in the presence of reinforcing filler particles. *Polymer* 1998;39:6369–76.
- [36] Yuan QW, Mark JE. Reinforcement of PDMS networks by blended and in-situ generated silica fillers having various sizes, size distributions, and modified surfaces. *Macromol Chem Phys* 1999;200:206–20.
- [37] Kozakiewicz J, Huang SJ. The effects of filler surface modifications on the properties of poly(dimethyl siloxane) elastomers. *Org Coat Plast Chem* 1981;44:343–6.
- [38] Kashiwagi T, Gilman JW, Butler KM, Harris RH, Shields JR, Asano A. Flame retardant mechanism of silica gel/silicas. *Fire Mater* 2000;24:277–89.
- [39] Tanahashi M, Hirose M, Lee J-C, Takeda K. Organic–inorganic nanocomposites prepared by mechanical smashing of agglomerated silica ultrafine particles in molten thermoplastic resin. *Polym Adv Technol* 2006;17:981–90.
- [40] Liu Y-L, Li S-H. Poly(dimethylsiloxane) star polymers having nanosized silica cores. *Macromol Rapid Commun* 2004;25:1392–5.
- [41] Briggs CC. In: Pritchard G, editor. *Calcium carbonate: plastics additives: an A–Z reference*. London: Chapman & Hall; 1998. p. 148–52.
- [42] Deodhar S, Shanmuganathan K, Patra P, Fan Q, Calvert P, Warner S, et al. Polypropylene based novel flame retardant nanocomposite compositions. In: *Technical Papers in Composites 2006 Convention and Trade Show American Composite Manufacturers Association*. St Louis, MO USA; October 18–20, 2006.
- [43] Xu X, Tao X, Gao C, Zheng Q. Studies on the steady and dynamic rheological properties of poly(dimethyl-siloxane) filled with calcium carbonate based on superposition of its relative functions. *J Appl Polym Sci* 2008;107:1590–7.
- [44] Hermansson A, Hjertberg T, Sultan B-A. The flame retardant mechanism of polyolefins modified with chalk and silicone elastomer. *Fire Mater* 2003;27:51–70.
- [45] Pritchard G. Fillers. In: Pritchard G, editor. *Plastics additives: an A–Z reference*. United Kingdom: Chaall; 1998. p. 241–51.
- [46] Park ES. Mechanical properties and processibility of glass-fiber, wollastonite, and fluoro rubber reinforced silicone rubber composites. *J Appl Polym Sci* 2007;105:460–8.
- [47] Nicholson WR, Rapson L, Shephard K. Flame retardant silicone foams, US Patent 6,084,002; 2000.
- [48] Shephard KL. Flame resistant silicone rubber wire and cable coating composition, US Patent 6,239,378; 2001.

- [49] George C, Pouchelon A, Thiria R. Composition polyorganosiloxanes vulcanisables à chaud utilisable notamment pour la fabrication de fils ou câbles électriques, French Patent 2,899,905; 2006.
- [50] Briggs CC. In: Pritchard G, editor. *Mica: plastics additives: an A–Z reference*. London: Chapman & Hall; 1998. p. 459–63.
- [51] Osman MA, Atallah A, Müller M, Suter UW. Reinforcement of poly(dimethylsiloxane) networks by mica flakes. *Polymer* 2001;42:6545–56.
- [52] Hanu LG, Simon GP, Mansouri J, Burford RP, Cheng YB. Development of polymer–ceramic composites for improved fire resistance. *J Mater Process Technol* 2004;153–154:401–7.
- [53] Hanu LG, Simon GP, Cheng YB. Preferential orientation of muscovite in ceramifiable silicone composites. *Mater Sci Eng A* 2005;398:180–7.
- [54] Mansouri J, Burford RP, Cheng YB. Pyrolysis behaviour of silicone-based ceramifying composites. *Mater Sci Eng A* 2006;425:7–14.
- [55] Ariagno D, Barruel P, Viale A. Heat-vulcanisable organopolysiloxanes, intended for coating of electrical cables. *European Patent* 0,467,800; 1992.
- [56] Branlard P, George C, Leuci C. Polyorganosiloxane compositions vulcanisable by hot process useful in particular for making electric wires or cables. *European Patent* 1,238,007; 2003.
- [57] Alexander G, Cheng Y, Burford R, Shanks R, Mansouri J, Hodzic A, et al. Fire resistant silicone polymer compositions, *World Patent* 2004,013,255; 2004.
- [58] Hanu LG, Simon GP, Cheng YB. Thermal stability and flammability of silicone polymer composites. *Polym Degrad Stab* 2006;91:1373–9.
- [59] Mansouri J, Wood A, Roberts K, Cheng Y-B, Burford RP. Investigation of the ceramifying process of modified silicone–silicate compositions. *J Mater Sci* 2007;42:6046–55.
- [60] Henrist C, Rulmont A, Cloots R, Gilbert B, Bernard A, Beyer G. Toward the understanding of the thermal degradation of commercially available fire-resistant cable. *Mater Lett* 2000;46:160–8.
- [61] Genovese A, Shanks RA. Fire performance of poly(dimethyl siloxane) composites evaluated by cone calorimetry. *Compos Part A Appl Sci Manuf* 2008;39(2):398–405.
- [62] Lynch TJ, Chen T, Riley D. Advances in ATH benefit composite products. *Reinforc Plast* 2003;9:44–6.
- [63] Troitzsch HJ. In: Gächter R, Müller H, editors. *Flame retardants: plastics additives*. Cincinnati: Hanser Publisher; 1993. p. 709–48.
- [64] Horn WE. In: Grand DAF, Wilkie CA, editors. *Inorganic hydroxycarbonates: their function and use as flame retardant additives: fire retardancy of polymeric materials*. USA: CRC Press; 2000. p. 285–352.
- [65] Lewin M. In: Le Bras M, Camino G, Bourbigot S, Delobel R, editors. *Fire retardancy of polymeric materials: strategies: fire retardancy of polymeric materials: the use of intumescent*. London: The Royal Society of Chemistry; 1999. p. 1–32.
- [66] Hiremath S, Roy S. Aluminium trihydrate (ATH)-a versatile material. *Bhel J* 2007;28:12–9.
- [67] Miyata S. Composite metal hydroxide and its use, *US Patent* 5,401,442; 1995.
- [68] Toporcer LH, Dibling MR. Flame retardant elastomeric composition, *US Patent* 5,260,372; 1993.
- [69] Tkaczyk JE, Klug FJ, Amarasakera J, Sumpter CA. Silicone composition with improved high temperature tolerance, *US Patent* 6,051,642; 2000.
- [70] Sweet R, Gallmeyer JH. A silicone composition useful in flame retardant applications, *World Patent* 2004,063,280; 2004.
- [71] Gilman JW, Jackson CL, Morgan AB, Richard Jr H. Flammability properties of polymer-layered-silicate nanocomposites: polypropylene and polystyrene nanocomposites. *Chem Mater* 2000;12(7):1866–73.
- [72] Leszczyńska A, Njuguna J, Pielichowski K, Banerjee JR. Polymer/montmorillonite nanocomposites with improved thermal properties. Part I: factors influencing thermal stability and mechanisms of thermal stability improvement. *Thermochim Acta* 2007;453:75–96.
- [73] Burnside SD, Giannelis EP. Synthesis and properties of new poly(dimethylsiloxane) nanocomposites. *Chem Mater* 1995;7(9):1597–600.
- [74] Burnside SD, Giannelis EP. Nanostructure and properties of polysiloxane-layered silicate nanocomposites. *Polym Sci Part B: Polym Phys* 2000;38:1595–604.
- [75] Ma J, Xu J, Ren J-H, Yu Z-Z, Mai Y-W. A new approach to polymer/montmorillonite nanocomposites. *Polymer* 2003;44:4619–24.
- [76] Wang SJ, Long C, Wang X, Li Q, Qi Z. Synthesis and properties of silicone rubber/organomontmorillonite hybrid nanocomposites. *J Appl Polym Sci* 1998;69:1557–61.
- [77] Yang L, Hu Y, Lu H, Song L. Morphology, thermal, and mechanical properties of flame-retardant silicone rubber/montmorillonite nanocomposites. *J Appl Polym Sci* 2006;99:3275–80.
- [78] Pape PG, Romenesco DJ. The role of silicone powders in reducing the heat release rate and evolution of smoke in flame retardant thermoplastics. *J Vinyl Addit Technol* 1997;3:225–32.
- [79] Iji M, Serizawa S. Silicone derivatives as new flame retardants for aromatic thermoplastics used in electronic devices. *Polym Adv Technol* 1998;9:593–600.
- [80] Nodera A, Kanai T. Flame retardancy of a polycarbonate-polydimethylsiloxane block copolymer: the effect of the dimethylsiloxane block size. *J Appl Polym Sci* 2006;100:565–75.
- [81] Nodera A, Kanai T. Flame retardancy of polycarbonate-polydimethylsiloxane block copolymer/silica nanocomposites. *J Appl Polym Sci* 2006;101:3862–8.
- [82] Yasuhiro H, Kazuhiko I. Polycarbonate resin composition and its molded articles, *US Patent* 6,664,313; 2003.
- [83] Barren JP, Chen FF-S, Osborn AJ. Polycarbonate resin blends containing titanium dioxide, *US Patent* 6,133,360; 2000.
- [84] Lupinski JH, Howkins CM. Flame retardant polycarbonate compositions, *US Patent* 5,153,251; 1992.
- [85] Zhong H, Wu D, Wei P, Jiang P, Li Q, Hao J. Synthesis, characteristic of a novel additive-type flame retardant containing silicon and its application in PC/ABS alloy. *J Mater Sci* 2007;42(24):10106–12.
- [86] Zhong H, Wei P, Jiang P, Wang G. Thermal degradation behaviors and flame retardancy of PC/ABS with novel silicon-containing flame retardant. *Fire Mater* 2007;31:411–23.
- [87] Zhong H, Wei P, Jiang P, Wu D, Wang G. Synthesis and characteristics of a novel silicon-containing flame retardant and its application in poly[2,2-propane-(bisphenol) carbonate]/acrylonitrile butadiene styrene. *J Polym Sci: Part B Polym Phys* 2007;45:1542–51.
- [88] Davidson NS, Wilkinson K. Flame retardant polymer composition, *European Patent* 0,393,959; 1990.
- [89] Krämer RH, Blomqvist P, Hees PV, Gedde UW. On the intumescence of ethylene-acrylate copolymers blended with chalk and silicone. *Polym Degrad Stab* 2007;92:1899–910.
- [90] Hermansson A, Hjertberg T, Sultan B-A. Linking the flame-retardant mechanisms of an ethylene-acrylate copolymer, chalk and silicone elastomer system with its intumescent behaviour. *Fire Mater* 2005;29:407–23.
- [91] Lipatov YS. *Polymer reinforcement*. Canada: ChemTech Publishing; 1995. pp. 361–389.
- [92] Hermansson A, Hjertberg T, Sultan B-A. Distribution of calcium carbonate and silicone elastomer in a flame retardant system based on ethylene-acrylate copolymer, chalk and silicone elastomer and its effect on flame retardant properties. *J Appl Polym Sci* 2006;100:2085–95.
- [93] Sultan B-A, Hermansson A, Hjertberg T. Flame retardant polymer composition, *European Patent* 1,316,581; 2003.
- [94] Huhtala J, Motha K. Flame retardant polymer composition comprising nanofillers, *European Patent* 1,512,718; 2005.
- [95] Krämer RH, Raza MA, Gedde UW. Degradation of poly(ethylene-co-methacrylic acid)-calcium carbonate nanocomposites. *Polym Degrad Stab* 2007;92(10):1795–802.
- [96] Santra RN, Mukunda PG, Nando GB, Chaki TK. Thermogravimetric studies on miscible blends of ethylene-methyl acrylate copolymer (EMA) and polydimethylsiloxane rubber (PDMS). *Thermochim Acta* 1993;219:283–92.
- [97] McNeill IC, Mohammed MH. Thermal analysis of blends of low density polyethylene, poly(ethyl acrylate) and ethylene ethyl acrylate copolymer with polydimethylsiloxane. *Polym Degrad Stab* 1995;50(3):285–95.
- [98] Santra RN, Samantaray BK, Bhowmick AK, Nando GB. In situ compatibilization of low-density polyethylene and polydimethylsiloxane rubber blends using ethylene-methyl acrylate copolymer as a chemical compatibilizer. *J Appl Polym Sci* 1993;49(7):1145–58.
- [99] Jana RN, Nando GB. Thermogravimetric analysis of blends of low-density polyethylene and poly(dimethyl siloxane) rubber: the effects of compatibilizers. *J Appl Polym Sci* 2003;90(3):635–42.
- [100] Jana RN, Mukunda PG, Nando GB. Thermogravimetric analysis of compatibilized blends of low density polyethylene and poly(dimethyl siloxane) rubber. *Polym Degrad Stab* 2003;80(1):75–82.
- [101] Li Q, Jiang P, Wei P. Synthesis, characteristic, and application of new flame retardant containing phosphorus, nitrogen, and silicon. *Polym Eng Sci* 2006;46:344–50.
- [102] Li Q, Jiang P, Su Z, Wei P, Wang G, Tang X. Synergistic effect of phosphorus, nitrogen, and silicon on flame-retardant properties and char yield in polypropylene. *J Appl Polym Sci* 2005;96:854–60.
- [103] Romenesco DJ, Shepard KL. Fire resistant thermoplastic silicone vulcanizates, *World Patent* 2000,046,291; 2000.
- [104] Zulfiqar S, Ahmad S. Thermal degradation of blends of PVAC with polysiloxane – II. *Polym Degrad Stab* 2001;71(2):299–304.
- [105] Andreasson U, Fagrell O, Sultan BA. Flame retardant polymer composition, *European Patent* 1,396,865; 2004.
- [106] Lomakin SM, Koverzanova EV, Shilkina NG, Usachev SV, Zaikov GE. Thermal degradation of polystyrene–polydimethylsiloxane blends. *Russ J Appl Chem* 2003;76(3):472–82.
- [107] McNeill IC, Basan S. Thermal degradation of blends of PVC with polydimethylsiloxane. *Polym Degrad Stab* 1993;39(2):139–44.
- [108] Zulfiqar S, Ahmad S. Thermal degradation of blends of PVC with polysiloxane – I. *Polym Degrad Stab* 1999;65:243–7.
- [109] Belva F, Bourbigot S, Duquesne S, Jama C, Le Bras M, Pelegrin C, et al. Heat and fire resistance of polyurethane–polydimethylsiloxane hybrid material. *Polym Adv Technol* 2006;17:304–11.
- [110] Santra RN, Roy S, Tikku VK, Nando GB. In situ compatibilization of thermoplastic polyurethane and polydimethyl siloxane rubber by using ethylene methyl acrylate copolymer as a reactive polymeric compatibilizer. *Adv Polym Technol* 1995;14(1):59–66.
- [111] Dong W, Zhang X, Liu Y, Wang Q, Gui H, Gao J, et al. Flame retardant nanocomposites of polyamide 6/clay/silicone rubber with high toughness and good flowability. *Polymer* 2006;47:6874–9.
- [112] Liu YL, Chou C-I. The effect of silicon sources on the mechanism of phosphorus–silicon synergism of flame retardation of epoxy resins. *Polym Degrad Stab* 2005;90:515–22.
- [113] Hsiue GH, Liu Y-L, Tsiao J. Phosphorus-containing epoxy resins for flame retardancy V: synergistic effect of phosphorus–silicon on flame retardancy. *J Appl Polym Sci* 2000;78:1–7.

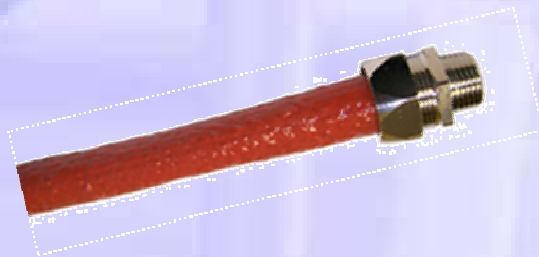
- [114] Kashiwagi T, Gilman JW. Silicon based flame retardants. In: Grand AF, Wilkie CA, editors. Fire retardancy of polymeric materials, vol. 10. New York: Marcel Dekker Inc.; 2000. p. 353–89.
- [115] Morgan AB, Bundy M. Cone calorimeter analysis of UL-94 V-rated plastics. *Fire Mater* 2007;31:257–83.
- [116] International Organization for Standardization. Fire tests. Reaction to fire. Part 1: rate of heat release from building products (cone calorimeter method), vol. 5660-1. Geneva: ISO; 1993(E).
- [117] Scharrel B, Hull TR. Development of fire-retarded materials – interpretation of cone calorimeter data. *Fire Mater* 2007;31:327–54.
- [118] Becker W, Rupprecht H, Troitzsch J. In: Troitzsch J, editor. Building: international plastics flammability handbook. Munich: Hanser Publishers; 1990. p. 93–284.
- [119] Limiting Oxygen Index (LOI): ASTM D2863-97. Standard test method for measuring the minimum oxygen concentration to support candle-like combustion of plastics (Oxygen Index).
- [120] <http://www.ul.com/plastics/flame.html>
- [121] Kaufmann W, Prager FH, Schiffer HW. In: Troitzsch J, editor. Electrical engineering: international plastics flammability Handbook. Munich: Hanser Publishers; 1990. p. 344–78.
- [122] Hong S, Yang J, Ahn S, Mun Y, Lee G. Flame retardancy performance of various UL94 classified materials exposed to external ignition sources. *Fire Mater* 2004;28:25–31.
- [123] Weil ED, Hirschler MM, Patel NG, Said MM, Shakir S. Oxygen index: correlations to other fire tests. *Fire Mater* 1992;16:159–67.
- [124] Lyon R. Fire and Flammability. Personal communication in symposium on Fire Safe Electronics, 2003.





## *Chapitre 2.*

# *Etude de la Matrice*





## **Synergie entre la silice et le platine pour obtenir un haut taux de résidu et une résistance au feu améliorée lors de la pyrolyse de formulations à base de silicone**

Plusieurs méthodes sont actuellement connues et appliquées pour améliorer le comportement au feu du silicone, telles que l'ajout de charges inorganiques, de platine (Pt) ou d'additifs organiques. Concernant l'ajout de platine, il a été montré qu'il améliore la stabilité thermique et le comportement au feu du silicone [1,2,3] via une modification du mécanisme de dégradation du silicone. La dégradation de formulations silicone exemptes de platine génère une grande quantité de petits cycles, notamment de l'hexaméthylcyclotrisiloxane ( $D_3$ ) et de l'octaméthyl-cyclotetracyclosiloxane ( $D_4$ ). En présence de Pt et de silice, des produits supplémentaires, le méthane et le dihydrogène sont également détectés. La dégradation du silicone, dans ce dernier cas, fait donc intervenir un processus de réticulation radicalaire [4]. Pour des formulations ne comportant pas de silice, l'action du platine sur l'amélioration de la stabilité thermique et du comportement au feu est beaucoup moins significative [1]. Il est suggéré que la silice améliore ces deux paramètres par la formation d'une couche barrière [5].

Afin de mieux comprendre les rôles respectifs du platine et de la silice, nous avons décidé d'étudier chaque étape du mécanisme de dégradation des formulations à matrice silicone. Cette étude est basée sur des formulations simples de silicone contenant un polydiméthylsiloxane (PDMS) téléchélique à groupements vinyle, de la silice fumée modifiée (21% en poids), et d'un catalyseur de Karstedt comme source de platine (200ppm équivalent platine). L'étude que nous proposons porte sur l'influence des paramètres suivants : le taux de platine, le taux et le type de silice, la masse molaire du PDMS et la nature des bouts de chaîne du silicone. L'ensemble des formulations a été caractérisé à l'aide d'analyses thermogravimétriques (ATG), de calorimétrie différentielle à balayage (DSC), d'un pyrolyseur couplé à une chromatographie couplée à un spectre de masse (py-GCMS) et enfin par microscopie à balayage couplée à une analyse X élémentaire (MEB/EDX).

Nous avons pu mettre en évidence un mécanisme de dégradation du silicone en présence de silice et de platine en trois étapes :

1. *Etape de réticulation* (au dessous de 400°C) : au cours de cette étape, le Pt catalyse la génération de radicaux et de ce fait induit une réticulation du réseau de chaînes. Cette étape est primordiale pour immobiliser les chaînes macromoléculaires.
2. *Etape de dépolymérisation des chaînes faiblement réticulées* (de 400 à 625°C) : elle est mise en évidence au cours de la première perte de masse importante lors de la dégradation du silicone en ATG. Cette perte de masse est liée à la volatilisation des cycles et des oligomères formés lors de la dépolymérisation des chaînes faiblement réticulées.
3. *Etape de dépolymérisation des chaînes fortement réticulées* (de 625 à 850°C) : celle-ci est associée à la deuxième étape de dégradation du silicone en ATG. Les chaînes silicones sont totalement converties en une phase inorganique probablement de type SiOC. Le résidu obtenu pour la formulation contenant le Pt est noir, brillant et dense, alors que celui sans Pt est blanc et fragile.

L'effet de synergie entre la Silice et le platine augmente le taux de résidu du silicone lors des tests en pyrolyse. La silice permet, lors de la mise en œuvre des formulations, la formation de liaisons hydrogènes entre ses groupements de surface (groupement hydroxyles) et les chaînes de silicone[6,7]. Grâce à cette immobilisation des macromolécules (immobilisation physique), et du fait que le platine induit une réticulation du réseau silicone (immobilisation chimique), une augmentation du taux de résidu est favorisée.

De nouvelles formulations à base de silicone peuvent être imaginées à partir de ces éléments de compréhension. Par exemple, la présence de groupements réactifs en surface de la silice telle que le D<sub>4</sub> ou les vinyles augmente l'immobilisation des chaînes de silicone non seulement par liaisons hydrogène, mais aussi par réticulation chimique grâce aux réactions radicalaires induites par le platine. Une seconde solution permettant le remplacement du platine consiste à ajouter un précurseur de radicaux agissant à plus haute température que le peroxyde utilisé lors de la vulcanisation.

### Références

---

1. MacLaury M. R., The Influence of Platinum, Fillers and Cure on the Flammability of Peroxide Cured Silicone Rubber, *J. Fire Flam.* 1979; 10 : 175-98
2. Hayashida K, Tsuge S, Ohtani H. Flame retardant mechanism of polydimethylsiloxane material containing platinum compound studied by analytical pyrolysis techniques and alkaline hydrolysis gas chromatography. *Polymer* 2003;44:5611–5616.
3. Lagarde R, Lahaye J, Bargain M. Mécanisme d'ignifugation d'élastomères organosiliciques par le platine, *European Polymer Journal* 1977;13:769-774.
4. Camino G, Lomakin S, Lazzari M. Polydimethylsiloxane thermal degradation Part 1. Kinetic aspects. *Polymer* 2001;42(6):2395-2402.
5. Buch RR. Rates of heat release and related fire parameters for silicones. *Fire Safety* 1991;17:1-12
6. Cohen Addad J.P., S. Touzet, Polydimethylsiloxane–silica mixtures: Intermediate states of adsorption and swelling properties, *Polymer* 1993; 34: 3490-3498.
7. Cohen Addad J.P., Ebengou R., Silica—siloxane mixtures. Investigations into adsorption properties of end-methylated and end-hydroxylated chains, *Polymer* 1992; 33: 379-383.



# High Residue Contents Indebted by Platinum and Silica Synergistic Action during the Pyrolysis of Silicone Formulations

Etienne Delebecq,<sup>†</sup> Siska Hamdani-Devarences,<sup>†,‡</sup> Julia Raeke,<sup>†</sup> José-Marie Lopez Cuesta,<sup>‡</sup> and François Ganachaud<sup>\*,†</sup>

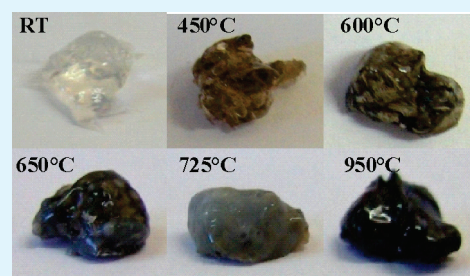
<sup>†</sup>Ingénierie des Architectures Macromoléculaires, UMR 5076 CNRS/ENSCM, 8 Rue de l'Ecole Normale, 34296 Montpellier Cedex, France

<sup>‡</sup>Centre des Matériaux de Grande Diffusion, Ecole des Mines d'Alès, 6 avenue de Clavières 30319 ALES Cedex, France

 Supporting Information

**ABSTRACT:** The synergistic role of platinum and silica as a way to increase the final residue of pyrolyzed silicone was investigated and explained, giving new interpretations. Conditions were first set to study the thermal degradation of silicones in the presence of platinum based on the simplest silicone/silica/platinum formulation. Numerous parameters, e.g., platinum and silica content or silica surface modifications, were varied to track their influences on the final residues. A thorough DSC study, together with SEM/EDX and Pyrolysis/GC-MS analyses, led us to propose a three-stage process. The key parameter governing thermal stability and final content of the residue is the conjugated actions of immobilizing/cross-linking PDMS chains. Silica particles tether silicone chains through physical interactions, i.e., hydrogen bonding, facilitating a platinum radically catalyzed cross-linking reaction. Practical implications and possible improvements on LSR formulations are finally given.

**KEYWORDS:** platinum cross-linking, silica H-bonding, immobilization, residue, thermal degradation



## I. INTRODUCTION

Polydimethylsiloxane (PDMS) or other silicone-based polymers are well-known for their excellent thermal and fire behavior.<sup>1</sup> Furthermore, the flame retardancy of silicones can be significantly improved by choosing specific additives, as recently reviewed by some of us.<sup>2</sup> One typical way of boosting the fire resistance of silicone consists in adding various specific fillers, which upon decomposition, melt or react with the silicone matrix; for instance, synthetic or natural calcium carbonates generate, upon heating, calcium oxide, which reacts with silica at 900 °C to produce a cohesive residue.<sup>3</sup> This approach is however restricted: even in highly filled commercial formulations sold as fire-retardant materials, silicone matrix count for at least 40 parts on the total formulations.<sup>2</sup> Indeed, too high a filler loading, for instance, of aluminum trihydrate, may ruin mechanical properties and limit the range of applications. Another way of doing this consists of adding small contents of high value specific additives to improve the ceramization of the materials. Typically, carbon nanotubes were recently introduced in conventional silicone formulations to provide self-extinguishing, highly cohesive residues.<sup>4,5</sup> Another possibility described in some patents<sup>6,7</sup> is to incorporate low contents of blends of metal oxides, e.g., TiO<sub>2</sub>, CeO, ZnO, and ZrO. For example, the pyrolysis of vinyl-terminated PDMS containing a trimethylsilyl terminated methylhydrosiloxane–dimethylsiloxane copolymer as a curing agent and 200 ppm of cesium octanoate as an additive produced a 52% residue yield (under a heating rate of 6.25 °C/min).<sup>8</sup> In many

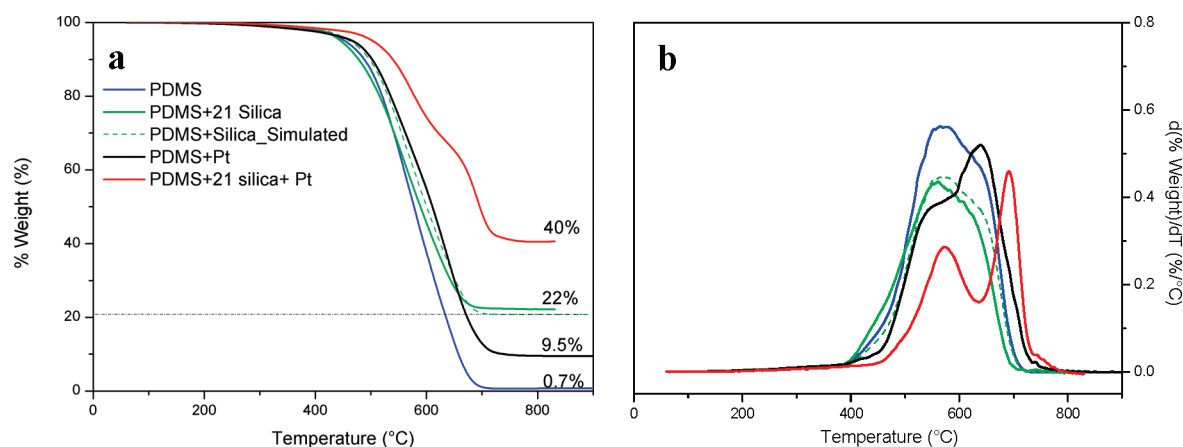
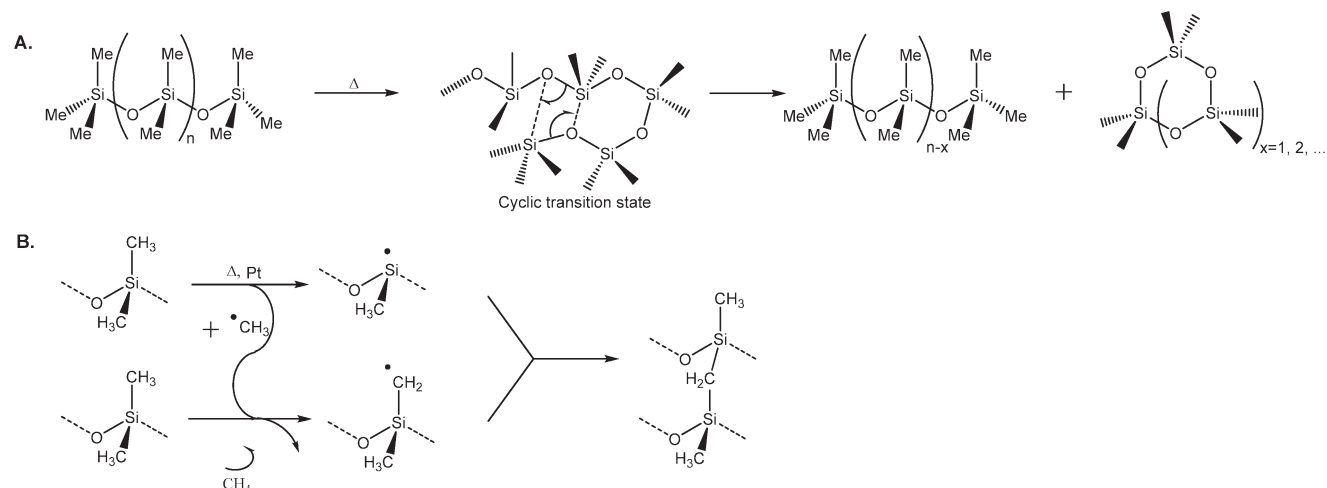
cases, however, the roles of each of these compounds, separately or in synergy, are not well-documented.

In contrast, the role of platinum (Pt) compounds in silicone fire retardancy has been described in detail in a few academic papers.<sup>9–11</sup> Indeed, the so-called Karstedt catalyst (platinum(0)-1,3-divinyl-1,1,3,3-tetramethyldisiloxane<sup>12</sup>) is widely used in industrial applications to produce cross-linked polymers via hydrosilylation.<sup>13</sup> Whereas neat silicone chains are known to degrade through a random scission reaction to produce volatile cyclic oligomers, mostly D<sub>3</sub> and D<sub>4</sub> (Scheme 1A),<sup>1</sup> in the presence of a platinum catalyst, the thermal stability and fire retardancy of silicone is largely improved. MacLaury<sup>9</sup> specifically studied by mass spectrometry the volatile products of silicones filled with 50 ppm of platinum. The major volatile components at 300 °C are methane and CO<sub>2</sub>, together with slight contents of water, a cyclic trimer, and ethylene as tracked by GC. At a higher temperature (600 °C), the major volatile products are dihydrogen and methane with very small amounts of released water, CO<sub>2</sub>, a cyclic trimer, and a tetramer. Hayashida et al.<sup>10</sup> recently proposed a complex radical-catalyzed mechanism to explain the flame retardant Pt activity, concordant with MacLaury findings (Scheme 1B). The 400–500 °C thermal treatment of a platinum-filled silicone proceeds through three chemical steps: (i) first, the radical homolytic break of the Si–Me bond by the catalytic action of the platinum atom at an

**Received:** December 10, 2010

**Accepted:** February 17, 2011



Scheme 1. (A) Volatilization of PDMS through a Random Scission Mechanism<sup>1</sup> and (B) Crosslinking Mechanism by Platinum<sup>10</sup>

**Figure 1.** Thermal stability of vinyl terminated PDMS/silica/platinum combinations measured by TGA at a heating rate of 50 °C/min under N<sub>2</sub>. Values given at the right of the curves represent the final residual content: (a) TG curves, (b) DTG curves.

elevated temperature to produce methyl and silyl radicals; (ii) second, the methyl radical abstraction of hydrogen from another methyl group to yield methane and a radical methyl grafted on the chain siloxane; and (iii) the macroradical attack to an adjacent polymeric chain inducing a cross-linking of the matrix. A close mechanism was also proposed by Lagarde et al.<sup>11</sup> in which the flame retardant action of Pt in PDMS occurs by preventing the formation of a complex transition, thus limiting the quantity of condensates formed.

MacLaury<sup>9</sup> showed that neat silicone chains in the presence and absence of platinum (50 ppm), produced similar and low residue contents, though platinum slightly increased the degradation temperature onset of about 20–30 °C. He also showed that platinum effectively changes the fire resistance of silicone formulations, albeit exclusively in the presence of vinyl groups and filler. For instance, at a Pt loading above 60 ppm, the char yield in the Chimney test was remarkably increased up to 50%. The practical fire-testing applications and the numerous factors spanned along this study do not allow one, unfortunately, to easily intuit the role of each of the components. Other authors, who have also studied the role of platinum, obtained much larger residue yields when systematically introducing silica or quartz

reinforcing filler than without it, for instance, as high as 73% for a 48% quartz-silica loaded sample.<sup>10</sup> They did not mention the necessity of having vinyl groups left in the formulations.

We have redone simple TG analyses and confirmed the importance of the filler (Figure 1). Vinyl terminated PDMS degraded from about 400 °C over 700 °C to produce a final residue yield of 0.7%; all PDMS was converted to volatile products, as expected from a random scission mechanism.<sup>14</sup> The incorporation of a small amount of Karstedt catalyst (200 ppm platinum metal, *vide infra*) in neat PDMS showed a slight 13 °C shift toward higher temperatures, both in the onset degradation temperature and the maximum rate of degradation, but increased the final residue yield (9.5%). The PDMS and silica blend follows the calculated degradation path from each element contribution, ending with a residue yield of 22%.<sup>3</sup> By adding Pt into PDMS–silica blending, the onset temperature shifted to 510 °C, and the final residue yield was 40%, much larger than for both neat PDMS–Pt and PDMS–silica blends. Such an increased residue yield can only be explained by a synergy of actions between silica and platinum toward silicone degradation. This paper thus aims at unraveling the role of silica in the thermal

**Table 1.** Main Characteristics of Bare and Modified Fumed Silicas Used in This Work

product	AEROSIL 150	AEROSIL R 812 S	AEROSIL R 106	vinylated silica
surface modifier	none	hexamethyldisilazane (HMDS)	octamethylcyclotetrasiloxane (D <sub>4</sub> )	vinyl silane
concentration of surface modifier (%) <sup>a</sup>		9	7	
silanol content (%) <sup>a</sup>	26	20	21	confidential
specific surface area by BET (m <sup>2</sup> /g)	150 ± 15	220 ± 25	250 ± 30	120 ± 4
average primary particle size (nm) <sup>b</sup>	14 (28 ± 3)	7 (9 ± 2) <sup>c</sup>	7 (- <sup>d</sup> )	- <sup>d</sup> (16 ± 3)

<sup>a</sup> Measured by one-pulse <sup>29</sup>Si solid-state NMR; see text for calculation details. <sup>b</sup> As given by the supplier and/or measured by Transmission Electronic Microscopy (values between parentheses). <sup>c</sup> From ref 15. <sup>d</sup> Not given or measured.

degradation of platinum-filled silicone formulations, giving new interpretations that, to our knowledge, were not specifically proposed in previous works. A model formulation is first set up, based on a preliminary product screening. Some parameters that may influence the Pt activity are then explored, including the nature and content of silica. From a complete DSC analysis on the model formulation and characterization of residues taken up at different temperatures by SEM/EDX and Pyrolysis/GC-MS, a three-stage degradation process is proposed, of greater complexity than the one proposed before (see Scheme 1B). Important implications and improvements for the ceramization of commercial liquid silicone rubber formulations are finally proposed.

## II. EXPERIMENTAL SECTION

**II.1. Materials.** Trimethyl- and vinyl-terminated polydimethylsiloxanes of various molar masses were purchased from ABCR and used without further purification. Three types of silica purchased from Evonik Degussa were tested (Table 1). One-pulse <sup>29</sup>Si solid-state NMR ( $\pi/6$  pulse, 60 s recycling delay on a Varian VNMRs, 400 MHz) was performed to characterize the silica surface. The concentration of grafted units is measured by the peak integration of HDMS or D<sub>4</sub> (*M* or *D*) silicon atoms compared to the sum of silicon atoms integration (eq 1). The silanol content is expressed in the same manner, by comparing the integration of Q<sub>3</sub> units relative to the integrations of all silicon peaks (eq 2):

$$\text{concentration of surface modifier (\%)} = \frac{I_M}{\Sigma I} \times 100 \quad (1)$$

$$\text{silanol content (\%)} = \frac{I_{Q_3}}{\Sigma I} \times 100 \quad (2)$$

In addition, a vinyl-functionalized silica was prepared in the “Ingénierie des Matériaux Polymères” laboratory (Lyon, France) and used as received.

The platinum(0)-1,3-divinyl-1,1,3,3-tetramethyldisiloxane complex (Karstedt catalyst, 10% platinum solution in xylene) was kindly given either by Gelest or by BlueStar Silicones. All platinum concentrations given in the paper are expressed in parts per million (ppm), calculated according to the platinum element. Two high-temperature radical generators, 2,3-dimethyl-2,3-diphenylbutane (DMDPB) and *tert*-butyl hydroperoxide (*t*-BuOOH), with half-life time  $t_{1/2} = 0.1$  h at 284 and 207 °C, respectively, were purchased from Akzo Nobel. THF (reagent grade, pure analysis, 99% purity) was used for the preparation of the Karstedt catalyst and radical generator.

**II.2. Methods.** Thermogravimetry (TG) analyses were performed on a Q50 from TA Instrument. A 20 mg sample in a platinum pan was heated from room temperature to 900 °C under a nitrogen flow (60 mL/min). The experiments were carried out at a heating rate of typically 50 °C/min (*vide infra*). The simulated weight loss plots were obtained by recording experimental TG curves of the different components separately, normalizing them

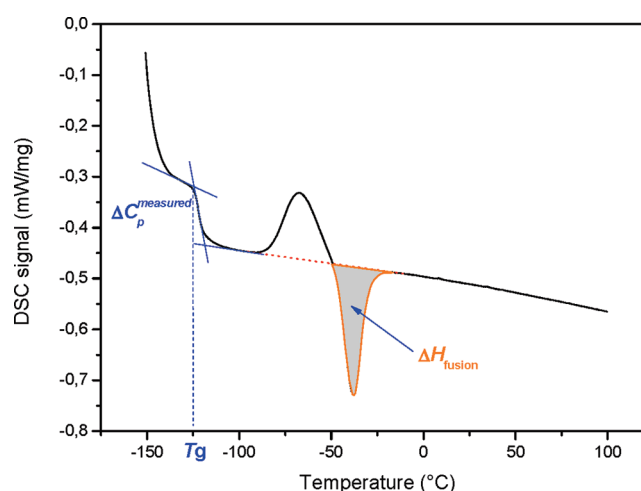


**Figure 2.** Illustration of calculation procedure on the DSC curve of the model blend (see text for details).

according to their contents in the formulation and adding them to simulate the TG curve that one would attend without synergistic effects between the different components.<sup>3</sup> The derivative weight loss curves were deconvoluted with OriginPro8 into two Gaussian peaks to determine both areas and temperatures at the peak maximum; all of the fitted curves presented a correlation coefficient superior to 0.98.

To compare the peak areas for samples containing various amounts of filler, all areas of the first peak were expressed as

$$A_1^{\text{corrected}} = \frac{A_1^{\text{measured}}}{100 - \% \text{Filler}} \quad (\text{eq. 3})$$

$A_1^{\text{measured}}$  quantifies the weight loss of the sample in its entirety, whereas  $A_1^{\text{corrected}}$  represents exclusively the content of degradation related to the polymer fraction.

By the same token, the second peak area is corrected using eq 4:

$$A_2^{\text{corrected}} = \frac{A_2^{\text{measured}}}{100 - A_1^{\text{measured}} - \% \text{Filler}} \quad (4)$$

where  $A_2^{\text{corrected}}$  now stands for the fraction of the polymer left after the first degradation step, which is degraded during the second step.

Differential scanning calorimetry analyses were carried out on a NETZSCH DSC200 calorimeter. Cell constant calibration was performed using indium, *n*-octadecane, and *n*-octane standards. Nitrogen was used as the purge gas. The 10–15 mg samples were sealed in hermetic aluminum pans. The thermal properties of degraded samples obtained at different temperatures were analyzed at 20 °C/min as an average value in order to observe the glass transition as well as crystallization/fusion processes. All of the reported temperatures are onset values. For each sample, the thermal history was erased with a first heating ramp up to 100 °C. From the DSC curve, glass transition temperature  $T_g$ , variation of heat capacity  $\Delta C_p$ , and heat of fusion ( $\Delta H_{\text{fus}}$ ) were measured with the software (see schematized

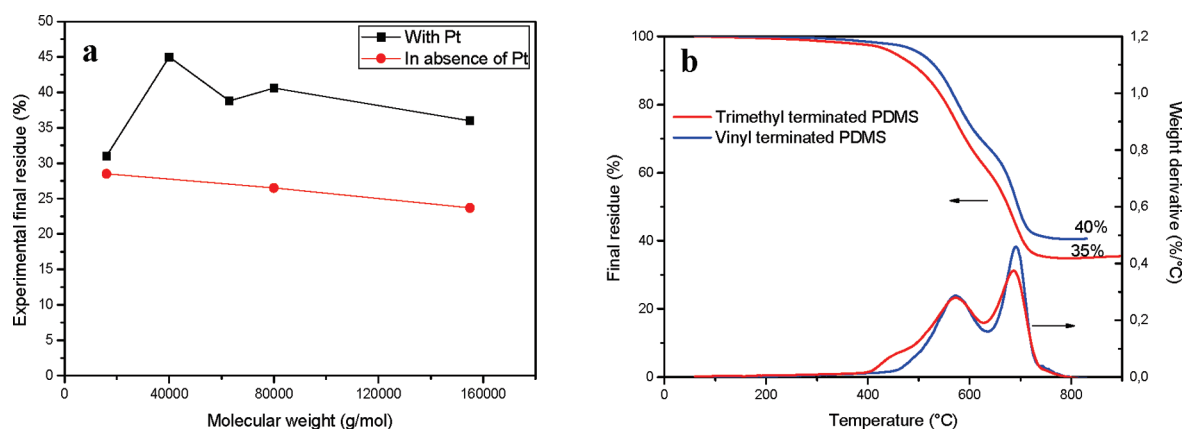


**Figure 3.** Influence of the nature of PDMS chains on the thermal degradation of a model silicone blending: (a) effect of average molecular weight on the final residue content; (b) effect of chain ends on TG and DTG profiles.

procedure on a DSC spectrogram in Figure 2).<sup>16</sup>  $\Delta H_{\text{fus}}$  allows calculation of the degree of crystallinity of the polymer, expressed as weight percent crystallinity (eq 5), using 61.3 J/g as the perfect heat of fusion for PDMS.<sup>17</sup>

$$\% \text{crystallinity} = \frac{-\Delta H_{\text{fus}}}{61.3 \times (100 - \% \text{Filler})} \times 100 \quad (5)$$

Variations in heat capacity, expressed per weight of silicone amorphous phase, were calculated from eq 6:

$$\Delta C_p = \frac{\Delta C_p^{\text{measured}}}{(100 - \% \text{Filler})} \times \frac{1}{100 - \% \text{crystallinity}} \quad (6)$$

Energy-dispersive X-ray (EDX) measurements were conducted as an integrated tool in environmental scanning electron microscopy (ESEM) to determine the elemental composition of the residue on micrographs with a magnitude of 300 $\times$ . Quantitative analyses of element content in plate residues were measured on ESEM micrographs using the XT Docu program. Samples were first heated to the desired temperature, and then the residues obtained were ground to obtain observable flat surfaces.

Py-GC/MS analyses were carried out on a Pyroprobe 5000 pyrolyser (CDS Analytical) interfaced to a 450-GC gas chromatograph (Varian) by means of a chamber heated at 110 °C. The column is a Varian VF-5 ms capillary column (30 m  $\times$  25 mm), and helium (1 mL/min) was used as the carrier gas. Samples of less than 1 mg were first placed in a quartz tube between two pieces of rockwool and successively flash pyrolyzed under helium at 250, 575, and 725 °C for 5 s. Then, the gases were drawn to the gas chromatograph for 5 min and subsequently from the GC transfer line to the ion trap analyzer of the 240-MS mass spectrometer (Varian) through the direct-coupled capillary column.

**II.3. Sample Preparations.** PDMS and silica were blended into a beaker glass, by extensive crushing and breaking off of silica agglomerates until a transparent paste was obtained. Karstedt catalyst or DMDPB (diluted in THF) was added, and then the blend was crushed again using a glass stirrer for at least 20 min to obtain a homogeneous blending. To remove solvent, the blend was dried in a vacuum at 50 °C overnight. The *t*-BuOOH radical generator was mixed as received, i.e., 70% solution in water, with the formulated paste, and blended as usual. The obtained transparent formulation was left under a fume hood for 1 week at room temperature to remove water (as confirmed by the absence of weight loss below 200 °C on TG curves). When not specified, the model formulation contains vinyl-terminated PDMS chains of an average molar mass of 60 000 g/mol, HMDS-modified fumed silica at 21 wt %, and 200 ppm of platinum. All sample compositions are given in Table S1, Supporting Information.

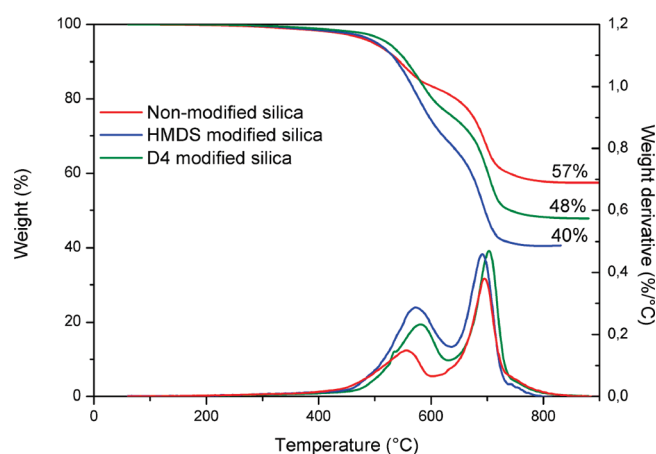


**Figure 4.** Influence of silica type on the thermal stability of silicone model formulation degradation.

### III. RESULTS AND DISCUSSION

**III.1. Variations on the Formulation.** Preliminary trials were carried out to derive a simple three-component formulation to be studied and establish the best TG analysis conditions to stress the line on the synergy between platinum and silica. Basically, telechelic vinyl silicone, fumed silica treated by HMDS, and the Karstedt catalyst were mixed and crushed with a small amount of THF to favor the introduction of the platinum catalyst (see sample compositions in Table S1, Supporting Information). TG weight loss curves and derivative curves (abbreviated DTG in the following) were systematically plotted (as in Figure 1, for instance) in order to observe in detail each degradation step of the PDMS blends.

**Nature of Silicone.** Different PDMS samples were purchased and introduced into a model formulation (see the Experimental Section). The effect of molecular weight of the vinyl-terminated PDMS on the final residue was first studied. The molecular weights ranged from 16 000 to 155 000 g/mol (Figure 3a). In the absence of platinum, the residue decreased as the molecular weight increased. For platinum-containing samples, the residue drastically increased up to 40 000 g/mol and, then, slightly decreased. The spectacular residue increase between 16 000 and 40 000 g/mol in the presence of platinum catalyst can be assigned to the threshold of critical molecular weight for

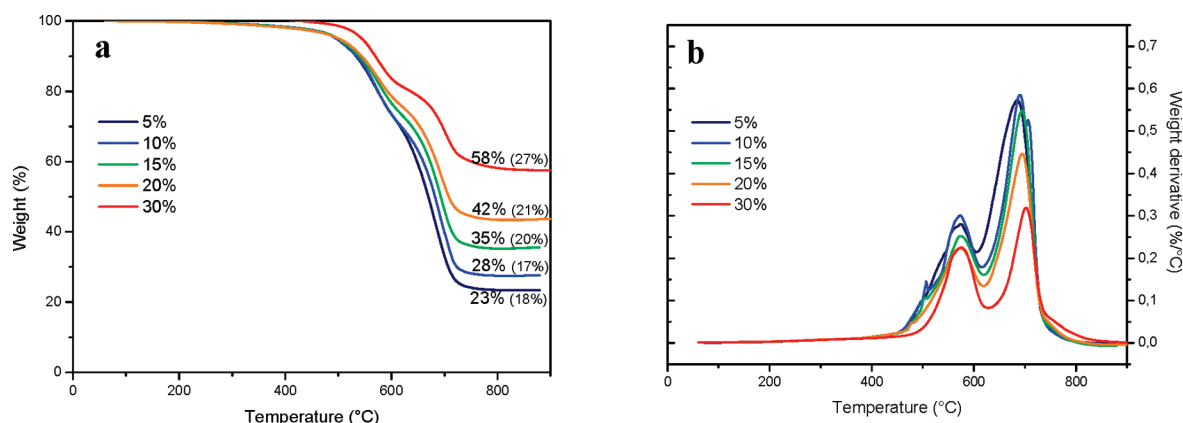


**Figure 5.** Effect of HMDS-treated silica content on the thermal stability of a model silicone formulation. Values on the TG curves give the final residues; those in parentheses are the extra residues (see text for details): (a) TG curves, (b) DTG curves.

entanglements, which is thought to lie somewhere between 21 000 and 30 000 g/mol.<sup>17,18</sup> Above this threshold, the number of entanglements increases while increasing the molecular weight. The fact that the mass between entanglements remains constant (measured around 12 000 g/mol<sup>19</sup>) explains why the content of residue does not further increase. We selected the vinyl-terminated PDMS with an average molar mass of 60 000 g/mol as the main matrix component in the following.

As summarized previously in the literature,<sup>2</sup> the silicone chain ends can play an active role during the thermal degradation, particularly vinyl groups, which easily react with radicals. Trimethyl-terminated PDMS was tested in place of vinyl chains of similar molar masses. A preliminary 5% degradation occurred around 400 °C (Figure 3b), but above 550 °C, both degradation profiles were similar. The final residue obtained at 900 °C was slightly less for trimethyl-terminated chains, 35% against 40% for vinyl-terminated PDMS. This value is nevertheless much higher than the silica content, so the synergistic effect between platinum and silica occurs even after vinyl reactive chain ends have been consumed. We chose in the following to work exclusively with vinyl-terminated chains, to stay close to commercial LSR formulations (*vide infra*).

**Nature and Content of Silica.** Different types of silica were incorporated into Pt–PDMS blending: bare silica and silica treated by hexamethyldisilazane (HMDS) or by octamethylcyclotetrasiloxane (D<sub>4</sub>) (experiments on vinyl-modified silica are also presented in section III.3). TG and DTG curves are given Figure 4.

Here, the type of grafting agent on the silica surface has a strong influence on the final residues. Indeed, both physical adsorption and covalent bonding are sources of polymer–filler interactions in the PDMS–silica composite.<sup>20–23</sup> Bare silica possesses many silanol groups on its surface that form hydrogen bonds with oxygens from the siloxane backbone (see Table 1);<sup>24,25</sup> the physical adsorption of PDMS on silica greatly enhances the final residue, with a final content close to 60%. Bare silica is however not useable in commercial formulations, because of its propensity of increasing blend bulk viscosity with aging (a phenomenon known as crepe hardening<sup>23</sup>). Large differences between HMDS and D<sub>4</sub>-modified silicas were seen also on thermal degradation, the latter producing a larger residue (40% against 48%). The presence of longer siloxane chains grafted to D<sub>4</sub>-modified silica favors cross-linking reaction of more PDMS chains onto silica surface through the platinum catalysis (*vide infra*). In the

following, we systematically worked with HMDS-modified fumed silica for two reasons: HMDS-treated silica is a model silica bearing exclusively trimethylsilyl units on the surface, and furthermore, it is by far the most widespread industrially.

The thermal degradation of a mixture containing 5–30% HMDS-modified silica in the presence of 200 ppm of platinum catalyst was then investigated. From the thermograms presented in Figure 5, it is clear that increasing the silica content produced superior residues than expected from the sole filler content. There was almost no change in onset temperature, except for the largest silica content, showing that the initial step of degradation, between 400 and 600 °C, is independent of the silica content. The extra residue (i.e., the difference between the experimental and the simulated residue) increases monotonously with the silica content (see values between parentheses in Figure 5). The more PDMS chains adsorbed on silica, the higher the residue. In the following, we chose to work at a 21 wt % silica loading, a conventional value in silicone formulations.

**Other Parameters.** Several blends containing PDMS and HMDS-modified silica were prepared while adding an increased content of Pt (from 1 to 400 ppm). The final residues and some DTG degradation profiles are plotted in Figure 6. From 1 to 25 ppm of Pt content, the final residue was almost constant and set at 24%, the slight variations being ascribed to the difficulty of obtaining homogeneous blends for samples containing less than 50 ppm (Figure 6a). Meanwhile, for a platinum content as low as 1 ppm, the degradation profile is drastically changed from a broad peak for the silica–PDMS blend (Figure 1b) to two well-defined peaks when Pt is added (Figure 6b). This indicates that the platinum induces cross-linking as proven by residues slightly larger than the silica content. From 50 ppm and beyond, the final residue increased with the platinum content to reach values as high as 47% residue under these experimental conditions. In the following, 200 ppm of platinum was selected as the model content to guarantee a clear synergistic action.

We tested also two heating rates, of 10 °C/min and 50 °C/min, since a fast heating rate in TGA may be more representative of a real fire expansion (Figure 7). At a low rate, the degradation curve of the PDMS–silica blending is slightly shifted to lower temperatures (around 40 °C). However, the final residue remains roughly constant to 24–26%. On the contrary, the PDMS–silica–Pt blend thermogram changes significantly while increasing the heating rate, shifting drastically the onset temperature of degradation (around 50%) and enhancing the final residue (from 30 to



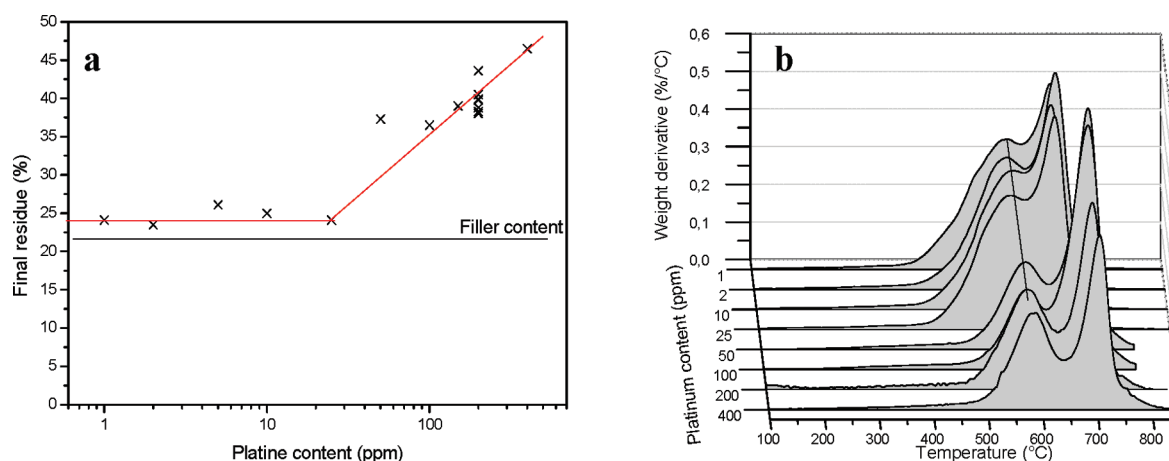


**Figure 6.** Influence of Pt content on the residue on a model silicone formulation degradation: (a) final residue as a function of Pt content (black straight line is filler content); (b) cascade plot of selected DTG curves (see platinum content on the z axis on the left-hand side).

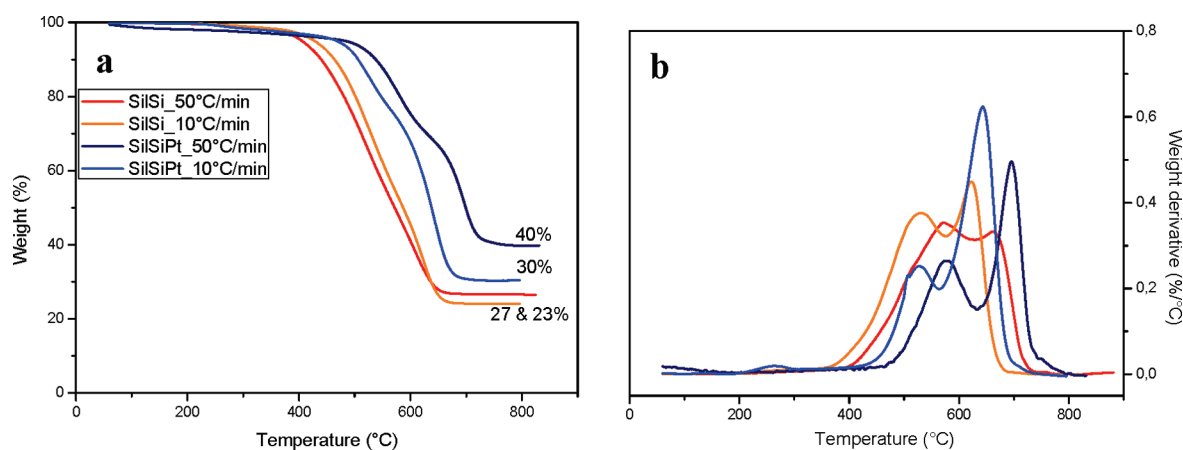


**Figure 7.** Effect of the heating rate on the PDMS degradation: (a) TG curves; (b) DTG curves.

40%). This result is in agreement with the study of Camino et al.,<sup>26</sup> who have shown in a kinetic study that, at a higher heating rate, PDMS thermal volatilization is dominated by the rate of diffusion and evaporation of oligomers produced during decomposition. The heating rate of 50 °C/min was finally kept for further degradation analysis.

**III.2. Degradation Mechanism.** The incorporation of both a silica and platinum catalyst into a silicone formulation has thus an outstanding effect on its thermal stability and also changes the degradation mechanism, as clearly shown in the derivative curves of TG analyses (see Figure 1, for instance). Neat PDMS or PDMS–silica presented broad peaks on TG derivative curves and PDMS in the presence of Pt, a slightly bimodal degradation peak. The combination of both silica (21%) and Pt (200 ppm) in PDMS resulted in two well-separated DTG degradation peaks (this is particularly obvious in Figures 5b and 6b, for instance). To further study the degradation mechanism, thermally treated samples were prepared by heating around 100 mg of the model formulation mixture with the furnace of a thermobalance, taking out the residue at selected temperatures, and analyzing them by DSC and SEM/EDX. Py-GC/MS performed at various temperatures was also done to track out the structures of volatile species.

**DSC Analyses.** From calorimetric measurements, the glass transition temperatures, the variations of heat capacity and degree of crystallinity were measured, as reported in Figure 8.

The complete DTG degradation profile is also plotted in the same figure for comparison.

The degradation process can be divided into three steps. During the first step, taking place from ambient temperature to 400 °C, negligible changes in weight (only 1.5 wt % loss) and a slight increase in  $T_g$  (from  $-124$  to  $-122$  °C) were observed, though the  $\Delta C_p$  remains constant, around 0.44 J/(g.K). The most probable explanation is that the mixture undergoes a heavy cross-linking step inducing small molecules to release, such as  $H_2$  or methane (see Scheme 1B). Between the cross-linking points, the silicone chains remain long enough to keep their mobility, and thus, the glass transition temperature stays constant. The extent of the cross-linking reaction is also confirmed by a strong rise in the degree of crystallinity from 16 to 38% (Figure 8). Below 400 °C, samples thermally treated crystallized more easily as the temperature increased and subsequently fell off. Several works have reported the constraint effect on the crystallization. Most of them showed that PDMS crystallization is enhanced by any type of preordering effect; cross-linking points,<sup>27</sup> chain entanglements,<sup>28</sup> or interaction with surfaces<sup>29</sup> reduce the chains fluctuations, lowering the overall activation energy of crystal formation.

The second step corresponds to the first degradation peak on the TGA derivative curve occurring in a temperature range from 400 to 640 °C. Here, a strong weight loss from 1.5 to 29 wt %

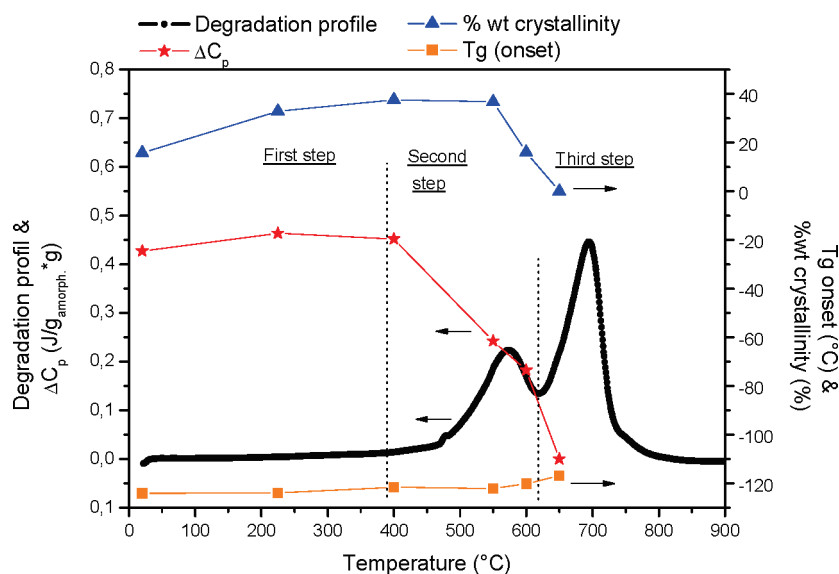


**Figure 8.** Glass transition temperature, variation of heat capacity, and percentage of crystallinity as determined by DSC on samples treated by TG and discarded at different temperatures. The black curve is the corresponding DTG profile.

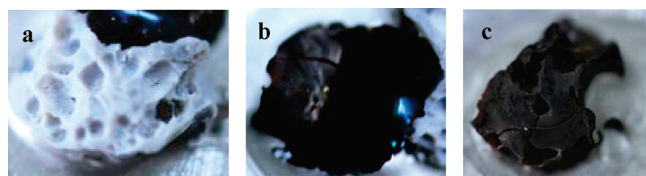


**Figure 9.** Residues of silicone after pyrolysis at 900 °C (a) without platinum (blank friable residue), (b) with 200 ppm platinum (shiny cohesive black residue), (c) residue from a radical generator (matte friable black residue).

occurred. The glass transition temperature slightly increased from  $-122$  to  $-117$  °C, and the  $\Delta C_p$  as well as the degree of crystallinity dropped off from  $0.44$  to  $0.17$  J/(g K) and from  $38$  to  $16\%$ , respectively. In this step, the silicone phase undergoes a volatilization process of highly mobile chains. The remaining dimethylsiloxane (D) units, mostly constrained around the cross-linking point (about  $8$  to  $10$  adjoining units, according to the literature<sup>30,31</sup>), do not participate in the glass transition, which leads to a decrease of the  $\Delta C_p$  value.<sup>32</sup>

The third step corresponds to the second peak degradation in DTG analysis observed at temperatures from about  $625$  to  $850$  °C. At this range of temperatures, a severe weight loss (about  $30$  wt %) as well as disappearances of glass transition and crystallization points were observed (Figure 8): the sample is no longer a polymer. The mechanism of degradation here consists of the removal of the highly constrained chains before the ceramization takes place to generate a large final residue.

**Complementary Analyses.** Visual observation showed that, in the absence of Pt, the obtained residue is a greyish white powdery solid, with some apparent holes in the material. Whereas, in the presence of Pt, the obtained residue is a hard and shiny black solid (see Figure 9).

A microstructure analysis by SEM images under a magnification of  $20\,000\times$  showed some microstructure changes under heat treatment (Figure 10). In the presence of platinum, the residues look dense, and increasing the temperature to  $900$  °C decreased the structure porosity, which signifies the ceramization

of the residue. In absence of platinum, the residue looks very fragile and more porous due to the absence of a cohesive phase between silica particles.

EDX analyses were carried out during these ESEM observations to analyze the contents of carbon and other elements in residues taken out at various temperatures (Figure 11). In all instances, the decrease of carbon element content while increasing the temperature is consistent with the loss of methyl groups.<sup>33</sup> Some differences were nevertheless seen between platinum-filled formulation and the blank experiment without platinum. Cross-linking the residue in the former resulted in a chemical structure with an increased level of oxygen and silicon and a decrease in the molecular level of carbon. In the absence of Pt, the final residue had a lower carbon content and resulted in a fragile residue. Note that the few carbon atoms remaining at  $900$  °C in this sample surely come from some remaining methyl groups on the silica surface (HMDS modification).

The volatile products released from sample degradation, and of molar mass larger than  $60$  g/mol, were differentiated by pyrolysis-GC/MS at  $250$ ,  $575$ , and  $725$  °C (Figure 12). Large cyclic and linear silicone oligomers were released at a low temperature ( $250$  °C), which confirmed that the slight degradation observed at low temperatures is only related to the release of free chains which are not involved in the cross-linking step. At higher temperatures ( $575$  and  $725$  °C), i.e., during the first and second steps of TG degradation, smaller cycles (including  $D_3$  and  $D_4$ ) devolatilized.

**Comprehensive Mechanism.** Before commenting on the degradation chemistry, the microstructure of silicone chains in the presence of silica is worth mentioning. According to a NMR relaxation study carried out by Litvinov et al.,<sup>34,35</sup> PDMS chains tethered onto the silica surface form two layers. The first layer at the interface consists of immobilized chains, and the second layer is composed of the mobile fraction of PDMS chains (Figure 13). At the edge of this layer settle highly mobile chains, and their degrees of freedom are close to those of neat silicone chains. According to their analyses, the immobilized fraction consists of about eight units of dimethylsiloxane pendant chains and is



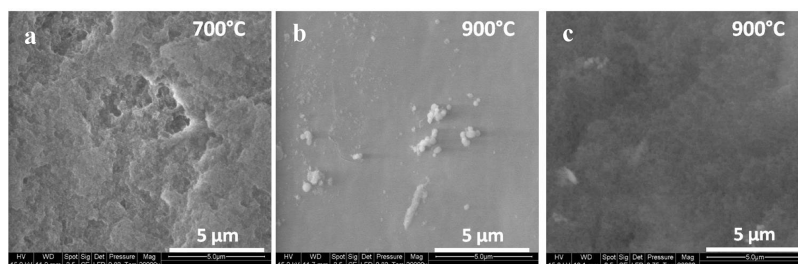


**Figure 10.** SEM images of silicone residues at (a) 700 °C, (b) 900 °C with platinum, and (c) in the absence of platinum at 900 °C (all pictures were taken under a magnification of 20 000 $\times$ ).

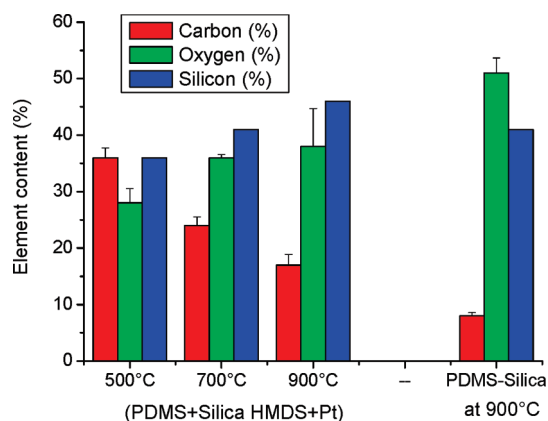


**Figure 11.** Pt influence on the element content of residue as determined by EDX.

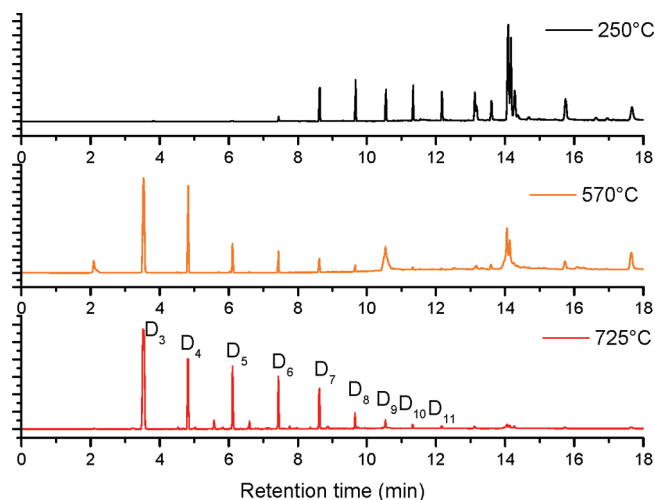


**Figure 12.** Py-GCMS chromatograms of model blending pyrolyzed at key temperatures.

independent of the total length of the PDMS chains. The mobility in this layer is comparable to the mobility of pure PDMS at temperatures slightly above  $T_g$ , while the outer layer is extremely mobile. In addition, they proved that the type of tethering (chains chemically linked or physically adsorbed on the silica surface) has no influence on the mobility of chains in each layer.

Below 400 °C, mostly a cross-linking reaction occurs, according to the pathway previously reported in the literature (Scheme 1B).

The fact that most free silicone chains are adsorbed onto silica surfaces allows a decreased level of freedom for these chains, and thus an efficient cross-linking. Highly mobile chains, as reported in Figure 13, may start volatilizing, but this reaction is quite odd. In the second step, the chains in the outer layer keep enough mobility between previously generated cross-link points to undergo easy depolymerization through random scission (Scheme 1A) and to produce large cycles. On the other hand, PDMS chains close to the surface are constrained and degrade only at high temperatures (third step). Since only low molar mass silicone loops are still present on this last step, principally  $D_3$  and  $D_4$ , the lowest volatile cyclic oligomers, are produced here.

Silica and Pt thus favor, respectively, chain adsorption on the surface and cross-linking, successively. Such joint immobilization action is the key factor in ensuring a final high residue. Moreover, the heterogeneous mobility between chain segments likely explains the two separate volatilization degradation steps observed in TG curves. Platinum has a definite role only during the first stage of heating, and only if introduced in the recipe at a sufficient content level (typically, 50 ppm under these particular conditions, see Figure 6A).<sup>36,37</sup> On the other hand, the adsorption of silicone chains on silica occurs most exclusively during the mixture preparation; thus, increasing the silica content (i.e., the specific surface of the filler) is a facile way to improve the final residue (Figure 5). In addition, chemical grafting on the silica surface, when silicone loops are available, may occur also during the first step (see differences between HMDS and  $D_4$ -treated silica, respectively, Figure 4).

Finally, we have shown that the residues obtained with or without platinum do not present the same elemental compositions and outward appearance. Ceramic materials form in the presence of platinum by bond reorganization during degradation at high temperatures.<sup>38</sup> Black SiOC is known to form during the thermal degradation of heavily cross-linked PDMS,<sup>39</sup> where the cross-linking density of the polymeric network has a strong influence on the ceramic yield as well as on the final composition of the glasses.<sup>40</sup> The SiOC network is stable up to 1000–1200 °C and, above these temperatures, decomposes to form a SiC ceramic phase.<sup>41</sup> Here, the Pt catalyzes the cross-linking reaction during the first step of the thermal treatment. After the second step of degradation, the mineralization of the material takes place at temperatures between 600 and 900 °C, producing SiOC glasses.<sup>42</sup>

**III.3. Implications and Improvements of LSR Formulations.** *Improving Platinum/Silica Synergy.* Chain immobilization by cross-linking has previously been confirmed by comparing the thermal stability of PDMS blends filled with different types of silica. We chose to introduce vinyl-modified silica, to produce higher final residue yields than those of  $D_4$  or HMDS-modified

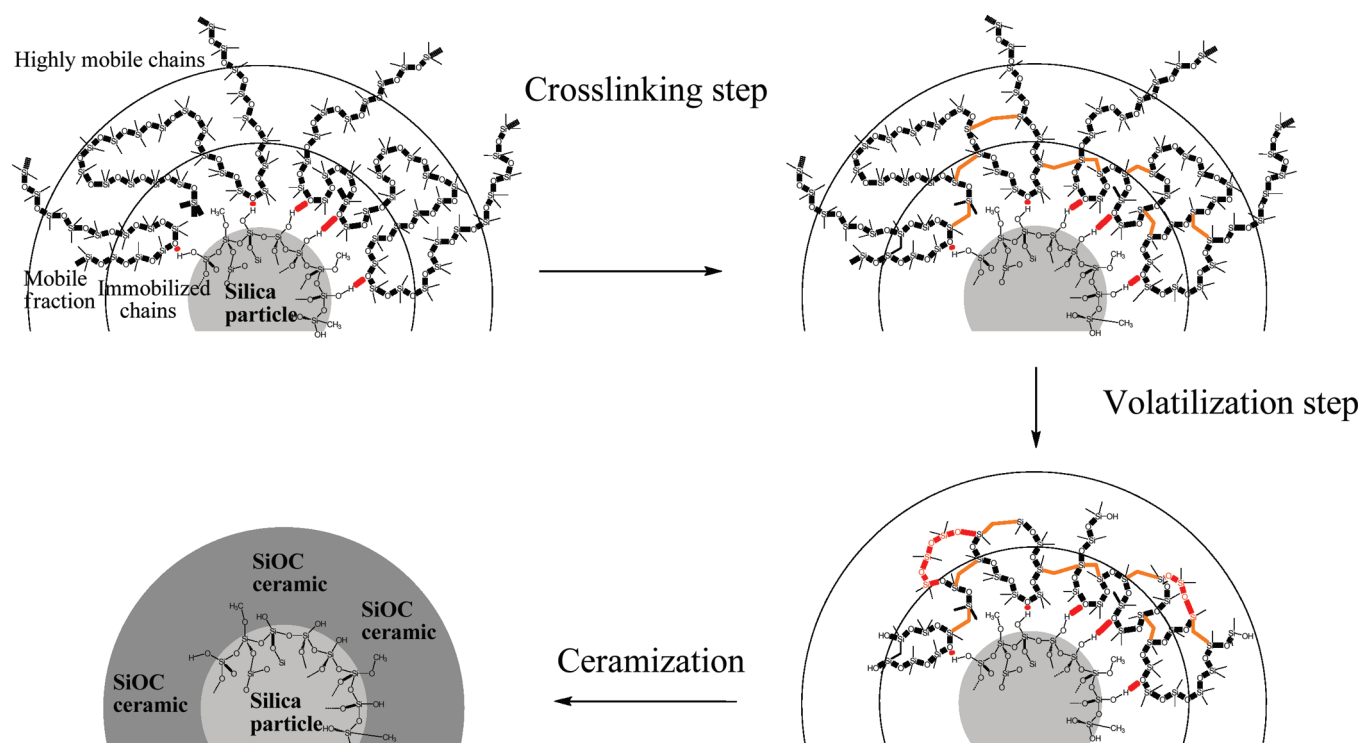


**Figure 13.** Modelization of silicone chain arrangement on a silica surface and their thermal degradation pathway.

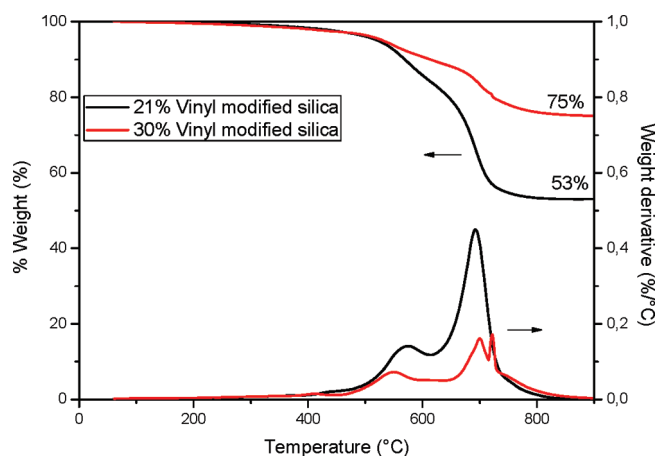


**Figure 14.** Influence of vinyl-modified silica content on TG profile and final residue.

silica (compare Figure 14 with Figure 4). The presence of vinyl groups on the silica surface indeed favors chemical cross-linking between PDMS chains and silica at high temperatures, promoted by a platinum catalyst, and resulting in lower volatilization and increased final residue yield. The fact that vinyl groups may react around 400 °C is explained by the exceptional stability of these groups close to the silica surface (see the TGA of vinyl silica, Figure S1, Supporting Information). Increased contents of vinyl-modified silica resulted in the greatest final residues gained in this study (Figure 14): the incorporation of 30 wt % vinyl-modified silica produced a 75% residue yield against 50% for 20 wt % filler loading. Therefore, the use of a cross-linking promoter as a grafting agent on the silica surface may fit with some applications that require a final large ceramic content, such as in the electrical cable industry.

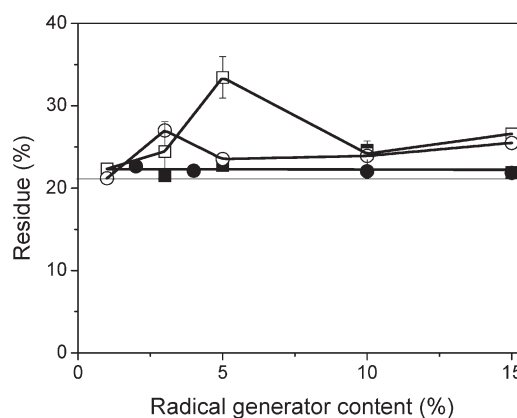


**Figure 15.** Influence of 2,3-dimethyl-2,3-diphenylbutane (DMDPB, black symbols) and *tert*-butyl hydroperoxide (*t*-BuOOH, open symbols) on the final residue of platinum-free model silicone formulations filled with HMDS-treated (circle) and vinyl-modified (square) silicas.

**Substituting Platinum.** We replaced in typical formulations Pt with two different types of radical generators, e.g., 2,3-dimethyl-2,3-diphenylbutane (DMDPB) and *tert*-butylhydroperoxide (*t*-BuOOH) at loading levels ranging from 1% to 15 wt % and filled either with HMDS-treated or vinyl-functionalized silica (Figure 15). The incorporation of both radical generators spawned again two separated degradation peaks in TG analyses (Figure S2, Supporting Information). An additional broad peak on the TG curve at a temperature between 100 and 300 °C was only observed for samples containing DMDPB and ascribed to the volatilization of radical generator degraded moieties, as supported by the weight loss that roughly corresponds to the DMDPB content. Using DMDPB did not basically change the final residue, set slightly above the filler content, as it did for blends with

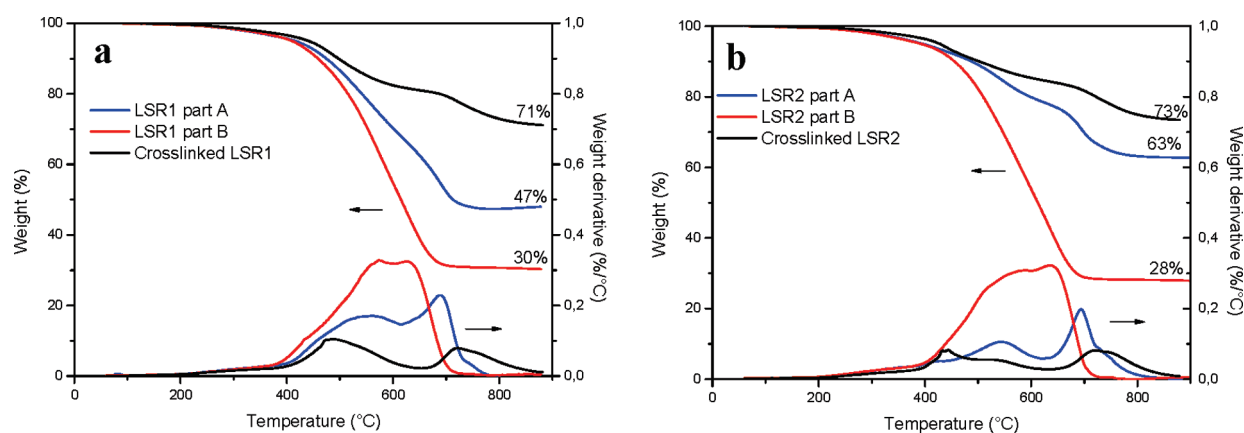


**Figure 16.** Two examples of commercial LSR formulations thermally degraded under a nitrogen flow.

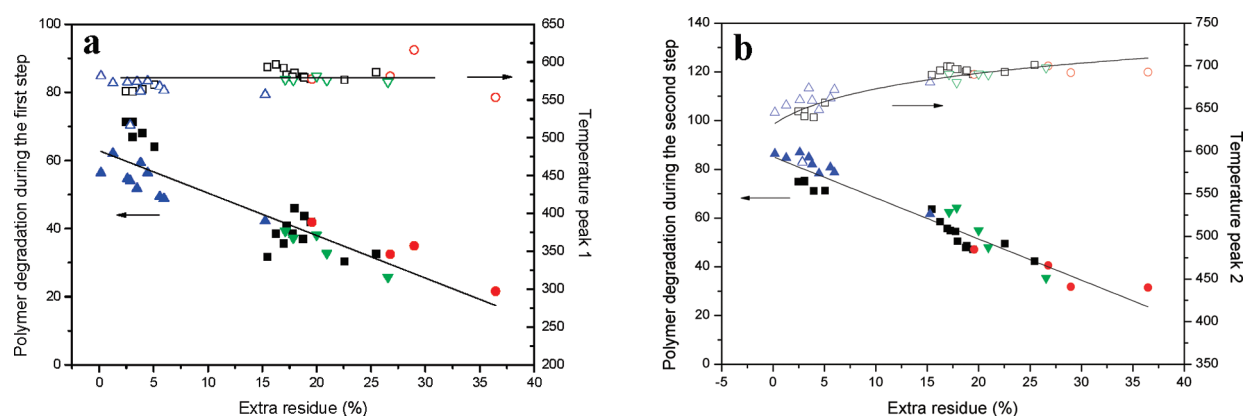


**Figure 17.** Peak area (solid symbols) and peak temperature (open symbols) as a function of extra residues for platinum content (black squares), silica type (red circles), silica content (green down triangles), and peroxide (blue up triangles) studies: (a) first peak on DTG; (b) second peak on DTG.

low platinum contents (Figure 6a). These radicals may volatilize rather than react on PDMS chains, certainly since they are not keen to abstract a proton or a methylene group from the PDMS chains. On the other hand, *t*-BuOOH filled at moderate contents (typically between 3 and 5 wt %) enhanced the final residue of both HDMS-treated and vinyl-functionalized silica blends, with an emphasis on the latter (residues of about 34 to 38% in a reproducible manner, see Figure 15). Note also the color of the residue, a black matte material which did not seem to ceramize as much as when filled with platinum (Figure 9c).

In most high-temperature vulcanizing (HTV) silicone formulations, the cross-linking of silicone chains is commonly ensured by peroxides.<sup>43–46</sup> Peroxides were conventionally classified in the literature into two categories:<sup>43,47,48</sup> “vinyl-specific” or “vinyl-non-specific” radical generators. “Non-specific” peroxides are typically decomposing at low temperatures,<sup>45,49,50</sup> and according to Loan,<sup>44</sup> the cross-linking reaction of PDMS is due to abstraction of the hydrogen on methyl on the  $\alpha$  position of the silicon atom followed by the coupling reaction between two polymer radicals. “Vinyl-specific” peroxides differ by their high decomposition temperature,<sup>49,51</sup> and their supposed propensity to favor addition exclusively on vinyl groups. The difference in reactivity of these two types of peroxide was explained thermodynamically by Dłuzneski,<sup>48</sup> stressing the difference in stability of the radicals: if the radical formed by abstraction of a hydrogen atom is more stable than the one from the peroxide, this latter is classified in the

family of “non-specific vinyl groups” and conversely. Recently, Baquey et al.<sup>52,53</sup> carried out a thorough fundamental study on model reactions between hexamethyldisiloxane ( $M_2$ ) and  $D_4$  using the two most common and representative types of peroxides: di-*tert*-butyl peroxide and dibenzoyl peroxide in the presence and absence of 2,2,5,5-tetramethylpiperidinyloxy (TEMPO) and 2,4-diphenyl-4-methyl-1-pentene, respectively, these latter aimed at trapping radicals as soon as they are formed to simplify the products analysis. Both types of peroxides were able to abstract hydrogen to a methyl, the difference between these two appearing in the fate of the  $Si-CH_2^\bullet$  radical: in the former, it would preferentially add to a vinyl group, whereas for the latter, aromatic groups seemed to attack radicals in competition with vinyl groups. Such hydrogen abstraction is believed to happen here with *t*-BuOOH: both HMDS-treated and vinyl-functionalized silicas participate in the cross-linking reaction and increase the final residue, although higher residues are generated when thermally stable vinyl groups are attached to the silica surface. This set of experiments proves that the presence of a carefully selected radical generator, which would not decompose during the vulcanization step but at higher temperatures, may replace to some extent Pt, a clear advantage from the industrial viewpoint in terms of cost.

*The Case of Commercial LSR Formulations.* Liquid silicone rubbers (LSR) consist of a 50:50 mixture of two components, A and B, which are prepared from the same base, i.e., silica and a

vinyl-terminated polydimethylsiloxane. Compound A additionally contains the platinum catalyst, whereas compound B adds on a few percent of hydrido-functionalized silicone chains as a cross-linker. In the course of a systematical LSR deformation study,<sup>54,55</sup> TGA for a typical formulation showed that compounds A and B produced 47 wt % and 30 wt % (basically the content of silica) residue at 900 °C, respectively (Figure 16a). For 30 Shore A grades, most of the studied commercial formulations presented a roughly constant difference between the residues of compounds A and B, around 15%. The slightly lower content of the extra residue compared to those presented before (*vide supra*) agrees with the fact that, in these formulations, the platinum only plays a catalytic role in the addition reaction of cross-linking: in other words, the Karstedt complex is added in much lower concentration than 200 ppm. In very singular formulations, however, the residue of part A was found to be more than 35% higher than the residue of part B (Figure 16b). Such differences in final residues of A + B may advise one of improved PDMS chain immobilization, either by incorporating particular kinds of silica and/or by combining the action of platinum and a radical generator introduced in the recipe. Thermal degradation of both the vulcanized materials on the other hand presented an improved final residue exceeding 70 wt % at 900 °C (Figure 16).

**III.4. Rationalizing the Degradation Pathway.** All experiments presented before gave various final residues via TG as a consequence of chain immobilization and cross-linking. Yet, in all formulations, we observed two degradation steps in DTG curves. Plotting the polymer degradation, deduced from each of the two different peak areas of DTG curves (see Experimental Section for precision) as a function of extra residues ( $R_{\text{exp}} - R_{\text{simul}}$ ) for all experiments, confirmed a monotonous linear decrease (Figure 17). Moreover, temperatures at the top of the first and second peaks remained constant and increased slightly, respectively. Master curves could be traced, showing that the proposed mechanism is universal from one recipe to another. The fact that the area under the first peak decreases while the temperature at the maximum of degradation remains constant is due to free parts of the mobile PDMS chains degrading at a roughly constant temperature. On the other hand, when the number of adsorption/entanglement points increases, the free PDMS amount also decreases, so that the polymer degradation is reduced. The decrease in area of peaks 1 and 2 is particularly exacerbated when increasing the silica content, an indication that chain immobilization through physical adsorption is the most important mode of immobilization prior to cross-linking.

One should however note that for peroxide–silica–PDMS blends, the volatilization extent is reduced compared to the platinum-containing samples, whereas the second degradation peak is exacerbated. The differences may lie in the density and/or homogeneity of the cross-linking reaction. In the case of platinum, principally, chains located close to the silica surface will generate cross-link points, whereas for peroxide, a homogeneous cross-linking density is expected. Thus, for equivalent chains immobilization, i.e., equal extra residue, platinum-containing samples may possess a fraction of mobile silicone chains, ready to volatilize, more important than in peroxide samples.

## CONCLUSIONS

A general mechanism of the polydimethylsiloxane degradation process entailing a synergy of actions of platinum and silica has

been presented in this article. Either one or the other component introduced in separated formulations does not produce high residues. Three steps are consecutively involved: cross-linking of PDMS chains adsorbed on silica, then volatilization of mobile chains, and finally volatilization/ceramization of the remaining constrained chain fragments. Physical adsorption of a PDMS chain onto a silica surface through hydrogen bonding is a compulsory prerequisite entailing large chemical cross-linking, below 400 °C, via radical Pt catalysis. The macroradical generated from PDMS methyl abstraction can react either with a neighboring PDMS macroradical (interchain cross-linking) or in some instances with organic groups on silica (most likely D<sub>4</sub> loops or vinyl groups). At temperatures from 400 to 640 °C, weakly retained chains depolymerize between cross-link points, releasing volatile small cycles. At high temperatures (typically from 650 °C), the volatilization of highly constrained chains generates a ceramization residue in high yield. Ceramic materials such as SiOC are most probably formed. From the formulation model, new progress was brought to develop silicone blends at a lower price with similar or better ceramization and final residue content. In particular, the presence of active groups toward Pt on the silica surface, such as vinyl groups, improved the content of the final residue. In addition, the use of an easily purchased radical generator of the type *tert*-butyl hydroperoxide was successfully applied to mimic in some ways the catalytic role of Pt. In a next study, we will look specifically at the influence of a prevulcanization step on final residue and ceramic microstructure.

## ASSOCIATED CONTENT

**S Supporting Information.** Table of compositions and degradation properties of the blends used in this study and TG degradation profiles of neat vinyl-modified silica and various silica–PDMS blends filled with DMDPB or *t*-BuOOH. This information is available free of charge via the Internet at <http://pubs.acs.org/>.

## AUTHOR INFORMATION

### Corresponding Author

\*Tel.: 33 4 67 14 72 96. Fax: 33 4 67 14 72 20. E-mail: francois.ganachaud@enscm.fr.

## ACKNOWLEDGMENT

The authors acknowledge S. Livi (IMP LMM INSA-Villeurbanne) and N. Durand for providing the vinyl-modified silica, B. Otazaghine for Py-GC MS studies, and C. Longuet for helpful comments on radical precursors.

## REFERENCES

- (1) Dvornic, P. R. In *Silicone-Containing Polymers*; Jones, R. G., Ando, W., Chojnowski, J., Eds.; Dordrecht, the Netherlands: Kluwer Academic Publisher, 2000; pp 185–212.
- (2) Hamdani, S.; Longuet, C.; Perrin, D.; Lopez-Cuesta, J.-M.; Ganachaud, F. *Polym. Degrad. Stab.* **2009**, *94*, 465–495 and references therein.
- (3) Hamdani, S.; Longuet, C.; Lopez-Cuesta, J.-M.; Ganachaud, F. *Polym. Degrad. Stab.* **2010**, *99*, 1911–1919.
- (4) Xu, J.; Razeed, K. M.; Roy, S. J. *Polym. Sci. B: Polym. Phys.* **2008**, *46*, 1845–1852.



- (5) Verdejo, R.; Barroso-Bujans, F.; Rodriguez-Perez, M. A.; de Saja, J. A.; Arroyo, M.; Lopez-Manchado, M. A. *J. Mater. Chem.* **2008**, *18*, 3933–3939.
- (6) Tkaczyk, J. E.; Klug, F. J.; Amarasekera, J.; Sumpter, C. A. U.S. Patent 6,051,642, 2000.
- (7) Ota, K.; Hirai, K. U.S. Patent 6,011,105, 1998.
- (8) Deshpande, G.; Rezac, M. E. *Polym. Degrad. Stab.* **2001**, *74*, 363–370.
- (9) MacLaury, M. R. *J. Fire Flam.* **1979**, *10*, 175–198.
- (10) Hayashida, K.; Tsuge, S.; Ohtani, H. *Polymer* **2003**, *44*, 5611–5616.
- (11) Lagarde, R.; Lahaye, J.; Bargain, M. *Eur. Polym. J.* **1977**, *13*, 769–774.
- (12) Karstedt, B. D. U.S. Patent 3,715,334, 1970.
- (13) Lewis, L. N.; Stein, J.; Gao, Y.; Colborn, R. E.; Hutchins, G. *Platinum Metals Rev.* **1997**, *41*, 66–75.
- (14) Radhakrishnan, T. S. *J. Appl. Polym. Sci.* **1999**, *73*, 441–450.
- (15) Saleh, K.; Cami, X. B.; Thomas, A.; Guigon, P. *KONA* **2006**, *24*, 134–145.
- (16) Cassel, B.; Hoult, R. *Technical note on Differential Scanning Calorimetry*. Website: [las.perkinelmer.com/content/TechnicalInfo/TCH\\_UseofSmartScan.pdf](http://las.perkinelmer.com/content/TechnicalInfo/TCH_UseofSmartScan.pdf) (accessed Feb 2011).
- (17) *Polymer Data Handbook*; Mark, J. E., Ed.; Oxford University Press: New York, 1999; p 420.
- (18) Andersson, L. H. U.; Johander, P.; Hjertberg, T. *J. Appl. Polym. Sci.* **2003**, *90*, 3780–3789.
- (19) Stepto, R. F. T.; Cail, J. I.; Taylor, D. J. *R. Mater. Res. Innov.* **2003**, *7*, 4–9.
- (20) Aranguren, M. I.; Mora, E.; MacOsco, C. W. *J. Colloid Interface Sci.* **1997**, *195*, 329–337.
- (21) Selimovic, S.; Maynard, S. M.; Hu, Y. *J. Rheol.* **2007**, *51*, 325–340.
- (22) Gun'ko, V. M.; Borysenko, M. V.; Pissis, P.; Spanoudaki, A.; Shinyashiki, N.; Sulim, I. Y.; Kulik, T. V. *Appl. Surf. Sci.* **2007**, *253*, 7143–7156.
- (23) DeGroot, J. V., Jr.; Macosko, C. W. *J. Colloid Interface Sci.* **1999**, *217*, 86–93.
- (24) Cohen Addad, J. P.; Touzet, S. *Polymer* **1993**, *34*, 3490–3498.
- (25) Cohen Addad, J. P.; Ebengou, R. *Polymer* **1992**, *33*, 379–383.
- (26) Camino, G.; Lomakin, S. M.; Lazzari, M. *Polymer* **2001**, *42*, 2395–2402.
- (27) Maxwell, R. S.; Cohenour, R.; Sung, W.; Solyom, D.; Patel, M. *Polym. Degrad. Stab.* **2003**, *80*, 443–450.
- (28) Maus, A.; Saalwachter, K. *Macromol. Chem. Phys.* **2007**, *208*, 2066–2075.
- (29) Dollase, T.; Wilhelm, M.; Spiess, H. W. *Interf. Sci.* **2003**, *11*, 199–209.
- (30) Roland, C. M.; Aronson, C. A. *Polym. Bull. (Berlin)* **2000**, *45*, 439–445.
- (31) Bordeaux, D.; Cohen Addad, J. P. *Polymer* **1990**, *21*, 743–748.
- (32) Aranguren, M. I. *Polymer* **1998**, *39*, 4897–4903.
- (33) Stevens, N. S. M.; Rezac, M. E. *Chem. Eng. Sci.* **1998**, *53*, 1699–1711.
- (34) Mingfei, W.; Bertmer, M.; Demco, D. E.; Blümich, B.; Litvinov, V. M.; Barthel, H. *Macromolecules* **2003**, *36*, 4411–4413.
- (35) Litvinov, V. M.; Barthel, H.; Weis, J. *Macromolecules* **2002**, *35*, 4356–4364.
- (36) Branlard, P.; George, C.; Leuci, C. European Patent 1,238,007, 2003.
- (37) Leuci, C.; Canpont, D. World Patent 2004064081, 2004.
- (38) Camino, G.; Lomakin, S.; Lageard, M. *Polymer* **2002**, *43*, 2011–2015.
- (39) Renlund, G. M.; Prochazka, S. A.; Doremus, R. H. *J. Mater. Res.* **1991**, *6*, 2716–2722.
- (40) Schiavon, M. A.; Redondo, S. U. A.; Pina, S. R. O.; Yoshida, I. V. P. *J. Non-Cryst. Solids* **2002**, *304*, 92–100.
- (41) Pantano, C. G.; Singh, A. K.; Zhang, H. *J. Sol-Gel Sci. Technol.* **1999**, *14*, 7–25.
- (42) Campostrini, R.; D'Andrea, G.; Carturan, G.; Ceccato, R.; Soraru, G. D. *J. Mater. Chem.* **1996**, *6*, 585–594.
- (43) Caprino, J. C.; Macander, R. F. In *Rubber Technology*, 3rd ed.; Morton, M., Ed.; Van Nostrand Reinhold: New York, 1987; pp 375–409.
- (44) Loan, L. D. *Rubber Chem. Technol.* **1967**, *40*, 149–176.
- (45) Thomas, D. R. In *Siloxane Polymers*; Clarson, S. J., Semlyen, J. A., Eds.; Prentice Hall: Englewood Cliffs, NJ, 1993; pp 567–615.
- (46) Brooke, M. R. In *Silicon in Organic, Organometallic and Polymer Chemistry*; Wiley: New York, 2000; pp 282–291.
- (47) Nijhof, L.; Cubera, M. *Rubber Chem. Technol.* **2001**, *74*, 181–188.
- (48) Dluzneski, P. R. *Rubber Chem. Technol.* **2001**, *74*, 451–492.
- (49) Dunham, M. L.; Bailey, D. L.; Mixer, R. Y. *Ind. Eng. Chem.* **1957**, *49*, 1373–1376.
- (50) Warley, R. L.; Feke, D. L.; Manas-Zloczower, I. *J. Appl. Polym. Sci.* **2005**, *97*, 1504–1512.
- (51) Bobear, W. J. In *Rubber Technology*, 2nd ed.; Morton, M., Ed.; Van Nostrand Reinhold: New York, 1973; pp 368–406.
- (52) Baquey, G.; Moine, L.; Degueil-Castaing, M.; Lartigue, J. C.; Maillard, B. *Macromolecules* **2005**, *38*, 9571–9583.
- (53) Baquey, G.; Moine, L.; Babot, O.; Degueil, M.; Maillard, B. *Polymer* **2005**, *46*, 6283–6292.
- (54) Yactine, B.; Boutevin, B.; Ganachaud, F. *Polym. Adv. Technol.* **2009**, *20*, 66–75.
- (55) Yactine, B.; Ratsimihety, A.; Ganachaud, F. *Polym. Adv. Technol.* **2010**, *21*, 139–149.

Supporting information for

# High Residue Contents Indebted by Platinum and Silica Synergistic Action during the Pyrolysis of Silicone Formulations

*By Etienne Delebecq, Siska Hamdani, Julia Raeke, José-Marie Lopez Cuesta and François Ganachaud*

Table S1. Compositions and degradation properties of the blends used in this study. The experimental errors for the results are estimated to be  $\pm 0.5\%$  for the final residue and  $\pm 1.5$  for the areas.

Parameter investigated	Additives composition			Results			Calculation		
	Silica treating agent	Silica content (wt%)	Pt content (ppm) or radical generator content (wt%)	Final residue (%)	Area under peak 1	Area under peak 2	Extra residue <sup>a</sup> (%)	A <sub>1</sub> <sup>corrected</sup>	A <sub>2</sub> <sup>corrected,b</sup>
Platinum content	HMDS	21	1	24.1	56.3	17.0	3.1	71.3	74.8
	HMDS	21	2	23.5	56.3	17.0	2.5	71.3	74.8
	HMDS	21	5	26.1	50.6	20.2	5.1	64.0	71.1
	HMDS	21	10	25.0	53.7	18.0	4.0	68.0	71.1
	HMDS	21	25	24.1	52.9	19.7	3.1	66.9	75.3
	HMDS	21	50	37.3	30.4	28.4	16.3	38.5	58.5
	HMDS	21	100	36.5	25.1	34.3	15.5	31.7	63.6
	HMDS	21	150	39.0	36.3	21.5	18.0	46.0	50.4
	HMDS	21	400	46.5	25.7	22.5	25.5	32.6	42.3
	HMDS	21	200	38.0	28.2	28.2	17.0	35.7	55.6
	HMDS	21	200	39.8	29.2	23.8	18.8	37.0	47.8
	HMDS	21	200	40.5	33.1	21.6	19.5	41.9	47.1
	HMDS	21	200	39.9	34.5	21.6	18.9	43.7	48.6
	HMDS	21	200	43.6	24.0	27.2	22.6	30.4	49.4



	HMDS	21	200	38.3	32.3	25.6	17.3	40.9	54.8
	HMDS	21	200	38.8	30.4	26.4	17.8	38.5	54.4
Silica type	Bare	21	200	57.5	17.1	19.5	36.5	21.6	31.4
	Vinyl <sup>c</sup>	21	200	50.0	27.6	16.3	29.0	34.9	31.8
	D4	21	200	47.8	25.7	21.6	26.8	32.5	40.6
	HMDS	21	200	40.6	33.1	21.6	19.6	41.9	47.1
Silica content	HMDS	5	200	23.4	35.1	38.1	17.9	37.2	64.2
	HMDS	10	200	27.5	35.2	34.0	17.1	39.3	62.4
	HMDS	15	200	35.2	32.3	28.8	20.0	38.1	54.9
	HMDS	20	200	41.0	26.2	25.8	20.9	32.8	47.9
	HMDS	30	200	56.3	18.1	18.5	26.6	25.7	35.4
Radical generator tBuOOH	Vinyl	21	1	22.3	49.0	25.4	1.3	62.1	84.7
	Vinyl	21	3	24.5	40.9	32.3	3.5	51.8	84.9
	Vinyl	21	5	36.3	33.3	28.1	15.3	42.2	61.6
	Vinyl	21	10	23.6	43.2	31.1	2.6	54.7	87.0
	Vinyl	21	15	26.6	38.9	32.4	5.6	49.3	80.8
	HMDS	21	1	21.2	44.5	29.8	0.2	56.4	86.4
	HMDS	21	3	27.0	38.5	31.8	6.0	48.8	78.8
	HMDS	21	5	24.8	46.9	26.4	3.8	59.3	82.1
	HMDS	21	10	23.9	42.6	30.3	2.9	54.0	83.2
	HMDS	21	15	25.5	44.5	27.0	4.5	56.4	78.3

<sup>a</sup> Extra residue = Experimental final residue – Simulated final residue; <sup>b</sup> the area under the second peak normalized to the remaining material amount after the 1<sup>st</sup> degradation peak; <sup>c</sup> Curve presented in Figure S1.

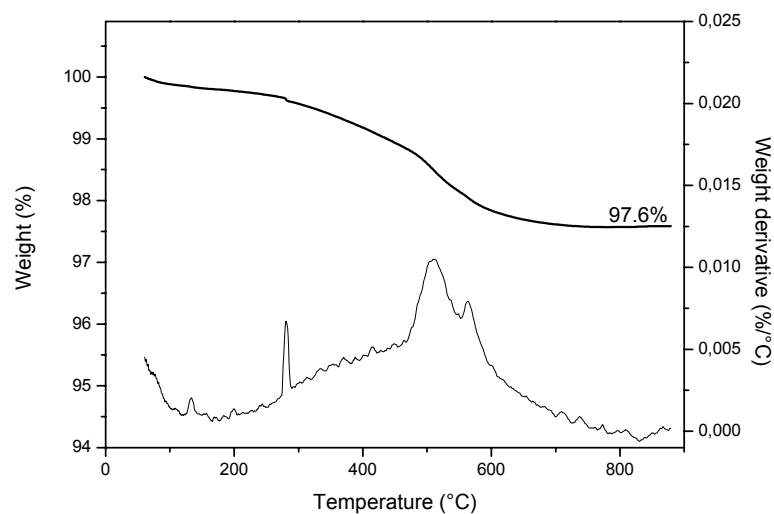


**Figure S1.** TG degradation profile of neat vinyl-modified silica.

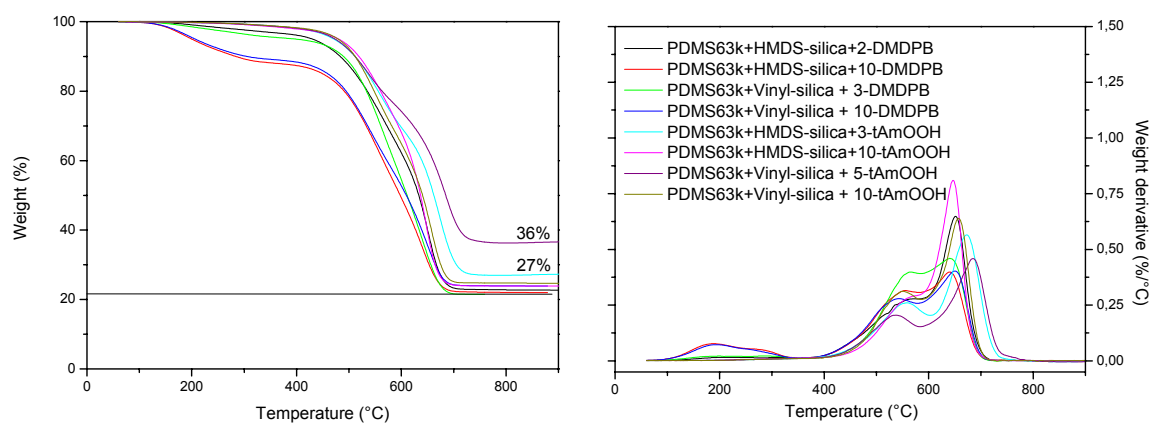


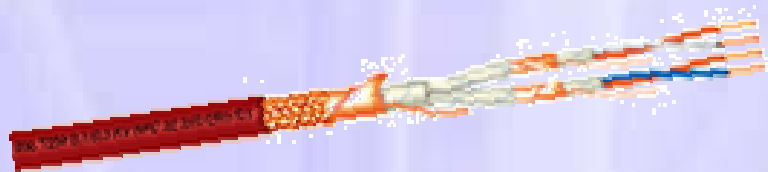
**Figure S2.** Examples of degradation profile of various 21% silica-PDMS blends (HMDS or vinyl modified silica) containing from 2 to 10wt.% of Dimethyl-2,3-diphenylbutane (DMDPB) or *tert*-butylhydroperoxide (*t*-BuOOH): a) TG curves; b) DTG curves.



# *Chapitre 3.*

## *Etude des Composites:*

### *«Stabilité Thermique»*





## **Etude des propriétés thermiques d'une matrice silicone contenant des charges à base de calcium ou d'aluminium : Préparation des mélanges et analyse de leur comportement thermique.**

Le polydiméthylsiloxane (PDMS) se distingue des polymères organiques carbonés par une stabilité thermique très importante, ce qui explique son utilisation fréquente pour des applications à haute température. Cependant, le silicone seul présente des caractéristiques mécaniques insuffisantes pour la plupart des applications, d'où la nécessité d'incorporer une ou plusieurs charges renforçantes dans les formulations. Il s'avère en effet que dans la plupart des cas, en plus de conférer des propriétés mécaniques intéressantes, telles que l'élasticité ou la résilience, l'ajout de charges minérales améliore également la stabilité thermique de la matrice. Une large gamme de charges a déjà été utilisée pour des formulations usuelles, par exemple dans des domaines d'application tels que la câblerie, et son action rapportée principalement dans des brevets. Parmi les nombreuses publications présentant une grande variété de charges incorporées dans les silicones, peu d'entre elles détaillent les mécanismes de dégradation thermique. Une connaissance détaillée de l'action de chaque type de charge et son rôle dans des formulations à matrice silicone à des températures élevées est indispensable pour la réalisation de formulations optimales vis-à-vis de la résistance au feu.

La première partie de cette étude a consisté à regarder le comportement thermique des charges seules. Elles ont alors été classées en trois catégories : les charges « neutres », celles contenant de l'eau et celles présentant des groupements hydroxyles en surface. Les charges sélectionnées pour cette étude sont le carbonate de calcium précipité (PCC), la calcite, et la wollastonite en ce qui concerne les charges « neutres », la chaux (hydroxyde de calcium), l'aluminium trihydraté (ATH) et la boehmite comme charges contenant de l'eau, et enfin le mica et l'alumine, présentant spécifiquement des groupements hydroxyles en surface. Les différentes formulations ont été réalisées en suivant le même protocole : l'incorporation des charges dans la matrice silicone est effectuée via un mélangeur interne (HAAKE) avant de réticuler à chaud et sous pression ces mélanges fins et stables. Le comportement thermique de ces composites a été étudié par analyse thermogravimétrique (ATG) sous atmosphère inerte (azote). L'étude de la stabilité thermique intrinsèque et du taux de résidu final des composites a montré des effets synergiques ou antagonistes lors de l'ajout de différentes charges, en

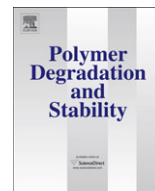


comparant la courbe de dégradation du composite obtenue expérimentalement avec celle obtenue par simulation.

L'incorporation du PCC, de la calcite ou de la wollastonite ne modifie pas la température de début de dégradation de la matrice silicone, en revanche, l'ajout de chaux accélère la dégradation de la matrice, à cause de la libération d'eau lors de la dégradation de la charge. Le même effet a été observé pour les composites contenant de l'ATH et de l'alumine. La libération d'eau est néfaste si elle se produit à une température inférieure à celle de début de dégradation de la matrice, car elle accélère la dégradation de cette dernière. Le mica est une charge connue pour porter des groupements hydroxyles en surface, c'est-à-dire ne libérant presque pas d'eau, et ne modifiant donc pas la température de dégradation du silicone. De même, la boehmite, charge libérant de l'eau mais à une température supérieure à celle de la dégradation du silicone, n'interfère donc pas.

Le résidu final du composite est indépendant du type de charge (calcium ou aluminium), mais la dégradation thermique est par contre fortement influencée par la nature de la charge (non-hydratée, contenant de l'eau, ou portant des groupements hydroxyles en surface). Dans le cas des mélanges contenant une charge à base de calcium, une réactivité entre le produit de dégradation de la charge et la silice (initialement présente ou issue de la dégradation du silicone) a également été mise en évidence. L'oxyde de calcium (CaO) obtenu par décomposition du carbonate de calcium ou de la chaux peut réagir avec la silice à haute température ( $>900^{\circ}\text{C}$ ) pour former trois nouvelles structures cristallines de type silicates de calcium : la wollastonite ( $\text{CaSiO}_3$ ), une variété allotropique de même formule stoechiométrique, mais de structure cristalline différente (notée  $\beta\text{CaSiO}_3$ ), et la larnite ( $\text{Ca}_2\text{SiO}_4$ ).

En plus de la nature des charges, leur forme (morphologie) et leur taille jouent également un rôle important sur les taux de résidu des composites. Les charges aciculaires ou sphériques apparaissent moins efficaces que les charges lamellaires ou rhomboédriques, et les charges nanométriques, moins intéressantes que les microniques. Si l'on considère le cas des charges libérant de l'eau, il s'avère que plus la taille de la charge est petite, plus sa surface spécifique est grande, cela conduit donc à une diminution du taux de résidu final du composite, à cause de sa forte réactivité de surface. Il existe néanmoins une exception : la chaux confère un taux de résidu final plus important, en raison de la réactivité de CaO avec la silice à haute température, qui contrecarre l'effet néfaste de l'eau.



# Calcium and aluminium-based fillers as flame-retardant additives in silicone matrices. I. Blend preparation and thermal properties

Siska Hamdani<sup>a</sup>, Claire Longuet<sup>a</sup>, José-Marie Lopez-Cuesta<sup>a</sup>, François Ganachaud<sup>b,\*</sup>

<sup>a</sup> Centre des Matériaux de Grande Diffusion, Ecole des Mines d'Alès, 6 avenue de Clavières 30319 ALES Cedex, France

<sup>b</sup> Institut Charles Gerhardt UMR5253 CNRS/UM2/ENSCM/UM1, Equipe Ingénierie et Architectures Macromoléculaires, Ecole Nationale Supérieure de Chimie de Montpellier, 8 Rue de l'Ecole Normale 34296 Montpellier cedex, France

## ARTICLE INFO

### Article history:

Received 8 March 2010

Accepted 20 April 2010

Available online 5 May 2010

### Keywords:

Silicone

Fire retardants

Fillers

Thermal degradation

Thermogravimetry

## ABSTRACT

This series investigates silicone composites with enhanced thermal behaviour for cable applications. Calcium and aluminium-based fillers introduced into silicone formulations were classified according to three categories: non-hydrated fillers such as  $\text{CaCO}_3$  (precipitated calcium carbonate and natural calcite) and wollastonite, water-releasing fillers such as calcium hydroxide, ATH, boehmite, and hydroxyl-functionalized fillers including alumina and mica. The fillers were first characterized in detail, and the thermal stability of their blends with silicone was recorded by thermogravimetric analyses. A discussion on various aspects of the filler morphology (size, microstructure, release profile with temperature) on the silicone stability is finally given.

© 2010 Elsevier Ltd. All rights reserved.

## 1. Introduction

Since the commercialization of silicones in the 40s', silicone industries have developed a variety of products, among which polydimethylsiloxane (PDMS) is the prevailing polymer. The structure of PDMS entails a wider range of operating temperatures for silicones than for most organic elastomers [1], thus covering a variety of specifications in e.g. civil engineering, transportation, aerospace, defence, textiles, cosmetics and electrical cable applications [2–5].

Silicone applications at high temperature for heat-resistant coatings of electrical cable were made possible thanks to three unique features: i) a remarkable resistance of PDMS at high temperature (PDMS starts to degrade at 300 °C [6,7]), ii) an outstanding reaction to fire (volatile cyclosiloxane release does not participate to the gas combustion [8]) and iii) the formation of silica ash from silicone degradation, acting as a mass transport barrier and delaying the volatilization of decomposition products [9]. Since the thus-generated silica powder is often of insufficient mechanical strength to generate a cohesive residue, several types of inorganic fillers are commonly incorporated into industrial silicone formulations, in complement to fumed or precipitated silica, to provide a better shielding effect [10].

In a recent review from the open and patent literatures, Hamdani et al. [11] described the incorporation of several types of fillers in silicone matrix in a view to improve mechanical properties, to lower production cost, and to enhance the thermal stability and fire behaviour of these composites [12]. Even if several papers have proposed ways to improve the thermal stability of silicone composites, few of these tried to correlate filler-silicone matrix interactions with their behaviour at high temperature. This series is thus devoted to the study of calcium and aluminium-based inorganic fillers as additives for a new generation of fire-resistant cables. In this first part, we describe the characteristics of the different fillers, their blending in a model silicone matrix and the thermogravimetric analyses of resulting composites. The second part will focus primarily on the content and state of the residue using a simulation of a fire test such as CR1 NFC 32 070 standard test (a fire test for electrical cables in France) [13]. Finally, the third part will describe the fire behaviour of similar silicone composites in conventional fire tests using the complementary cone calorimeter and micro calorimeter techniques.

## 2. Materials and methods

### 2.1. Materials

The silicone matrix, kindly supplied by Bluestar Silicones, contains 74.4 wt% of vinyl-terminated polydimethylsiloxane ( $M_w$  of 550,000 g/mol), 25 wt% of  $D_4$ -modified silica and 0.6 wt% of

\* Corresponding author. Tel.: +33 4 67 14 72 96; fax: +33 4 67 14 72 20.  
E-mail address: [francois.ganachaud@enscm.fr](mailto:francois.ganachaud@enscm.fr) (F. Ganachaud).

**Table 1**  
Physical and thermal properties of the fillers used in this study.

	Fillers	Formula	Chemical Composition <sup>a</sup>	Particle shape	Mean particle size and deviation (μm) <sup>b</sup>	SSA (m <sup>2</sup> /g) <sup>c</sup>	Density (g/cm <sup>3</sup> )		Weight loss at 900 °C (%)		XRD Crystalline form <sup>d</sup>
							Exp. <sup>e</sup>	Litt. <sup>f</sup>	Exp. <sup>g</sup>	Simul. <sup>h</sup>	
Ca-based	Precipitated calcium carbonate (PCC)	CaCO <sub>3</sub>	CaCO <sub>3</sub>	Oblate/spherical (aggregates)	0.074 ± 0.015	20.57 ± 0.04	2.67 ± 0.01	2.7	45.0 ± 0.4	44	Calcite
	Calcite	CaCO <sub>3</sub>	CaCO <sub>3</sub> (98.0%) MgCO <sub>3</sub> (0.4%) Fe <sub>2</sub> O <sub>3</sub> (0.1%)	Rhombohedral	1.0 ± 0.3	6.49 ± 0.33	2.69 ± 0.01	2.7	43.8 ± 0.1	44	Calcite Quartz
	Calcium hydroxide	Ca(OH) <sub>2</sub>	Ca(OH) <sub>2</sub>	Rhombohedral	1.1 ± 0.5	5.44 ± 0.79	2.29 ± 0.01	2.2	29.4 ± 0.7	24	Portlandite Calcite
	Wollastonite	CaSiO <sub>3</sub>	CaO (46.15%), SiO <sub>2</sub> (51.60%) Fe <sub>2</sub> O <sub>3</sub> (0.77%) Al <sub>2</sub> O <sub>3</sub> (0.34%) MnO (0.16%) MgO (0.38%) TiO <sub>2</sub> (0.05%) K <sub>2</sub> O (0.05%)	Acicular	7.4 ± 6.7	3.74 ± 1.15	2.92 ± 0.01	2.9–3.1	1.4 ± 0.4	0	Wollastonite Calcite
Al-based	Aluminum trihydrate (ATH)	Al(OH) <sub>3</sub>	Al <sub>2</sub> O <sub>3</sub> ·3H <sub>2</sub> O	Rhombohedral	0.9 ± 0.3	6.01 ± 0.04	2.43 ± 0.01	2.4	35.2 ± 0.5	35	Gibbsite
	Boehmite	AlOOH	Al <sub>2</sub> O <sub>3</sub> (83.00%) Fe <sub>2</sub> O <sub>3</sub> (0.02%) SiO <sub>2</sub> (0.04%) Na <sub>2</sub> O (0.50%)	Acicular	0.37 ± 0.11	40 <sup>i</sup>	3.01 ± 0.01	3	17.7 ± 0.1	15	Boehmite
	Alumina	Al <sub>2</sub> O <sub>3</sub>	α-Al <sub>2</sub> O <sub>3</sub>	Spherical	0.013 <sup>i</sup>	94.28 ± 0.05	NM <sup>j</sup>	4 <sup>k</sup>	5.3 ± 0.3	0	Aluminum oxide
	Mica	KAl <sub>2</sub> (Si <sub>3</sub> Al)O <sub>10</sub> (OH) <sub>2</sub>	SiO <sub>2</sub> (51.0%) Al <sub>2</sub> O <sub>3</sub> (32.0%) K <sub>2</sub> O (8.5%) MgO (0.6%)	flake-like, lamellar/platelet	6.8 ± 9.6	5.87 ± 0.75	2.78 ± 0.01	2.8–3	5.5 ± 0.1	— <sup>l</sup>	Muscovite, Kaolinite, Quartz

<sup>a</sup> Given by the supplier, the remaining content to reach 100% in some fillers is supposed to be of water.

<sup>b</sup> From ESEM photos, using a size measuring software (see text).

<sup>c</sup> From BET measurements.

<sup>d</sup> From XRD.

<sup>e</sup> From He Pycnometer.

<sup>f</sup> From reference [15] for all fillers but mica [16].

<sup>g</sup> Measured by TGA.

<sup>h</sup> Making stoichiometric calculation according to the filler decomposition pathway (see Scheme 1).

<sup>i</sup> Given by the supplier.

<sup>j</sup> Non measurable.

<sup>k</sup> Density of micro-sized natural alumina.

<sup>l</sup> Could not be calculated, according to the unknown precise chemical structure.

2,5-dimethyl-2,5-di(tertbutylperoxy)hexane as a crosslinking agent. It was specifically prepared for this study in order to avoid the presence of any other additives in the formula. On SEM micrographs, silica aggregates can be seen (Figure S1), the nature of which was confirmed by EDX mapping (*vide infra*). The thermal behaviour of the silicone matrix alone is in agreement with previously reported figures [14] (Figure S1). Precipitated calcium carbonate (PCC), wollastonite, and boehmite were kindly supplied by Solvay, Nyco minerals and Nabaltec respectively. ATH was purchased from Martinswerk, alumina from Evonik and mica from Kaolin International. Table 1 presents the formula and filler compositions as given by the suppliers, whereas the SEM micrographs of the different fillers are given in supporting information (Figure S2).

## 2.2. Methods

Thermogravimetric analyses (TGA) were carried out on a Perkin–Elmer 7 thermal analysis system (Perkin–Elmer, Norwalk, CT). The filler and composite samples ( $10 \pm 2$  mg) were heated in an alumina ceramic crucible from 50 to 900 °C at a heating rate of 10 °C/min under a nitrogen flow rate of 20 ml/min. The simulated weight loss plots were obtained by recording experimental TG curves of the different components separately, normalizing them according to their contents in the formulation and adding them to simulate the TG curve that one would attend without synergistic effects between the different components. An example is given in Figure S1 for the Bluestar Silicones matrix. The simulated curve was obtained by overlapping the curves of silica (grey dotted curve, normalized by multiplying by 0.25) and PDMS (black dotted curve, normalized by multiplying by 0.744). One sees here that hydrogen bonding between silicone and silica provides a better experimental thermal stability of the matrix compared to the simulated TG curve (black and grey solid curves, respectively).

SEM (Scanning electron microscopy) microstructure analyses were acquired on a Hitachi S-4300 environmental scanning electron microscope (ESEM) using an acceleration voltage of 15 kV. Filler morphology and distribution at the surface and in the bulk of the composites were assessed by immersing the composite sample in liquid nitrogen and fracturing it before SEM observations. Energy-dispersive X-Ray (EDX) measurements were conducted as an integrated tool in ESEM to determine the elemental composition of residue on micrographs with a magnitude of 300×. Apparent filler particle size and distribution were measured on ESEM micrographs using XT Docu program as an integrated program in ESEM.

Helium Pycnometer was used to measure the density of filler. Powder sample was weighted and then placed in the measurement chamber of pycnometer. The test was carried out using helium gas under pressure of 100–150 bar and a capillary pressure of 134.44 MPa to ensure the drainage of sample. The density of the filler was calculated according to powder standard measurements.

To measure the specific surface area of the fillers by nitrogen adsorption, small samples (~1 g) of dry powder of fillers were degassed at 25 °C under vacuum for 800–1000 min to remove physically adsorbed gases (water vapour). They were then immediately analyzed in a BET (Brunauer Emmet Teller) instrument (SA 3100, Coulter Instrument Co) by weighing the samples before and after the analysis. The specific surface area values were calculated automatically by the system software and are reported as square meters per gram.

X-Ray Diffraction (XRD) analyses of finely ground filler and final residues were performed on a Bruker X-ray diffractometer using Cu K $\alpha$  radiation.

## 2.3. Sample preparation

Composite formulations consisting of 20 wt% of silica and 20 wt % of filler were prepared using a HAAKE internal mixer at a temperature of 45 °C, shear rate of 40 rpm and mixing time of 50 min. The HAAKE internal mixer has two rotors running in a contra-rotating way to blend the filler and matrix. Thereafter, filled silicone was crosslinked under heat pressure of 90 bar at 150 °C during 15 min to obtain a plate of elastomer with dimensions of 10 cm × 10 cm × 0.4 cm.

## 3. Results

### 3.1. Filler characterizations

Before investigating the influence of the various fillers on the thermal stability of a silicone composite, the selected calcium and aluminium-based fillers were characterized by a variety of techniques, which main results are given in Table 1.

#### 3.1.1. Filler morphologies and particle sizes

The fillers presented various forms and mean particle sizes, as noted in Table 1. The corresponding particle sizes were measured on SEM micrographs taken under magnification of 20000×, except for Mica (2000×) for which particles were too large to use such zooming (Figure S2). All fillers present a large particle size distribution. PCC is composed of big agglomerates of particles bound together, whereas calcite shows independent particles. Calcium hydroxide contains very large agglomerates, probably because of the water absorbed by these very hygroscopic particles. Wollastonite is a mix of big stone-like particles and small particles. ATH particles are hexagonal rhombohedra assembled into large blocks. Boehmite showed crystal bunches of acicular (needle-like) particles that form fragile crystalline agglomerates, and alumina is composed of spherical particles. According to supplier, boehmite and alumina have mean particle sizes of 300 nm and 13 nm respectively (for this latter, the average particle size could not be measured from ESEM micrographs analysis). (Flake-like) mica forms agglomerates of lamellar platelets but some independent particles were also found. From the mean particle size measurement of fillers obtained from ESEM micrographs, one can particularly stress out the large particle size distribution of wollastonite and mica (Table 1).

#### 3.1.2. Physical properties

The different filler characteristics are quoted in Table 1, among which their densities, measured by He pycnometry, the specific surface area (SSA), obtained by BET, and the crystalline structures from XRD analyses. When available, these experimental values were compared with ones obtained from the literature or from simulation (see Table 1 for details).

The filler densities compared well with values mentioned in the literature. Such comparison could not be done for the alumina nanoparticles, so light and fine that, even when the measuring chamber was completely filled by the sample, its density still could not be measured by He Pycnometry. Note that PCC, composed of agglomerated nano-sized particles, exhibits the same density as calcite, a natural calcium carbonate mineral.

Specific surface area (SSA) measurements provide information about the filler surface in a view of potential interfacial interactions with the matrix. According to SSA values, alumina logically exhibits the highest SSA whereas wollastonite displays the lowest one. Calcite value is three times less than PCC.

XRD analyses confirmed the crystalline form of fillers and their impurities. Some impurities were observed in calcite, calcium

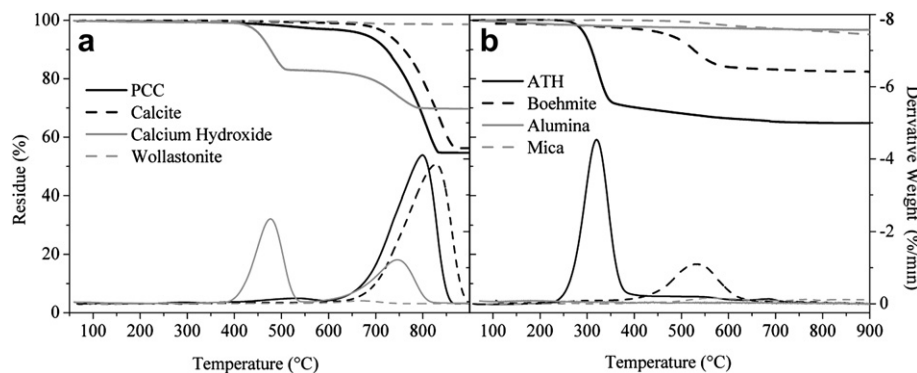


**Fig. 1.** TG analyses (weight loss curves at the top and derivatives on the bottom) of (a) calcium and (b) aluminium-based fillers under inert atmosphere at a heating rate of 10 °C/min.

hydroxide, and mica (i.e. in natural mineral products), while synthetic PCC, ATH, boehmite and alumina do not present any crystalline impurities. The most common impurities found in calcite natural mineral and in muscovite mica are quartz and kaolinite + quartz, respectively. The presence of calcite in calcium hydroxide may come from sample contamination by CO<sub>2</sub> in atmosphere, thus reacting with Ca(OH)<sub>2</sub> particles to form CaCO<sub>3</sub> [15].

### 3.1.3. Thermal stability of fillers

The weight losses of the different fillers were determined by thermogravimetry under nitrogen at a heating rate of 10 °C/min from 50 to 900 °C. Experimental filler residues were compared to simulated ones from stoichiometric calculation based on the degradation pathway intrinsic to the filler structure. Fig. 1 shows the different behaviours of calcium- and aluminium-based filler under thermal treatment.

**3.1.3.1. Ca-based fillers.** Among all fillers, calcium carbonates showed the highest weight loss, i.e. 44%, which corresponds exactly to the theoretically predicted value assuming the release of CO<sub>2</sub> during filler decomposition (Scheme 1a). PCC produced the same final weight loss than calcite, but started to decompose at slightly larger temperature (the onset temperature of degradation is shifted of 50 °C between PCC and calcite, see Fig. 1a). Strong degradation of PCC occurred from 600 °C to 850 °C, with a derivative peak centred

at 810 °C, while the main degradation event of calcite was observed from 650 °C to 900 °C (maximum derivative at 830 °C). The shift of temperature is either due to the difference in size of PCC and calcite, or to the natural impurities that calcite contains, such as quartz and Fe<sub>2</sub>O<sub>3</sub>, which may contribute to enhance the thermal stability of calcite [16–19]. It should be stressed here that CO<sub>2</sub> release during calcium carbonate decomposition is an endothermic reaction [20].

Calcium hydroxide started to decompose in a temperature range of 400–830 °C, releasing 30 wt% of volatiles, mainly water. Two degradation steps were observed: the first one, set between 400 °C and 600 °C, released 24 wt% of H<sub>2</sub>O, in agreement with the theoretical value (Scheme 1a). The further 6 wt% experimental weight loss observed during the second step of degradation (between 600 °C and 830 °C) could be ascribed to calcite impurities seen by XRD (see Table 1), since in the TG curve, the slope of the second release coincides with those of PCC and calcite degradation (Fig. 1a).

Wollastonite should show no weight loss even after heating up to 900 °C; the 1 wt% of weight loss observed here is tentatively explained by the presence of a small amount of calcite impurity.

**3.1.3.2. Al-based fillers.** The experimental weight loss of ATH filler (35 wt%) is in agreement with stoichiometric calculation (release of three water molecules, see scheme 1b), and confirms observations from the literature [21]. ATH loses weight from 190 °C to 800 °C according to a three-step degradation scheme: the first step

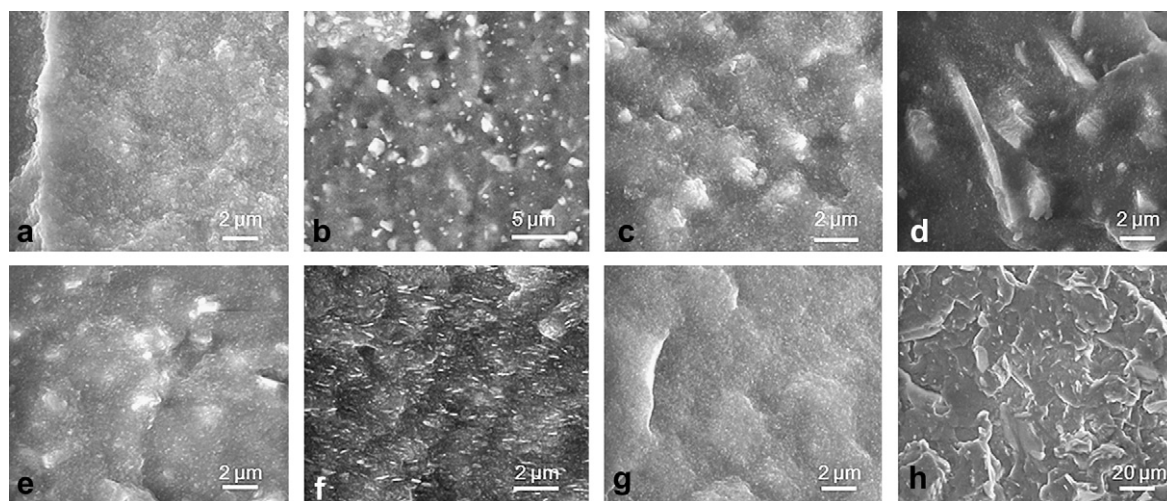
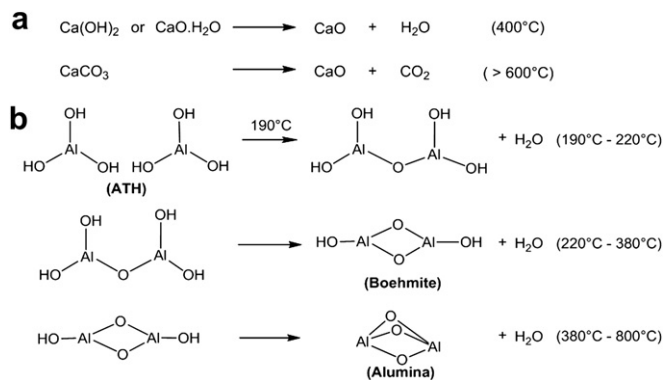


**Fig. 2.** Morphologies, as observed by ESEM, of silicone composites containing Ca-based (on top) and Al-based (on bottom) fillers: a) PCC, b) calcite, c) Ca(OH)<sub>2</sub>, d) wollastonite, e) ATH, f) boehmite, g) alumina, h) mica.





**Scheme 1.** Chemical degradation steps of a) Ca-based fillers and b) Al-based fillers [21,29].

proceeds very slowly from 190 °C to 220 °C (hardly visible on TG curve), the second step (strong) from 220 °C to 380 °C (peak at 320 °C), and the third step from 380 °C to 800 °C (very slow). In a recent review, Troitzsch wrote that the degradation of ATH starts between 180 °C and 200 °C [22], whereas Hancock showed that the main degradation temperature of ATH varies with the mean particle size: fine ATH filler starts to degrade around 190 °C, and coarse ATH filler degrades above 220 °C [21]. The present TG data shows that high temperatures must be reached to degrade completely ATH, without going through a step of boehmite formation and degradation. According to Hancock and Rotheron, this is probably due to the presence of some isolated hydroxyls, which need to diffuse on relatively long distances before they can react. The ATH we used here is composed of fine particles (Figure S2) in agreement with its TG profile.

Boehmite displayed similar simulated and experimental weight losses (18 wt%), and an initial degradation temperature at 380 °C which agrees again with the Scheme 1b. Strong degradation was observed from 380 °C to 550 °C (peak at 520 °C), showing the conversion of boehmite into alumina. Alumina should not degrade

even after heating at 900 °C, only a phase transition from crystalline to amorphous is expected [21]. Very low degradation of alumina filler was observed experimentally, a 5 wt% weight loss indebted to dehydroxylation from alumina surfaces or to the loss of lightest alumina nanoparticles during TG measurement.

Finally, mica showed a weight loss of 5 wt% starting from 330 °C and going on up to temperatures of 900 °C. This weight loss is closed to the water loss reported previously in literature (4.5 wt%) [25] and is indebted to a very slow mica dehydroxylation [23]. Indeed, water molecules are distributed among mica surface but also confined in the mica network [24]. According to Schomburg and Zwahr [25], the adsorbed water content in mica is released up to a temperature of approximately 300 °C. Further dehydroxylation from 500 °C to 1000 °C occurs before achieving structural decomposition and formation of high temperature phases. The presence of kaolinite as impurity in mica was also confirmed by close observation of the TG curve, through the presence of an initial degradation temperature at 300 °C and a peak centred at 550 °C [26].

### 3.2. Silicone composites

#### 3.2.1. Filler distribution in silicone composites

SEM micrographs were systematically taken to observe the distribution of the different fillers in the final composites. Fig. 2 presents all pictures taken under magnification of 20000×, except for mica which magnification was 2000× to see the largest particles (to be compared with the initial matrix, Figure S1, and the filler morphologies, Figure S2).

Calcium-based fillers were easily incorporated in the silicone matrix during blending in HAAKE internal mixer. There were no neat differences of filler distribution in matrix between nano-sized (PCC) and micro-sized  $\text{CaCO}_3$  (calcite). Bigger particle size and large particle size distribution of calcite and wollastonite gave at first sight an impression of inhomogeneous blending due to the large distribution of particle size; nevertheless, while zooming on SEM analysis, a homogeneous blending was established.

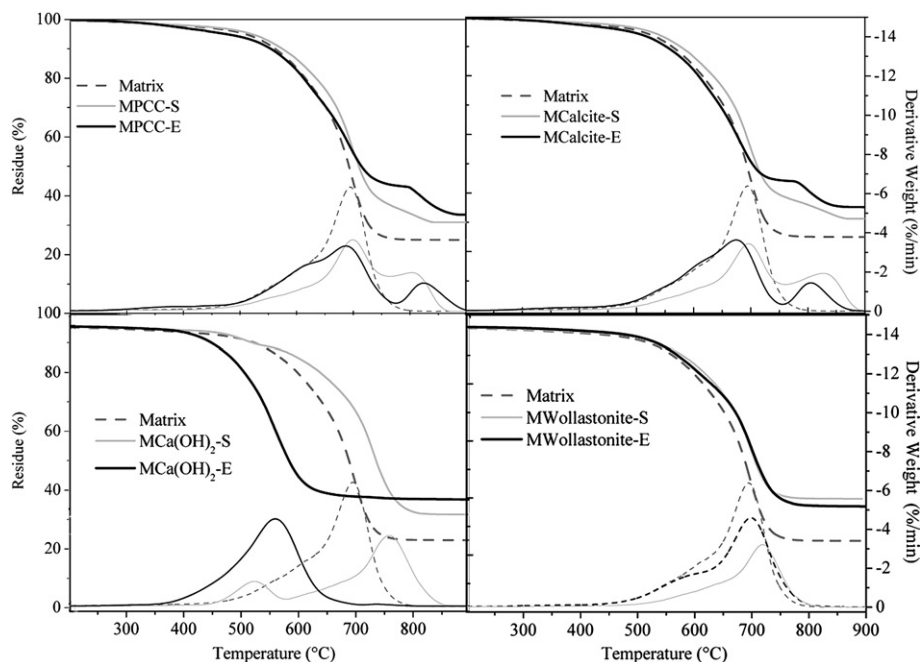
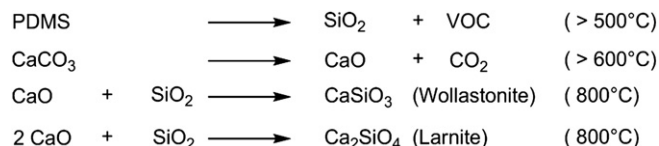


**Fig. 3.** TG curves (weight loss curves at the top and derivatives on the bottom) of silicone composites containing Ca-based fillers. The nature of the fillers are given in labels on the curves (S = simulated curve, E = experimental curve).





**Scheme 2.** Successive reactions in the degradation of CaCO<sub>3</sub> silicone composites [29]. (VOC: Volatile organic compound).

Water-containing fillers (calcium hydroxide, ATH and boehmite) were also easily incorporated in the silicone matrix by mechanical blending, but their distributions in the final composite were not as homogeneous as those observed for the non-hydrated fillers. For instance, the harsh mixing conditions allowed breaking the larger aggregates of calcium hydroxide, but some agglomerates were still found in the final composite. Contrary to CaCO<sub>3</sub>-based fillers, the dispersion of hydroxyl-containing fillers in the silicone matrix seems to depend on their average particle size and particle shape: the higher the surface area, the higher the content of hydroxyl groups and the worst the filler dispersion in matrix. Some large agglomerates of alumina nanoparticles were found in silicone composite even after extensive blending, whereas massive mica flakes showed a better distribution within the matrix. The acicular shape of boehmite made its incorporation into the matrix easier than for rhombohedral-shaped fillers such as ATH or calcium hydroxide.

### 3.2.2. Thermal behaviour of composites

Even though silicone alone is known to display one of the greatest thermal stability among all elastomeric polymers (see Figure S1), some filler additions can be required when targeting demanding final fire-protective applications. Thermal stability of silicone composites were measured by thermogravimetric analyses under inert atmosphere at a heating rate of 10 °C/min. Experimental curves (E) were compared to simulation curve (S) to see the synergistic or antagonist effect of each filler toward silicone composites (see experimental part for the description of the calculation of the simulated curve).

**3.2.2.1. Ca-based composites.** Silicone composites containing PCC and calcite showed an identical thermal behaviour (Fig. 3). Calcite produced slightly higher final residues (35 wt%) than PCC (33.5 wt %), probably due to the presence of traces of other impurities in calcite such as quartz or Fe<sub>2</sub>O<sub>3</sub>. Indeed, transition metal oxides, such as Fe<sub>2</sub>O<sub>3</sub>, have been reported to increase the fire resistance of silicones [27,28]. Both composites degraded according to a two-step pathway, the first step starting at around 500 °C, the second step from about 780 °C (with a minor variation of 20 °C between calcite and PCC). The first degradation step occurs at the same

temperature than the degradation of matrix, converting silicone into VOCs (cyclsiloxanes) and silica. Otherwise saying, CaCO<sub>3</sub> has no influence on the thermal stability of silicone composites at low temperature (below 600 °C). However, once CaCO<sub>3</sub> fillers degraded into CaO at about 680 °C (Fig. 3), *in situ* reaction between silica and CaO formed new crystals (typically wollastonite, calcium silicate or larnite) [29] which form a barrier layer on the surface of matrix residue (Scheme 2). This synergetic effect was confirmed by the larger residue content observed after the second step degradation (at temperatures of 800 °C) compared to the simulated curve (Fig. 3).

XRD analysis from residues of composites of calcium carbonate showed the formation of wollastonite and calcium silicate crystals exclusively, which minerals are CaSiO<sub>3</sub> polymorphs. Both of them differed by their crystalline form as shown by the XRD pattern of residues of PCC and calcite silicone composites, presenting some identical peaks (Fig. 4).

Unlike CaCO<sub>3</sub> fillers, calcium hydroxide silicone composite decomposed in one step, with an onset temperature of degradation at 400 °C, i.e. earlier than the onset of the matrix alone (500 °C). The final weight loss was observed as early as 650 °C, with an experimental residue of 39 wt% against 34 wt% for the calculated one. As shown before, filler decomposition at 400 °C releases water which promotes earlier matrix degradation, but in the mean time it also produces CaO which reacts with SiO<sub>2</sub> at high temperature, again to form new crystals, as for PCC and calcite. Since larger contents of CaO are available from calcium hydroxide degradation (Scheme 2), not only calcium silicate and wollastonite but also larnite crystals were tracked on the XRD pattern of the final residue (Fig. 5). Here, the experimentally observed larger residue than theoretically expected can be explained by the synergistic effect of calcite and silica that co-crystallize to form a barrier layer on the surface and limit further volatilization of the composite.

The thermally stable wollastonite slightly lowered the one-step degradation rate of the composite to produce 37 wt% of final residue (Fig. 3). No synergistic effect may be suggested here, since the simulated and experimental curves almost perfectly overlay on the full temperature range. Besides, the absence of *in situ* co-crystallization led to a slightly lower experimental final residue than the simulated curve.

**3.2.2.2. Al-based composites.** Fig. 6 shows the different TG curves and derivatives obtained for Al-based silicone composites. ATH silicone composite was degraded in two steps, a first slow degradation from 240 °C to 440 °C, and a further rapid degradation between 450 °C and 720 °C. ATH composites first step degradation occurred at higher temperature than ATH filler (190 °C), probably because some water may have been removed by silicone chain adsorption on the filler surface during the HAAKE mixing. The

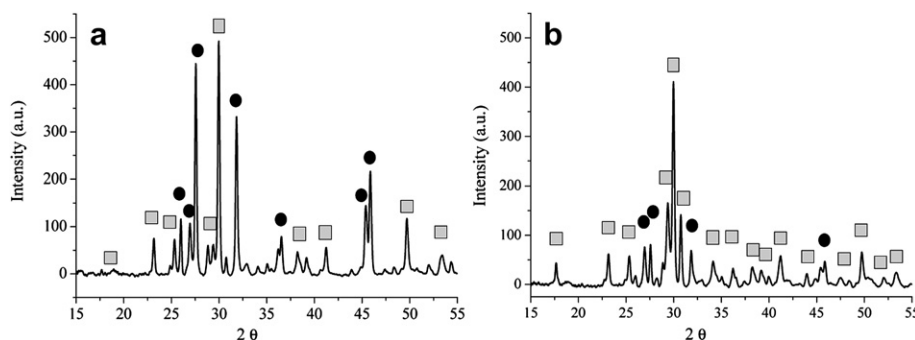


**Fig. 4.** XRD pattern from composite residues of (a) precipitated calcium carbonate and (b) calcite (■ Wollastonite, ● Calcium silicate).

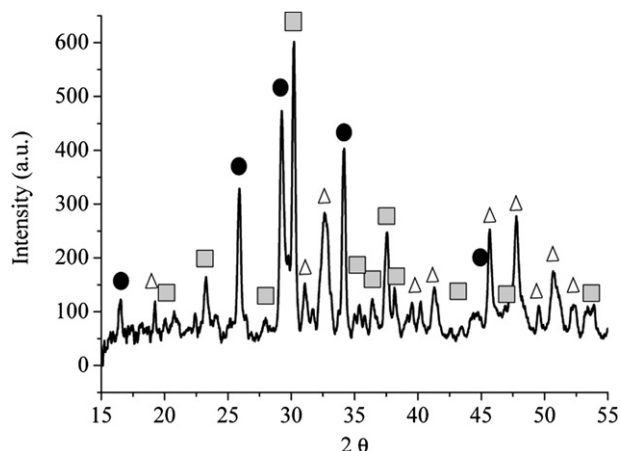


Fig. 5. XRD pattern from the residue of calcium hydroxide composites (■ Wollastonite, ● Calcium silicate, △ Larnite).

weight loss observed in the first step degradation may only be caused by the filler degradation, since the simulated and experimental curves overlay quite nicely. This first step converted ATH into boehmite, so that the second step degradation was identical to that seen for boehmite decomposition. The experimental residue was slightly larger than expected (35 against 33 wt%): by releasing water during its degradation, ATH probably degraded the matrix earlier to produce a silica ash layer that retarded further degradation.

Boehmite composite also degraded in two steps, with a first fast degradation from 500 °C, where both filler and matrix degraded, and then a slow degradation from temperature up to 650 °C with dehydroxylation of alumina obtained from water-free boehmite. The fact that the residue of boehmite composite is lower than expected may be explained by the large surface area developed by the filler, for which a high content of hydroxyl groups on the surface generally increases the catalytic degradation of silicone matrix

through cyclosiloxane devolatilization. In addition, acicular particles of boehmite could not promote the formation of a barrier layer to limit the degradation of matrix.

Mica and alumina are both fillers that do not degrade in their bulk but only loses few percent of water by dehydroxylation of hydroxyl groups on their surface. Both mica and alumina composites were degraded through a one step weight loss and produced a final residue of about 38 wt%. Alumina nanoparticles lowered the initial degradation temperature of silicone composites for at least 100 °C due to catalytic degradation of matrix by hydroxyl groups on the surface of alumina particles. Mica composite was degraded from 480 °C, far from the 300 °C observed for the onset of mica dehydroxylation, presumably because its surface hydroxyl groups were engaged via hydrogen bonding with silicone chains. At temperature up to 560 °C, composite degradation occurred at a faster rate than matrix alone due to mica dehydroxylation and silicone degradation. The fact that the simulated and experimental residue of mica composite coincide may be due to the fact that the mica morphology (big flake-like particles) limited volatile release through a barrier effect. Such effect was reasonably not observed for the spherical and small alumina particles.

#### 4. Discussion

Several types of fillers have already been used in silicone, particularly in patents. Still, some persistent questions remain on the better filler choices for improving the thermal stability of silicone composites, especially in electrical cable applications. The present discussion, mainly relying on TG analyses, tries to correlate the thermal stability of silicone-filled composites with: i) the filler mineral-type, ii) the impact of water release from fillers iii) the filler particle size and morphology. To argue on these points, the composites were classified into three groups: 1. Composites containing non-hydrated fillers (calcium carbonate fillers, i.e. PCC, calcite, and wollastonite); 2. Composites containing water-releasing fillers (calcium hydroxide, ATH and boehmite); 3.

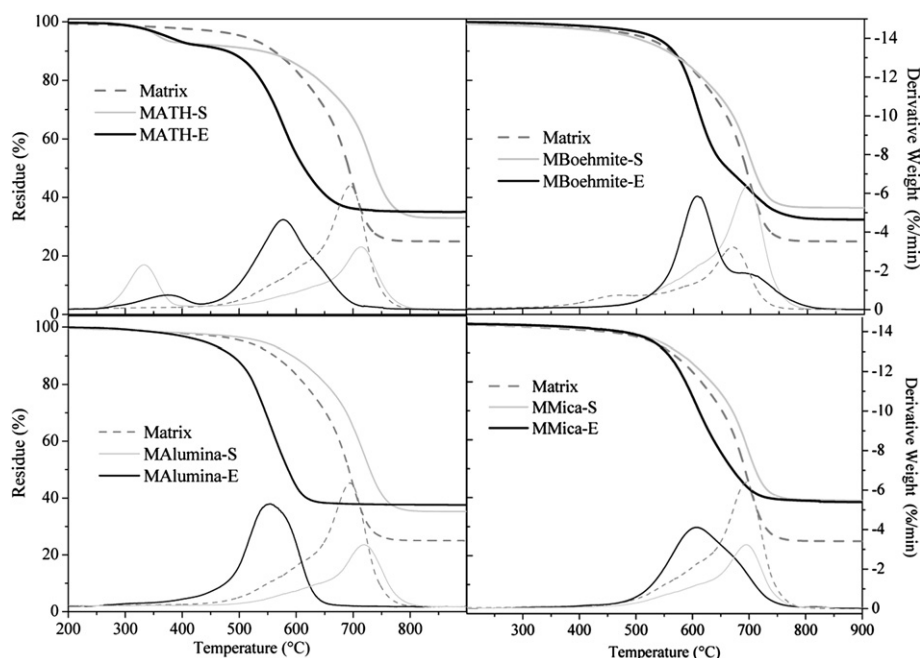


Fig. 6. TG curves of Al-based silicone composite. Fillers nature is indicated in the labels (S = simulated curve, E = experimental curve).

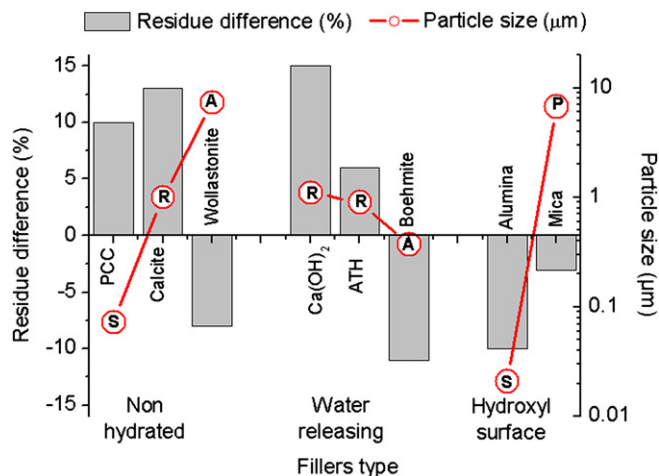


Fig. 7. Influence of particle sizes and filler morphologies on the improvement of final residue (the letter in the sphere indicates the filler morphology: S = spherical, A = acicular, P = platelet, R = rhombohedral).

Composites containing fillers with hydroxyl groups on surface (alumina and mica).

The content and mechanical resistance of the final residue are certainly the most important parameters when testing the thermal stability of electric cable-driven formulations. For this reason, we tried in this first part to correlate the nature of the fillers with the final residue of composite, especially looking at the influence of their particle size (or surface area) and morphology. Fig. 7 summarizes the effect of particle size and filler type on the final residue of the silicone composite, which variation is expressed as the residue difference ( $R_d$ ) given as:

$$R_d = \frac{\%R_{Exp} - \%R_{Sim}}{\%R_{Sim}} \times 100\%$$

where  $R_{Exp}$  is the experimental residue and  $R_{Sim}$  the simulated residue.

#### 4.1. Non-hydrated fillers

Calcium carbonates improve the final residue of silicone composites, surely because of *in situ* co-crystallization phenomena between the CaO matter produced by  $\text{CaCO}_3$  fillers and the matrix at high temperature. The failure on the residue improvement for wollastonite composite might be caused by the absence of co-crystallization and the acicular morphology, which does not induce a heat and mass barrier as platelet, spherical or rhombohedral fillers do. Also, natural and macro-sized calcium carbonate (calcite) improved the thermal stability of silicone composites better than synthetic and nano-sized calcium carbonate (PCC). Such result was probably due to the presence of impurities in the former and also the fact that large rhombohedral particles of calcite were more efficient as heat and mass barrier than nano-sized spherical PCC particles. Since there is no obvious trend on the  $\text{CaCO}_3$  filler particle size versus silicone composite thermal stability, probably macro-sized non-hydrated fillers would be economically more interesting to use than nano-sized ones.

#### 4.2. Water-releasing fillers

Water-releasing fillers are a priori avoided in commercial applications since they catalyze the silicone degradation and generate cracks in the final residue [1,30]. However, the addition of

water-releasing filler is not systematically detrimental to the composite. In fact, its effect mainly depends on numerous factors: type (aluminium or calcium-based filler), morphology, particle size, surface area, initial degradation temperature of the filler and quantity of water released by filler decomposition.

Calcium-based fillers have been shown to induce a slight synergistic effect on the final residue (PCC, calcite, and calcium hydroxide) which was not observed in silicone composites containing aluminium-based fillers. This is due to the formation of new crystals by successive *in situ* reactions during the degradation of  $\text{CaCO}_3$  or  $\text{Ca(OH)}_2$  in the silicone composites (Scheme 2). Calcium hydroxide thus presented more interesting results in terms of increasing the final residue compared to ATH or boehmite, benefiting from the co-crystallization.

Smaller particle size of water-releasing filler led to lower residue. This is correlated to a larger surface area that increases the surface contact between filler-matrix and therefore enhances the water release impact to promote thermal degradation of silicone. Besides, composites containing rhombohedral fillers show more synergistic effect on final residue than acicular fillers due to their capacity to induce a barrier effect.

Calcium hydroxide or ATH starts to degrade at lower temperature than silicone matrix, therefore the degradation of composites starts earlier with these two fillers, whereas for boehmite which starts to degrade at the same temperature as silicone matrix, no degradation of silicone composites were observed at lower temperature. Lower onset temperature of composite degradation thus leads to earlier barrier layer formation, which may retard the degradation of the matrix, to finally increase the final residue.

#### 4.3. Fillers with hydroxyl groups on their surface

The presence of hydroxyl groups on the surface of alumina and mica induced an early thermal degradation of silicone composite due to catalytic activity of hydroxyl groups on the filler surface. Consequently, alumina with smaller particle size and bigger surface area degrades more silicone chains than bigger particles of mica. On the other hand, the heat barrier build by platelet mica particles at higher temperature is more effective to slow down the degradation of corresponding composites.

Considering the effect of hydroxyl groups on the thermal degradation of silicone, the surface dehydroxylation of the filler would a priori be required. Moreover, surface modification aims at facilitating the composite processing and at improving the mechanical properties of composite [31–33]. For most low-cost applications however, using large filler particles would probably be enough. Note that the substitution of non-treated silica with silane-treated silica showed only little increases both on the initial degradation temperature and on the residue of silicone composites [34].

## 5. Conclusion

Thermal degradation of silicone composite is modified by incorporating aluminium and calcium-based fillers. At high temperature, two mechanisms have been observed: i) a co-crystallization due to the reaction between the degradation products of calcium-based fillers ( $\text{CaO}$ ) with matrix ( $\text{SiO}_2$ ) to form wollastonite, calcium silicate, or larnite at high temperature; ii) a barrier layer formation thanks to platelet or rhombohedral fillers which tend to limit both heat and mass transfers.

The final residue of silicone composites depends on the filler nature (non-hydrated/water-releasing/hydroxyl surface) rather than the filler type (aluminium or calcium-based fillers). For non-hydrated fillers, both morphology and reactivity with the matrix

(co-crystallization) are important. In the case of calcium-based fillers, higher CaO availability resulted in better co-crystallization and increased final residue. Platelet or rhombohedral fillers were found more efficient than spherical or acicular fillers. The impurities in filler also seem to influence the thermal stability of silicone. In the case of water-releasing fillers and fillers with hydroxyl groups on surface, platelet/rhombohedral and/or micro-sized fillers increase the final residue compared to acicular and/or nanoparticles, again here, thanks to an efficient barrier effect.

The next part of this series will specifically explore the performance of final residues while burning the composites in a furnace, mimicking a French standard applied to cable fire resistance testing.

## Acknowledgments

We are most grateful to Bluestar Silicones for providing all the necessary silicone raw materials to carry out this study. We also thank Solvay, Nyco Minerals and Nabaltec for donating PCC, Wollastonite and Boehmite, respectively.

## Appendix. Supplementary material

Supplementary data associated with this article can be found in the online version at doi:10.1016/j.polyimdegradstab.2010.04.013.

## References

- [1] Dvornic PR. In: Jones RG, Ando W, Chojnowski J, editors. Thermal stability of polysiloxanes: silicone-containing polymers. Dordrecht, the Netherlands: Kluwer Academic Publisher; 2000. p. 185–212.
- [2] Danner B. Amino-functional silicone waxes 2009. US 7,511,165.
- [3] Dubief C, Cauwet D. Utilization in cosmetic for tropical applications of an aqueous dispersion based on organosiloxanes and a crosslinked copolymer of acrylamide/neutralized 2-acrylamido 2-methylpropane sulfonic acid 2009. EP 1992, 0920, 525.
- [4] Branlard P, George C, Leuci C. Polyorganosiloxane compositions vulcanisable by hot process useful in particular for making electric wires or cables 2003. EP 1,238,007.
- [5] Eikhenbaum IG. Heat-resistant unit 1995. US 5,418,274.
- [6] Grassie N, Macfarlane IG. The thermal degradation of polysiloxane-I poly (dimethylsiloxane). Eur Polym J 1978;14:875–84.
- [7] Camino G, Lomakin S, Lazzari M. Polydimethylsiloxane thermal degradation. Part 1. Kinetic aspects. Polymer 2001;42(6):2395–402.
- [8] Buch RR. Rates of heat release and related fire parameters for silicones. Fire Saf J 1991;17:1–12.
- [9] Hsieh F-Y. Shielding effects of silica-ash layer on the combustion of silicones and their possible applications on the fire retardancy of organic polymers. Fire Mater 1998;22:69–76.
- [10] Mansouri J, Burford RP, Cheng YB, Hanu L. Formation of strong ceramified ash from silicone-based compositions. J Mater Sci 2005;40:5741–9.
- [11] Hamdani S, Longuet C, Perrin D, Lopez-Cuesta J-M, Ganachaud F. Flame retardancy of silicone-based materials. Polym Degrad Stab 2009;94:465–95.
- [12] Pritchard G. Fillers. Chaall, United Kingdom. In: Pritchard G, editor. Plastics additives: an A–Z reference. New York: Springer; 1998. p. 241–51.
- [13] Kaufmann W, Prager FH, Schiffer HW. In: Troitzsch J, editor. International plastics flammability handbook 2nd edition: electrical engineering. Munich: Hanser Publishers; 1990. p. 344–78.
- [14] Liu Y-L, Li S-H. Poly(dimethylsiloxane) star polymers having nanosized silica cores. Macromol Rapid Commun 2004;25:1392–5.
- [15] Patnaik P, editor. Handbook of inorganic chemicals. New York: McGraw Hill; 2002.
- [16] Utracki LA, editor. Clay-Containing Polymeric Nanocomposites, Vol. 1. United Kingdom: Rapra Technology Limited; 2004. p. 77.
- [17] Criado JM, Ortega A. A study of the influence of particle size on the thermal decomposition of calcium carbonate by means of constant rate thermal analysis. Thermochim Acta 1992;195:163–7.
- [18] Beruto DT, Searcy AW, Kim MG. Microstructure, kinetic, structure, thermodynamic analysis for calcite decomposition: free-surface and powder bed experiments. Thermochim Acta 2004;424:99–109.
- [19] Garcia CE, Arranz MA, Leton P. Effects of impurities in the kinetics of calcite decomposition. Thermochim Acta 1990;170:7–11.
- [20] L'vov BV, Polzik LK, Ugolkov VL. Decomposition kinetics of calcite: a new approach to the old problem. Thermochim Acta 2002;390:5–19.
- [21] Hancock M. In: Rothon R, editor. Principal types of particulated fillers: particulate-filled polymer composites. 2nd ed. United Kingdom: Rapra Technology Limited; 1995. p. 85–8.
- [22] Troitzsch HJ. In: Gachter R, Muller H, editors. Flame retardants: plastics additives. Cincinnati: Hanser Publisher; 1993. p. 709–48.
- [23] Guggenheim S, Chang T-H, Koster Van Groos AF. Muscovite dehydroxylation: high-temperature studies. Am Mineral 1987;72:537–50.
- [24] Sakuma H, Kawamura K. Structure and dynamics of water on muscovite mica surfaces. Geochim Cosmochim Acta 2009;73:4100–10.
- [25] Schomburg J, Zwahr H. Thermal differential diagnosis of mica mineral group. J Therm Anal Calorim 1997;48(1):135–9.
- [26] Murray HH, editor. Developments in clay science 2: applied clay mineralogy. Amsterdam: Elsevier; 2007. p. 180.
- [27] Fujiki H, Tanaka M. Silicone coated base material and air bag base material 1995. EP 0,669,419.
- [28] Dubois R, Pouchelon A, Pusineri C. Use of mixtures with base of Pt and of transition metal compounds other than Pt for improving the resistance to arc tracking and to arc erosion of silicon elastomers. 1998. WO 98,029,488.
- [29] Hermansson A, Hjertberg T, Sultan B-A. The flame retardant mechanism of polyolefins modified with chalk and silicone elastomer. Fire Mater 2003;27: 51–70.
- [30] Genovese A, Shanks RA. Fire performance of poly(dimethyl siloxane) composites evaluated by cone calorimetry. Compos Part A Appl Sci Manuf 2008;39(2):398–405.
- [31] Yuan QW, Mark JE. Reinforcement of PDMS networks by blended and in-situ generated silica fillers having various sizes, size distributions, and modified surfaces. Macromol Chem Phys 1999;200:206–20.
- [32] Osman MA, Atallah A, Kahr G, Suter UW. Reinforcement of Poly(dimethylsiloxane) networks by montmorillonite platelets. J Appl Polym Sci 2002;83: 2175–83.
- [33] Park ES. Mechanical properties and processability of glass-fiber, wollastonite, and fluoro rubber reinforced silicone rubber composites. J Appl Polym Sci 2007;105:460–8.
- [34] Park SJ, Cho KS. Filler–elastomer interactions: influence of silane coupling agent on crosslink density and thermal stability of silica/rubber composites. J Colloid Interface Sci 2003;267:86–91.



# Supporting information for

## “Calcium and aluminum-based fillers as flame-retardant additives in silicone matrices. I. Blend preparation and thermal properties”

By S. Hamdani, C. Longuet, F. Ganachaud, J. Lopez-Cuesta\*

Submitted to « *Polymer Degradation and Stability* »

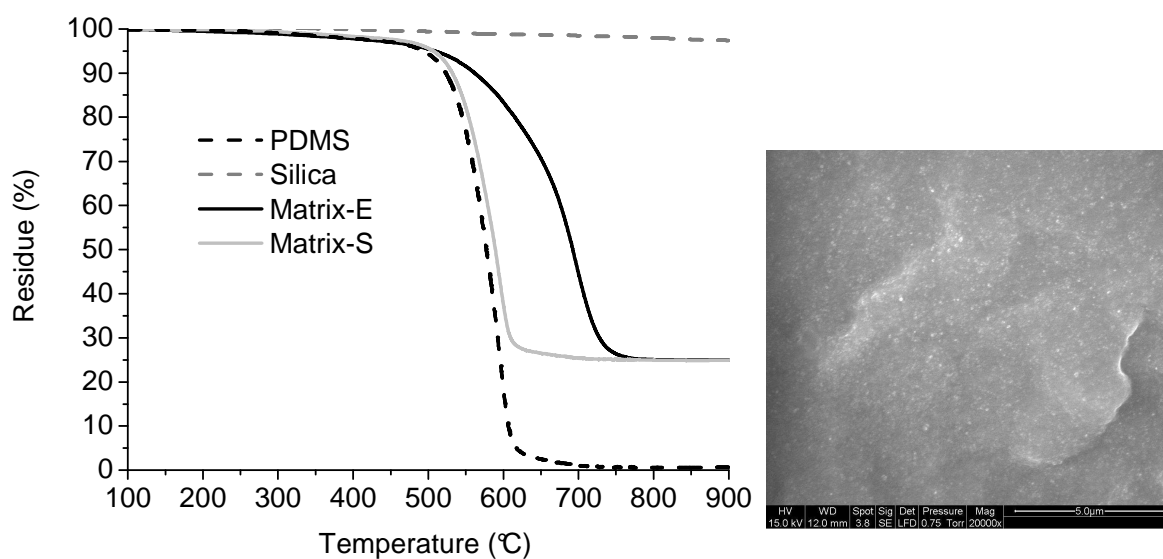


Figure S1. Thermal behavior and morphology of silicone matrix as observed by SEM (the bar on the bottom of the photo represents 5 µm).



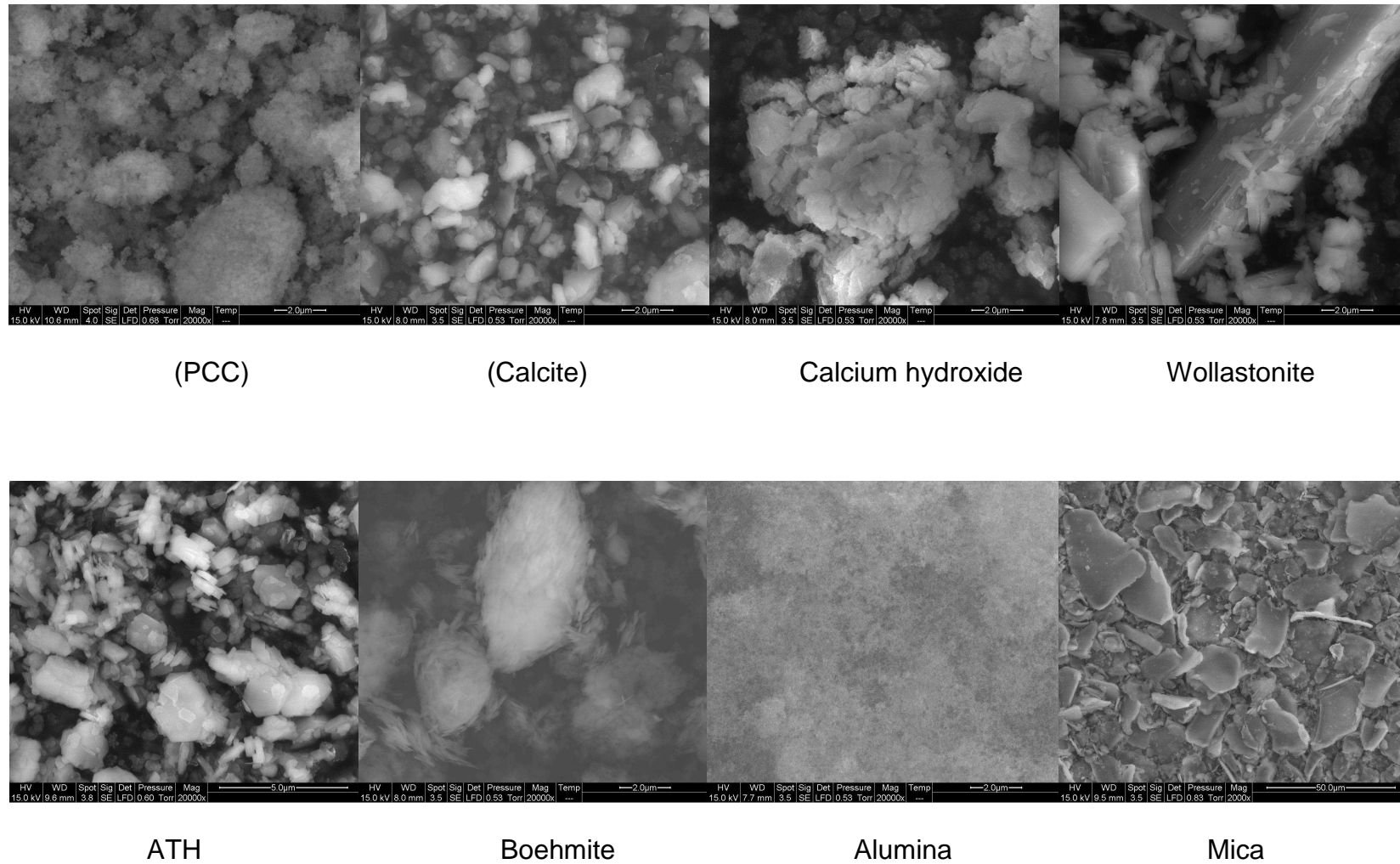


Figure S2. ESEM micrographs of the various fillers used in this study at magnification of 20.000x, except mica (2.000x) (the scale is given on each photo).

# *Chapitre 4.*

## *Etude des Composites:*

### *« Cohésions du Résidus »*





## **Etude de la cohésion du résidu des composites à matrice silicone contenant des charges minérales à base de calcium ou d'aluminium après pyrolyse en conditions extrêmes**

L'utilisation de gaines en câblerie à base de silicones requiert des formulations présentant une bonne cohésion du résidu après combustion afin d'assurer le fonctionnement des câbles électriques au cours d'un incendie. Une isolation suffisante du conducteur métallique pour éviter les coupures de courant est alors requise. La résistance demandée et les contraintes imposées sont résumées dans la norme Française NF C 32-070 CR1. Afin d'atteindre cet objectif, plusieurs types de charges minérales ont été ajoutées dans des formulations industrielles à matrice silicone utilisées en câblerie [1,2,3,4,5]. A l'échelle du laboratoire, il existe peu de techniques d'analyse permettant d'étudier la cohésion des résidus. Il est possible d'étudier les propriétés mécaniques des cendres grâce à la mesure du module de rupture (« flexural strength » en anglais), ou par micro-indentation, mais ces méthodes nécessitent des échantillons avec une surface régulière, c'est-à-dire présentant une surface lisse et peu poreuse. Ce n'est pas le cas pour nos résidus, de morphologies très variables selon la charge ajoutée : des résidus très poreux et fragiles, ou d'autres au contraire compacts et très durs, comportant cependant dans tous les cas des surfaces irrégulières. De ce fait, une nouvelle méthode rendant compte de la cohésion des résidus a été développée. Nous avons considéré, dans un premier temps, la variation de volume de l'échantillon avant et après combustion, puis nous avons mesuré la résistance à la compression. La formulation idéale pour la câblerie pourrait être ainsi celle ne présentant aucune variation de volume et affichant une résistance maximale à la compression.

Les différentes formulations présentées dans le chapitre 3 sont pyrolysées dans un four en se rapprochant des conditions de pyrolyse extrême de la norme NFC 32070 CR1, mais en absence de chocs mécaniques réguliers au cours du test. Les résidus sont ensuite caractérisés par plusieurs méthodes : par compression (via une presse ADAMEL) pour mesurer la résistance à la rupture du résidu, par déplacement de mercure pour étudier la variation de volume avant et après pyrolyse au four. La structure des résidus est également caractérisée par diffraction des rayons X (DRX) pour observer les structures cristallines présentes ou créées *in*

*situ*, ou par imagerie par microscopie électronique à balayage (MEB) pour mettre en évidence leur morphologie. Cette dernière méthode est couplée à une sonde permettant l'analyse dispersive en énergie des rayons X (EDX) pour mesurer le taux des éléments présents tels que le carbone, le silicium, l'oxygène, l'aluminium ou le calcium.

Il a été montré que d'une manière générale, l'incorporation de charges à base de calcium conduit à une très bonne cohésion des résidus par rapport à celles à base d'aluminium. Ils possèdent une meilleure résistance à la compression, mais présentent une contraction de volume après pyrolyse, sauf pour la formulation contenant la chaux. L'analyse DRX a mis en évidence la formation de nouveaux cristaux lors de la combustion, et les photos MEB montrent la constitution de couches vitreuses en surface des résidus, deux facteurs qui améliorent apparemment la résistance à la compression des composites. La cristallisation et l'absence de libération de gaz dégradant le silicone (par exemple la vapeur d'eau) amènent à un résidu très cohésif et compact. Dans le cas de la chaux, la libération d'eau lors de la pyrolyse endommage la matrice silicone et crée une porosité à l'intérieur du résidu. Dans ce cas, le résidu subit une augmentation de volume et affiche une faible compacité, ce qui conduit à une plus faible résistance à la compression. Cependant, cette dégradation est en partie compensée par une cristallisation *in situ* qui maintient une cohésion correcte du résidu. Même si la wollastonite n'induit pas la formation de nouveaux cristaux, les photos MEB montrent une organisation suggérant l'existence d'interactions entre la wollastonite et la silice à l'état vitreux, de façon suffisante pour améliorer la résistance à la compression.

Si l'on considère maintenant les résidus des composites contenant des charges à base d'aluminium, ils apparaissent très fragiles, et montrent un gonflement très important, notamment pour les mélanges contenant de l'ATH ou de l'alumine. La libération d'eau et l'absence d'interactions entre les charges à haute température (charges à base d'aluminium et de silice) conduisent à des résidus très poreux et peu cohésifs. Le mica, comme la wollastonite, montrent une résistance à la compression légèrement meilleure que les autres formulations, ceci est peut être dû à leur capacité à interagir avec la silice à haute température, à l'état vitreux.

L'incorporation dans le composite à base de mica de charges permettant la formation de nouveaux cristaux à haute température, et/ou de charges pouvant fondre telle que les poudres

de verre (glass frits), améliore la résistance à la compression du résidu. Les charges libérant de l'eau, quant à elles, induisent une porosité à l'intérieur du résidu et son gonflement. Ces deux phénomènes sont engendrés par la libération de produits volatiles tels que l'eau, les cyclosiloxanes (produits de dégradation de la matrice), et le CO<sub>2</sub>. On peut donc conclure qu'une morphologie très poreuse est induite par expansion de volume (gonflement). Un résidu très compact provient d'une contraction de volume, ceci a priori grâce à l'apparition de nouveaux cristaux à haute température.

Pour conclure, l'incorporation de charges neutres comme le PCC et la calcite améliore la résistance à la compression du résidu, bien qu'il y ait libération de CO<sub>2</sub>. Le test de compression montre que l'incorporation de PCC semble plus intéressante pour améliorer la cohésion du résidu. Cependant, ces deux composites présentent une contraction de volume très importante par rapport aux autres charges. Au vu de ces résultats, de nouvelles formulations sont envisagées en associant différents types de charges pour limiter la variation de volume et, en même temps, améliorer la résistance à la compression.

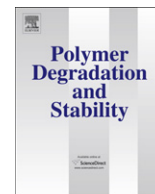
## Références

---

1. Shephard KL. Flame resistant silicone rubber wire and cable coating composition. US Patent 6,239,378; 2001
2. George C, Pouchelon A, Thiria R. Compositions Polyorganosiloxanes vulcanisables à chaud utilisables notamment pour la fabrication de fils ou câbles électriques. France Patent 2,899,905; 2006.
3. Ariagno D, Barruel P, Viale A. Heat-vulcanisable organopolysiloxanes, intended for coating of electrical cables. European Patent 0,467,800; 1992
4. Branlard P, George C, Leuci C. Polyorganosiloxane compositions vulcanisable by hot process useful in particular for making electric wires or cables. European Patent 1,238,007; 2003.
5. Ota K, Hirai K. Flame retardant silicone rubber composition for coating electrical wire and cable. US Patent 6,011,105; 1998.







## Calcium and aluminium-based fillers as flame-retardant additives in silicone matrices II. Analyses on composite residues from an industrial-based pyrolysis test

Siska Hamdani-Devarennnes<sup>a</sup>, Audrey Pommier<sup>a</sup>, Claire Longuet<sup>a</sup>,  
José-Marie Lopez-Cuesta<sup>a,\*\*</sup>, François Ganachaud<sup>b,\*</sup>

<sup>a</sup> Centre des Matériaux de Grande Diffusion, Ecole des Mines d'Alès, 6 avenue de Clavières, 30319 ALES Cedex, France

<sup>b</sup> Institut Charles Gerhardt UMR5253 CNRS/UM2/ENSCM/UM1, Equipe Ingénierie et Architectures Macromoléculaires, Ecole Nationale Supérieure de Chimie de Montpellier, 8 Rue de l'Ecole Normale, 34296 Montpellier Cedex, France

### ARTICLE INFO

#### Article history:

Received 18 February 2011

Received in revised form

12 May 2011

Accepted 28 May 2011

Available online 12 June 2011

#### Keywords:

Silicone

Fillers

Calcium

Aluminium

Pyrolysis

Residue

### ABSTRACT

The second part of this series, devoted to the study of model fire-resistant silicone composites filled with calcium or aluminium-based material which would meet cable industry specifications, focuses on residues obtained after extreme pyrolysis adapted from the NFC 32070 CR1 French standard. Several methods of analysis (among them ESEM, EDX, XRD, Hg pycnometer, and compression tests) have been carried out in order to investigate the microstructure, volume variation, and compression behaviour of silicone composite residues. Calcium-based fillers produced more cohesive residues than aluminium-based fillers. Indeed, the co-crystallisation taking place during pyrolysis, as shown in the first part of this series (Hamdani, S. et al., Polym Degrad Stab, 2010, 95, 1911–1919), produced a dense and strong residue. The strong internal porosity and absence of new crystal formation in residues of aluminium-based filled composites resulted in their low compressive resistance. In addition, water release during the degradation of the latter fillers, favoured residue expansion, high interior porosity and thus weak compression resistance.

© 2011 Elsevier Ltd. All rights reserved.

### 1. Introduction

The demand for electric cables able to operate during a fire and limit fire propagation is constantly increasing. Government regulations in various countries now specify that essential electrical circuits be protected in order to ensure the safety of persons inside the building and also to permit the firemen to be more efficient in controlling and extinguishing fires. Such systems include, for example, alarms, telephones, lighting, elevators, ventilation, fire pumps, and so on. Therefore, depending on the country of application, national standard tests of different difficulties have to be passed before launching electrical cables with improved fire resistant coatings. In France particularly, the NFC 32070 CR1 standard test imposes that cables sustain electrical power after burning at a high heating rate (above 80 °C/min) in inert atmosphere while being periodically mechanically shocked during the test. The

temperature is finally maintained at 900 °C for 15 min. The test is passed if the cables retain electrical insulation under thermal and mechanical stresses [1]. In England, the national standard test of BS EN 50200:2006, based on European standard EN 50200, implies a direct application to the cable of a flame from a propane burner, giving a constant temperature attack of a notional 842 °C. This method allows testing cables used in emergency circuits [2]. In Australia, the fire test condition for cables, known as Australian Standard AS/NZS3013:1995, requires that the cable be fired in air up to 1050 °C and maintained at a maximum firing temperature for 30 min, then sprayed with a water jet. The test is valid if the residue resists the small mechanical shocks from the water spray.

To fulfil these requirements and avoid e.g. short circuits during the fire, a silicone coating producing a cohesive residue after burning is particularly sought. From this prospective, different studies have been carried out to understand the cohesion residue mechanism in polymers and several methods have also been proposed to obtain a strong char, for example by incorporation of nanofillers into composites [3,4]. Nevertheless, to our knowledge there is still only a limited number of papers that reported the characterisation of cohesion residue of composites, in particular for

\* Corresponding author. Tel.: +33 4 67 14 72 96; fax: +33 4 67 14 72 20.

\*\* Corresponding author. Tel.: +33 4 66 78 53 34; fax: +33 4 66 78 53 65.

E-mail addresses: [jose-marie.lopez-cuesta@mines-ales.fr](mailto:jose-marie.lopez-cuesta@mines-ales.fr) (J.-M. Lopez-Cuesta), [francois.ganachaud@enscm.fr](mailto:francois.ganachaud@enscm.fr) (F. Ganachaud).

silicone composites. Mansouri et al. [5] characterised the residue of silicone composite by flexural strength measurement on pyrolysed samples, using the three-point bend method. This method measured the mechanical properties of a bulk residue, while in our case, we are also interested in measuring the influence of surface layering on the residue cohesion. Laoutid et al. [3] used a micro-indentation test to evaluate the mechanical behaviour of EVA combustion residue. The material was submitted to a plastic deformation by penetration of an indenter forced into the material under a load and recorded as a function of the depth of the indentation. Unfortunately, this method requires a residue with two parallel faces, which is not the case for our residues.

Since the NFC 32070 CR1 standard test specifications are hardly passed by most current high-tech silicone formulations, it requires further fundamental research to understand the role of each potential fire-resistant additive. The present series of papers thus aims at considering the role of calcium and aluminium-based inorganic fillers as additives for a new generation of fire-resistant cables. In the first part of this series [6], we described the characteristics of a variety of fillers chosen for this work, their blending in a model silicone matrix and the thermogravimetric analyses of resulting composites. From these, we classified silicones composites into three groups regarding their thermal behaviour, whether they contain inert fillers, water-releasing fillers, or hydroxyl-functionalized fillers. Non-hydrated fillers improved the thermogravimetric stability of silicone, while water-releasing and/or hydroxyl-decorated fillers depressed it.

The current study focuses primarily on the content and cohesion of the residue arising from a simulation of an extreme fire test such as NFC 32 070 CR1 standard test, but without exerting mechanical shocks during burning. Samples were fired in stainless steel tubes, a confinement corresponding roughly to working in inert atmosphere. The high heating rate imposed here is believed to mimic conditions from a real fire case. In this paper, complementary understandings about the role of each kind of filler, introduced in the silicone cable formulation, on the cohesion residue (compared to thermal stability, as reported in the first part of this series [6]) are given. The third part will describe the fire behaviour of similar silicone composites in fire tests using complementary calorimeter techniques.

## 2. Experimental part

### 2.1. Materials

The silicone matrix, kindly supplied by Bluestar Silicones, contains 74.4 wt.% of vinyl-terminated polydimethylsiloxane ( $M_w$

of 550,000 g/mol), 25 wt.% of D<sub>4</sub>-modified silica and 0.6 wt.% of 2,5-dimethyl-2,5-di(tert-butyl peroxy)hexane as a crosslinking agent. Precipitated calcium carbonate (PCC), wollastonite, and boehmite were supplied by Solvay, Nyco minerals and Nabaltec respectively. ATH was purchased from Martinswerk, alumina from Evonik and mica from Kaolin International. For a complete and thorough characterisation of all fillers, see the supporting information (Table S1).

### 2.2. Sample preparation

Fillers were incorporated into the silicone matrix using a HAAKE internal mixer at a temperature of 45 °C, shear rate of 40 rpm and mixing time of 50 min. The HAAKE internal mixer has two rotors running in a contra-rotating way to blend the filler and the matrix. All composites contained 20 wt% of silica and 20 wt% of filler. Thereafter, filled silicone was cross-linked under heat pressure of 90 bars at 150 °C during 15 min to obtain plates of 100 × 100 × 3.8 mm. The effectiveness of mixture dispersion was confirmed by ESEM analysis as reported previously [6].

### 2.3. Sample pyrolysis

Samples with dimension of 20 × 15 × 3.8 mm or 10 × 10 × 3.8 mm, depending on applied tests, were confined in a paired system of stainless steel tubes ( $\varnothing_1 = 30$  mm, and  $\varnothing_2 = 35$  mm) to limit thermo-oxidation by oxygen in air and ash contamination of the furnace (Fig. 1). In order to simulate real fire conditions, the thermal ramp was adapted from CR1 NFC 32070 standard test. Typically, samples were burned in a Nabertherm furnace from 40 °C to 940 °C in a 40 min time lag followed by an isotherm at 940 °C during 15 min.

### 2.4. Characterisation of residues

A Hitachi S-4300 environmental scanning electron microscope (ESEM) was used to acquire analyses on the microstructure of silicone composite residues under a magnification of 5000× using an acceleration voltage of 15 kV. Energy-dispersive X-Ray (EDX) measurements were conducted as an integrated tool in ESEM to determine local elemental composition on micrographs with a magnitude of 300×. The averaged element contents were measured from three observation points, on the surface and on the fractured side of the residues, during ESEM analysis.

**Table 1**  
Structure behaviour, volume variation, XRD, and EDX elemental analysis of residues.

Filler	Microstructure		Volume variation (%)	Co-crystallisation observed by XRD analysis	Ca or Al relative to Si element content (%)			
	Inside	Outside			Composite		Residue	
					Surface	Interior	Surface	Interior
PCC	Dense with low porosity	Rough with ceramic layer	$-52.4 \pm 2.9$	Wollastonite, Calcium silicate	$20.4 \pm 0.9$	$18.9 \pm 0.7$	$63.3 \pm 0.7$	$67.3 \pm 0.3$
Calcite	Dense with low porosity	Rough with ceramic layer	$-47.9 \pm 0.2$	Wollastonite, Calcium silicate	$15.0 \pm 0.2$	$15.5 \pm 0.6$	$38.7 \pm 0.7$	$40.6 \pm 0.2$
Wollastonite	Smooth and fillers found everywhere	Filler not bound to matrix	$-7.0 \pm 5.3$	Wollastonite	$4.5 \pm 2.5$	$12.0 \pm 0.4$	$26.9 \pm 0.3$	$24.9 \pm 2.0$
Calcium hydroxide	Dense with low porosity (crater like) and cottony	Rough with ceramic layer but slightly cottony	$10.2 \pm 2.3$	Wollastonite, Calcium silicate, Larnite	$0.7 \pm 0.2$	$15.9 \pm 0.7$	$47.3 \pm 0.5$	$50.3 \pm 0.3$
ATH	High porosity (crater like)	Rough	$59.5 \pm 9.3$	None	$15.7 \pm 0.1$	$15.7 \pm 0.4$	$37.1 \pm 1.3$	$38.5 \pm 0.4$
Boehmite	Low porosity and cottony	Smooth	$24.7 \pm 4.3$	None	$15.6 \pm 0.9$	$15.9 \pm 0.3$	$41.9 \pm 0.5$	$41.8 \pm 0.3$
Alumina	Smooth and cottony	Smooth	$57.7 \pm 2.4$	None	$20.3 \pm 1.0$	$21.3 \pm 1.4$	$34.7 \pm 0.5$	$31.2 \pm 0.3$
Mica	Porous and big void among mica particles	Fillers well bound to matrix	$18.1 \pm 0.1$	Muscovite	$4.8 \pm 0.3$	$5.2 \pm 0.2$	$19.0 \pm 1.4$	$13.9 \pm 0.2$

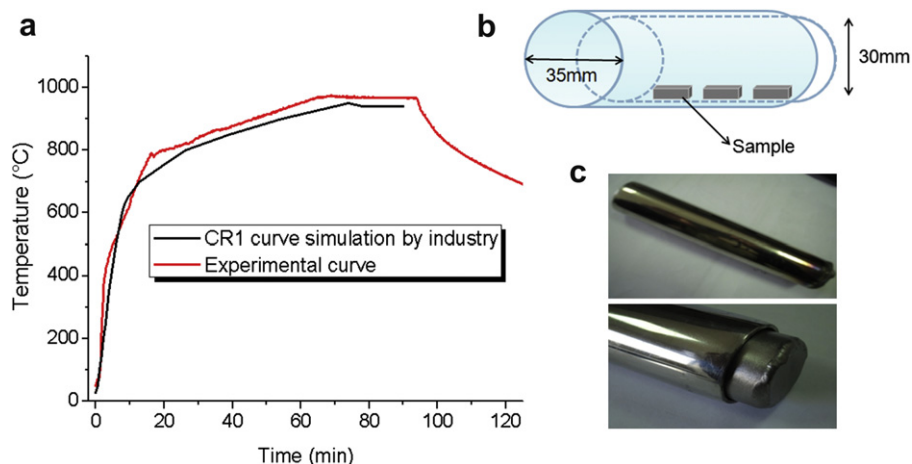


**Fig. 1.** Pyrolysis ramp of our sample (red curve), compared to the one used in industry to meet the NFC 32070 CR1 test (black curve) (a), the scheme (b) and photos (c) of paired tubes used during pyrolysis (For interpretation of the references to color in this figure legend, the reader is referred to the web version of this article.).

X-Ray Diffraction (XRD) analyses of finely ground filler and final residues were performed on a Bruker X-ray diffractometer using Cu K $\alpha$  radiation.

Volume variations before and after pyrolysis were measured by the mercury immersion method using Archimedes principle. An unfired sample (composite) with dimension of  $20 \times 15 \times 4$  mm was placed into a beaker glass filled with Hg. The displaced Hg was weighed to define the initial volume of the sample (volume of composite) by taking Hg density as  $13.6 \text{ g/cm}^3$ . After pyrolysis, the volume of residue was measured similarly to the non-pyrolysed sample in Hg. The volume variation is calculated by using Equations (1) and (2) as follows:

$$\text{Volume variation (\%)} = \frac{(\text{Volume})_{\text{residue}} - (\text{Volume})_{\text{composite}}}{(\text{Volume})_{\text{composite}}} \times 100\% \quad (1)$$

in which the volume of residue or composite is calculated by

$$\text{Volume (cm}^3\text{)} = \frac{\text{Weight of the displaced Hg (g)}}{13.6 \text{ (g cm}^{-3}\text{)}} \quad (2)$$

The breaking resistance of the residue was measured using a compression tool (Fig. S1), connected to a 10 daN Zwick detector in an ADAMEL mechanical testing machine. Typically, burned samples were pressed by a cylindrical sensor with diameter 4 mm (initial sample dimension  $100 \times 100 \times 4$  mm) at compression rate of 1 mm/min under which the applied force (N) and the compression depth (mm) to break down the material were recorded. The results were reprocessed to determine the energy required to attain the maximum force, and the slope up to the first crack under the test (Fig. 2). The area under the peak of maximum force was considered as the energy required to destroy the material (when the force curve reaches a plateau, synonymous with powder compression, or shuts down, for a material that breaks into pieces, *vide infra*). The slope was taken as an indicator of the surface stiffness. The test was applied to at least 10 samples, because of the poor repeatability of the technique, from which most representative curves were taken and averaged.

### 3. Results

As stated in the introduction, composite samples were burned in a furnace under extreme pyrolysis conditions, according to NFC

32070 CR1 specifications. Silicone test materials were confined in paired stainless steel tubes with limited air content. Pyrolysis ranged from  $40^\circ\text{C}$  to  $940^\circ\text{C}$  over 40 min, followed by an isotherm at  $940^\circ\text{C}$  during 15 min. Residues were then characterised by examining their inner and outer microstructures (by ESEM and optical microscopy), by determining their chemical transformation (by EDX elemental analysis and XRD analysis) and by estimating their cohesion (by volume variation and compressive resistance tests).

The structure of the matrix residue (no filler apart from 25 wt% silica) was first observed by ESEM and optical microscopy, as shown in Fig. S2. These blank analyses are necessary as a reference point compared to filled sample residue. Microstructures of matrix residue were relatively smooth and had few cracks, but some agglomerates of silica particles were found on the surface (Fig. S2). The cracks on the surface residue were principally attributed to the release of volatile products during silicone degradation.

#### 3.1. Structure of surface residues by optical microscopy

The general appearance of residues of silicone composites after pyrolysis in extreme condition is presented in Fig. 3. Macroscopic

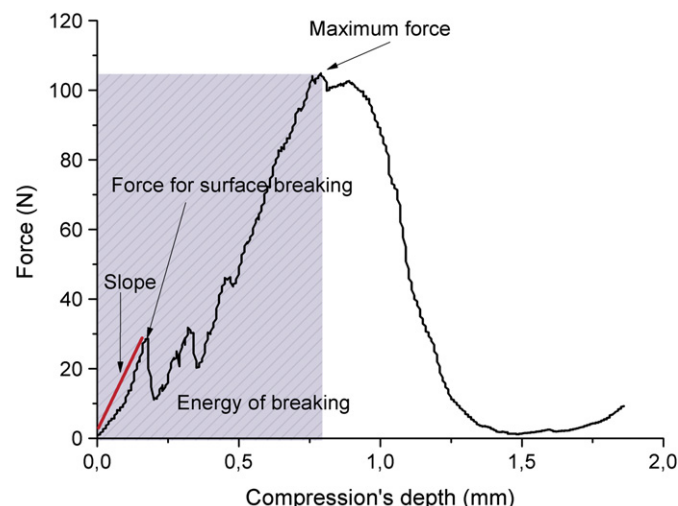


**Fig. 2.** Data observations from the compression test of residue PCC composite.

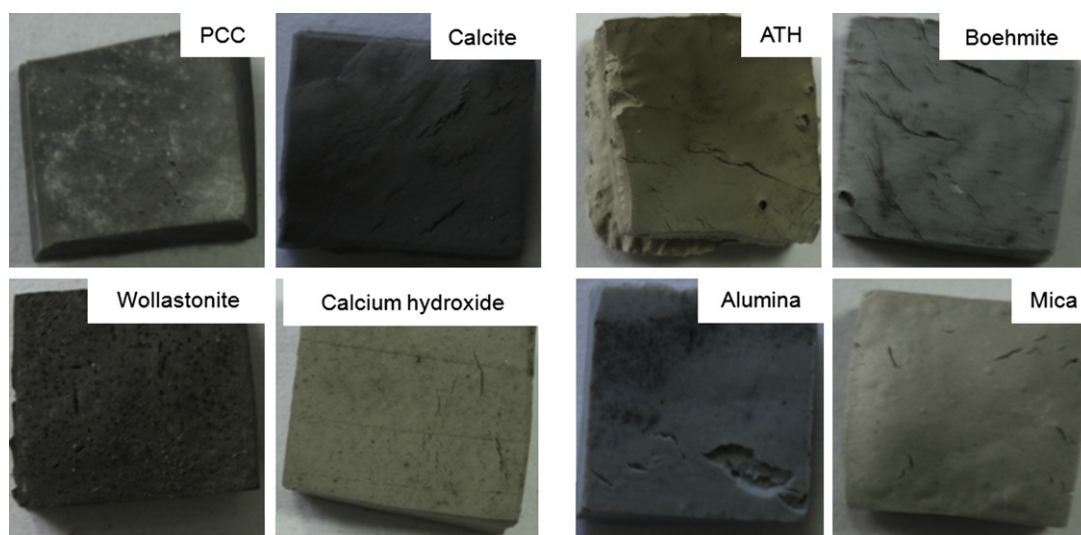


Fig. 3. Photographs of the surface morphologies of the residues (composites containing calcium- (left) or aluminium- (right) based fillers).

observation by optical microscopy was also systematically done on the microstructure of surface residues (Fig. 4).

Silicone composites containing nano-sized calcium carbonate (PCC), micro-sized calcium carbonate (calcite) or wollastonite produced residues with a very small amount of cracks on the surface. The residue of calcite composites exhibited slightly more cracks on the surface compared to PCC or wollastonite. In addition, silicone composites containing calcium hydroxide presented more cracks on the surface, probably because of water release from filler degradation.

All aluminium-based fillers presented cracks on their surfaces. High water release through thermal decomposition of ATH led to formation of numerous cracks everywhere on the surface, bigger than those from calcium hydroxide or boehmite composites. Residue of silicone composites containing mica and alumina also presented numerous cracks covering the surface. Volatiles released during the combustion may be water, CO<sub>2</sub>, or cyclic siloxanes, all of which entail crack formation in the composites during the test. Lower crack formation on calcium carbonates and wollastonite comes from the fact that volatiles released displayed no interactions with silicone during degradation at low temperature [6].

### 3.2. ESEM analyses

From ESEM images under magnification of 5000 $\times$ , a continuous ceramic layer was observed on the surface of PCC and calcite composite residues (Fig. 5). The surface residue of wollastonite composite presented some big filler particles slightly attached to the amorphous structure of matrix residue through a ceramic layer. The surface of calcium hydroxide composite was rough and cottony due to matrix degradation by water molecules released from the filler, and traces of cracks were also observed on the surface residue. Thanks to EDX analyses, we have identified that the cottony materials contains silicon atoms. Silica, either silica filler or silica from silicone degradation (mainly fumed silica) tends to accumulate near the surface without sinking through the polymer melt layer during the burning process [7].

In Fig. 6, no obvious porosities were observed on the surface of ATH and boehmite composites, probably because they degraded at rather low temperature (below 500 °C). It is supposed that structural rearrangement of the residual network could occur while burning the composite up to 940 °C. ATH presented rough surface with some cottony agglomerates and traces of cracks, while boehmite showed, on the micrometer scale, a smoother surface.

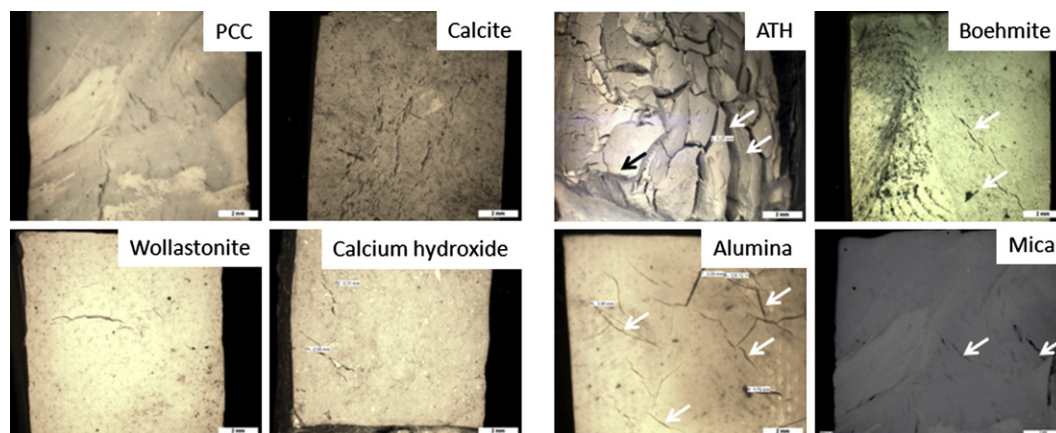


Fig. 4. Surface morphologies from residues of silicone composite containing calcium- (left) or aluminium- (right) based fillers as observed by optical microscopy. Pictures were taken from the top of the samples with a magnification of 25 $\times$ .



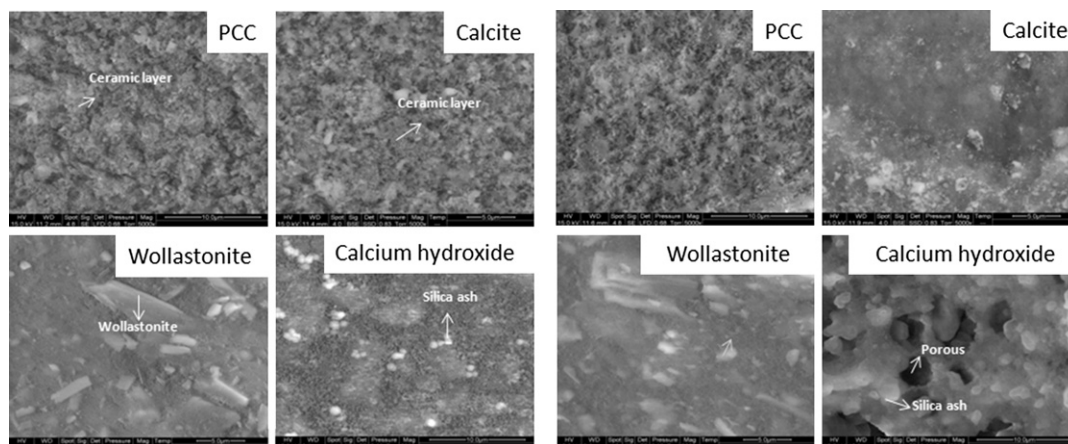


Fig. 5. ESEM images on surface (left) and interior (right) microstructures of pyrolysis residues from silicone composites containing calcium-based fillers.

Alumina composite also exhibited smooth surface residues. The sample containing mica presents surface residue with some individual mica particles found on the surface, apparently with a better cohesion to matrix residue than wollastonite particles.

The internal residue of composites containing calcium carbonates presented a minor porosity (Fig. 5), probably due to  $\text{CO}_2$  gas release during pyrolysis, with few ceramic continuous layers. While the internal residue of composites containing wollastonite presented no porosity, some isolated particles of wollastonite filler were found as well as cotton-like materials. Inside calcium hydroxide's residue, the crater-like surface was surrounded by ceramic materials. The big holes formation could be explained by matrix degradation due to strong water release from filler decomposition. It is suggested that these water molecules catalyse the degradation of the neighbouring silicone chains to release volatile and to leave holes behind them.

All aluminium-based fillers presented almost similar microstructure in their core, in which crater-like holes are surrounded by cottony materials (Fig. 6). However, ATH residue seemed to have bigger pores than other fillers, probably due to the larger water release from ATH degradation. Smaller fillers such as boehmite and alumina presented low porosity and cottony internal structure. A porous structure and big voids were observed among mica particles inside the residue of mica-based composite. Note that an observation by ESEM at high magnification, of the interior residues of mica and wollastonite composites showed the presence of micro-bridges in both cases (Fig. 7).

### 3.3. XRD analysis

XRD analysis of bulk residues confirmed the results previously reported in the first paper of this series devoted to thermogravimetric analyses [6]. The diffractograms of PCC, calcite, and calcium hydroxide residues are presented in Fig. S3. Ceramic-like materials in PCC and calcite residues were found to be composed of wollastonite and calcium silicate; two different  $\text{CaSiO}_3$  crystalline forms arose from *in-situ* crystallisation between  $\text{CaO}$  in filler and  $\text{SiO}_2$  in matrix. The XRD analysis of wollastonite confirmed the presence of filler in the residue, since wollastonite was stable during pyrolysis at  $940^\circ\text{C}$ .  $\text{CaO}$  from calcium hydroxide degradation product also reacted with silica to form wollastonite, calcium silicate, and larnite ( $\text{Ca}_2\text{SiO}_4$ ). The lower decomposition temperature of calcium hydroxide made the  $\text{CaO}$  available earlier and in higher content than calcium carbonate's composites to crystallise with silica. ATH, boehmite, and alumina residues did not lead to new crystallisation steps at high temperature. All of them degraded to form amorphous  $\text{Al}_2\text{O}_3$ , not visible on XRD. As for wollastonite, mica particles maintained their crystallinity after pyrolysis.

### 3.4. Elemental analyses by EDX

EDX analyses from ESEM images were carried out to obtain averaged elemental contents. Fig. 8 presents the Ca or Al element content (relative to Si element content) inside and at the surface of

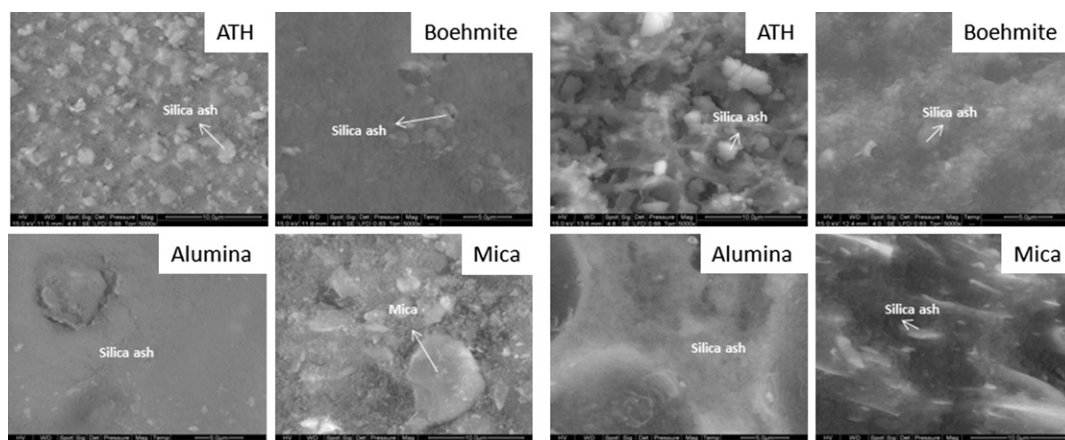


Fig. 6. ESEM images on surface (left) and interior (right) microstructure of pyrolysis residues from silicone composites containing aluminium-based fillers.



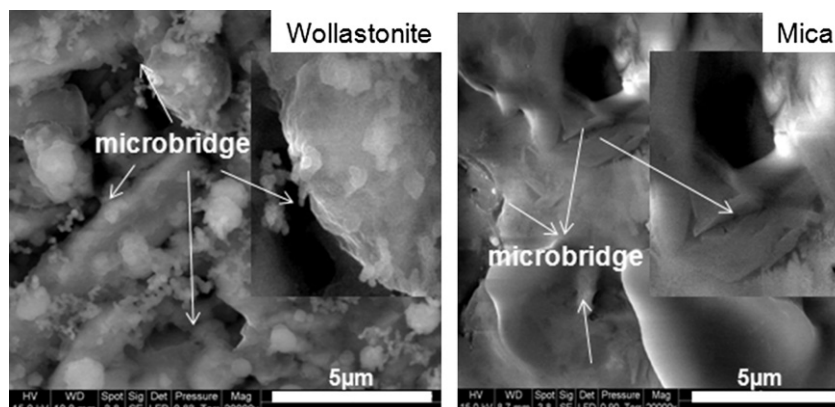


Fig. 7. Interior microstructures of pyrolysis residues from silicone composites containing wollastonite and mica under magnification of 20,000 $\times$ .

composites and residues. Note that increased Ca or Al content can also be interpreted as lower Si content.

In composites containing aluminium-based filler, ATH and boehmite residues showed almost homogeneous Al element distribution in the core (interior) and surface (exterior) of composites (Fig. 8a), but a slight difference was observed in alumina and mica composites. After pyrolysis, an increase of Al element content on the surface of mica and alumina residues were observed (Fig. 8b). Residue of mica has a richer Al content on the surface than alumina residue, which suggests either filler migration to surface, silica volatilisation or polymer ablation during pyrolysis.

Conversely, compositions of residues and composites of calcium-based fillers did not show such regular tendency. PCC and wollastonite composites presented slightly higher Ca content on its surface than in the interior, contrary to calcite, although differences are tenuous. Larger differences of Ca content on the surface and in the interior were found for the composites containing calcium hydroxide (Fig. 8a). After pyrolysis, all residues of calcium-based fillers except wollastonite have lower Ca content on surface than

inside the residues, which may designate silica migration to surface (Fig. 8b), whereas higher Ca content on surface of wollastonite residue was presumably caused by polymer ablation, which left more wollastonite particles on the surface of the residue (see ESEM image Fig. 5).

### 3.5. Volume variation analysis

Volume variations were determined by the Hg displacement technique by comparing samples before and after pyrolysis. In this method done at atmospheric pressure, the internal porosity is ignored since Hg cannot penetrate into the internal closed pores (measuring the porosity of the samples would imply to use a mercury porosimeter working at high pressures that would break such brittle samples). Incorporation of aluminium or calcium-based fillers severely modified the volume variation of residues, as presented in Table 1. The residues of PCC and calcite composites presented high residual shrinkage, 52% and 48% respectively. Incorporation of wollastonite had almost no influence on the

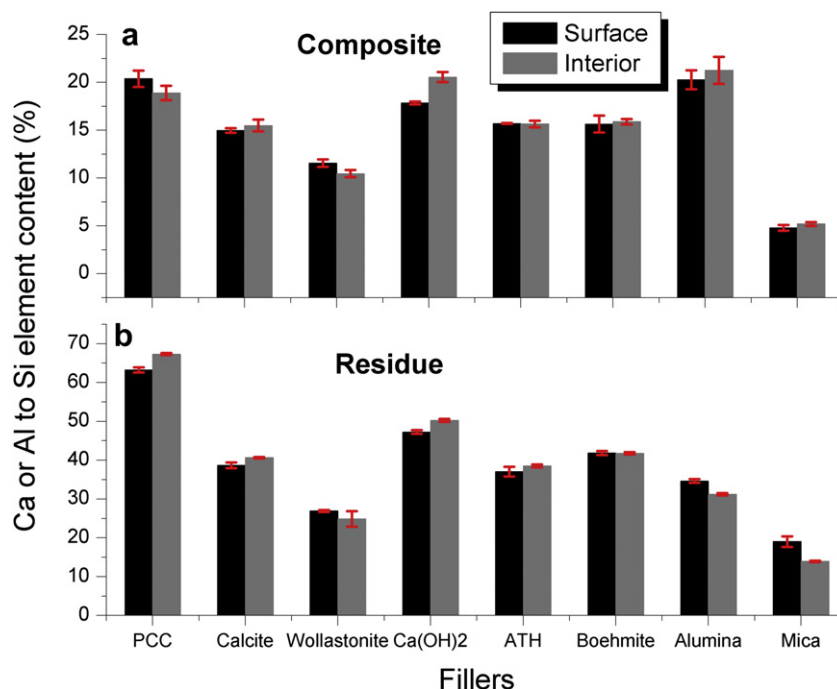
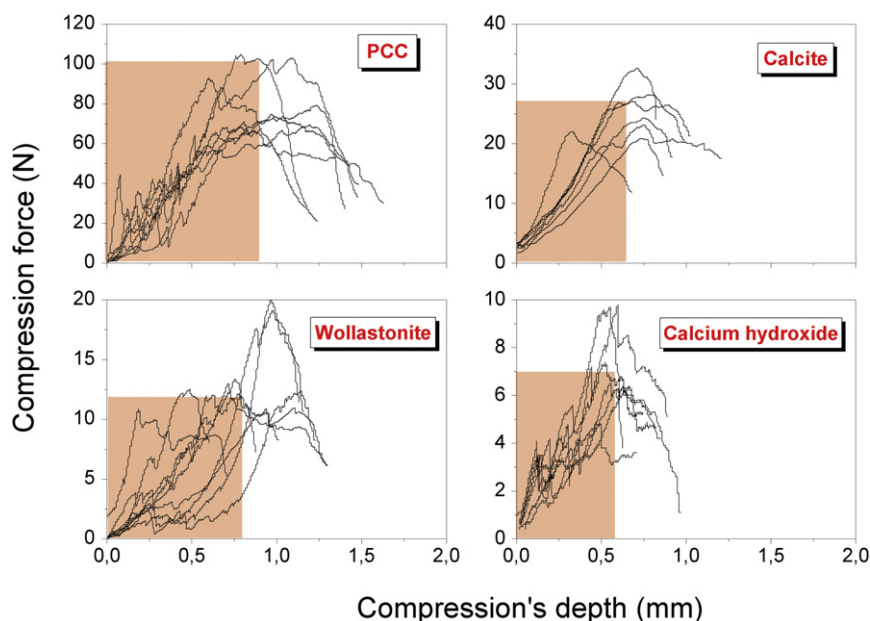


Fig. 8. Elemental analyses of Al or Ca contents (normalised by Si contents) inside (interior) and outside (surface) of composites and residues.



**Fig. 9.** Experimental curves from compression tests of residues from silicone composites containing calcium-based filler. Salmon zone is delimited by the average force and average time to break down the residue, as calculated from all curves (see values in Table 2).

volume variation of composite's residue (7% shrinkage). Contrary to other calcium-based fillers, incorporation of calcium hydroxide resulted in 9% expansion volume of residue. All aluminium-based fillers presented significant volume expansions, large ones for ATH and alumina (60% and 58% respectively), while boehmite and mica exhibited lower volume expansion (25% and 18% respectively).

### 3.6. Compression tests

Originally, micro-indentation measurements were planned to evaluate the mechanical strength of the residues [3]. Since most of

these were brittle, we took advantage of this fragility to generate some "destruction curves" so as to discriminate between the different pyrolysed materials. Figs. 9 and 10 present the experimental curves from compression tests of calcium and aluminium based residues, respectively. As stated in the experimental part, the compression test was applied to at least 10 samples, because of the poor repeatability of the technique, especially for aluminium-based material residues. From all curves, we recorded the maximum force required to break down the bulk residue, noticed maximum compression force (N), and the compression's depth at which this breaking occurs (mm), including the area under the maximum force corresponding to energy required to break down residues

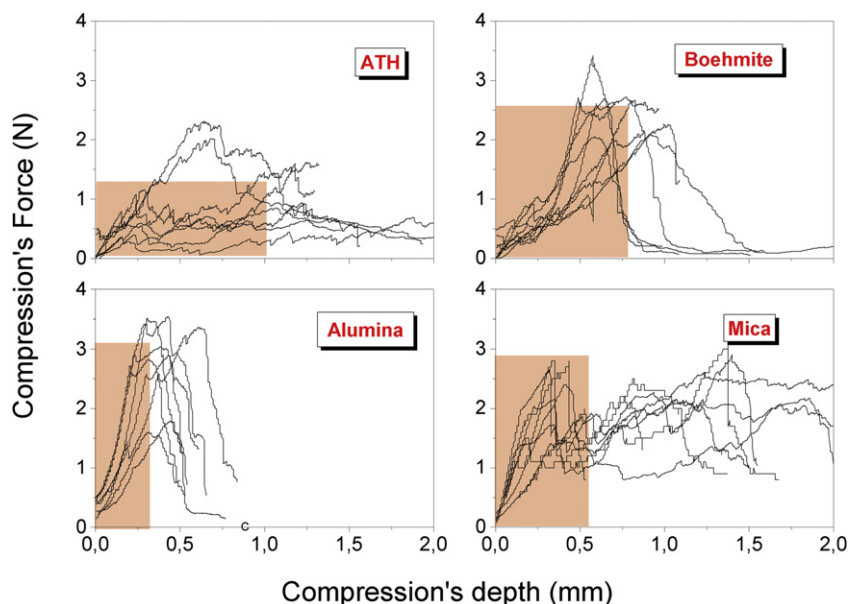


**Fig. 10.** Experimental curves from compression tests of residues from silicone composites containing aluminium-based filler. Salmon zone is delimited by the average force and average time to break down the residue, as calculated from all curves (see values in Table 2).

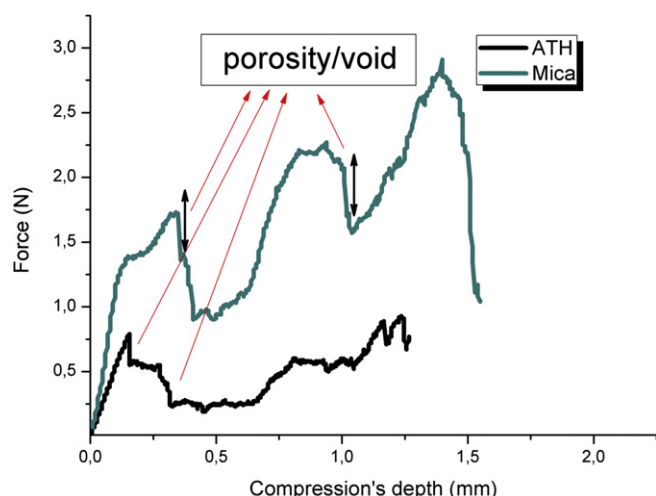


**Fig. 11.** Selected compression curves of residues of composites containing ATH and mica, showing the effect of the porosity on the compression measurements.

(N mm), and finally the slope up to the first peak under compression (N/mm) (see an example of data considered on the compression curve of PCC composite in Fig. 2). Note that the first peak that appears under test is assigned to a rupture of the surface layer. For porous residues, when the cylindrical sensor passes through a pore, the force goes down until the cylindrical sensor touches back the residue and then increases again, and this step is repeated until the maximum force is attained. For example, residues of mica and ATH composites which present some porosity, showed crenellated compression curves (Fig. 11).

All data were compiled, averaged and compared in Table 2 and Fig. 12. The residues containing aluminium-based fillers presented almost identical average values of maximum force of compression, energy, and penetration depth of cylindrical sensor (%) to attain the maximum force of bulk residues. Even so, residue of mica composite required slightly higher force and energy to break down. The residue of alumina composite differed slightly, showing the lowest sensor penetration to break down; this residue gave highly powdered ashes compared to the others, in agreement with its brittleness and poor mechanical resistance.

More dissimilarity was observed for the residues of calcium-based composites. In general, they presented better compressive behaviours than ones of aluminium-based composites. PCC showed an outstanding compressive resistance of its residue compared to other tested calcium-based fillers; automatically it also required

the highest sensor penetration (%) to break down the residue of very dense structure. Instead, bigger particle size of natural calcium carbonate (calcite) presented lower compressive resistance, thus less dense residue. However, residue of calcite composite presented higher force and energy required to break down their residues compared to wollastonite and calcium hydroxide composites. The decrease in force, which correlates with a decrease in energy and sensor penetration (%), means that residue of calcite composite was more cohesive and denser than residue of wollastonite and calcium hydroxide composite.

The appearance of residues after the compression tests is presented in Fig. 13. All residues of calcium-based filler and mica formed small fragments which maintained their integrity. ATH, boehmite, and alumina residues were literally squashed down to form ashes-like bits. Such final state can be correlated with the form of the compression curve quite easily: upstanding residue materials such as those obtained from calcium-based materials broke suddenly and went down to the origin rapidly (Fig. 9, except for calcium hydroxide). Conversely, crumbly materials sustain a given force even at high compression depth (see example of ATH, Fig. 10). Alumina compression curve is the only exception of compression/state of the broken residue correlation: indeed, these materials were far too crumbly to be carefully characterised by compression.

#### 4. Discussion

All data gained in the results part are summarised in Tables 1 and 2. In order to determine the cohesion of all residues obtained here by pyrolysis, two main parameters are considered (volume variation and residue behaviours under compression) and compared with external parameters (volatile release, new crystal and/or char formation and filler/polymer interaction).

##### 4.1. Effect of volatile release to volume variation

Silicone composites containing water-releasing fillers presented almost identical residue microstructures, with high porosity and crater-like morphology inside, and amorphous (smooth) and cracked surface. These porosities and cracks were induced by water and volatile products released from the filler and matrix degradation, respectively. All of these also resulted in volume expansion, proportional to the content of water released, principally. Lower volume expansion of boehmite based composition compared to ATH one was observed because boehmite degradation released only 18 wt% of water against 35 wt% for ATH. Also, the temperature of water release is primordial: boehmite

**Table 2**  
Compression resistance's behaviour of Ca and Al-based residues.

Filler	Surface			Bulk residue			
	Force (N) <sup>a</sup>	Compression depths (mm) <sup>a</sup>	Slope (N/mm) <sup>a</sup>	Maximum force (N)	Compression depths (mm) <sup>a</sup>	Sensor Penetration (%) <sup>c</sup>	Energy (10 <sup>-3</sup> J) <sup>b</sup>
PCC	27.36 ± 3.55	0.10 ± 0.02	0.470 ± 0.178	90.07 ± 15.07	0.91 ± 0.23	50.4	33.1 ± 7.1
Calcite	2.78 ± 0.38	0 <sup>d</sup>	0.103 ± 0.012	24.71 ± 2.95	0.71 ± 0.05	35.7	10.93 ± 1.66
Wollastonite	3.91 ± 0.80	0.17 ± 0.04	0.027 ± 0.003	11.97 ± 1.05	0.85 ± 0.11	24.1	4.09 ± 0.60
Calcium Hydroxide	3.99 ± 0.50	0.14 ± 0.02	0.092 ± 0.024	7.83 ± 1.32	0.57 ± 0.05	13.7	2.41 ± 0.59
ATH	0.74 ± 0.18	0.21 ± 0.04	0.007 ± 0.003	1.21 ± 0.51	1.06 ± 0.39	17.4	0.86 ± 0.51
Boehmite	0.43 ± 0.15	0.20 ± 0.06	0.007 ± 0.002	2.55 ± 0.41	0.80 ± 0.17	16.8	0.89 ± 0.26
Alumina	2.04 ± 0.54	0.27 ± 0.05	0.019 ± 0.008	2.87 ± 0.38	0.37 ± 0.06	6.10	0.70 ± 0.18
Mica	1.81 ± 0.34	0.27 ± 0.07	0.021 ± 0.006	3.01 ± 0.55	0.75 ± 0.44	16.6	1.18 ± 0.72
Matrix 25% Silica	1.91 ± 0.21	0.09 ± 0.03	0.055 ± 0.020	2.64 ± 0.39	0.29 ± 0.06	8.10	0.45 ± 0.16

<sup>a</sup> Collected for the first time residue is broken under compression.

<sup>b</sup> At the maximum force.

<sup>c</sup> Calculated by considering the volume variation of residue.

<sup>d</sup> The outer layer of calcite residue did not generate a specific compressive resistance (see Fig. 9).

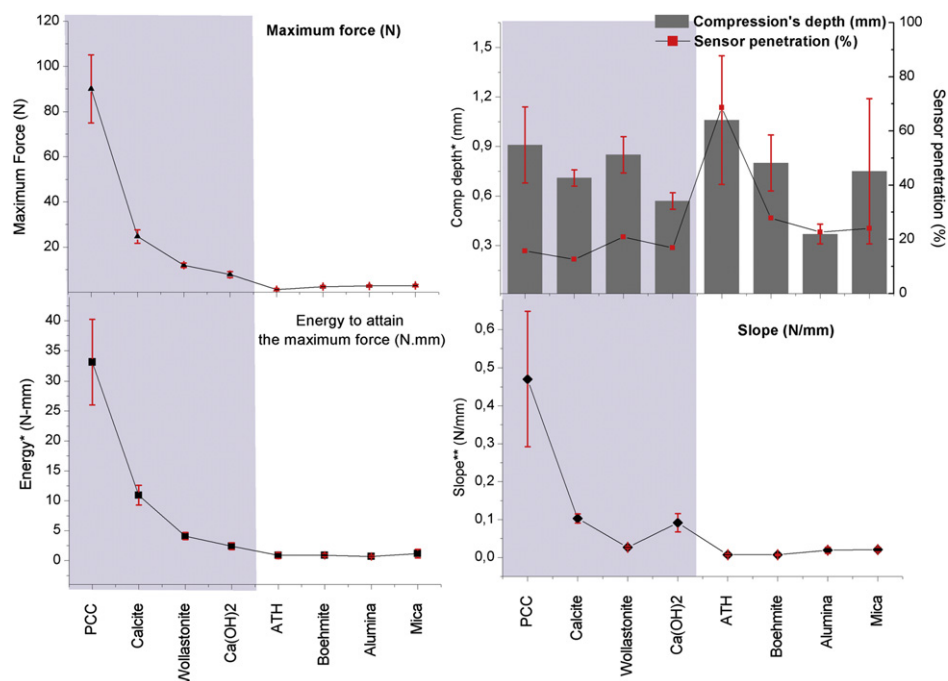


**Fig. 12.** Compressive behaviours of residues silicone composite containing aluminium and calcium-based filler (zones in grey and white separates calcium- from aluminium-filled silicone composite residues).

releases water at about the same temperature as silicone degradation (from 380 °C to 550 °C), so that it has a lower catalytic effect on silicone degradation than ATH, which initial degradation temperature is rather low (from 220 °C to 380 °C) [6]. High volume expansion of alumina fillers can be explained by the very high surface area developed by the nanoparticles, so that more hydroxyl groups were able to promote silicone degradation. Unless other fillers, low volume expansion of mica contributed to filler good cohesion to matrix surface. In addition, as reported previously by Mansouri et al. [5], mica could produce a eutectic liquid at high temperature to facilitate the formation of a strong ceramic layer. This eutectic liquid of mica can form at the interface on heating around 900 °C to act as a bridge between the silicon dioxide particles and the mica particles, giving a coherent structure at the firing temperature. Lamellar shape and big particle size

of mica bound well to the matrix to form an effective protective layer and limit the volume variation.

Silicone composites containing CO<sub>2</sub>-releasing fillers were shown to induce almost no porosity inside the residue, and on the contrary led to a severe shrinkage. They even showed higher volume shrinkage than for wollastonite. CO<sub>2</sub> release during sample pyrolysis did not result in matrix degradation, thus confirming that this gas is inert towards silicones. In addition to that, co-crystallisation occurring at high temperature surely helped to densify the residue and to reduce the porosity, resulting in the shrinkage of the residues. The shrinkage volume of residue observed for wollastonite composite is attributed only to the loss of cyclic siloxanes during matrix degradation, since wollastonite is inert towards silicone.

Calcium hydroxide showed a behaviour in-between the two former cases. Whereas volume expansion would be expected since

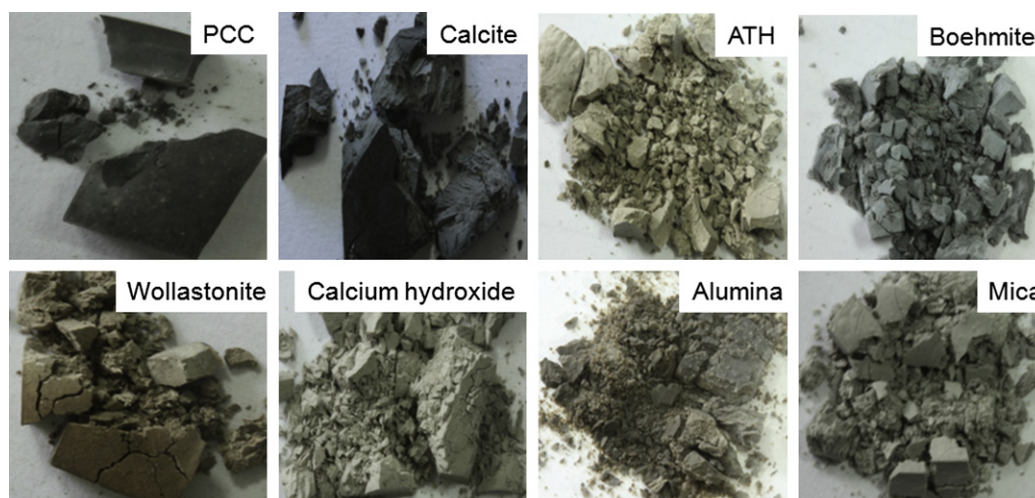


**Fig. 13.** Residues appearance after compression tests.



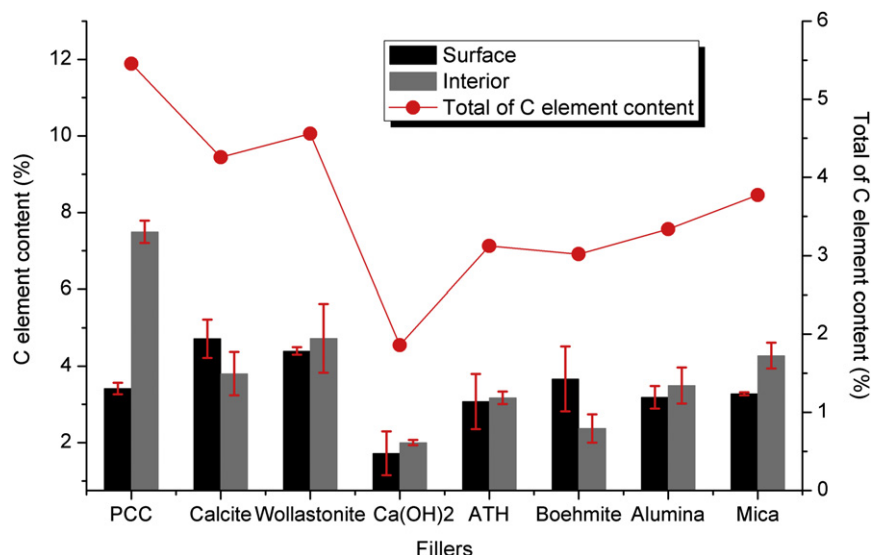


Fig. 14. Carbon element content in the residues of silicone composite. Total C element content is the addition of C element content on surface and interior of residue.

water release shall promote matrix degradation, co-crystallisation involving calcium oxide should also limit its volume expansion, as for the other Ca-based composites. It seems that water release had a low catalytic effect on matrix degradation, since calcium hydroxide degradation temperature occurs at the same time than matrix degradation (between 400 °C and 600 °C).

#### 4.2. Effect of co-crystallisation to compression behaviour

The occurrence of co-crystallisation in residues was believed to be at the origin of their compression resistance. Co-crystallisation between filler and matrix at high temperature modifies the microstructure of residue, providing denser residue and improving its structural strength. The unsatisfactory compression behaviour of residue of silicone composite containing aluminium-based filler is certainly due to the absence of co-crystallisation at high temperature.

PCC and calcite presented better compression resistance because they have a very compact residue as the result of structure rearrangement by co-crystallisation. Compared to calcite, the nano-sized of calcium carbonate in PCC surely presents higher surface activity towards silica in co-crystallisation (for a complete characterisation of particle sizes and structures, see [6]). Thanks to co-crystallisation, calcium hydroxide composite showed better compressive resistance than all-water releasing fillers even though it presented high interior porosity due to water-release. Unlike in residue of aluminium-based fillers, these interior porosities were surrounded by a continuous ceramic layer (glassy layer) as seen in ESEM images (Fig. 5) because volatiles release (water or cyclic siloxanes) was followed by a successive co-crystallisation at high temperature, which densifies the residue. Unfortunately, the interior porosity makes the residue of calcium hydroxide composite more fragile than wollastonite composite. Residue of silicone composite containing wollastonite also showed good cohesion, even though wollastonite filler did not co-crystallise with silicone matrix nor did it bind to the matrix.

#### 4.3. Char formation to residue content

Shephard [8] has reported that increasing contents of wollastonite into silicone resulted in a tough resinous char, i.e. a partly carbonaceous residue, with few surface cracks and high surface

integrity. This char formation was confirmed here by the high total carbon element content measured for wollastonite residue, as well as in the interior of the mica residue (Fig. 14). Lamellar shape of mica or wollastonite favours a mass barrier effect which limits the volatile release. Also, the occurrence of micro-bridge formation between wollastonite particle and matrix residue should increase ash strength.

Nano-fillers of PCC and alumina composites also presented high carbon element content in their residues. The presence of nano-particles in polymer induces tortuosity in volatiles' release pathway [9–11]. Hence, carbon-rich residue of PCC presents better compressive resistance of PCC than calcite; similarly, the carbon-rich char formation in alumina residue results in slightly higher compressive resistance than ATH or boehmite (Table 2). Nevertheless, this char formation is not enough to provide high compressive resistance of residue. Submicronic boehmite showed no improvement in charring residue; its acicular particle shape seems not to be able to increase either the tortuosity in composite or mass barrier on surface.

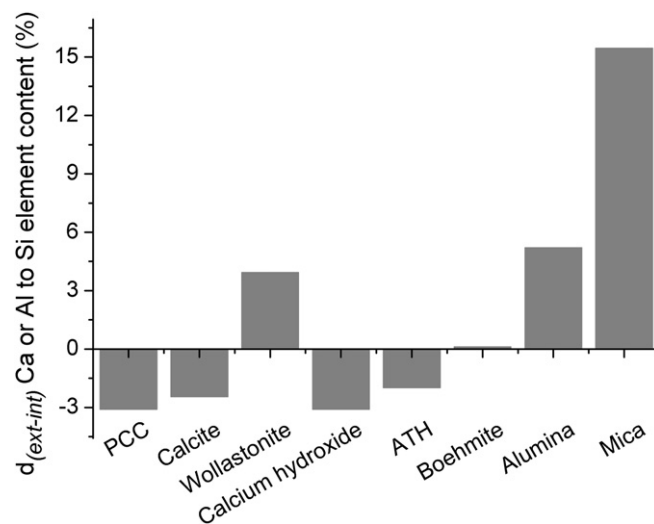


Fig. 15. Differences between Ca or Al to Si element content on surface and interior of silicone composites after pyrolysis.

We also calculated the difference between Ca or Al to Si element content in surface and interior of residue, express as  $d_{(\text{ext-int})}$  in Equation (3).

$$d_{(\text{ext-int})}(\%) = \frac{(\% \text{Element})_{\text{Surface}} - (\% \text{Element})_{\text{Interior}}}{(\% \text{Element})_{\text{Surface}} + (\% \text{Element})_{\text{Interior}}} \times 100 \quad (3)$$

where % Element refers to Al or Ca element content to Si element content on surface or interior of residue. The positive values of  $d_{(\text{ext-int})}$ , presented in Fig. 15 indicates some filler accumulation at the surface of the material and/or polymer ablation. Mica, wollastonite, and alumina fillers showed higher Al or Ca element content on surface of residue. PCC filler was on the opposite rather located inside the residue, where charring mostly occurred, as seen in Fig. 14.

Large size and high filler density of wollastonite and mica particles [6] do not speak in favour of their migration to the surface. Since both of them sustain the tested temperature, and do not transform at high temperature, the presence of excess mica or wollastonite on residue surface can thus only be attributed to polymer ablation during burning, leaving filler poles on the burned material. On the opposite, the presence of alumina particles on surface of residue could likely be ascribed to filler migration to surface, since alumina nanoparticles exhibit very small filler density [6].

## 5. Conclusions

The state of the residues of calcium and aluminium-based composites after pyrolysis has been observed by different techniques of microscopy (optical and scanning electronic microscopy), elemental analysis (XRD, EDX) and physical characterisation (volume expansion, compression curves). The filler nature and the co-crystallisation and/or charring at high temperature are the two key parameters to achieve a cohesive residue. Filler nature strongly influences the residue's morphology by the formation of interior porosity, indirectly also varying its volume. The presence of water from filler degradation weakens the residues, because of interior porosity, and expands their volume. Besides, co-crystallisation is believed to control the residues' compression resistance. As a matter of fact, the presence of cracks is not important, since the surface effect on the compressive resistance of bulk residue is not significant. All residues of composites containing aluminium-based fillers are fragile without any cohesion residue, due to the absence of filler-matrix interaction at high temperature (co-crystallisation). On the group of residues containing calcium-based fillers, residue of PCC presented the strongest ceramified residue. Residue of PCC composite is tough and very dense, and as a consequence, it requires more energy to break down under compression compared to calcite, wollastonite and calcium hydroxide. For this particular filler, co-crystallisation and char formation in the interior of residue explain such interesting result. Mica and wollastonite also showed slightly better cohesion residue thanks to char formation.

The above conclusions can be challenged in regards of the NFC 32070 CR1 standard test. In our simplified pyrolysis test, we did not check the influence of the presence of the copper wire and of the mechanical shocks. Those two process variations can however be discussed based on volume variation analysis and compressive test, respectively. The copper wire expands with temperature: if the material shrinks during pyrolysis, cracks will likely form and weaken the cable. On the other hand, volume expansion would

inherently degrade the cable homogeneity, not considering the copper wire. One should thus seek a material filled with additives so that volume variation would be nil. Concerning the shock resistance, the compression tests predicted that a ceramic material be used to pass such drastic specification. A combination of fillers should provide a material both with no volume variation and sufficient ceramization behaviour. The use of a filler able to co-crystallise with silica, and to degrade without releasing water is thus highly recommended to obtain composites with good cohesion residue. Alternatively, adding to the formulation a filler that forms a liquid phase at high temperature (for example glass frits) could be an advantage, in order to strengthen the residue through micro-bridge formations between mica or wollastonite particles with silica. Using a calcium carbonate filler alone (either PCC or calcite) provokes a very high residual shrinkage, whereas boehmite or mica does not generate a cohesive residue. Optimised combination of PCC or calcite with aluminium-based filler such as boehmite or mica could be of prime interest to limit the volume variation inappropriate for electrical cable applications. Real industrial tests are currently performed on optimised formulations arising from this comprehensive study.

## Acknowledgements

We are most grateful to Bluestar Silicones for providing all the silicone raw materials that were necessary to carry out this study. We also thank Solvay, Nyco Minerals and Nabaltec for donating PCC, Wollastonite and Boehmite, respectively.

## Appendix. Supplementary data

Supplementary data associated with this article can be found in the online version, at doi:10.1016/j.polymdegradstab.2011.05.019.

## References

- [1] Kaufmann W, Prager FH, Schiffer HW. Electrical engineering. In: Troitzsch J, editor. International plastics flammability handbook. 2nd ed. Munich: Hanser; 1990. p. 344–78.
- [2] British Standard BS EN 50200. Method of test for resistance to fire of unprotected small cables for use in emergency circuits. British Standard Institution; 2006.
- [3] Laoutid F, Ferry L, Leroy E, Lopez Cuesta JM. Intumescent mineral fire retardant systems in ethylene–vinyl acetate copolymer: effect of silica particles on char cohesion. *Polym Deg Stab* 2006;91:2140–5.
- [4] Beyer G. Flame retardancy of nanocomposites based on organoclays and carbon nanotubes with aluminium trihydrate. *Polym Adv Technol* 2006;17: 218–25.
- [5] Mansouri J, Burford RP, Cheng YB, Hanu L. Formation of strong ceramified ash from silicone-based compositions. *J Mater Sci* 2005;40:5741–9.
- [6] Hamdani S, Longuet C, Lopez-Cuesta JM, Ganachaud F. Calcium and aluminum-based fillers as flame-retardant additives in silicone matrices. I. Blends preparation and thermal properties. *Polym Deg Stab* 2010;95:1911–9.
- [7] Mansouri J, Burford RP, Cheng YB. Pyrolysis behaviour of silicone-based ceramifying composites. *Mater Sci Eng A* 2006;425:7–14.
- [8] Shephard KL. Flame resistant silicone rubber wire and cable coating composition. May 2001. United States Patent 6239378.
- [9] Leszczyńska A, Njuguna J, Pielichowski K, Banerjee JR. Polymer/montmorillonite nanocomposites with improved thermal properties. Part I: Factors influencing thermal stability and mechanisms of thermal stability improvement. *Thermochim Acta* 2007;453:75–96.
- [10] Burnside SD, Giannelis EP. Synthesis and properties of new poly(dimethylsiloxane) nanocomposites. *Chem Mater* 1995;7(9):1597–600.
- [11] Burnside SD, Giannelis EP. Nanostructure and properties of polysiloxane-layered silicate nanocomposites. *Polym Sci Part B Polym Phys* 2000;38: 1595–604.





Supporting information for

**“CALCIUM AND ALUMINUM-BASED FILLERS AS FLAME-RETARDANT ADDITIVES IN SILICONE MATRICES II. ANALYSES ON COMPOSITE RESIDUES FROM EXTREME PYROLYSIS TEST”**

By S. Hamdani-Devarennnes, A. Pommier, C. Longuet, J. Lopez-Cuesta, F. Ganachaud\*

Submitted to « *Polymer Degradation and Stability* »



Figure S 1 : ADAMEL compression tool

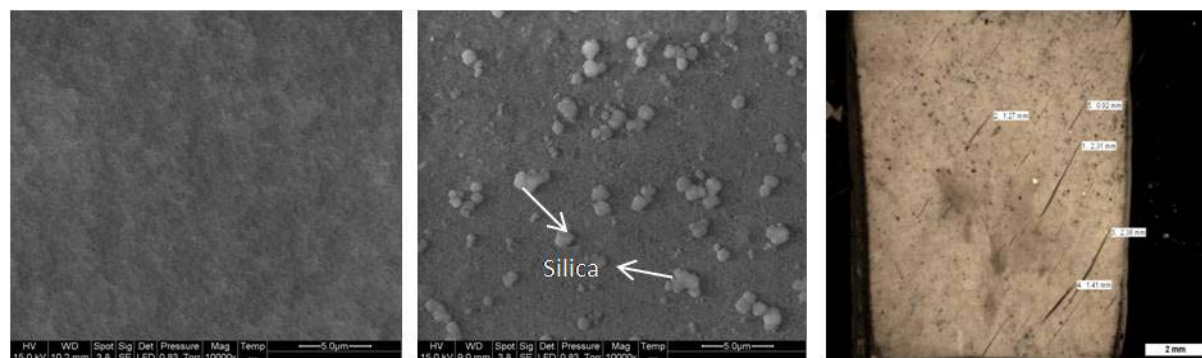


Figure S 2. Images of matrix residue in the interior (a) and exterior (b) of residue (by ESEM), and the general performance of surface residues taken by optical microscopy (c)

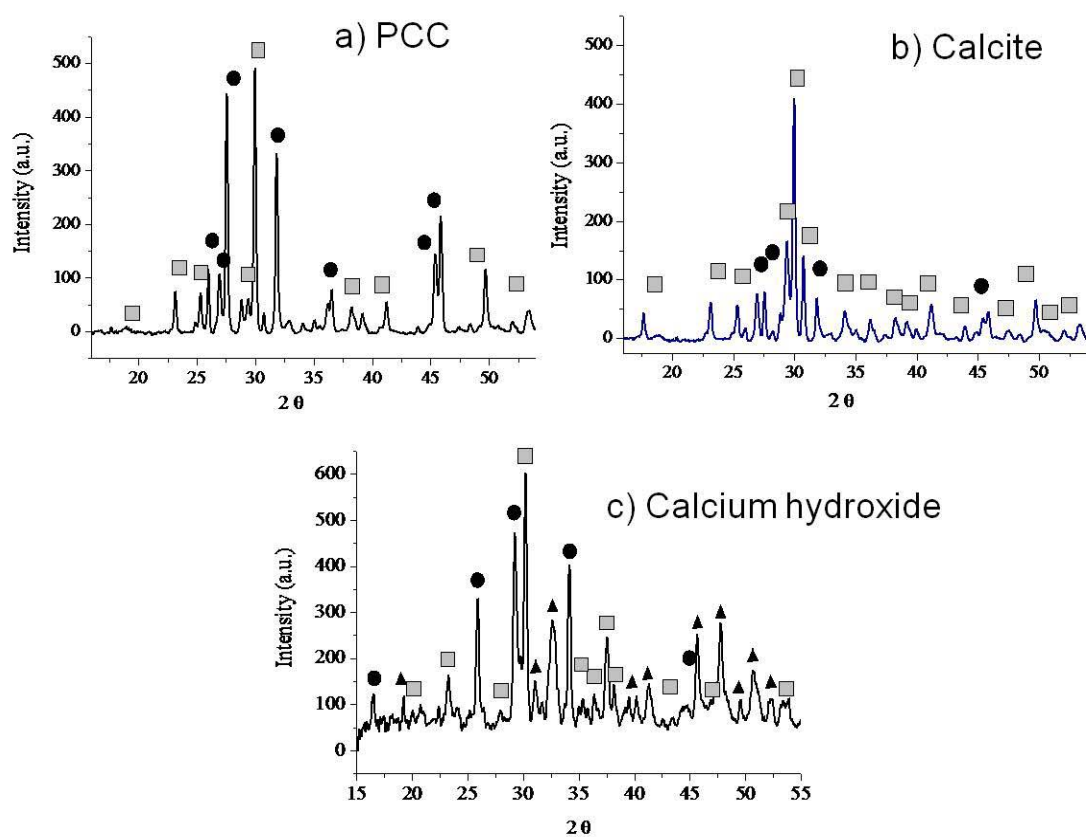


Figure S 3. Diffractograms of pyrolysis residue from PCC, calcite, and calcium hydroxide composites.

Table S 1. Commercial information and characterization data on the fillers used in this study.

	<i>Fillers</i>	<i>Formula</i>	<i>Chemical composition</i>	<i>Particle shape<sup>a</sup></i>	<i>Mean particle size and deviation (<math>\mu\text{m}</math>)<sup>b</sup></i>	<i>SSA (<math>\text{m}^2/\text{g}</math>)<sup>c</sup></i>	<i>Crystalline form<sup>d</sup></i>
Ca based	Precipitated calcium carbonate (PCC)	$\text{CaCO}_3$	$\text{CaCO}_3$	Oblate/spherical (aggregates)	$0.074 \pm 0.015$	$20.57 \pm 0.04$	Calcite
	Calcite	$\text{CaCO}_3$	$\text{CaCO}_3$ (98%) $\text{MgCO}_3$ (0.4%) $\text{Fe}_2\text{O}_3$ (0.1%)	Platelet	$1.0 \pm 0.3$	$6.49 \pm 0.33$	Calcite Quartz
	Calcium hydroxide	$\text{Ca}(\text{OH})_2$	$\text{Ca}(\text{OH})_2$	Platelet	$1.1 \pm 0.5$	$5.44 \pm 0.79$	Portlandite Calcite
	Wollastonite	$\text{CaSiO}_3$	$\text{CaO}$ (46.15%), $\text{SiO}_2$ (51.6%) $\text{Fe}_2\text{O}_3$ (0.77%) $\text{Al}_2\text{O}_3$ (0.34%) $\text{MnO}$ (0.16%) $\text{MgO}$ (0.38%) $\text{TiO}_2$ (0.05%) $\text{K}_2\text{O}$ (0.05%)	Acicular, and lamellar	$7.4 \pm 6.7$	$3.74 \pm 1.15$	Wollastonite Calcite
Al based	Aluminum trihydrate (ATH)	$\text{Al}(\text{OH})_3$	$\text{Al}_2\text{O}_3 \cdot 3\text{H}_2\text{O}$	Hexagonal platelet	$0.9 \pm 0.3$	$6.01 \pm 0.04$	Gibbsite
	Boehmite	$\text{AlOOH}$	$\text{Al}_2\text{O}_3$ (83%) $\text{Fe}_2\text{O}_3$ (0.02%) $\text{SiO}_2$ (0.04) $\text{Na}_2\text{O}$ (0.50%)	Acicular	$0.37 \pm 0.11$	$40^\circ$	Boehmite
	Alumina	$\text{Al}_2\text{O}_3$	$\alpha\text{-Al}_2\text{O}_3$	Spherical	$0.013^i$	$94.28 \pm 0.05$	Aluminum oxide
	Mica	$\text{KAl}_2(\text{Si}_3\text{Al})\text{O}_{10}(\text{OH})_2$	$\text{SiO}_2$ (51%) $\text{Al}_2\text{O}_3$ (32%) $\text{K}_2\text{O}$ (8.5%) $\text{MgO}$ (0.6%)	Flake like, Lamellar/platelet	$6.8 \pm 9.6$	$5.87 \pm 0.75$	Muscovite Kaolinite, Quartz

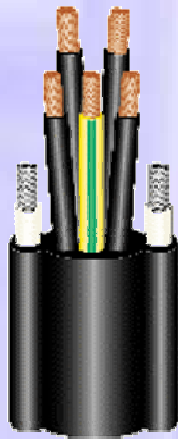
<sup>a</sup> from SEM observation, <sup>b</sup> from image analyses of SEM by XT-Docu, <sup>c</sup> BET measurements; <sup>d</sup> from XRD; <sup>e</sup> as given by the supplier.



# *Chapitre 5.*

## *Etude des Composites:*

### *« Comportement au Feu »*







## **Etude du comportement au feu de composites silicone comportant des charges minérales à base de calcium ou d'aluminium**

Ce chapitre est consacré à la compréhension de la réaction au feu de la matrice silicone en présence des différentes charges à base de calcium ou d'aluminium. Pour cela, nous avons comparé huit formulations différentes, identiques à celles décrites dans les chapitres 3 et 4. Le comportement au feu a été étudié grâce à un cône calorimètre, opérant à différentes irradiances (35, 50 et  $75\text{ kW/m}^2$ ), et à un microcalorimètre de combustion (PCFC). Lors de l'analyse de la réaction au feu au cône calorimètre, nous avons considéré la stabilité thermique du composite et/ou la formation d'une couche barrière. Pour ce faire, les structures des résidus produits lors du test au cône calorimètre ont été caractérisées par microscopie électronique à balayage (MEB) afin de mettre en évidence leur morphologie et également par analyse par diffraction des rayons X (DRX) pour observer la nature des structures cristallines présentes ou formées in situ. D'autre part, les analyses réalisées à l'aide du PCFC ont permis de définir la température correspondante au PHRR (Peak Heat Release Rate), utilisée pour les caractérisations au pyrolyseur couplé GC/MS (Py-GC/MS), ceci afin de déterminer la nature des volatils libérés lors de la dégradation des composites. Ces courbes HRR obtenues sont ensuite comparées avec la dérivée des courbes de perte de masse mesurées par analyse thermogravimétrique (ATG), sous atmosphère inerte, pour comprendre l'influence de la nature des volatils dégagés sur le HRR.

En général, les composites comportant les charges à base de calcium présentent un meilleur comportement au cône calorimètre. Deux formulations sortent du lot, celles contenant soit le mica, soit la wollastonite, une troisième s'en rapproche, celle où la calcite a été ajoutée. Le mica produit un effet barrière majoritaire, ainsi que la wollastonite, dont la stabilité thermique conférée domine cependant son comportement général. Enfin, la réaction au feu du composite à base de calcite est totalement liée à sa stabilité thermique. En revanche, l'incorporation de charges libérant de l'eau ou du  $\text{CO}_2$ , des gaz participant à l'effet endothermique, conduit à un comportement au feu moins bon que pour ces trois premières formulations. La microscopie électronique à balayage (MEB) nous a permis de mettre en évidence la formation de couches protectrices, indépendamment de l'irradiance. Par ailleurs, les analyses des résidus en DRX ont permis de montrer la formation de nouvelles structures cristallines uniquement à haute irradiance ( $75\text{ kW/m}^2$ ) dans le cas de l'hydroxyde de calcium et du CCP, ce qui améliore le comportement au feu de ces composites.

L'analyse des images des résidus par MEB nous a permis de différencier le type d'effet barrière obtenu en fonction de la charge ajoutée. Le mica, qui présente la meilleure résistance au feu, forme une couche barrière avec les particules en surface ainsi qu'à l'intérieur. L'incorporation des charges libérant de l'eau et/ou dégradant fortement la matrice silicone telles que l'ATH, la boehmite, l'alumine, et l'hydroxyde de calcium, conduisent à une surface fissurée, dont le taux de fissures augmente avec l'irradiance. Ces fissures créent des chemins permettant l'accélération de la dégradation du substrat, et la détérioration de la résistance au feu du composite.

La technique PCFC limite la prise en compte des effets barrières. Les essais réalisés selon cette méthode calorimétrique ont mis en exergue la stabilité thermique des composites silicones, que l'on peut attribuer à l'immobilisation des chaînes de silicone, ainsi qu'un léger effet endothermique. En ce qui concerne l'amélioration du PHRR et du HR (Heat Release), l'ajout d'ATH et d'hydroxyde de calcium était bénéfique de par leur effet endothermique, alors que l'ajout de wollastonite et de carbonate de calcium ne l'était pas, ces charges n'induisant pas d'immobilisation des chaînes macromoléculaires. Le faible PHRR du mica, malgré son absence d'effet endothermique, est attribué à sa capacité à immobiliser les chaînes de silicone via ses groupements hydroxyles de surface, et donc à limiter la production de macrocycles thermiquement instables. L'analyse de la composition des volatils produits au PHRR confirme la formation unique de cyclosiloxanes tendus ( $D_3$  et  $D_4$ ), ce qui limite non seulement l'augmentation du HRR (Heat Release Rate) mais aussi celle du HR (Heat Release).

Nous pouvons donc en conclure que le meilleur comportement au feu pour des composites silicone est obtenu principalement grâce à la stabilité thermique de la matrice, plutôt qu'à un effet endothermique, et dans le cas particulier du mica, grâce à un effet barrière. Cet effet barrière sera plus ou moins important en fonction de la stabilité thermique du minéral incorporé, ou comme pour le mica, grâce à sa morphologie. Enfin, la combinaison des essais au cône calorimètre et au PCFC apparaît être une approche prometteuse pour comprendre la contribution de chaque charge à la réaction au feu dans la matrice silicone. Ainsi, le PCFC permet d'observer essentiellement des processus élémentaires de réaction au feu en fonction de la température pour des échantillons microscopiques, alors que le cône calorimètre intègre la réaction au feu en phase condensée, et permet de visualiser des effets barrières.

# Calcium and aluminum-based fillers as flame-retardant additives in silicone matrices. III. Investigations on fire reaction

S. Hamdani-Devarennnes, C. Longuet, R. Sonnier, F. Ganachaud, J-M. Lopez-Cuesta\*

Submission to « Polymer Degradation and Stability »

**Abstract:** The fire resistance behavior of silicone composites containing calcium and aluminum-based fillers has been investigated using two calorimetry methods, namely a cone calorimeter and a Pyrolysis Combustion Flow Calorimeter (PCFC). Based on cone calorimeter test results, the fire reaction of PCC, calcite, calcium hydroxide, ATH, boehmite, and alumina composites is related to their thermal stability, while for mica and wollastonite composites, a barrier effect is also considered. In PCFC, thermal stability is believed to be the main factor governing the good fire reaction of silicone composite. Indeed, chain immobilization limits the production of volatile, combustible molecules, such as in mica, calcium hydroxide, and ATH composites. Using both techniques, the endothermic effect was not established as an efficient flame retardancy mechanism for these systems.

## I. Introduction

Polymers are a fundamental part of our modern society, for their unique properties of elasticity, lightness and durability. All organic polymers are nevertheless combustible, and when exposed to heat, they generate smoke and hazardous products. Fire safety in most buildings then depends upon the fire resistance of these materials. There are diverse approaches to enhance the fire stability of polymers. Nowadays, strong emphasis is given on non-halogenated flame retardants and nano-scaled additives [1]. Besides these, the use of polymers with higher thermal stability and better fire behaviour, such as silicone-based polymers, has been developed as a new, future approach to flame retardants materials [2]. For this reason, more research has been addressed to improve flame retardant properties of silicone, including addition of fillers, structure modification of silicone by incorporation of flame retardant heteroatoms into siloxane backbone, or formulation issues [3]. In our previous papers, we reported the thermal behavior and the cohesion residue of silicone composites containing aluminum and calcium-based fillers [4,5].

The flame retardant mechanism in silicone composite in the presence of mineral filler(s) is believed to take place in the condensed phase because of the formation of a barrier layer by silica [6]. In presence of platinum (Pt), a possible mechanism is the formation of highly crosslinked structure of melting polymer through the radical degradation of silicone chains [7,8,9]. While burning, silicones also show a slow decomposition rate without flame dripping and minimal sensitivity to external heat flux and low or almost zero emissions of toxic smokes [10]. It is not surprising that due to their unique properties against fire, PDMS (polydimethylsiloxane) has been put in the top list of polymers for applications at high temperature such as in electrical wire and cable [11,12,13].

This part on calorimetric studies is the last of our series of investigations on the thermal and fire behaviour of silicone composites, filled with calcium and aluminum-based fillers, and which are dedicated to electrical cable applications. As a matter of fact, polymeric materials, such as organic plastics and silicones, have been extensively used as part of an insulation coating for electrical cables and wires [14,15]. While most of organic polymers are acceptable for their general insulation properties, in areas of fire, they can lead to a spread of flames, an emission of smoke and a release of combustion products that are dangerous to humans and injurious to equipment and human health. Furthermore, these insulating materials may not provide a high temperature resistance during a long period of time.

Cone calorimeter test has been widely used to characterize the fire behaviour of various materials including polymers. This test is at present the most advanced method for assessing materials' reaction to fire at a small scale. The cone calorimeter brings quantitative analysis to materials flammability research by investigating parameters such as heat release rate (HRR), time to ignition (TTI), total heat release (THR), mass loss rate (MLR), and their derivatives. The HRR measurements can be further interpreted by looking at average HRR, peak HRR and time to peak HRR. Heat Release Rate is the key measurement required to assess the fire hazard of materials and products as it quantifies fire size, rate of fire growth and consequently the release of associated smoke and toxic gases [16]. It is considered as the single most important variable in characterizing the 'flammability' of organic materials and their consequent fire hazard [17]. The reduction of flame spread is the most important flame retardancy target in developing fire scenario. Under heat flux of  $50\text{ kW/m}^2$ , the HRR for most silicones falls within the range of  $60\text{--}150\text{ kW/m}^2$  [10].

Beside cone calorimeter test, a smaller scale of fire test has also been developed these last few years. Pyrolysis Combustion Flow Calorimeter (PCFC) is known a viable method for determining combustion parameters of materials at a micro-scale and observe some phenomena that would probably not be observed on a bench scale fire test such as in the cone calorimeter test [18]. In PCFC test, the controlled pyrolysis of sample in an inert gas stream is followed by high temperature oxidation of the volatile pyrolysis products. One is thus able to study separately the pyrolysis in the condensed phase and the combustion in the gas phase [18]. As a reminder, some of the tested fillers are non-combustible gas-emitting materials: hydroxide fillers, such as aluminum hydroxide, boehmite, and calcium hydroxide, split off water, and carbonate fillers (calcite and PCC) split off carbon dioxide. These types of fillers have been known to improve the flame retardant of polymer by physical action through gas dilution or cooling due to their endothermic decomposition [19].

This work will be presented in two parts: the first part will focus on the cone calorimeter and their residues analysis, and the second part will be focused on Pyrolysis Combustion Flow Calorimeter (PCFC) test and the analysis of related volatiles products by Py-GC/MS. For both part, a rapid discussion on the factors that influence the fire reaction of silicone composites, in the conditions of the considered method, is given.

## **II. Materials and Methods**

### **II.1. Materials**

The silicone matrix was gently supplied by Bluestar Silicones (France). It contains 74.4wt% of vinyl-terminated polydimethylsiloxane (Mw of 550000g/mol), 25wt% of D<sub>4</sub>-modified silica and 0.6wt% of 2,5-dimethyl-2,5-di(tert-butyl peroxy)hexane as a crosslinking agent. PCC, wollastonite, and boehmite were kindly supplied by Solvay, Nyco minerals and Nabaltec respectively. ATH was purchased from Martinswerk, alumina from Nabaltec and mica from Kaolin International (Table S2 in supporting).

### **II.2. Sample preparation**

Composite formulations consisting of 20wt% of silica and 20wt% of filler were prepared using a HAAKE internal mixer at a temperature of 45°C, shear rate of 60 rpm and mixing time of 60 minutes. The HAAKE internal mixer has two rotors running in a contra-rotating



way to blend the filler and matrix. Thereafter, filled silicone was cross-linked under heat pressure of 90 bars at 150°C during 15 minutes to obtain a plate of elastomer with dimensions of 100mmx100mmx4mm.

### II.3. Methods

A cone calorimeter (Fire Testing Technology, UK) was used to characterize the forced flaming behavior according to ISO 5660. Plaque specimens of 100mm×100mm×4mm were burned horizontally in 21% of oxygen atmosphere using different incident heat flux of 35, 50, and 75kW/m<sup>2</sup> in the presence of an igniter' spark. The heat release rate (HRR), time to ignition (TTI) total heat release (THR), mass loss rate (MLR), and their derived values were quantified. THR value was calculated over the first 500 seconds. All measurements were repeated (between 3 and 5 specimens) and the results were averaged. Then, the surface morphology of residues from cone calorimeter tests was observed on a Hitachi S-4300 environmental scanning electron microscope (ESEM) using an acceleration voltage of 15kV. Crystallinity of finely ground residue was checked on a Bruker X-ray diffractometer (XRD) using Cu K $\alpha$  radiation.

Pyrolysis Combustion Flow Calorimeter (PCFC) apparatus from FTT-UK was used to pyrolyze 3±1 mg of sample by heating up to 780°C at a heating rate of 1°C/s under a nitrogen flow, and the gases produced during pyrolysis were sent into a combustor and burnt at a temperature of 900°C in the presence of oxygen (20%). PHRR and heat release (HR) of samples were noted and each measurement was performed at least five times (up to ten times). The results were averaged with an error of less than 5%, while the error on temperature of PHRR ( $T_{\text{PHRR}}$ ) measurement is less than 1%. The gases produced at temperature of PHRR observed during the PCFC test were characterized by Py-GC/MS. Py-GC/MS analyses were carried out on a Pyroprobe 5000 pyrolyser (CDS Analytical) interfaced to a 450-GC gas chromatograph (Varian) by means of a chamber heated at 110°C. The column is a Varian Vf-5ms capillary column (30m\*25mm) and helium (1mL/min) was used as the carrier gas. Less than one mg samples were first placed in a quartz tube between two pieces of quartz wood, and successively flash pyrolysed for 5s under helium at PHRR temperature measured using PCFC test for each composite. Then the gases were sent to the gas chromatograph for five minutes and from the GC transfer line to the ion trap analyzer of the 240-MS mass spectrometer (Varian) through the direct-coupled capillary column.

The thermal decomposition was investigated with thermogravimetry (TG) using a TGA Pyris Manager 6. All measurements were performed at least three times for  $10 \pm 0.5$  mg sample under nitrogen with a heating rate of  $10^\circ\text{C}/\text{min}$ . The standard deviation for the TG results was about  $\pm 0.5$  wt%.

### **III. Results and discussion**

#### **III.1. Cone calorimeter and their residues analyses**

The fire properties of the composites were evaluated by cone calorimetry under different heat fluxes of 35, 50, and  $75\text{kW}/\text{m}^2$ . All steps during burning process and the results obtained such as PHRR, TTI, THR and their derivatives for silicone composites will be discussed in detail. The residues obtained were also characterized in order to better understand the fire reaction of filler incorporated into flame retardant mechanism of silicone composite.

##### **III.1.1. Burning process during cone calorimeter test**

The burning process during cone calorimeter test was observed for all silicone composites under all heat fluxes. Figure 2 presents the burning step from the step at which the fire already spread over the sample surface. In all cases, similar stages were observed: before TTI, one sees the development of few opaque smokes. After TTI, fire started to develop, until it spreads over the whole surface without drips. The substrates successively generated white platelets with bumpy surfaces. All composites showed almost the same appearance: on surface, there were white solid platelets, and on the interior of residues a thick cemented layer was observed, as in Figure 1d. Unless other composites, mica and wollastonite composites always presented scratches on surface through the formation of thin layers before the platelets formation (Figure S1).



Figure 1. Silicone composites transformation during burning (after TTI) in cone calorimeter test (a) fire spread, (b): white solid platelet formation, and (c) appearance of the final residue. (d) structure at the surface and inside the residues.

During combustion in cone calorimeter test, the heat released by sample combustion at different heat fluxes was recorded. HRR curves are presented in Figure 2 and Figure 3 for calcium and aluminum-based filled composites, respectively. As seen in Figure 2, at heat flux of  $35\text{kW/m}^2$ , all composites containing calcium-based fillers presented identical burning behavior with HRR curves presenting a plateau shape. According to the model proposed by Schartel et al. for HRR curves' interpretation [20], the initial strong increase in HRR stops when an efficient char layer forms and decreases HRR. The formation of a thick outer layer as observed during and after combustion (Figure 1) is in agreement with this study. Increasing heat flux to  $50\text{kW/m}^2$  slightly modified the HRR curves of PCC composites by generating two HRR peaks. Calcium hydroxide composite completely changed its HRR curve by formation of several peaks, whereas wollastonite and calcite composites maintained their burning behavior. Finally, under higher heat flux ( $75\text{kW/m}^2$ ) calcite, wollastonite, and calcium hydroxide composites presented identical HRR curves. The HRR increased instantly after TTI, and then a small plateau was formed before reaching the HRR maximum. This small plateau was not observed in PCC composite, whereas a small peak was found before HRR maximum.

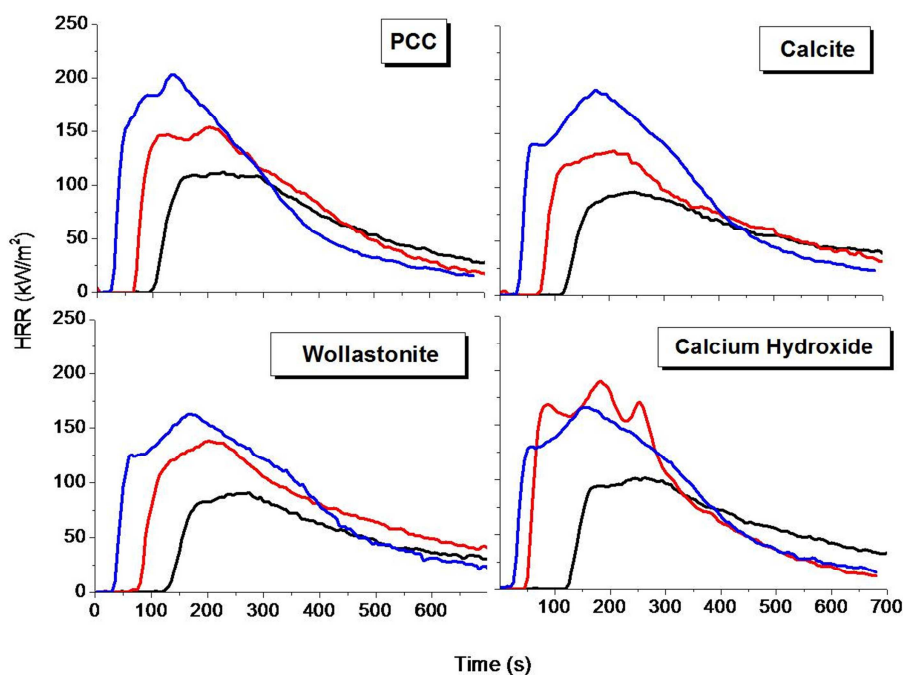


Figure 2. HRR curves of silicone composites containing calcium-based fillers measured at heat flux of 35, 50, and 75kW/m<sup>2</sup> (black, red, and blue lines, respectively).

Unlike calcium based filler composites, silicone composites containing aluminum-based fillers presented various burning behaviors (Figure 3), with the exception of mica composite. Under low heat flux, mica and boehmite presented identical shape of HRR peaks with a regular HRR diminution after their HRR maximum. ATH and alumina composites also presented similar plateau-like curves with several peaks of HRR. Increasing heat flux to 50kW/m<sup>2</sup> did not influence the burning behavior of mica and boehmite composites, but accelerated their initial ignition (TTI). The HRR curves of ATH and alumina composites also presented identical shape; even though ATH maintained its maximum HRR curve during a longer period of time than alumina composite. Finally, at 75kW/m<sup>2</sup>, mica composite showed an unclear peak of HRR and a longer combustion time. ATH, boehmite, and alumina composites burned the same way according to their HRR curves, even if alumina was consumed faster. The HRR increased instantly after TTI, and then progressed more slowly until PHRR was attained, after which, the HRR decreased rapidly. Compared to other composites, the presence of several peaks of HRR was clearly observed for ATH composite before attaining PHRR.

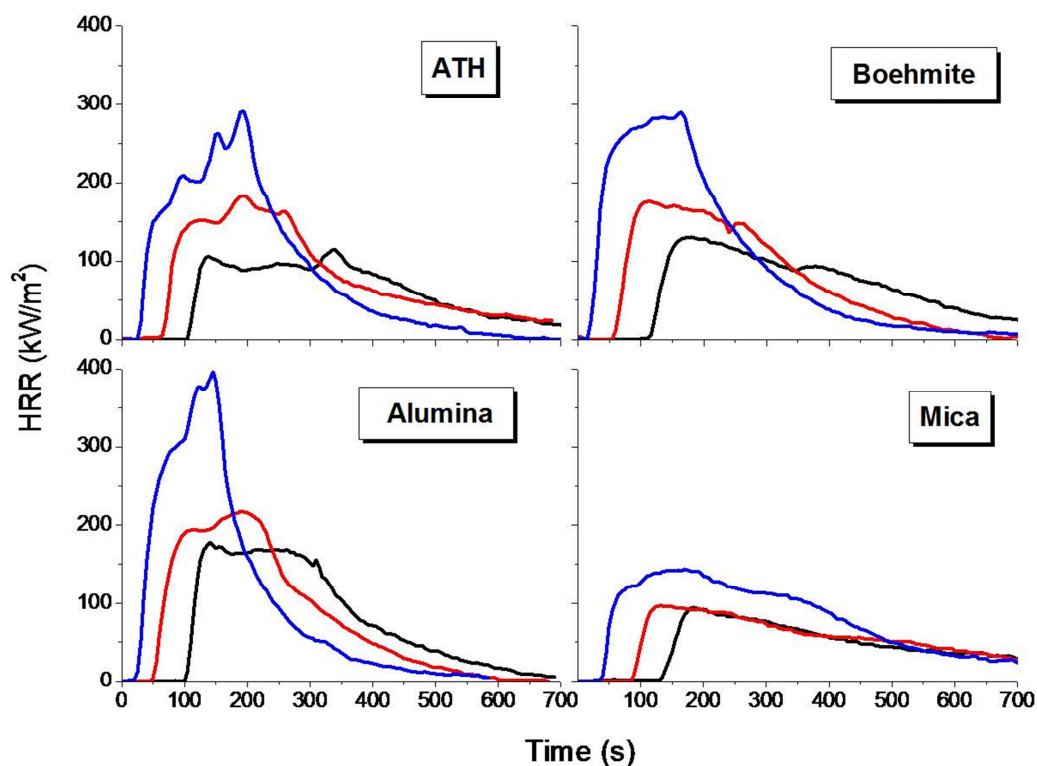


Figure 3. HRR curves of silicone composites containing aluminium-based fillers measured at heat flux of 35, 50, and 75kW/m<sup>2</sup> (black, red, and blue line respectively).

Beside HRR curves, the weight loss of silicone composites during burning in cone calorimeter was also tracked to investigate the relationship between heat release and sample degradation, given by the weight loss as a function of time (in %/s). Except for calcium hydroxide and wollastonite composites, all mass loss rates during combustion were coherent with heat release evolution, i.e. a plateau seen on HRR curve was related to a low degradation rate of composites (Figure S2). The first exception, calcium hydroxide composite weight loss, is presented Figure 4a. The mass loss rate under heat flux of 35kW/m<sup>2</sup> is lower than the one for 50kW/m<sup>2</sup>, owing to the different shapes of HRR, namely a plateau for low heat flux, and several peaks for the higher one. For wollastonite composite, the other special case, the mass loss rate slowed down after around 465 seconds of combustion and even reached a similar mass loss rate as under a heat flux of 50kW/m<sup>2</sup> (indicated by an arrow in Figure 4b). This is probably due to the formation of microbridges between silica and wollastonite particles at high temperature, observed in our previous work [5], and perhaps limiting the composite decomposition.

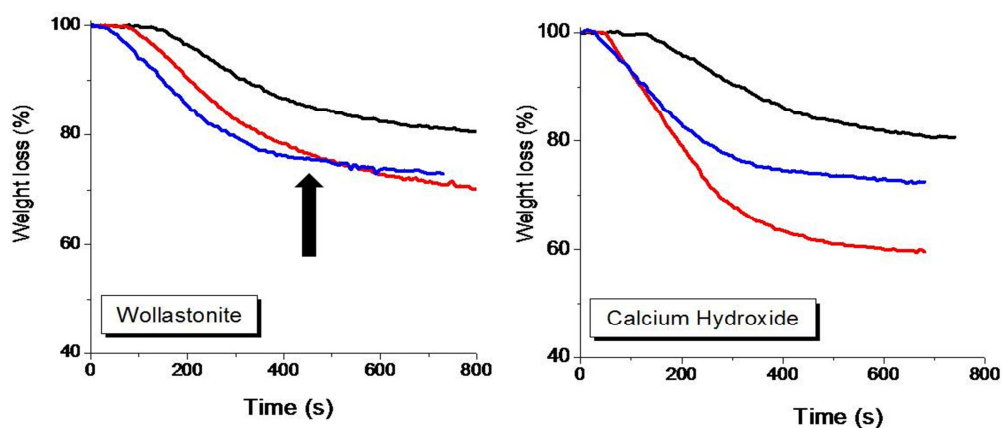


Figure 4. The weight loss of calcium hydroxide and wollastonite composites during combustion test in cone calorimeter at different heat fluxes: 35, 50, and 75kW/m<sup>2</sup> (black, red, and blue line respectively).

### III.1.2. PHRR, TTI, and THR

The fire behavior of silicone composites in terms of TTI, PHRR, and THR during cone calorimeter test was measured. Based on TTI and PHRR data, the fire performance index (FPI) was calculated by dividing TTI by PHRR. Also, the THR of composites were determined as THR after 500 seconds test since the sample combustion reached the stabilization after this time (see HRR curves in Figure 2 and Figure 3). All these data taken at different heat fluxes are reported in Figure 5.



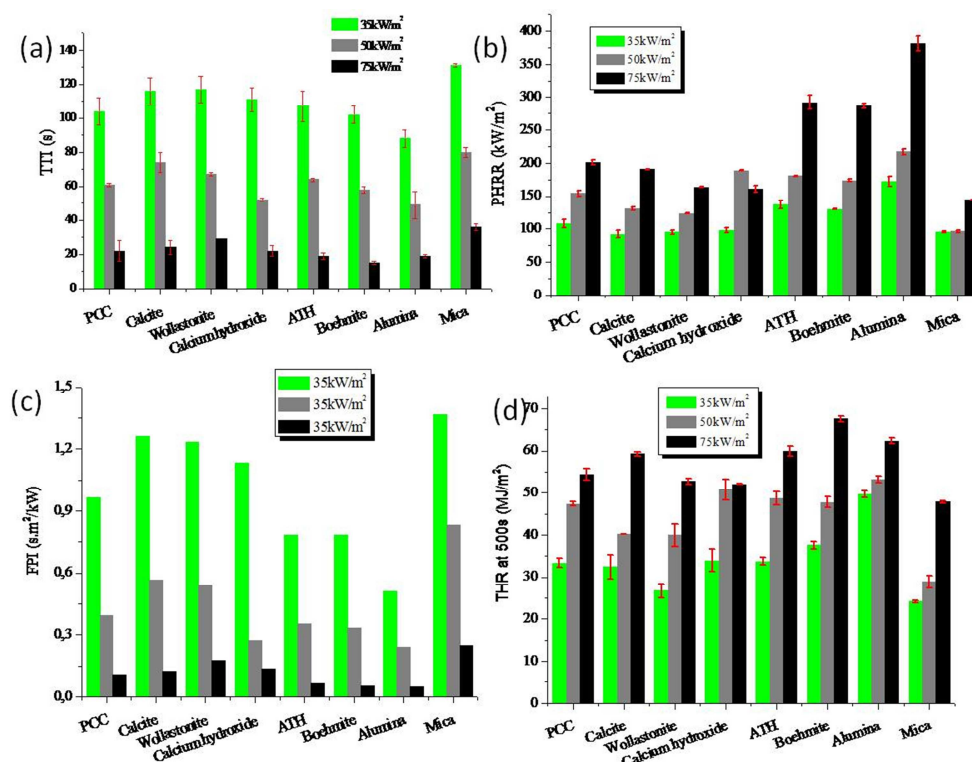


Figure 5. (a) TTI, (b) PHRR, (c) FPI, and (d) THR of silicone composites under cone calorimeter test at different heat fluxes.

First, TTI behavior showed a regular trend with heat flux (Figure 5a). For all formulations tested, mica composite always presented the highest TTI. Among calcium-based filler composites, wollastonite and calcite composites presented higher TTI than PCC and calcium hydroxide composites. ATH and boehmite, as well as calcium hydroxide were ignited earlier (low TTI) than mica, wollastonite, and calcite composites. Alumina composite presented basically the lowest TTI under low heat fluxes and one equal to boehmite at high flux.

The PHRR of composites varied sensibly as a function of heat flux. For all irradiance, mica composite always presented the lowest PHRR, while alumina composite presented the highest one. Calcite composite constantly presented lower PHRR than its nanoparticle calcium carbonate counterpart (PCC). In addition, ATH and boehmite composites systematically presented close PHRR values.

The FPI was obtained by dividing the TTI by PHRR; higher numbers of FPI indicates better flame performance [21]. According to their FPI values given in Figure 5c, under low and medium heat fluxes (35 and 50 kW/m<sup>2</sup>), mica presented the best fire behavior, followed by calcite and wollastonite composites. On the other hand, at high heat flux (75 kW/m<sup>2</sup>), calcium

hydroxide composite presented slightly better fire behavior than calcite, while mica and wollastonite composites still maintained their fire performance. Conversely, ATH, boehmite and alumina exhibited very poor fire performance whatever the heat flux.

Finally, THR obtained from cone calorimeter test after 500s burning are given in Figure 5d. As observed previously in TTI and PHRR, THR increased by increasing the heat flux, and calcium-based filler composites generally presented lower THR than aluminum based-filler composites. Mica composite presented the lowest THR among all silicone formulations and under all heat fluxes, whereas alumina composite presented the highest THR among all composites. For the other composites, at low heat flux of  $35\text{kW/m}^2$ , wollastonite presented the lowest THR after mica composite, and calcite composite THR was slightly less than for PCC composite. PCC, calcium hydroxide, and ATH composites presented almost comparably high THR. Under medium heat flux, wollastonite and calcite composites exhibited the same THR, slightly higher than mica. The THR of PCC, ATH, and boehmite composite was higher than the ones for wollastonite and calcite composites. THR of calcium hydroxide was only slightly lower than alumina composite one. Finally, at high heat flux ( $75\text{kW/m}^2$ ), wollastonite, PCC, and calcium hydroxide composites presented almost equivalent values of THR (again higher than mica). Behind them, calcite and ATH composites presented slightly lower THR than for alumina composite. Surprisingly, boehmite composite exhibited the highest THR during combustion at this testing temperature. Some parameters that may explain these results will be explained in detail in the next part of this paper.

### III.1.3. Crystallinity of residues

XRD analyses were carried out on all residues of composites containing aluminum and calcium-based fillers after cone calorimeter test. As mentioned in our previous paper [4], this co-crystallisation occurs as the result of interaction between fillers-matrix residues at high temperature. Under heat flux of 35 and  $50\text{kW/m}^2$ , there was no co-crystallisation found in residues; presumably, in these conditions, the temperature in the condensed phase was not high enough since the reaction occurs only at temperature above  $800^\circ\text{C}$ . At  $75\text{kW/m}^2$  however, calcium hydroxide composites generated wollastonite crystals ( $\text{CaSiO}_3$ ) (Figure 6a), and PCC formed a small amount of larnite ( $\text{Ca}_2\text{SiO}_4$ ) (Figure 6b). Nano-sized calcium carbonate (PCC) degraded earlier than bigger particle size of calcium carbonate (calcite), ensuring co-crystallization reaction only for PCC composite. The presence of calcite in PCC

residue could signify either an incomplete burning of composite during cone calorimeter test, or the carbonation of CaO produced from PCC decomposition during combustion.

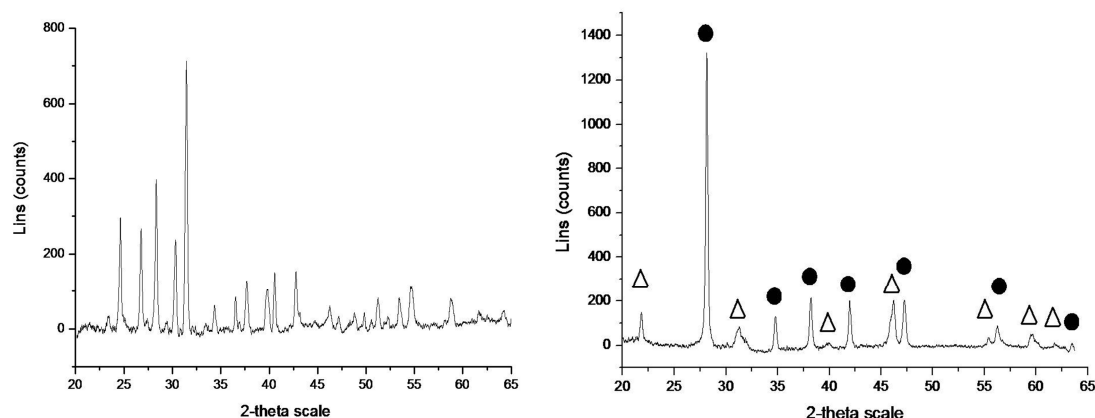


Figure 6. XRD pattern after cone calorimeter test at heat flux of 75kW/m<sup>2</sup> of the residues of (a) calcium hydroxide composite (all peaks belong to wollastonite) and (b) PCC composite (● Calcite, △ Larnite (Ca<sub>2</sub>SiO<sub>4</sub>)).

### III.1.4. Analyses of residues appearances

In Figure 7 are presented typical cohesive residues appearance for mica and wollastonite composites in one hand, and less cohesive residues of water-releasing fillers such as calcium hydroxide and ATH. For the same heat flux, the solid platelets formed after burning of ATH, alumina and boehmite composites were always smaller than the ones observed for composites containing mica and calcium-based fillers. The difference in HRR curve between calcium hydroxide composite burned under heat flux of 35kW/m<sup>2</sup> and 50kW/m<sup>2</sup> resulted in different residue appearance. The calcium hydroxide composite burned under heat flux of 50kW/m<sup>2</sup> resulted in damage surface layer, while the one burned under lower heat flux resulted in cohesive outer layer (Figure S3).

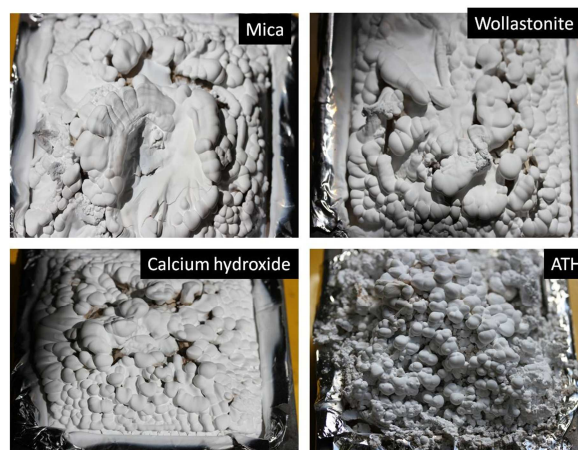


Figure 7. Different appearances of residues silicone composites after cone calorimeter test (heat flux of  $35\text{kW/m}^2$ ).

The microstructure of surface and interior of residues after cone calorimeter test at different heat fluxes was observed by SEM under magnification 5000x and 20000x. In this article, only SEM images of PCC, wollastonite, calcium hydroxide, mica and ATH composites will be presented in Figure 8 and Figure 9 for their surface and interior residues. The microstructures of other composites' residues can be found in the supporting information (Figure S4 and Figure S5).

The surface residues of all silicone composites after cone calorimeter test presented identical microstructure for all heat fluxes. The presence of some porosity was clearly observed under magnification of 20000x. This porosity is a consequence of volatile release during matrix or filler decomposition. Among all residues, only mica residue (at all heat fluxes) exhibited clearly the presence of filler particles on surface owing to the polymer ablation during combustion (Figure 8). The surface microstructures of residues after cone calorimeter test are different with ones observed after pyrolysis test under extreme conditions [5]. After pyrolysis to  $940^\circ\text{C}$  which corresponds to extreme conditions, each composite presented continuous surface layer. In addition, not only mica but also wollastonite composite's residues presented filler presence on the surface. Under cone calorimeter test, the sample does not reach high enough temperature for structure rearrangement to take place. The fact that sample burning in cone calorimeter occurs in the presence of oxygen has also probably favored silica ash formation.

The interior morphology of residues varied more significantly than those observed on their surfaces (Figure 9). The presence of big particle fillers was observed in the interior of residues, but not the nano-sized particle fillers. Therefore, under magnification of 20000x, the presence of PCC, alumina, and boehmite particles were not observed. In general, all composites presented interior microstructure's evolution with heat fluxes, except for alumina composites which systematically led to a smooth fragile residue. Boehmite and PCC composites presented smooth microstructures under low heat fluxes, but some big holes, which were ascribed to volatiles release, appeared at higher heat flux, especially for PCC. The presence of calcite, ATH and calcium hydroxide particles were observed on residues after test at heat flux of  $35\text{kW/m}^2$ , but it decreased when the heat flux increased. Calcite and calcium

hydroxide particles were no more observed only after test at heat flux of  $75\text{kW/m}^2$ , while ATH filler was hardly seen at  $50\text{kW/m}^2$ . This is probably due to filler phase conversion during their decomposition. Under heat flux of  $75\text{kW/m}^2$ , calcium hydroxide composite presented a glassy sintered residue's microstructure, which may confirm the formation of new crystal (wollastonite) observed previously with XRD analysis. At all heat fluxes, the interior residue of ATH composite presented some big porosity which increased by increasing the heat flux, whereas calcite and calcium hydroxide composites only presented low porosities. Finally, big particles of wollastonite and mica particles were always found in the interior of the residues, indicating a high thermal stability of these fillers towards temperature even under heat flux of  $75\text{kW/m}^2$  during cone calorimeter test.

The different residue's morphologies from cone calorimeter tests correlate quite well with the shape of HRR curves. For example, under heat flux of  $35\text{kW/m}^2$ , PCC composite presented HRR curve with plateau, while ATH composite presented several peaks. When the burning process was stopped at the time when the PHRR was attained, and then sample morphology was observed, different microstructures were found. SEM images of PCC composite's residue showed less porosity than for one observed in ATH composite (Figure S6), and these microstructures are identical with their microstructure at the end cone calorimeter test (Figure 8).



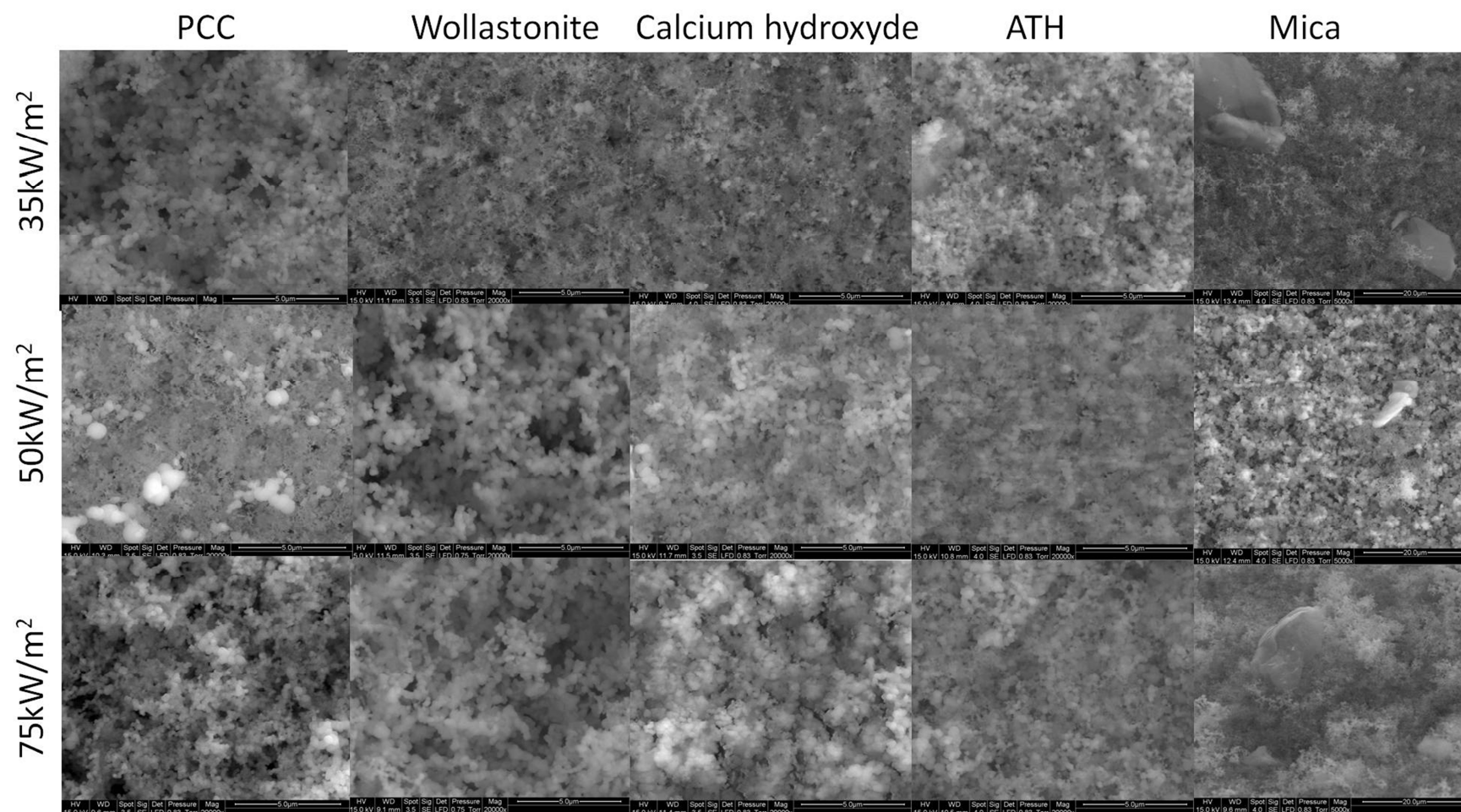


Figure 8. SEM images (20000x) on the surface of residues after cone calorimeter test (except residue of mica is under magnification of 5000x).



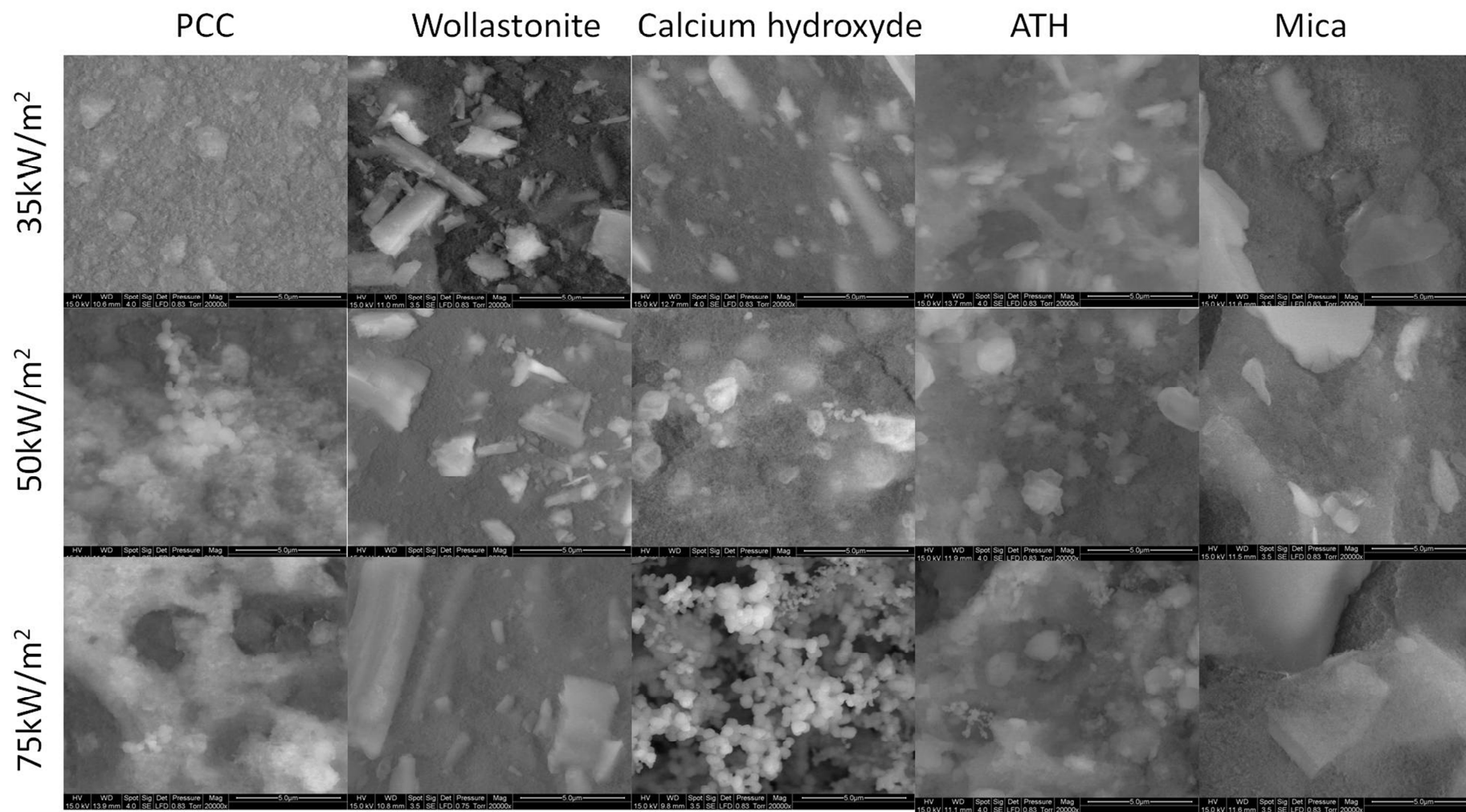


Figure 9. SEM images (20000x) on the interior of residues after cone calorimeter test.

### III.1.5 Influence of the thermal stability of silicone composite

The polymer ignition is only initialized when the combustible volatiles are produced in enough quantity to start a flame. In silicone polymer, the degradation was initiated by releasing the lower immobilized chains to form big volatiles molecules (cyclic or oligomer) [9]. Incorporation of aluminum and calcium-based filler into silicone composites modified their thermal stability, leading to different onset temperature, final residue [4], and probably the type of volatiles evolved.

In cone calorimeter test under different heat fluxes, the initial combustion of composite (TTI) shows a good correlation with their onset degradation temperature (the temperature of 2% weight loss obtained by TG analysis, Figure S8). Mica composite showed higher TTI at the onset temperature, probably because of the interference of its oxygen barrier action [22]. Therefore, mica particles were able to delay silicone degradation at the surface, where the presence of oxygen accelerates decomposition of siloxane chains [23].

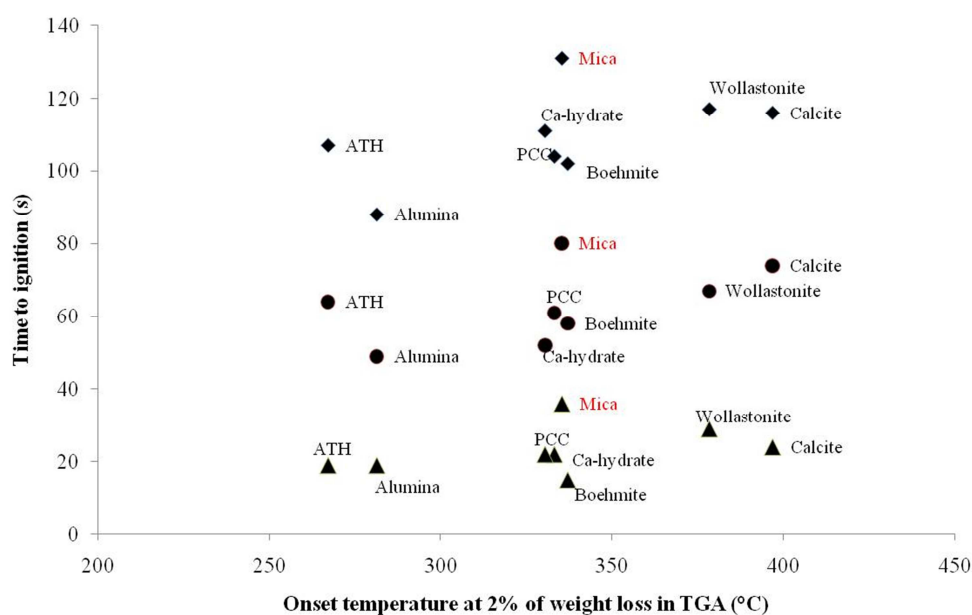


Figure 10. The relation between onset temperature and TTI of silicone composites in cone calorimeter test at different heat fluxes (diamonds, circles, and triangles are under 35, 50, and 75kW/m<sup>2</sup> respectively).

Since the TTI of silicone composites is influenced by their thermal stability, some factors that may influence silicone thermal stability should be considered. The presence of water or hydroxyl groups on filler surface triggers the silicone degradation to produce more volatile

products [4]. So, a lower TTI means a depression of thermal stability, i.e. an acceleration of silicone degradation, automatically resulting in higher production of volatiles, including combustible ones, as observed by lower THR in cone calorimeter. A good correlation between TTI and THR of composites was found (Figure 11). Under heat flux of  $75\text{kW/m}^2$ , all silicone composites ignited earlier, generating higher quantity of degraded substrates compared to lower heat fluxes (Figure S2). These correlations (Figure 10, Figure 11) demonstrate clearly the strong influence of thermal stability of silicone composite to their fire reaction in terms of TTI and THR under the cone calorimeter test.

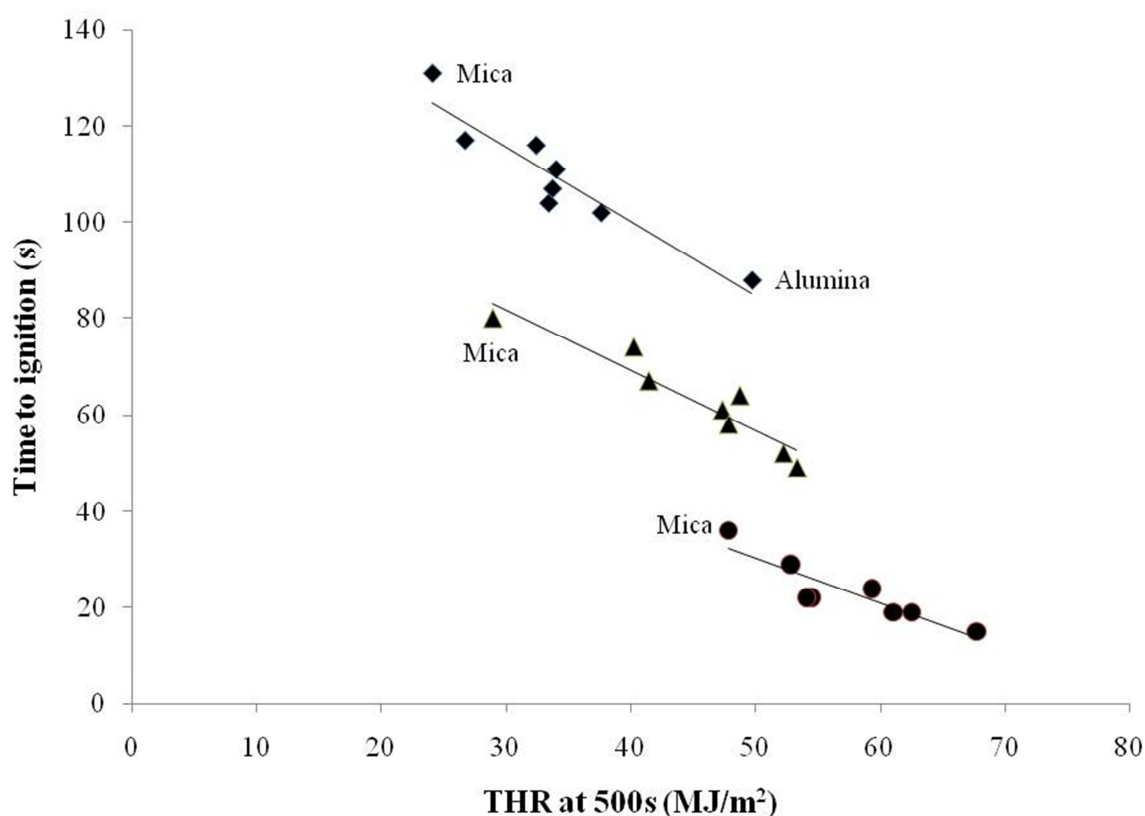


Figure 11. The relation between THR and TTI of silicone composites under different heat fluxes (circles:  $75\text{kW/m}^2$ , triangles:  $50\text{kW/m}^2$ , and diamond:  $35\text{kW/m}^2$ ).

### III.1.5. Discussion on the factors influencing the fire reaction of silicone composites in cone calorimeter test

Flame retardant mechanism of silicone has been reported in the literature to occur through the formation of a silica ash insulating layer limiting heat or mass transfer [6,10]. Silicone composite containing calcium or aluminium-based fillers also presented the formation of thick silica layer on surface, during and after burning process in cone calorimeter test. The filler-

matrix interaction at high temperature and the presence of lamellar filler in the interior of residues also have a role as barrier layer in silicone. Moreover, the good correlation between onset temperature, TTI, and THR highlighted the influence of thermal stability silicone composite toward their fire reaction. The role of these different factors is now discussed in detail.

### **Influence of surface (silica ash and barrier layer formation)**

Based on residue's appearance and SEM images of surface and interior residues, several types of residues formed during combustion of silicone composites in cone calorimeter test can be sketched (Figure 12). The difference in residue's appearance of each composite is related to their burning behavior (HRR curve). Residues showing a cohesive surface (less cracks) showed a HRR curve with a plateau, such as for mica composite, whereas in the presence of cracks and small white platelets found all over the surface, HRR curve exhibits some peaks (Figure 7, and Figure S3), for example while burning ATH composite. The volatiles release, either from filler or matrix degradation, generates cracks by breaking down the outer layer; these cracks create the pathway for further substrate degradation and facilitate the diffusion of combustible volatiles, which generate peaks in HRR curves.

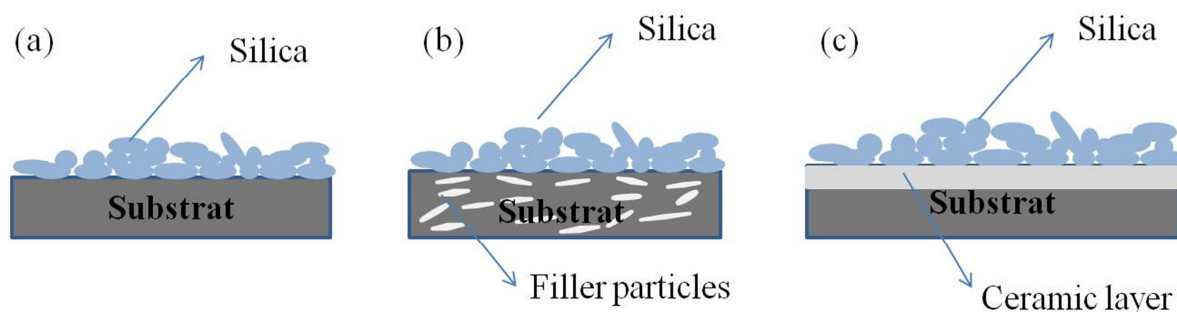


Figure 12. Sketches of different types of residues of silicone composites: thick silica layer on surface, and in interior (a) without barrier layer, (b), the presence of particle of filler, and. (c) with ceramified residue.

Besides, the insulating efficiency on surface is different for each composite, depending on the filler incorporated. An adequate surface insulating layer will slow down the mass and heat transfer and delay fuel transfer to fire. Even if there are some cracks on surface, the presence of filler left in the composite (Figure 12.b) or the formation of ceramified residue (Figure 12.c) would form an efficient barrier layer in the interior of residue. This barrier layer would

be able to feed back the energy from flame spread, thus limiting the surface area exposed to incident heat flux and lowering substrate degradation. The presence of filler was observed in the interior residue of mica and wollastonite composites at all heat fluxes, due to high thermal resistance of filler. So far, mica and wollastonite composites which exhibit this type of residue presented the best fire reaction under cone calorimeter test.

The barrier layer through ceramization in the interior of residue is due to the co-crystallization between filler and matrix at the tested temperature. The better fire resistance of calcium hydroxide under heat flux of  $75\text{kW/m}^2$  is ascribed to filler matrix interaction (co-crystallisation) that lowers the PHRR. The co-crystallization occurring in PCC composite failed to reduce its PHRR (still higher than calcite), but it decreased the THR. The crystal formation in silicone flame retardant system containing chalk (natural calcium carbonate) has also been reported to improve its flame retardancy through the formation of a protective layer [24,25,26,27].

### **Thermal stability effect**

High thermal stability composite requires higher temperature (higher TTI) to produce volatiles, and lower quantity of substrate (silicone) will be degraded, thus lowering THR. Since the composite is degraded slowly, the diffusion of combustible volatile towards the gaseous phase is limited (HRR). The better fire reaction of wollastonite composite compared to calcite one, and calcite compared to PCC composites, under cone calorimeter test, is believed to arise from a better thermal stability. Mica composite always presented the best fire reaction under cone calorimeter test at all heat fluxes by showing the highest TTI, the lowest PHRR and THR [4]. This efficient fire behavior is attributed to the formation of a barrier layer. Residue microstructure of mica showed the presence of filler particles not only in the interior but also on the surface. Besides, the thermal stability also takes place in mica fire reactions, as for other fillers, but chain immobilization by surface hydroxyls of mica favors the generation of small cyclics that are less combustible, delaying it TTI. Finally, the lamellar shape (high aspect ratio) of mica particle can act as oxygen barrier, where it is known that oxygen favors silicone degradation.

## **Water release and endothermic effect**

On the opposite, the presence of water promotes silicone degradation, and accelerates volatiles productions, including combustible volatiles feeding the flame initiation. As a result, composites containing a water-releasing filler generally presented lower TTI than other composites that are thermally stable. The high PHRR presented by calcium hydroxide, ATH, and boehmite composites, distinctly observed from heat flux of  $50\text{kW/m}^2$ , confirmed this point. The very high catalytic effect of hydroxyl groups on surface of alumina particles (exhibiting a very high surface area) toward silicone thermal stability resulted in catastrophic fire reaction of silicone composite, even under low heat flux.

The water release from filler decomposition is also producing an endothermic effect during conventional organic polymer combustion process. Here however, silicone degradation by water competes with this endothermic effect, which is not significant enough to lower the HRR. For example, at heat flux of  $35\text{kW/m}^2$ , calcium hydroxide, which releases 24% of water, and calcium carbonate fillers, which release 45wt% of  $\text{CO}_2$  [4], presented identical PHRR than those of the other composites. These results signify the absence of gas dilution or endothermic effect from the gases released by fillers. This hypothesis was confirmed by the high PHRR of ATH and boehmite composites, even though they released high quantity of water during their degradation (35wt% and 18wt% respectively [4]).

## **III.2. PCFC and analysis of volatiles pyrolysis products**

The PCFC test was performed in order to evaluate the fire retardant mechanism of silicone composite. Using this technique, the barrier effect is thus neglected, while in the cone calorimeter test, all phenomena occur in the same time. Here, the heat release evolution during sample pyrolysis in PCFC test is presented simultaneously with the mass loss rate during pyrolysis in TG analysis. TG analysis was carried out under  $\text{N}_2$  at heating rates of  $10^\circ\text{C/min}$ , and the details of the results have been reported in our previous work [4]. Py-GC/MS was carried out on temperature of the maximum HRR attained under PCFC test to identify the volatiles released liable to PHRR. All results obtained from PCFC test and analysis of their related volatiles pyrolysis products in Py-GC/MS and TG analysis are summarized in Table 1. Figure S7 presented the TG analysis of silicone composites under  $\text{N}_2$  at heating rate of  $10^\circ\text{C/min}$  to  $800^\circ\text{C}$ .



### III.2.1. PCFC test result

In exception for certain temperature in ATH and PCC composites, the HRR curves observed in PCFC test generally more or less correlated with the derivative weight curves of composites from TG analysis at heating rate of 10°C/min, as demonstrated in Figure 13 and Figure 14. It may signify that the weight loss observed from the pyrolysis in the TGA temperatures range could be related to the release of combustible gas in PCFC test. The temperature at the maximum HRR was shifted to higher temperatures than the peak degradation in TGA, presumably because of higher heating rate in PCFC test.

The HRR curves from PCFC and weight loss from TG analysis for silicone composites containing calcium-based filler is presented in Figure 13. In PCC and calcite composites, the second peak of derivative weight was due to the filler decomposition ( $\text{CaCO}_3$ ) to release  $\text{CO}_2$ , resulting in a slight increase (almost negligible) of HRR. Probably during  $\text{CO}_2$  release, it provoked the coproduction of combustible volatile. In wollastonite composite, all weight loss during pyrolysis in TG is related to the production of combustible volatiles. Thus, in the case where the composite weight loss does not increase the HRR, it can be considered as the production of non combustible volatiles or endothermic gases such as water and  $\text{CO}_2$ .

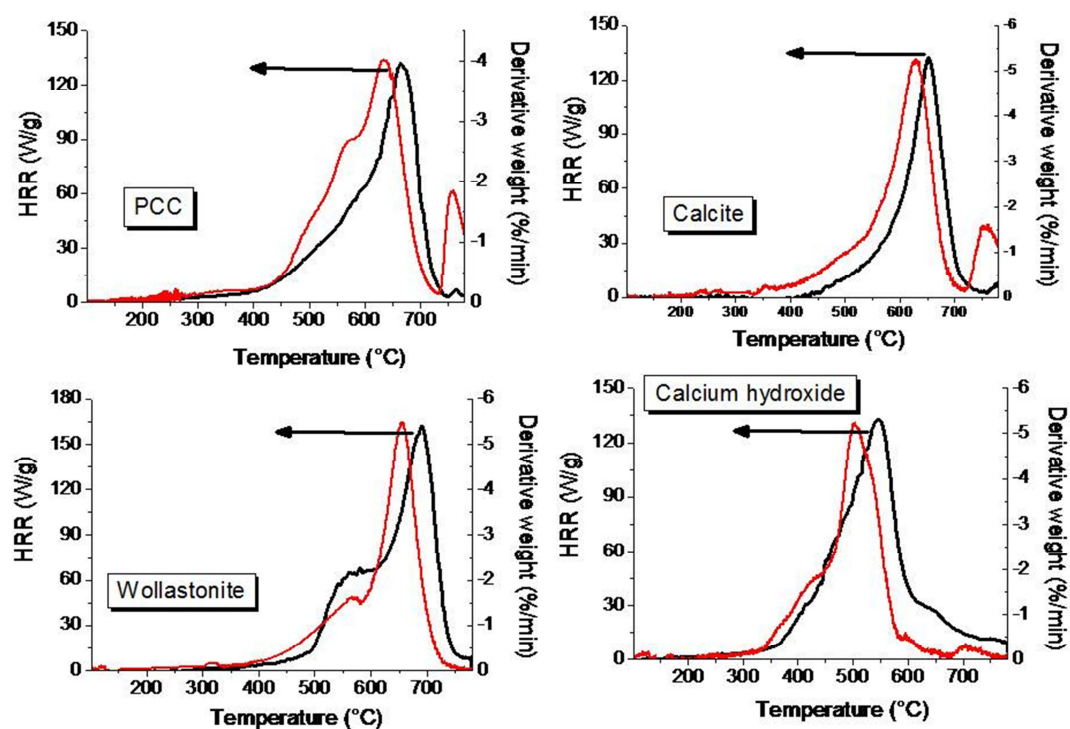


Figure 13. HRR curves of silicone composites containing calcium based filler (black line) and its relation to their derive curves of TG degradation at heating rate of 10°C/min (red line)

In ATH composite (Figure 14), the absence of HRR peaks during composite degradation at ranges temperatures of 220°C to 350°C proved clearly that the water production did not increase the HRR. The second peak HRR observed in boehmite composite is related to the ‘pseudo’ second peak on it derivative weight. Nonetheless, this weight loss is related to volatilization of combustible materials that quite strongly increased the HRR. In mica, weight loss observed in TGA derivative weight from temperature before 420°C did not increase the HRR, because this range temperature is related to mica dehydroxylation. The same case was observed for alumina composite, since the pyrolysis products at lower temperatures did not influence the HRR.

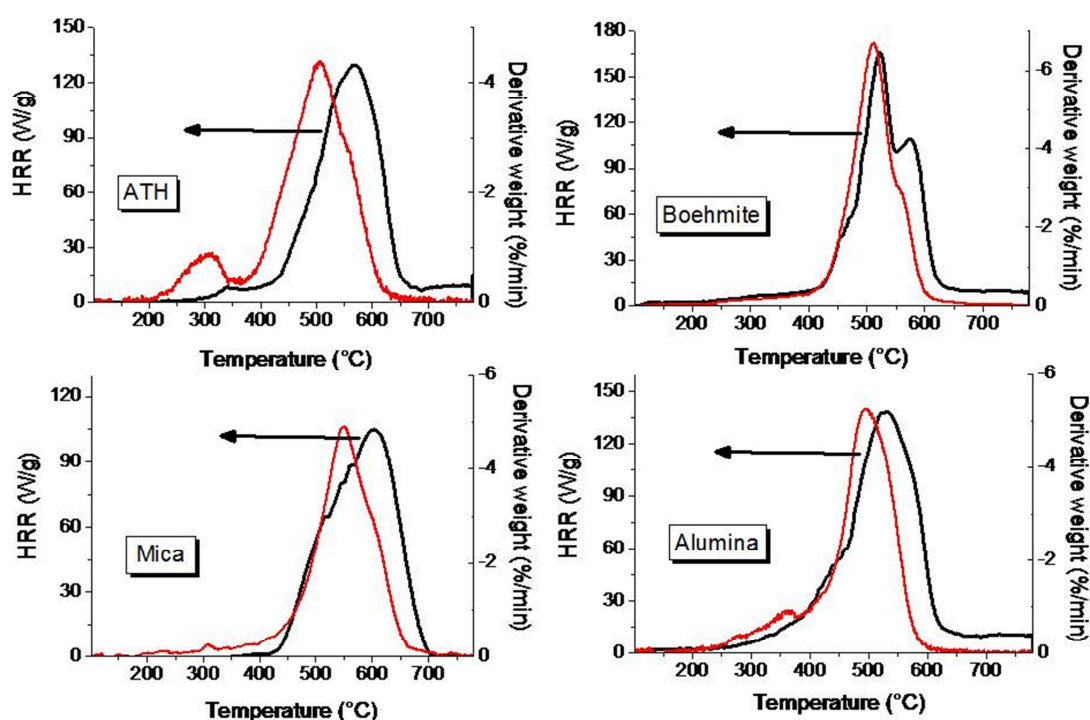


Figure 14. HRR curve of silicone composites containing aluminum based filler (black line) and its relation to their derive curves of TG degradation at heating rate of 10°C/min (red line)

All silicone composites presented more or less the same HR under PCFC test. Aside calcium hydroxide composite which presented slightly lower HR, boehmite and alumina composites presented conversely slightly higher HR than other formulations. Among all calcium-based filler composites, the lowest PHRR was obtained by the calcium hydroxide composite, and the highest one from combustion of wollastonite composite. Almost identical PHRR was

observed for calcium carbonate fillers (PCC and calcite), even though PCC attained its PHRR at slightly higher temperature than calcite (only 10°C difference). In other words, PCC and calcite presented the same fire behavior under PCFC test. In aluminum-based filler composites group, mica composite presented the lowest PHRR which occurred at the highest temperature. ATH composite presented only slightly higher PHRR than mica. The PHRR of boehmite and alumina composites occurred almost at the same temperature, but alumina presented lower PHRR than boehmite.

### III.2.2. Characterization of the volatiles from composites pyrolysis

In TG analysis, the weight loss observed was related to total volatile products including water and CO<sub>2</sub> from filler decomposition, and other cyclic or linear siloxanes from matrix degradation. According to the composite weight loss during TG analysis (Table 1), the most abundant products in silicone composite degradation comes from silicone (PDMS) degradation. Therefore, the silicone composite was subjected to successive flash pyrolysis under helium at given temperature for 5s. The volatile released from sample degradation and of molar mass larger than 60 g/mol were characterized and are presented in Figure 15.

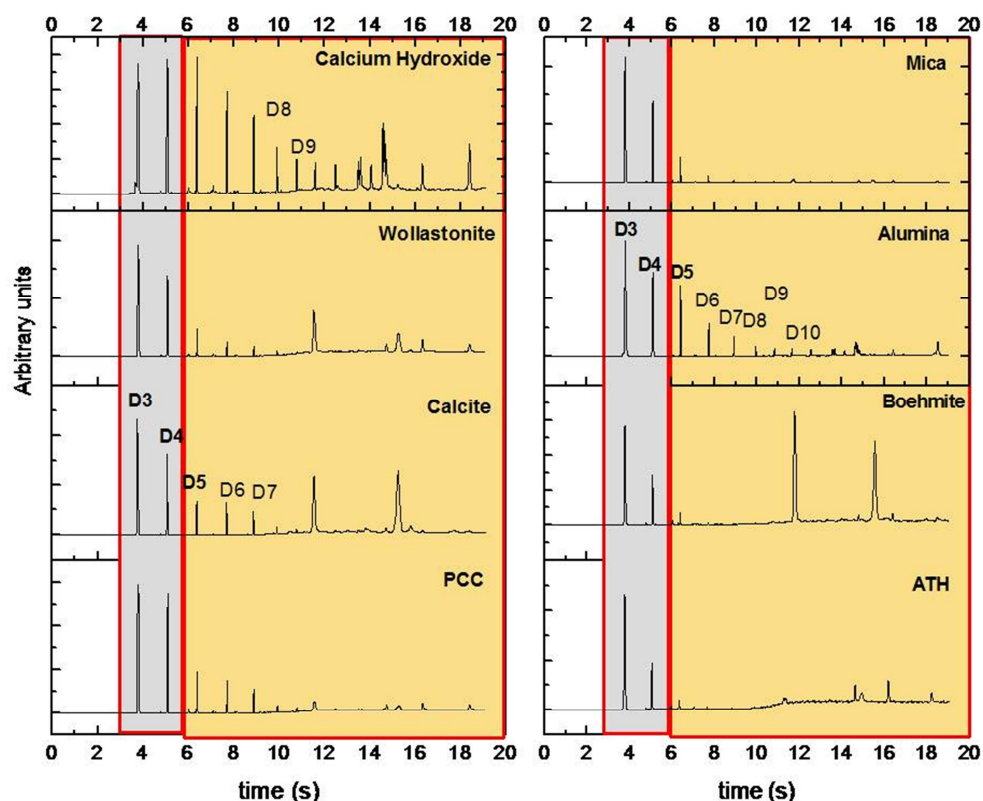


Figure 15. GC-MS chromatograms of calcium and aluminum-based composites at the temperature of peak HRR during PCFC test. Grey zone entails the smaller cyclosiloxanes (D<sub>3</sub> and D<sub>4</sub>), while the yellow zone is the domain of bigger molecules elution (from D<sub>5</sub> and including silicone oligomers).

D<sub>3</sub> and D<sub>4</sub> volatiles were always present as pyrolysis products of silicone composites containing calcium and aluminum-based fillers (Figure 15). The decomposition products of vinyl-terminated PDMS at elevated temperatures are principally cyclic oligomers hexamethyltrisiloxane (trimer; D<sub>3</sub>) and octamethyltetrasiloxane (tetramer; D<sub>4</sub>), with small amounts of methane and traces of linear oligomers [28,29]. Moreover, under flash pyrolysis, silicone degradation produces cyclic oligomers, with tetramer being the most abundant one, accompanied by other volatiles such as linear pentasiloxane or rearranged oligomeric siloxane compounds (e.g. tetrasiloxane, 3,5-diethoxy-1,1,1,7,7,7-hexamethyl-3,5-bis(trimethylsiloxy) [30]. Based on GC/MS chromatograms in Figure 15, the total composition of D<sub>3</sub> and D<sub>4</sub> produced during PHRR temperature is presented in Table 1.

Table 1. HR from PCFC test, Py-GC/MS, and TG analysis from different formulations of silicone composites.

<i>Filler</i>	<i>HR (kJ/g) in PCFC</i>	<i>Total D<sub>3</sub>, and D<sub>4</sub> formed at TPHRR by Py-GC/MS (%)</i>	<i>Weight loss (wt%) at 780°C by TG analysis [4]</i>		
			<i>Composite</i>	<i>Filler<sup>a</sup></i>	<i>Matrix<sup>b</sup></i>
PCC	14.6	82	67.4	5.0	62.4
Calcite	15.5	32	65.1	2.9	62.2
Wollastonite	15.8	34	58.8	0.3	58.5
Calcium hydroxide	13.6	53	60.9	5.9	55.0
ATH	14.7	74	65.0	7.0	58.0
Boehmite	17.8	46	61.1	3.5	57.6
Alumina	16.7	64	62.7	1.1	61.6
Mica	14.2	93	60.1	1.1	59.0

<sup>a</sup>, calculated as 20wt% of Ca or Al based filler loading by = 0.2\*filler weight loss in TG analysis at 780°C [4], <sup>b</sup>: Weight loss of matrix = weight loss of composites – weight loss of filler,

### III.2.3. Factors influencing the PHRR (W/g)

A good correlation between production of D<sub>3</sub> and D<sub>4</sub> with PHRR was observed (Figure 16). Composite which produced more D<sub>3</sub> and D<sub>4</sub> at temperature of HRR maximum presented

lower PHRR. Higher production of D<sub>3</sub> and D<sub>4</sub> automatically indicates the lower production of bigger volatiles molecules. It seems that high production of these large molecules (bigger than D<sub>4</sub>) is correlated with a high peak HRR, probably by feeding the combustion in the gas phase. It signifies that these large molecules are highly combustible.

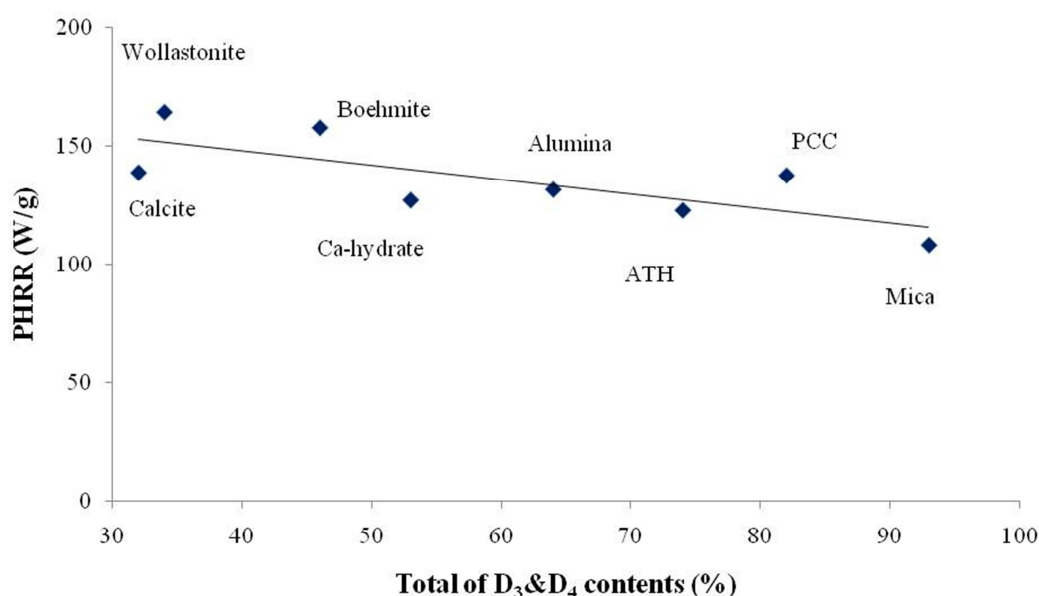


Figure 16. PHRR (W/g) versus contents of volatiles pyrolysis products from silicone composite PCFC test.

However, this correlation is not perfect, because it did not take into account the endothermic effect by filler decomposition which slowdowns the pyrolysis. Thus, the heat enthalpy decomposition of fillers decomposition were calculated using the enthalpy data (Table S1) for each component [31] by equation:  $\Delta H = H_{\text{product}} - H_{\text{reactant}}$ , where  $H$  is enthalpy. The enthalpies of endothermic gas emitting fillers are presented in Table 2.

<i>Filler</i>	<i><math>\Delta H_f</math> of filler decomposition (kcal/mole)</i>
CaCO <sub>3</sub>	42.9
Ca(OH) <sub>2</sub>	25.9
ATH	661.6
Boehmite	496.2

Table 2. Theoretical enthalpy of filler decomposition,

Water released from ATH and boehmite decomposition absorbed more heat than water or CO<sub>2</sub> released from calcium hydroxide and calcium carbonate fillers. Consequently, the decomposition of ATH and boehmite is supposed to have more endothermic effect than calcium hydroxide, or calcium carbonate. The relationship between the endothermic effect and the PHRR of silicone composites is shown in Figure 17. It can be seen that, the water released from filler decomposition has higher endothermic effect toward silicone compared to CO<sub>2</sub> release because of higher filler decomposition enthalpy. Higher quantity of water release led to lower PHRR of composite. Higher water content from ATH and calcium hydroxide decomposition resulted in their lower HRR than boehmite. Meanwhile, there is no influence of CO<sub>2</sub> quantity released from calcium carbonate to the PHRR of silicone composites. Such correlation confirms the important role of composite's thermal stability, rather than endothermic effect by filler, in the fire reaction of silicone composite containing calcium carbonates filler and water releasing filler.

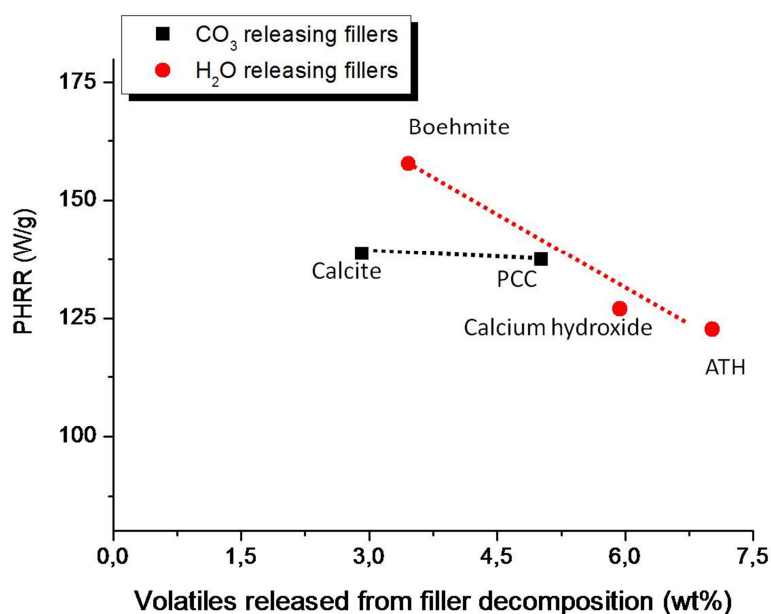


Figure 17. Contents of CO<sub>2</sub> and water release relationship to PHRR of silicone composite (dot lines are only guides for the eyes).

#### III.2.4. Factors influencing the fire reaction of silicone composites under PCFC test

Based on above correlations, the production of small cyclic (as the consequence of thermal stability) and the endothermic effect are considered as the main parameters that influence the fire behavior of silicone composite in PCFC test. The immobilization of siloxane chain has



been known to increase the thermal stability of silicone by generating, exclusively, less combustible small cyclics.

Due to their identical endothermic effect by CO<sub>2</sub> release, and their “inert” behavior toward silicone degradation [4], PCC and calcite presented almost identical fire reactions as observed by PCFC. Consequently, higher quantity of CO<sub>2</sub> released from PCC than calcite pyrolysis in PCFC test has no influence to their PHRR and HR. In addition, there is no influence of their filler particle size (nano-particle and micro-size) to their fire reaction in PCFC test.

In the absence of endothermic effect, mica composite still presented the lowest PHRR in PCFC test. This fact may be attributed to the chain immobilization generated by hydroxyl on mica surface. Highly immobilized siloxane chains limit large cyclics production. As seen in Table 1, mica produced high quantity of D<sub>3</sub> and D<sub>4</sub>. Unfortunately its PHRR was attained at lower temperature than inert fillers composites (calcium carbonate and wollastonite), surely because of the catalytic effect of surface hydroxyls towards silicone degradation.

In case of alumina, the catalytic effect due to hydroxyl groups on the high surface area of these nanoparticles particularly deteriorated the thermal stability of its composite. Thus, the maximum HRR was attained at lower temperature, and a large quantity of matrix was degraded, which resulted in high HR. In return, the combustion of alumina composite produced higher small molecules due to chain immobilization by filler. Consequently, alumina composite presented lower PHRR compared to boehmite or wollastonite composite. Nevertheless, the chain immobilization due to hydroxyl surface on alumina did not give as big an influence as in mica composite because of higher surface activity (surface area) of alumina.

The absence of chain immobilization and endothermic effect in wollastonite composite resulted in its worst fire behavior under PCFC test. As a matter of fact, wollastonite composite liberated some large oligomers (Figure 15), not immobilized on the filler (wollastonite does not have hydroxyl groups on surface). This fact leads to not only higher composite's HR but also to higher PHRR.

For water-releasing fillers, it seems that there is a competition between the endothermic effect to lower PHRR in one side, and the degradation of silicone backbone due to catalytic effect to increase PHRR on the other side. In calcium hydroxide composite, water released occurs at the same temperature with silicone decomposition, and in large quantity (5.9%, see Table 1).

So even though it produced more big volatiles molecules (Figure 15), it still presented the lowest PHRR and even also the lowest HR. Better flame retardancy of calcium hydroxide is purely attributed to the endothermic effect by water release from filler decomposition. Water release was able to cool down the condensed phase and the volatiles produced, thus limit the HRR. Higher endothermic effect provoked by ATH resulted in lower PHRR than for calcium hydroxide, but a slightly higher HR, probably because of higher catalytic effect by water release in ATH to silicone degradation that evoked more volatiles release from matrix (58% against 55%, see Table 1).

Boehmite composite presented high PHRR which occurred at lower temperature and the highest HR. The presence of water accelerated silicone degradation to produce more volatiles in one hand, and on the other hand, the small quantity of water lead to lower endothermic effect than ones from ATH or calcium hydroxide.

#### **IV. Conclusions**

The fire reaction of silicone composites containing calcium and aluminum based fillers has been investigated using cone calorimeter and PCFC tests. The residues after cone calorimeter test and the gas production at the maximum HRR in PCFC test were also characterized in order to better understand the mechanism of their fire reaction. The combination of both calorimeter methods (cone calorimeter and PCFC) appeared to be a good strategy to understand the flame retardant mechanism of silicone composite.

In cone calorimeter test, the fire behavior of silicone composites in terms of TTI, PHRR, and THR varied in the presence of calcium and aluminum-based fillers. In all formulations tested, increasing the heat flux resulted in a decrease in TTI and an increase in PHRR and THR. The fire reaction in silicone composites is owing to composite thermal stability and/or the formation of a barrier layer. In exception of mica composite, silicone composites containing calcium-based fillers presented better fire behavior than the ones containing aluminum-based filler. Mica and wollastonite composites exhibited better fire behavior than other silicone composites that release endothermic gas such as CO<sub>2</sub> or H<sub>2</sub>O. According to this result, the endothermic effect is not an efficient flame retardancy mechanism for these systems. The fire reaction of PCC, calcite, calcium hydroxide, ATH, boehmite, and alumina composites were attributed to their thermal stability, while mica and wollastonite composites showed both a

thermal stability and a barrier effect. The fire reaction of mica composite is governed by barrier effect, but in wollastonite composite, thermal stability is more significant.

In PCFC, the influence of endothermic effect is almost negligible, and thermal stability is suggested to be the main factor determining the efficient fire reaction of silicone composites. Chain immobilization limits the production of big volatile molecules that are combustible, thus increasing the thermal stability of the silicone matrix. Mica, calcium hydroxide, and ATH composites presented better fire behavior (low peak of HRR). In mica composite, the presence of hydroxyl groups on surface that immobilize the siloxane chain in one hand, also promotes silicone degradation on the other hand. Therefore, mica composite presented lower PHRR but at lower temperature. The absence of chain immobilization by wollastonite led to very bad fire reaction of wollastonite composite in PCFC test.

The cone calorimeter and PCFC tests on silicone composites containing calcium and aluminum-based fillers highlighted the significance of thermal stability on their fire reaction. Moreover, the presence of fillers having good thermal resistance, or which are able to form new crystal with matrix at high temperature (co-crystallisation), influence the fire reaction of silicone composite by barrier effect. For calcium hydroxide composite, the co-crystallization takes place at high heat flux and modifies its fire reaction from thermal stability to barrier layer formation. The particularity of ceramic promoter filler is its potential to generate an effective barrier layer, hopefully improving its fire behavior under strong heat flux. Based on this result, calcite would probably exhibit better fire resistance under cone calorimeter test at higher heat flux than  $75\text{kW/m}^2$ .

## V. REFERENCES

- 1 Nelson G.L., Morgan A.B, Wilkie C.A., In: Wilkie C.A., Morgan A.B, Nelson G.L., editors. Fire retardancy in 2009: Fire and Polymers V. Materials and concepts for fire retardancy. Washington: American Chemical Society; 2009, p: 1–7.
- 2 Dvornic, P.R. In: Jones R.G., Ando W., Chojnowski J., editors. Thermal Stability of Polysiloxanes, *in* Silicone–Containing Polymers. Dordrecht, the Netherlands: Kluwer Academic Publisher; 2000, p: 185-212.
- 3 Hamdani S., Longuet C., Perrin D., Lopez-Cuesta J-M., Ganachaud F., Flame retardancy of silicone-based materials, *Polym. Degrad. Stab.*, 2009; 94: 465–495.
- 4 Hamdani S., Longuet C., Lopez-Cuesta J-M., Ganachaud F., Calcium and aluminum-based fillers as flame-retardant additives in silicone matrices. I. Blends preparation and thermal properties, *Polym. Degrad. Stab.*, 2010; 99: 1911-1919.
- 5 Hamdani-Devarennnes S., Longuet C., Lopez-Cuesta J-M., Ganachaud F., Calcium and aluminum-based fillers as flame-retardant additives in silicone matrices II. Analysis of composites residues from normed pyrolysis test. *Submitted to Polym. Degrad. Stab.*
- 6 Hshieh F-Y. Shielding effects of silica-ash layer on the combustion of silicones and their possible applications on the fire retardancy of organic polymers. *Fire Mater.*, 1998; 22: 69-76.
- 7 MacLaury, M. R., The Influence of Platinum, Fillers and Cure on 50 the Flammability of Peroxide Cured Silicone Rubber, *J. Fire Flam.*, 1979; 10: 175-198.
- 8 Hayashida K., Tsuge S., Ohtani H., Flame retardant mechanism of polydimethylsiloxane material containing platinum compound studied by analytical pyrolysis techniques and alkaline hydrolysis gas chromatography. *Polymer*, 2003; 44: 5611–5616.
- 9 Delebecq E., Hamdani S., Raeke J., Lopez-Cuesta J-M., Ganachaud F., High Residue Contents Indebted by Platinum and Silica Synergistic Action during the Pyrolysis of Silicone Formulation, *Submitted to ACS Appl. Mater. Interfaces*.
- 10 Buch, R.R., Rates of heat release and related fire parameters for silicones, *Fire Saf. J.*, 1991; 17: 1-12.
- 11 George C, Pouchelon A, Thiria R. Hot-vulcanizable Polyorganosiloxane Compositions Useful Particularly For Manufacturing Electrical Cables or Wires, European Patent EP2007,/003,248; 2007.
- 12 Shephard KL., Flame resistant silicone rubber wire and cable coating composition, US Patent 6,239,378; 2001.
- 13 Ota K., K. Hirai, Dow Crowning Toray Silicone Co., Flame-Retardant Silicon Rubber composition for coating electrical wire and cable, US Patent 006,011,105; 2000.
- 14 Beauchamp M., Flame resistant electric cable. US Patent 5,705, 774; 1998.
- 15 Kunieda S., Ishino S. Nakai T., Hirai K., Matsushita T., Takeshita K., Process for insulating high voltage electrical conducting media US Patent 5,369,161; 1994.

- 16 Morgan A.B., Bundy M., Cone calorimeter analysis of UL-94 V-rated plastics. *Fire Mater.*, 2007; 31: 257–283.
- 17 Babrauskas V., Peacock R.D., Heat release rate: The single most important variable in fire hazard, *Fire Saf. J.*, 1992; 18(3): 255-272.
- 18 Lyon R.E., Walters R.N., Pyrolysis combustion flow calorimetry, *J. Anal. Appl. Pyrolysis*, 2004; 71: 27–46.
- 19 Trotsch H.J. In: Gachter R, Muller H, editors. *Flame Retardants: Plastics Additives*. Cincinnati: Hanser Publisher; 1993, p: 709-748.
- 20 Schartel B., Hull TR., Development of fire-retarded materials – interpretation of cone calorimeter data, *Fire Mater.*, 2007; 31: 327–354.
- 21 Cogen J.M., Lin T.S., Lyon R.E., Correlations between pyrolysis combustion flow calorimetry and conventional flammability tests with halogen-free flame retardant polyolefin compounds, *Fire Mater.*, 2009; 33:33–50.
- 22 Porter J.P., Ray W.D., High density polyethylene article with oxygen barrier properties, US Patent 5,153,039; 1992.
23. Camino G., Lomakin S., Lazzari M., Polydimethylsiloxane thermal degradation Part 1. Kinetic aspects, *Polymer*, 2001; 42(6): 2395-2402.
- 24 Hermansson A., Hjertberg T., Sultan B.A., The flame retardant mechanism of polyolefins modified with chalk and silicone elastomer, *Fire Mater.*, 200; 27: 51–70.
- 25 Krämer R.H., Blomqvist P., Hees P.V., Gedde UW. On the intumescence of ethylene-acrylate copolymers blended with chalk and silicone. *Polym. Degrad. Stab.*, 2007; 92: 1899-1910.
- 26 Hermansson A., Hjertberg T., Sultan B.A., Linking the flame-retardant mechanisms of an ethylene-acrylate copolymer, chalk and silicone elastomer system with its intumescent behaviour, *Fire Mater.*, 2005; 29: 407–423.
- 27 Hermansson A., Hjertberg T., Sultan B.A., Distribution of Calcium Carbonate and Silicone Elastomer in a Flame Retardant System Based on Ethylene–Acrylate Copolymer, Chalk and Silicone Elastomer and Its Effect on Flame Retardant Properties, *J. Appl. Polym. Sci.*, 2006; 100: 2085–2095.
- 28 Radhakrishnan T.S., New Method for Evaluation of Kinetic Parameters and Mechanism of Degradation from Pyrolysis–GC Studies: Thermal Degradation of Polydimethylsiloxanes, *J. Appl. Polym. Sci.*, 1999; 73: 441–450.
- 29 Deshpande G., Rezac M.E., The effect of phenyl content on the degradation of poly(dimethyl diphenyl) siloxane copolymers, *Polym. Degrad. Stab.*, 2001; 74: 363–370.
- 30 Camino G., Lomakin S., Lagueard M., Thermal polydimethylsiloxane degradation. Part 2. The degradation mechanisms, *Polymer*, 2002; 43(7): 2011-2015.
- 31 Patnaik P., editor. *Handbook of Inorganic Chemicals*. McGraw Hill New York; 2002.

Supporting information for

**“Calcium and aluminum-based fillers as flame-retardant additives in silicone matrices. III. Calorimetry / Flammability studies”**

By S. Hamdani-Devarennnes, C. Longuet, R.Sonnier, F. Ganachaud, J.M. Lopez-Cuesta\*

Submitted to « Polymer Degradation and Stability »

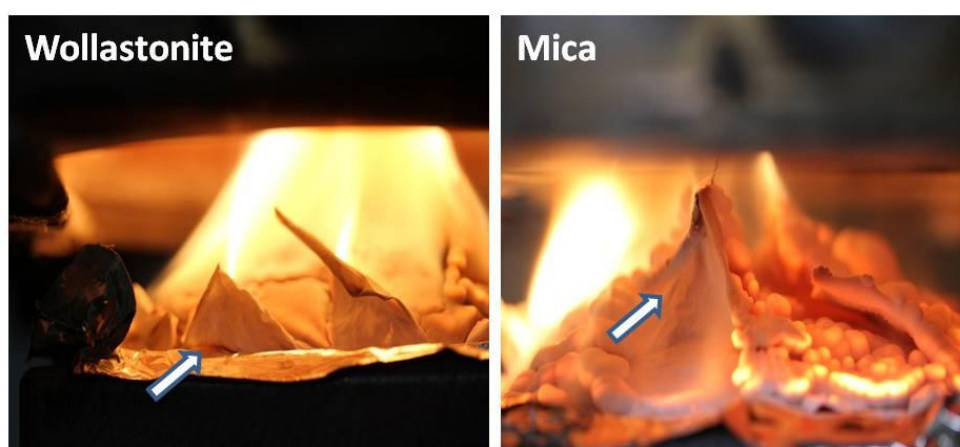


Figure S 1. The scratches on surface composites containing mica and wollastonite (under heat flux of  $50\text{kW/m}^2$ ) during cone calorimeter test.



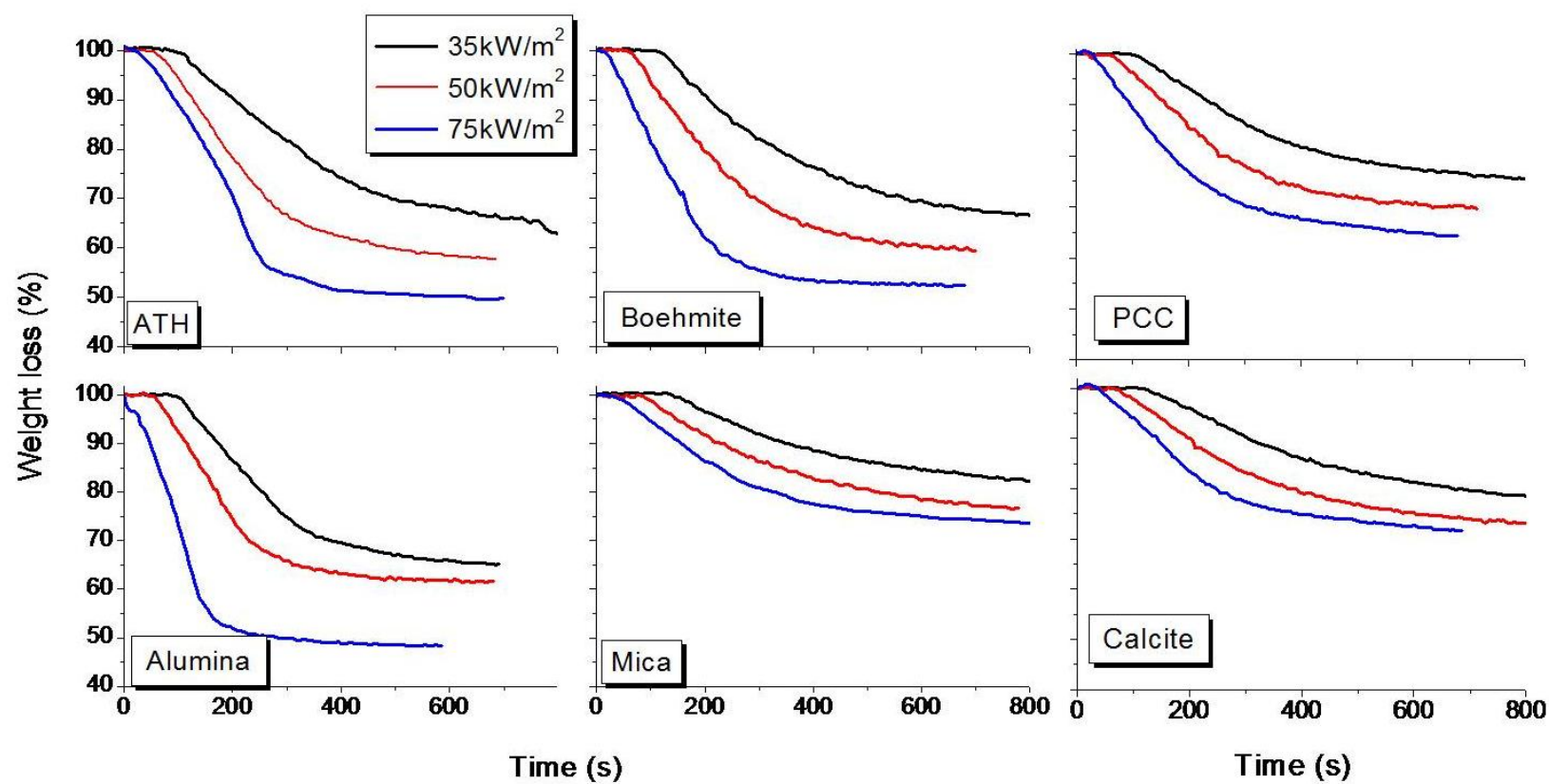


Figure S 2. Weight loss rate of silicone composites during cone calorimeter test (heat flux of 35kW/m<sup>2</sup>).

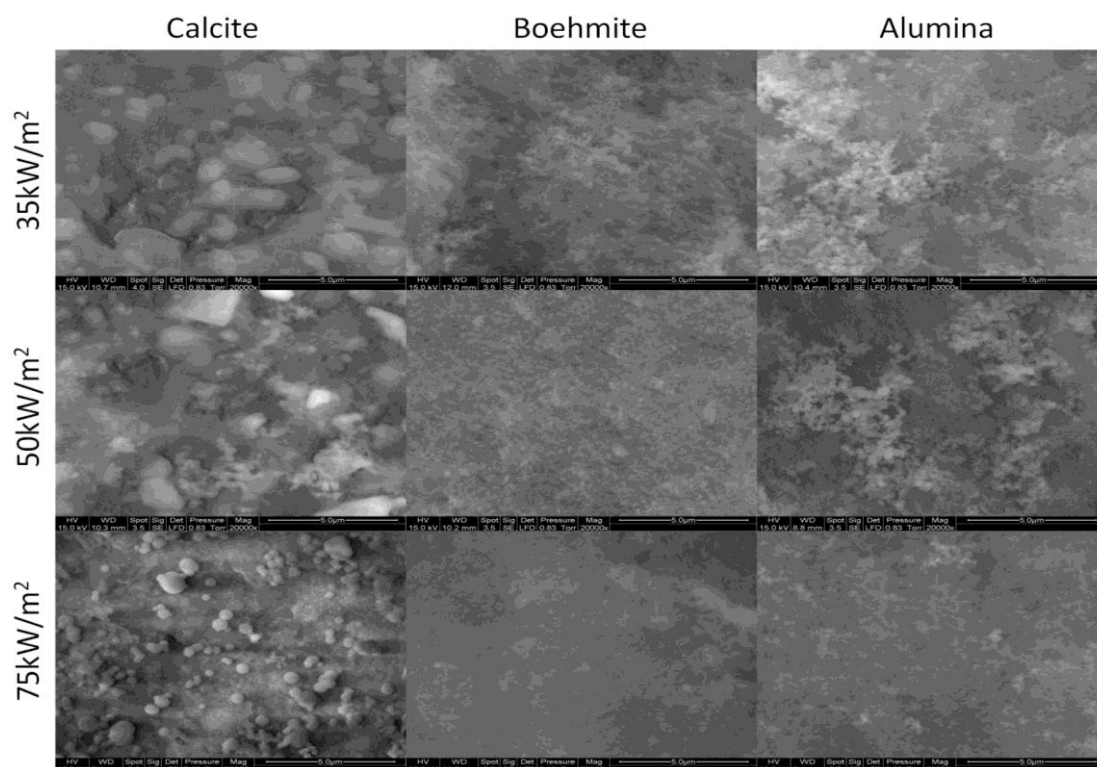


Figure S 5. SEM images (20000x) on the interior of residues after cone calorimeter test.

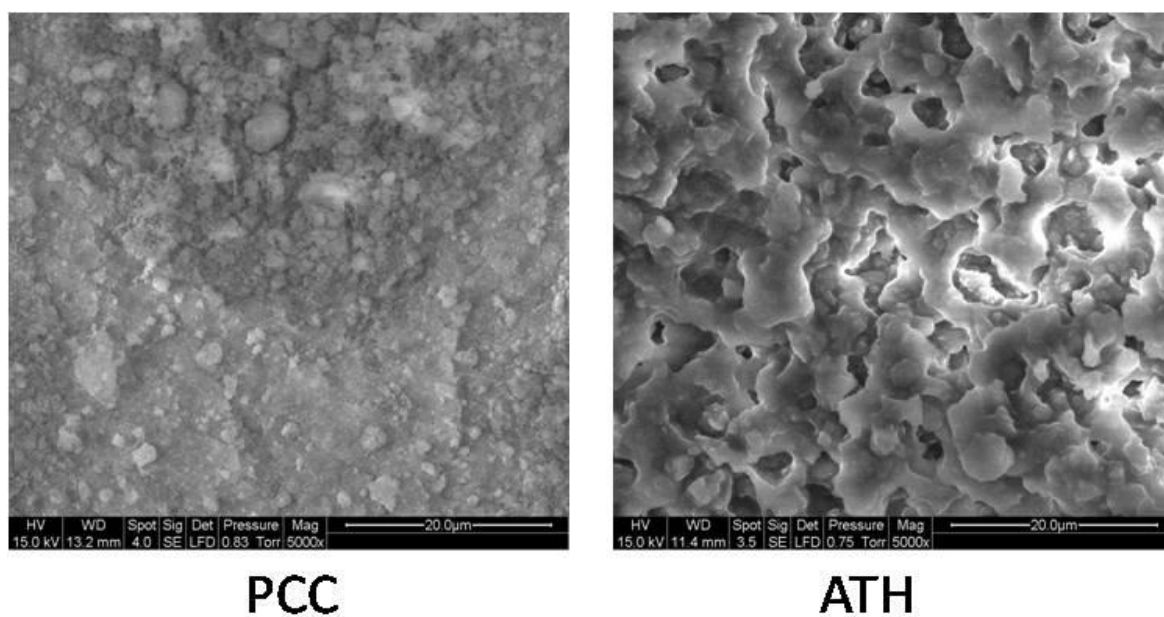


Figure S 6. SEM images of PCC and ATH residues taken for sample while the peak of HRR is attained under heat flux of  $35\text{kW/m}^2$ .

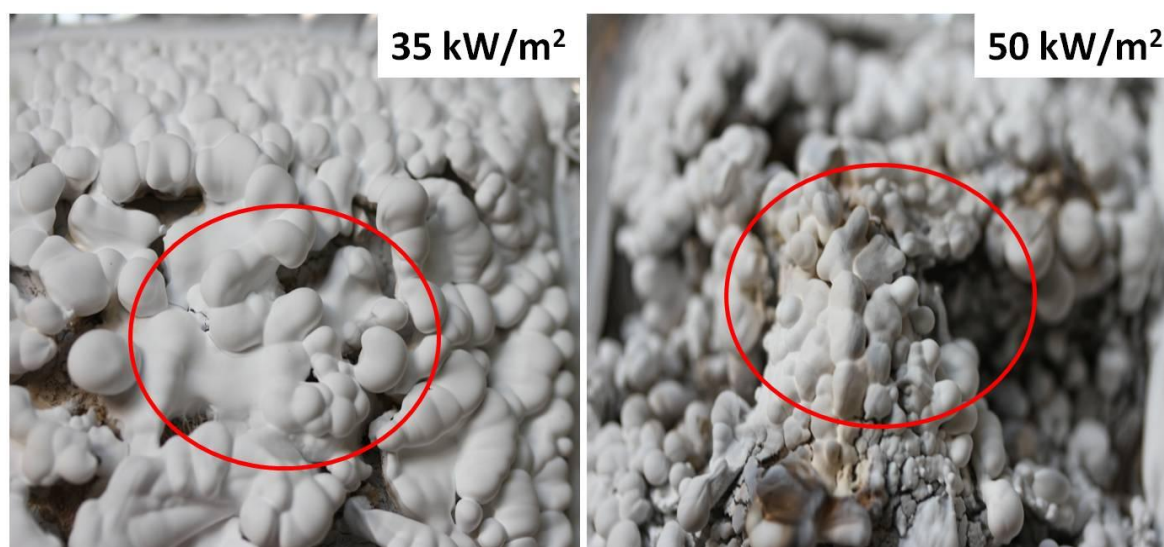


Figure S 3. The different of residue appearance of silicone composites containing calcium hydroxide after cone calorimeter test under heat flux of  $35\text{ kW/m}^2$  and  $50\text{ kW/m}^2$ .

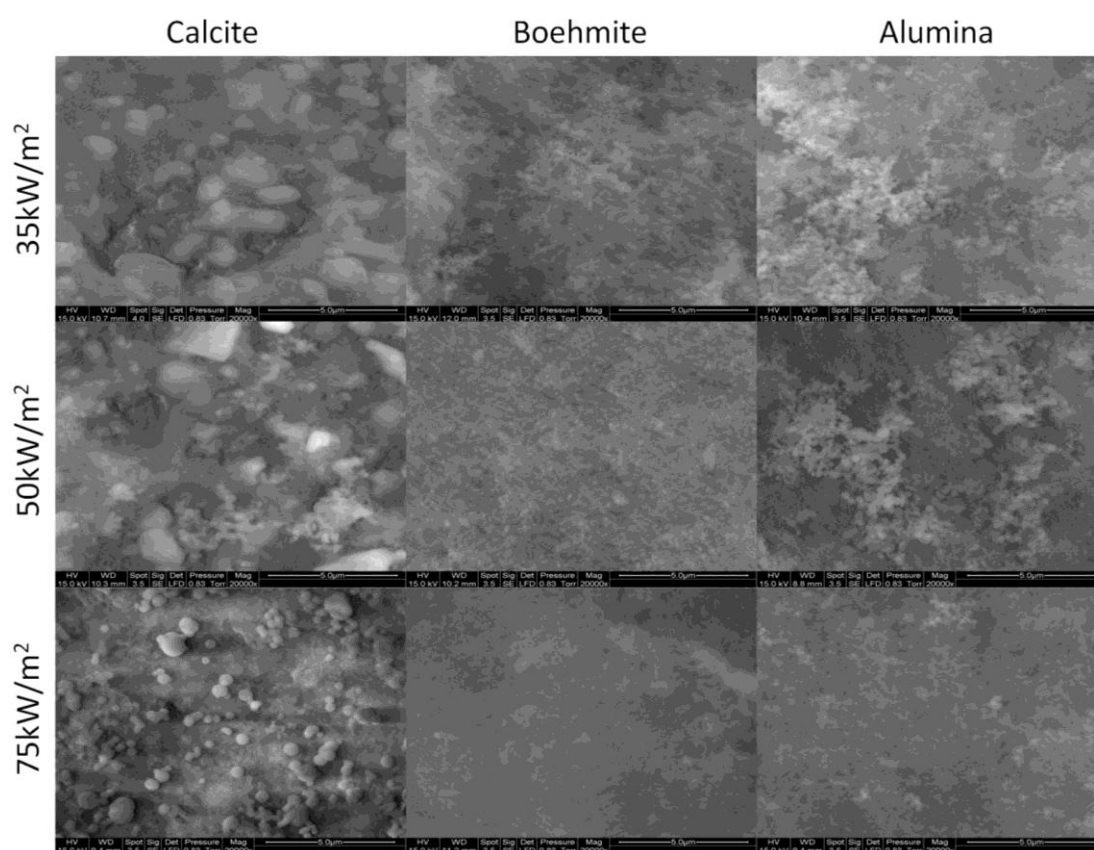


Figure S 4. SEM images (20000x) on the surface of residues after cone calorimeter test.

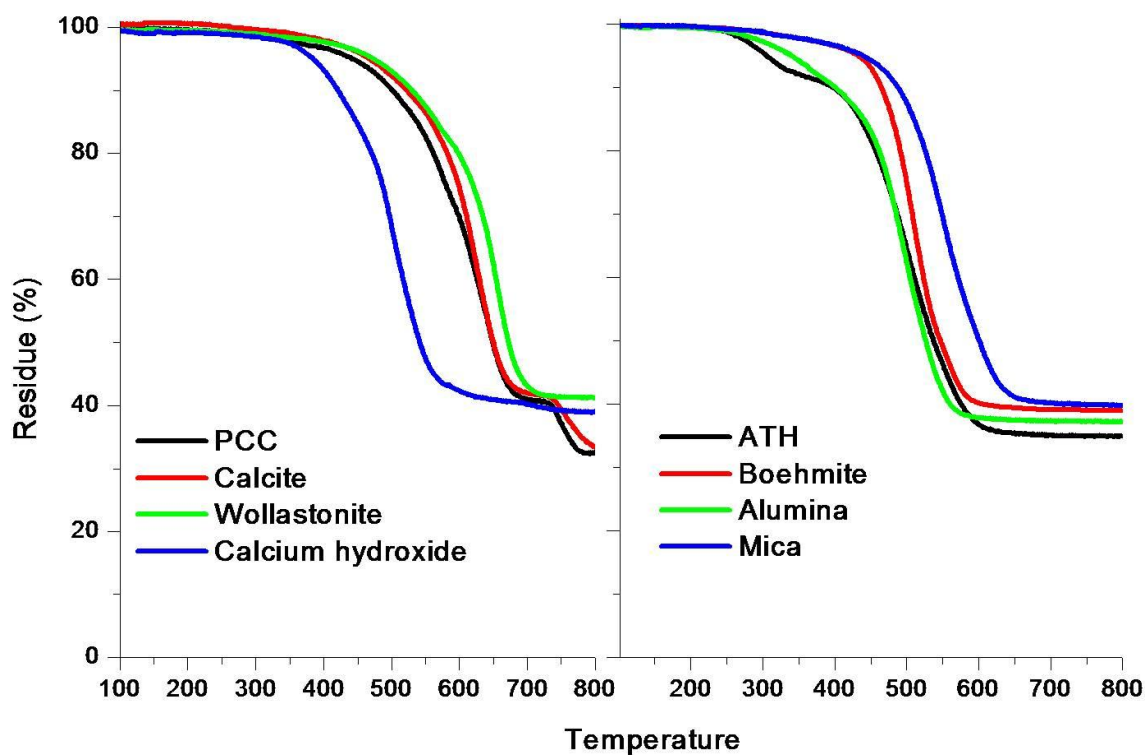


Figure S 7. Degradation of silicone composites by TG analysis at heating rate of 10°C/min

<i>Molecule</i>	<i>Enthalpy (kcal/mole)</i>
CaCO <sub>3</sub>	-288.6
Ca(OH) <sub>2</sub>	-235.5
ATH	-612.5
BHT	-472.0
CaO	-151.7
H <sub>2</sub> O	-57.8
CO <sub>2</sub>	-94.0
Al <sub>2</sub> O <sub>3</sub> -amorph	-390.0

Table S 1. Enthalpy energy of each filler and its decomposition products [<sup>1</sup>]

<sup>1</sup> Patnaik P. Editor. Handbook of Inorganic Chemicals. McGraw Hill New York 2002.



Table S 2. Commercial information and characterization data on the fillers used in this study.

	<i>Fillers</i>	<i>Formula</i>	<i>Particle shape</i>	<i>Mean particle size and deviation (<math>\mu\text{m}</math>)<sup>b</sup></i>	<i>SSA (<math>\text{m}^2/\text{g}</math>)<sup>c</sup></i>	<i>XRD Crystalline form<sup>d</sup></i>	<i>Filler residue at 780°C<sup>f</sup></i>
Ca based	Precipitated calcium carbonate (PCC)	$\text{CaCO}_3$	Oblate/spherical (aggregates)	$0.074 \pm 0.015$	$20.57 \pm 0.04$	Calcite	25.1
	Calcite	$\text{CaCO}_3$	Platelet	$1.0 \pm 0.3$	$6.49 \pm 0.33$	Calcite Quartz	14.6
	Calcium hydroxide	$\text{Ca}(\text{OH})_2$	Platelet	$1.1 \pm 0.5$	$5.44 \pm 0.79$	Portlandite Calcite	1.3
	Wollastonite	$\text{CaSiO}_3$	Acicular, Lamellar/platelet	$7.4 \pm 6.7$	$3.74 \pm 1.15$	Wollastonite calcite	29.7
Al based	Aluminum trihydrate (ATH)	$\text{Al}(\text{OH})_3$	Hexagonal, platelet	$0.9 \pm 0.3$	$6.01 \pm 0.04$	Gibbsite	35.1
	Boehmite	$\text{AlOOH}$	Acicular	$0.37 \pm 0.11$	40e	Boehmite	17.3
	Alumina	$\text{Al}_2\text{O}_3$	Spherical	0.013f	$94.28 \pm 0.05$	Aluminum oxide	3.1
	Mica	$\text{KAl}_2(\text{Si}_3\text{Al})\text{O}_{10}(\text{OH})_2$	Flake like, Lamellar/platelet	$6.8 \pm 9.6$	$5.87 \pm 0.75$	Muscovite, Kaolinite, Quartz	3.6

<sup>a</sup> given by the supplier, the remaining content to reach 100% in some fillers is supposed to be of water; <sup>b</sup> from ESEM photos, using a size measuring software (see text); <sup>c</sup> from BET measurements; <sup>d</sup> from XRD; <sup>e</sup> given by the supplier; <sup>f</sup>: by TG analysis under Nitrogen at heating rate of 10°C/min.

# *Conclusion Générale*









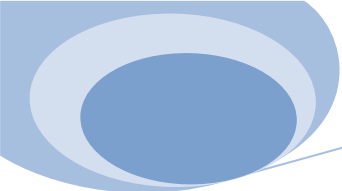
## Conclusion générale et perspectives

Ce travail de thèse a consisté à étudier d'un point de vue bibliographique (articles et brevets) et expérimental la dégradation thermique de composites silicones, à travers la céramisation au platine de la matrice silicone, et l'ajout de différentes charges sélectionnées pour apporter une meilleure cohésion du résidu, et un comportement au feu amélioré. Ce travail a été divisé en cinq chapitres présentant chacun un article en anglais publié, soumis ou en passe de l'être.

La première partie du travail consistait en une mise au point bibliographique décrivant l'état de l'art sur l'utilisation de silicones à fortes températures. Nous avons extrait de cette étude une meilleure compréhension des mécanismes de dégradation du silicone, en présence ou non de charges ou d'additifs employés pour l'amélioration des propriétés thermiques et du comportement au feu. Particulièrement, la discussion a porté sur l'effet des mécanismes de dépolymérisation et/ou de céramisation, en fonction de la structure du polymère, des conditions de chauffage, et de l'ajout d'additifs (i.e. à moins de 5% en poids de charges). Nous avons également recensé dans ce chapitre l'utilisation de silicones simples ou fonctionnalisés comme additif de retard de flamme dans différentes matrices polymères.

Le second chapitre concernait la compréhension des mécanismes de dégradation du polymère silicone. Pour cela, la formulation d'un mélange modèle, contenant un PDMS téléchélique vinylé, de la silice fumée et traitée, et des quantités catalytiques de platine, a été mise au point puis testée en ATG. L'influence du taux de Pt, du taux et de la nature des groupements de surface des silices utilisées, a été discutée. Une augmentation du taux du résidu est favorisée par à un effet de synergie entre la silice et le platine : la première immobilise les chaînes macromoléculaires par adsorption, alors que le second induit des réactions de réticulation du réseau silicone. On a pu constater que l'immobilisation des chaînes de silicone dès les plus basses températures était la clé pour une bonne stabilité thermique. À partir de ces éléments de compréhension, de nouvelles formulations ont été imaginées. Par exemple, la présence de groupements réactifs vinylés en surface de la silice favorise l'immobilisation des chaînes de silicone, non seulement par liaisons hydrogène, mais aussi par réticulation des chaînes grâce aux réactions radicalaires induites par le platine.

Les trois derniers chapitres étaient ensuite consacrés à l'étude des composites de silicone chargés par différents types de minéraux à base de calcium et d'aluminium. Les premières comprennent le carbonate de calcium précipité CCP (particules nanométriques obtenues

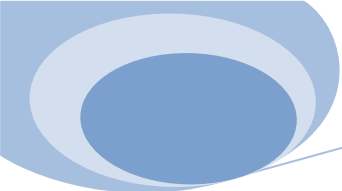


industriellement), la calcite ( $\text{CaCO}_3$  naturelle), la wollastonite ( $\text{CaSiO}_3$ ), et l'hydroxyde de calcium ( $\text{Ca(OH)}_2$ ), les secondes comprennent le trihydroxyde d'aluminium ( $\text{Al(OH)}_3$  ou  $\text{Al}_2\text{O}_3 \cdot 3\text{H}_2\text{O}$ ), la boehmite ( $\text{AlOOH}$  ou  $\text{Al}_2\text{O}_3 \cdot \text{H}_2\text{O}$ ), l'alumine ( $\text{Al}_2\text{O}_3$ ), et le mica.

La première étude, rapportée dans le chapitre trois, présentait l'étude du comportement thermique des charges, et la stabilité thermique des composites par ATG. Nous avons constaté que le résidu final du composite est indépendant du type de charge (à base de calcium ou d'aluminium), alors que la dégradation thermique est fortement influencée par la composition chimique de la charge (non-hydratée, contenant de l'eau, ou portant des groupements hydroxyles en surface). Leur forme (morphologie) et leur taille jouent également un rôle important sur le taux de résidus des composites. Les charges aciculaires ou sphériques apparaissent moins efficaces que les charges lamellaires ou rhomboédriques, et les charges nanométriques, moins intéressantes que celles de tailles microniques. Une meilleure efficacité des mélanges contenant une charge à base de calcium, de par la réactivité entre le produit de dégradation de la charge et la silice, a également été mise en évidence lors de la dégradation du composite pour des températures supérieures à  $900^\circ\text{C}$ .

Le chapitre quatre rapportait l'étude de la cohésion des résidus des composites pyrolysés sous des conditions extrêmes selon la norme française NF C 32-070 CR1, mais sans chocs mécaniques réguliers pendant l'essai. La cohésion des résidus finaux a particulièrement été testée par une méthode originale de compression et corrélée avec la microstructure, la composition élémentaire, et l'état cristallin des résidus. Ainsi la cristallisation et l'absence de libération de gaz dégradant le silicone (par exemple la vapeur d'eau) amènent à un résidu très cohésif et compact. Au contraire, la libération d'eau et l'absence d'interactions entre les charges à haute température conduisent à des résidus très poreux et peu cohésifs. Le mica et la wollastonite ont montré une résistance à la compression légèrement supérieure à celle des autres charges, grâce à leur capacité à interagir avec la silice à haute température. Le test de compression a mis en exergue que l'incorporation de CCP dans le silicone améliore la cohésion du résidu par rapport aux autres charges, mais celui-ci présente une contraction de volume trop importante pour l'application câblerie.

Enfin, le dernier chapitre décrivait, dans le détail, une étude du comportement au feu des composites. L'influence de chaque charge sur l'action retardatrice de flamme du silicone a été étudiée à l'aide du cône calorimètre et du microcalorimètre. Particulièrement, une analyse approfondie des résidus et des gaz libérées lors de la combustion du composite a été réalisée.



Au cours de cette étude, il a été montré que les charges lamellaires présentaient la meilleure efficacité au cône calorimètre. Contrairement à d'autres matrices polymères, nous n'avons pas pu mettre en évidence dans le silicone un effet significatif des nanoparticules. Par ailleurs, l'ajout de charges induisant un effet endothermique ne modifie par notablement la réaction au feu du composite silicone. Au vu de ces résultats, nous en avons conclu que les facteurs principaux pour l'amélioration du comportement au feu des silicones étaient liés à la stabilité thermique de la matrice et/ou à la génération d'un effet barrière, soit via l'incorporation de charges lamellaires, soit par la formation d'un résidu céramisé.



Grâce aux connaissances acquises au cours de cette thèse, nous pouvons maintenant imaginer développer de nouvelles formulations à base d'élastomère silicone plus efficaces pour des applications à hautes températures, notamment pour le comportement au feu en câblerie. Lors des études effectuées sur les composites, nous avons étudié principalement trois paramètres, à savoir leur stabilité thermique sous gaz inerte (par ATG), la cohésion des résidus après pyrolyse en milieu confiné (au four, dans des tubes en inox) et le comportement au feu en présence d'oxygène (via un cône calorimètre). A l'heure actuelle, la formule satisfaisant à ces trois paramètres n'est pas triviale ; il faudra donc faire des compromis afin d'adapter la formulation du composite au paramètre clé recherché. Dans le Tableau 1, le type d'additif(s) permettant de répondre au mieux à chaque paramètre est donné, d'abord individuellement, puis deux à deux, et enfin tous paramètres confondus. De plus, nous avons fait une distinction entre les résultats correspondant aux essais présentés dans les publications, et ceux réalisés dernièrement en perspectives du travail, et non présentés dans ce manuscrit. Enfin pour pouvoir obtenir un matériau répondant aux trois paramètres, nous avons imaginé une matrice améliorée que nous décrirons ci-dessous.

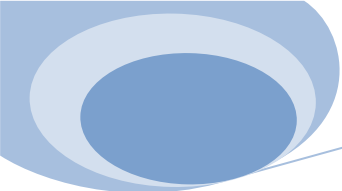
Pour obtenir un composite présentant une bonne stabilité thermique, à notre connaissance, l'utilisation d'une charge unique est suffisante. De plus, nous avons constaté que la wollastonite et le carbonate de calcium étaient les plus satisfaisants. Par ailleurs, nous avons pu montrer, dans le cas du carbonate de calcium, que la taille des particules employées n'avait pas d'influence. En plus d'une bonne stabilité thermique, ces composites ont également montré une bonne cohésion des résidus. Le composite à base de carbonate de calcium présente une bonne résistance à la compression mais une forte contraction de volume, alors que celui à base de wollastonite présente une variation de volume modérée mais une résistance à la

compression faible. Si l'application visée ne nécessitait pas de maintenir le volume du matériau, par exemple pour des textiles coupe-feu où la contraction des fibres imprégnées n'est pas rédhibitoire, le CCP seul serait alors parfait.

Tableau 1. Choix des additifs permettant de répondre aux différents paramètres décrits dans le texte. En blanc : essais publiés ; en bleu : essais prospectifs déjà réalisés ou en cours (non publiés) ; en rose : formulation idéale imaginée.

<i>Paramètres</i>	<i>Stabilité thermique</i>	<i>Cohésion des résidus</i>	<i>Comportement au feu</i>
<i>Stabilité thermique</i>	Wollastonite ou Calcite		
<i>Cohésion des résidus</i>	CCP ou Wollastonite	CCP ou Wollastonite	
	Wollastonite + Poudres de verre	Wollastonite + Poudres de verre Boehmite + Calcite + Poudres de verre	
<i>Comportement au feu</i>	Wollastonite	Wollastonite ou Calcite	Mica ou Wollastonite
			CCP + Mica
	<i>Matrice améliorée</i>		

Pour obtenir un matériau présentant un résidu cohésif, il faut viser à la fois une bonne résistance à la compression et une faible variation de volume. Afin de contrôler la forte contraction de volume observée avec le CCP, nous avons décidé de l'associer au mica, qui lui conduisait à une expansion de volume. La proportion choisie dans un premier temps a été de 50% en poids de chaque charge. Cette formulation n'était pas idéale, car malgré une variation de volume correctement contrôlée, la résistance à la compression s'est calquée sur le comportement du composite contenant uniquement du mica, et non selon un compromis entre les deux charges. Il faudrait donc tester un mélange de charge présentant un taux de mica inférieur à celui de CCP. Si nous regardons de plus près les autres paramètres, nous constatons que la stabilité thermique est identique à la composition contenant uniquement du mica ; par contre, ce composite mixte a montré un meilleur comportement au feu que ceux

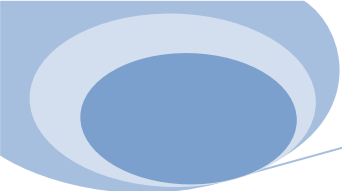


possédant une des deux charges seules. Au vu de ces résultats nous en avons conclu que pour une cohésion optimale des résidus, il faudrait associer une charge lamellaire et une charge céramisante (pouvant induire une co-cristallisation à haute température, c'est-à-dire une céramisation du résidu), et/ou un additif dit « agent liant », par exemple un borate du zinc ou des poudres de verre (« glass frits »). En effet, le facteur limitant pour la charge céramisante est la forte contraction de volume qu'elle induit, pouvant conduire à l'apparition de fissures. Ce facteur limitant devrait pouvoir être compensé par l'addition d'un agent liant, ce dernier comblant les fissures, limitant la contraction de volume et permettant la liaison entre les phases du résidu. Selon l'étude bibliographique, un mélange de mica avec des poudres de verre a montré une bonne cohésion du résidu de silicone grâce à la formation d'un état vitreux à haute température [1].

Une autre formulation à base de boehmite, de calcite et de poudres de verres (glass frits) a été testée au laboratoire afin de diminuer la variation de volume. Cependant, cette formulation ne s'est encore une fois pas avérée être idéale, car la résistance à la compression du résidu était assez faible (d'environ 10N pour une variation de volume de 3%). Une des possibilités qui pourrait permettre d'améliorer à la fois la résistance à la compression des résidus, la variation de volume et la tenue thermique serait l'association de wollastonite et de poudres de verres dans des proportions respectives de 80% et 20% en poids. Lors de certains essais récents, nous avons constaté que cette formulation améliorait légèrement la résistance à la compression (14N au lieu de 12N pour la wollastonite) et par la même occasion limitait la variation de volume (+3,8% au lieu de -7%). De plus, ce mélange a montré une meilleure stabilité thermique que celui comprenant l'association mica+CCP, bien que plus faible que celle mesurée pour la formulation ne contenant que de la wollastonite. Ces résultats sont expliqués par l'effet catalytique des hydroxyles de surface des poudres de verres sur la stabilité thermique de la silicone. Avec l'aide de la littérature et des essais réalisés, nous pouvons donc supposer que l'incorporation d'agents liants tels que les borates de zinc, en lieu et place des poudre de verres, pourrait être intéressante à tester.

Concernant l'amélioration uniquement du comportement au feu, les tests préliminaires ont permis de mettre en avant deux types de charge, la wollastonite et le mica. Ici encore, des mélanges de charges ont été testés et l'association CCP+mica, sous une irradiance de  $50\text{kW/m}^2$ , a montré une diminution significative du PHRR ( $116\text{kW/m}^2$  au lieu de  $134\text{kW/m}^2$ ). Si l'on considère l'amélioration simultanée du comportement au feu et de la stabilité





thermique, nous avons pu montrer que l'ajout de wollastonite était un bon compromis, et à l'heure actuelle aucune association de charges testées n'est arrivée à ce niveau. Enfin dans le cas de l'amélioration du comportement au feu et de la cohésion du résidu, nous avons vu précédemment que la wollastonite ou la calcite conduisait aux meilleurs résultats. Si l'on considère des tests limités à une irradiance de  $75 \text{ kW/m}^2$ , la charge céramisante la plus intéressante est l'hydroxyde de calcium. En revanche, si ces tests étaient poussés jusqu'à  $100 \text{ kW/m}^2$ , la calcite et le CCP pourraient être plus efficaces car ils ne libèrent pas d'eau et la température atteinte dans ce cas serait suffisante pour amorcer une céramisation des résidus. Les essais sous différentes irradiances au cône calorimètre ont montré que l'association de charges lamellaires (mica) et de charges céramisantes s'avérerait particulièrement efficace, sachant que ces dernières peuvent en plus permettre de maîtriser la variation de volume. Le matériau ainsi obtenu pourrait être utilisé sur une plage d'irradiance de 35 à  $100 \text{ kW/m}^2$  tout en conservant une bonne efficacité.

Enfin, si l'on devait imaginer une formulation idéale répondant à tous les paramètres, il serait certainement nécessaire de changer la matrice de base. En effet, si à la place d'une silice modifiée D<sub>4</sub> nous utilisons une silice modifiée vinyle, nous pourrions améliorer l'immobilisation des chaînes et ainsi augmenter le taux de résidu. De plus, l'ajout d'un additif donneur de platine, tel que le catalyseur de Karstedt, a montré son efficacité pour faciliter la céramisation tout en induisant également une augmentation du taux de résidu. L'association de ces deux composés dans la matrice initiale couplée avec l'ajout d'une charge lamellaire présentant un facteur de forme (aspect ratio) élevé (wollastonite ou mica), d'une charge céramisante (initiateur d'oxyde de calcium) et d'un additif tel que le borate du zinc pourrait permettre d'améliorer à la fois la céramisation du résidu, la stabilité thermique et également d'obtenir un meilleur comportement au feu.

## Référence

1. Mansouri J., R. P. Burford, Y. B. Cheng, L. Hanu, 2005, Formation of strong ceramified ash from silicone-based compositions, J. Mater. Sci., 40 (2005) 5741–5749



# **Etude fondamentale du comportement au feu de composites silicones : stabilité thermique, résidus sous pyrolyse et tests calorimétriques**

---

## **RESUME :**

Cette thèse avait pour but de comprendre le comportement thermique de composites silicones. Pour cela, une étude bibliographique complète sur le comportement au feu des silicones comme matrice ou en tant que retardateur de flamme a tout d'abord été réalisée. Ce travail a permis de définir une stratégie permettant d'améliorer la stabilité thermique de la matrice mais également du composite silicone. Une première étude expérimentale a été consacrée à l'étude de l'influence de l'ajout de platine et de silice sur le comportement thermique d'un composite silicone modèle. Nous avons pu montrer que l'immobilisation des chaînes macromoléculaires était le facteur clef pour une céramisation efficace. Dans une deuxième partie, des composites silicones dans lesquels nous avons incorporé des charges à base soit de calcium, soit d'aluminium ont été testés selon trois différents protocoles de dégradation thermique. Nous avons d'abord mis en exergue le fait que la nature chimique (charge non hydratée, contenant de l'eau ou portant des groupements hydroxyles en surface), la taille et la morphologie des charges influençaient fortement le comportement thermique du silicone. Nous avons ensuite montré que la formation de nouvelles structures cristallines et l'absence de libération de gaz dégradant la matrice conduisaient à des résidus très cohésifs, après pyrolyse extrême. Enfin, des tests calorimétriques ont montré que l'amélioration du comportement au feu des composites était liée à la stabilité thermique et/ou à la génération d'une couche barrière.

---

## **MOTS-CLES :**

Comportement au feu, composite, pyrolyse, cohésion résidu, test calorimétrique, céramisation

---

## **Fundamental study on the fire behavior of silicone composites: thermal stability, cohesion residues, and calorimeter tests**

---

## **SUMMARY:**

This PhD work has been devoted to the study of the thermal behavior of silicone composites. A preliminary review on the flame retardancy of silicone reported numerous works devoted to the development of thermally-resistant silicone composites or silicone polymers used as flame retardant agents in other organic polymer matrices. The first part of our experimental work highlighted the key role of macromolecular chain immobilization, through the synergy of platinum and silica, in generating high ceramized residue content after thermal gravimetry. The second part of this work was dedicated to the study of silicone composites filled with either calcium or aluminum-based fillers. The filler nature (non hydrated, water releasing or hydroxyl groups on the surface), the morphology and the particle size strongly influenced the thermal behavior of silicone composites. The analyses on composites residues after extreme pyrolysis showed that the formation of new crystalline structures and the absence of water release favored the residue ceramization. The investigation on fire reaction of silicone composites finally granted their outstanding properties to the matrix thermal stability and/or a barrier layer formation.

---

## **KEYWORDS:**

Fire behavior, composite, pyrolysis, residue cohesion, calorimetric test, ceramization.

---

## **DISCIPLINE : Chimie des Matériaux**

---

## **LABORATOIRE :** Ecole des Mines d'Alès – CMGD

6, Avenue de Clavières - 30319 Alès Cedex – FRANCE

Ecole Nationale Supérieure de Chimie de Montpellier, ICGM-Equipe IAM

8, Rue de l'Ecole Normale - 34296 Montpellier Cedex 5 - FRANCE